

# **INTEGRATION OF GEO-ELECTRICAL AND GEOTECHNICAL PARAMETERS OF LATERITIC SOILS THROUGH LABORATORY AND FIELD STUDIES**

Thesis

Submitted in partial fulfilment of the requirement for the degree of  
**DOCTOR OF PHILOSOPHY**

By

**NIMI ANN VINCENT**



DEPARTMENT OF CIVIL ENGINEERING  
NATIONAL INSTITUTE OF TECHNOLOGY KARNATAKA  
SURATHKAL, MANGALORE – 575025  
September, 2018

## DECLARATION

*by the Ph.D. Research Scholar*

I hereby *declare* that the Thesis entitled “**Integration of geo-electrical and geotechnical parameters of lateritic soils through laboratory and field studies**” which is being submitted to the **National Institute of Technology Karnataka, Surathkal** in partial fulfilment of the requirements for the award of the Degree of **Doctor of Philosophy in Civil Engineering**, is a *bonafide report of the research work carried out by me*. The material contained in this Research Thesis has not been submitted to any University or Institution for the award of any degree.

**NIMI ANN VINCENT**

(Register No. 135009CV13F02)

Department of Civil Engineering

Place: NITK, Surathkal

Date: 14/09/2018

## CERTIFICATE

This is to *certify* that the Research Thesis entitled “**Integration of geo-electrical and geotechnical parameters of lateritic soils through laboratory and field studies**” submitted by **Ms. NIMI ANN VINCENT**, (Register Number: **135009CV13F02**) as the record of the research work carried out by her, is *accepted as the Thesis submission* in Partial fulfillment of the requirements for the award of degree of Doctor of Philosophy.

**Dr. K. N. Lokesh**  
**Research Guide**  
(Signature with Date and Seal)

**Dr. R. Shivashankar**  
**Research Guide**  
(Signature with Date and Seal)

**Dr. Varghese George**  
**H. O. D. Civil and Chairman – DRPC**  
(Signature with Date and Seal)

**DEDICATED TO  
MY FAMILY**

## **ACKNOWLEDGEMENT**

I extend my heartfelt gratitude to my research supervisor Dr. K. N. Lokesh, Professor, Civil Engineering Department, NITK Surathkal, for his support and timely advice for the completion of my research program and preparation of the Thesis.

With great pleasure I acknowledge my sincere gratitude to my research Co-supervisor Dr. R. Shivashankar, Professor, Civil Engineering Department, NITK Surathkal, for all his inspiration, relentless guidance, encouragement and help in successful completion of the research program. His keen engineering and scientific insight has helped me enormously in improving the technical content and practical relevance of the thesis.

I am greatly indebted to RPAC members, Prof. K. Swaminathan of civil engineering department and Prof. M. K. Nagaraj from department of applied mechanics for their timely evaluation and valuable suggestions during the progress of the research work.

I am thankful to Prof. Varghese George, Head of civil engineering department and chairman of DRPC, Dr. Jayalekshmi, Secretary DRPC. I take this opportunity to thank former department heads namely, Prof. K. N. Lokesh and Prof. Venkat Reddy for their timely help during my entire research period.

I sincerely thank Prof. Katta Venkataramana, Dean (Academic) for his continuous and wholehearted support during my entire research period.

I gratefully acknowledge the support and help rendered by Ms. Gayathri V. L., Ms. Jinu Mary Jacob, Ms. Haritha P. A., Ms. Sreelekshmy Sreedevi, Ms. Divya Nath (Former M.Tech. Students of GTE) for the successful completion of my experimental work. Special thanks to my friends Mr. Ugwal Prakash, Ms. Shannon Pinto, Mr. Virupaksha H. S., and Mr. Vignesh Bhat for their help in conducting the field tests. I sincerely thank the geotechnical engineering laboratory staff, especially Mr. Yathish Saliyan for the help rendered by him during the experimental stages of the work.

I wish to thank Proto Engineering Solutions and Stamina Engineering works for fabricating the soil resistivity box and related accessories precisely. I also wish to thank Gennext chemicals, for the timely supply of chemicals needed for the experiments.

I also like to extend my gratitude to all the teaching faculty and supporting staff of the civil engineering department, for their encouragement, help and support provided during the research work. My thanks are also due to the office staff of Civil Engineering Department.

I would like to express my sincere gratitude to the authorities of NITK Surathkal, for providing me excellent facilities and comfortable stay in the campus.

I wish to thank my IIT colleagues, Ms. Aswathy R (IITD), Mr. Ganesh Kailas (IITK), Mr. Jeevan Joseph and Mr. Ansaf V Karim, (IITB) for finding me the inaccessible literatures without any delay and for sharing their technological knowledge with me. I also thank my friends Greeshma and Sandhya for clearing my doubts and giving valuable suggestions during the progress of my research work.

I would like to thank my best friend Ms. Biji C Thomas, who stood beside me during all the tough times unconditionally. I thank all my friends at NITK who were always supportive and friendly to me.

I thank my mother, Mrs. Annie Vincent for the great sacrifices she has done for my education and bright future. I thank my father, Mr. P. C. Vincent who always inspired me and gave freedom in following my career dreams. I thank my husband, Dr. Appu Abraham and my mother in law, Dr. Mary Abraham for the forbearance and full hearted support offered me during my studies, without which my research dreams wouldn't have been fulfilled. More than anything, I would like to thank my three years old little champ, Master Abie Appu Abraham, who patiently cooperated, when his mother was busy with the research and studies.

I would like to remember The Almighty for providing such a splendid learning experience in my lifetime through this journey.

Lastly, I thank all my well-wishers who have directly or indirectly supported me in the need of the hour.

Nimi Ann Vincent

## ABSTRACT

All physical matters involve electricity. Soil has been considered as a specific electrolyte with free ions in the pore water and free electrons in the electrical double layer. This electrical nature of the soil has been studied, and applied to predict various soil parameters by various researchers. In this study, electrical resistivity (ER) of laterites and lateritic soils at controlled and natural field conditions are measured and compared with various engineering properties. Laboratory measurement of electrical resistivity is done using a soil resistivity box, a dc power supply and two high precision multimeters and the field ER measurements are done using signal stacking resistivity meter. The effect of various geotechnical parameters such as water content, dry density, porosity, degree of saturation, percentage of ions and degree of compaction, in controlling the electrical resistivities of lateritic soil samples are studied. Quantitative correlations are obtained between strength and electrical resistivity of lateritic soils, in regulated laboratory conditions.

Vertical Electrical Soundings (VES) were conducted at 14 locations in NITK campus. Standard Penetration Tests (SPT) were also conducted up to 10 to 12m depth at the same locations where VES were conducted. True resistivities at different soil layers interpreted were correlated with the SPT blow counts at the same depth. Overall, there exists a good correlation between SPT and ER. A comparison is made on the laboratory and field electrical resistivity in lateritic formations for surface soil samples.

Electrical behaviour of soil stabilised with cement/lime is also studied. Quantitative correlations are developed between electrical resistivity and strength parameters. The multiple regression models developed can be used to predict the 7<sup>th</sup> day unconfined compressive strength of the soil-cement/lime mix, in the freshly prepared state itself, so that if it doesn't meet the performance criteria, it can be remixed with additional cement/lime and wastage of material can be prevented. A graphical method is introduced in this study which predicts the shrinkage limit (point of just saturation at maximum compaction) of the soil. The results of this research, propose that by properly managing the uncertainties and ubiquitous resistivity measurement errors, Electrical Resistivity tomography can be applied as a pre-investigation method in sites, preceding to direct testing methods like Standard Penetration Test to reduce labour, cost and time involved and to increase efficiency of the testing programme.

**Key words:** electrical resistivity, laterites, unconfined compressive strength, soil-cement/lime, shrinkage limit, Standard Penetration Test





# TABLE OF CONTENTS

DECLARATION		
CERTIFICATE		
ACKNOWLEDGEMENT		
ABSTRACT		
TABLE OF CONTENTS		i
LIST OF FIGURES		ix
LIST OF TABLES		xxiii
NOMENCLATURE		xxiv
<b>1</b>	<b>INTRODUCTION</b>	<b>1</b>
	1.1 General	1
	1.2 Scope the study	1
	1.3 Objectives	2
	1.4 Organisation of the Thesis	2
<b>2</b>	<b>LITERATURE REVIEW</b>	<b>7</b>
	2.1 General	7
	2.2 Electrical Resistivity and Conductivity	7
	2.3 Applications of Resistivity Measurements in Groundwater Studies	8
	2.4 Specific Applications of Resistivity Measurements in Concrete Engineering	10
	2.5 Electrical Resistivity Applications in Soil Mechanics	10
	2.5.1 Electrical resistivity tomography for characterizing cracks in soils.	12
	2.5.2 Electrical resistivity measurements for evaluation of swell-shrinkage properties of expansive soils.	13
	2.5.3 Electrical resistivity measurements for quantifying soil hydraulic parameters	13

2.5.4	Correlations of Electrical Resistivity with Strength Properties by previous researchers	13
2.5.5	Electrical Resistivity Measurements and SPT	14
2.5.6	Cone penetration and vane shear test with ER measurements	15
2.6	Factors Affecting Soil Resistivity	16
2.6.1	Effects of Soil Type	16
2.6.1(a)	Basic Structure of Clay	17
2.6.1(b)	Clay Water Interaction	21
2.6.2	Effect of temperature	22
2.6.3	Effect of water content	23
2.6.4	Effect of degree of saturation	24
2.6.5	Effect of hydraulic conductivity	24
2.6.6	Effect of void ratio/porosity	25
2.6.7	Effect of pore fluid composition	26
2.6.8	Effect of dry density and degree of compaction	26
2.7	Laboratory Electrical Resistivity Measurements	26
2.7.1	Two probes measurements	26
2.7.2	Four probes measurements	27
2.8	Field Electrical Resistivity Measurements	28
2.8.1	Survey Methods and Electrode Configurations	29
2.8.2	True resistivity and apparent resistivity	29
2.8.3	Interpretation of electrical resistivity sounding data	31
2.8.4	Inverse Slope Method	32
2.9	Laboratory Resistivity vs Field Resistivity	33
2.10	Lateritic Soils	33
2.10.1	Electrical resistivity studies on laterites	35
2.11	Electrical resistivity of contaminated soils	35
2.11.1	Case study on heaving of soil due to acid contamination	35

2.12	Electrical Resistivity Studies on Engineering Properties of Soil-Cement/Lime	36
2.12.1	Stabilisation of soils	37
2.12.2	Electrical resistivity of stabilised soils	37
2.13	Summary	39
<b>3</b>	<b>LABORATORY EXPERIMENTAL INVESTIGATIONS ON LATERITIC SOILS</b>	<b>41</b>
3.1	Introduction	41
3.2	Sample Preparation	41
3.3	Geotechnical Properties of Soil	42
3.4	Test Procedures	43
3.4.1	Water content	43
3.4.2	Specific gravity test	43
3.4.3	Liquid limit and Plastic limit	43
3.4.4	Shrinkage limit	43
3.4.5	Compaction characteristics	44
3.4.6	Sieve analysis and Hydrometer analysis	44
3.4.7	Falling Head Permeability test	44
3.4.8	Unconfined compression tests	45
3.4.9	Triaxial compression test	45
3.4.10	Energy-dispersive X-ray spectroscopy (EDAX)	46
3.4.11	Electrical Resistivity of Soil	46
3.4.11(a)	Fabrication of Soil Resistivity Box	46
3.4.11(b)	Calibration of soil resistivity box	47
3.4.11(c)	Test procedure for soil resistivity measurement	48
3.4.11(d)	Measurement of California Bearing Ratio (CBR) and Electrical Resistivity	51
3.5	Results and Discussions	52
3.5.1	Basic Geotechnical parameters of the soil samples	52
3.5.2	Energy-dispersive X-ray spectroscopy (EDAX )	53

3.5.3	Correlations of Geotechnical Parameters with Soil	57
	Electrical Resistivity	
3.5.3(a)	Soil Resistivity with Moisture Content	57
3.5.3(b)	Resistivity- dry density relationships	58
3.5.3(c)	Effect of degree of saturation on soil resistivity	62
3.5.3(d)	Correlation of Electrical resistivity with Porosity	63
3.5.3(e)	Effect of percentage of fine fraction on electrical resistivity at saturated and partially saturated states	64
3.5.3(f)	Resistivity vs Light Compaction	66
3.5.3(g)	Variation of Resistivity with heavy compaction	69
3.5.3(h)	Resistivity with compaction effort	73
3.5.3(i)	Soil Resistivity with Elemental Composition	73
3.5.3(j)	Correlation of permeability with resistivity	74
3.5.3(k)	Correlation of Resistivity with Shear Strength parameters	74
3.5.3(l)	Correlation of Resistivity with Unconfined Compressive Strength (UCS)	76
3.5.3(m)	Correlation of Resistivity with CBR	77
3.6	Summary	78
<b>4</b>	<b>FIELD EXPERIMENTAL INVESTIGATIONS</b>	<b>79</b>
4.1	Introduction	79
4.2	Laterites and Lateritic Soils	80
4.3	Electrical Resistivity Method	81
4.4	Vertical Electrical Soundings (VES)	82
4.5	Interpretation of the Apparent Resistivity data	83
4.6	Standard Penetration Test (SPT) and Borehole sampling	84
4.7	Results and Discussions	84

	4.7.1	Correlation of SPT (N) with Electrical Resistivity(ER)	85
	4.7.2	Correlation between field and laboratory electrical resistivity of soil samples at shallow depths	109
	4.8	Summary	111
<b>5</b>		<b>LABORATORY ELECTRICAL RESISTIVITY STUDIES ON CEMENT STABILIZED SOIL</b>	<b>113</b>
	5.1	Introduction	113
	5.2	Electrical Resistivity of Stabilised Soils	114
	5.2.1	Effect of cement content	114
	5.2.2	Effect of degree of saturation	114
	5.2.3	Effect of water content on electrical resistivity	114
	5.2.4	Effect of curing time on electrical resistivity	114
	5.3	Materials used	115
	5.4	Cement	115
	5.5	Test method	116
	5.6	Results and Discussions	116
	5.6.1	Variation of resistivity with time of curing	118
	5.6.2	Resistivity with compaction effort	126
	5.6.3	Variation of resistivity with cement content	128
	5.6.4	Resistivity with porosity	133
	5.6.5	Scanning Electron Microscope (SEM) Analysis	135
	5.6.6	Resistivity with Unconfined Compressive Strength (UCS)	140
	5.6.7	Resistivity with cohesion	143
	5.6.8	Resistivity with angle of internal friction	144
	5.6.9	Resistivity with split tensile strength	146
	5.7	Summary	148
<b>6</b>		<b>LABORATORY ELECTRICAL RESISTIVITY STUDIES ON LIME STABILIZED SOIL</b>	<b>149</b>
	6.1	Introduction	149
	6.2	Materials used	150

6.2.1	Shedi soil and River sand	150
6.2.2	Lime	150
6.3	Compaction	150
6.4	Test method	151
6.5	Results and Discussions	151
6.5.1	Variation of resistivity of soil-lime with time of curing	161
6.5.2	Variation of resistivity with lime content	161
6.5.3	Variation of resistivity with compaction effort	165
6.5.4	Variation of Resistivity with Porosity	167
6.5.5	Scanning Electron Microscope Images (SEM)	169
6.5.6	Correlation of Resistivity with UCS value	174
6.5.7	Correlation of resistivity with angle of friction	176
6.5.8	Correlation of resistivity with cohesion	177
6.5.9	Correlation of Resistivity with Split Tensile Strength	179
6.6	Summary	181
<b>7</b>	<b>STUDIES ON RESISTIVITY-MOISTURE CONTENT RELATIONSHIP</b>	<b>183</b>
7.1	Introduction	183
7.1.1	States and Limits of Consistency	183
7.1.2	Atterberg limits – Importance in soil behaviour	184
7.1.3	Resistivity-water content relationship	184
7.2	Resistivity-moisture content studies on Lateritic Soils	185
7.2.1	Test materials	185
7.2.2	Test method	186
7.2.3	Results and Discussions	187
7.3	Electrical resistivity- moisture content studies on Phosphoric acid contaminated Shedi soil and Bentonite blended Shedi soil	192
7.3.1	Is Shrinkage limit the lowest limit?	192
7.3.2	Materials used	193
7.3.2.1	Shedi Soil	193

7.3.2.2	Bentonite	194
7.3.2.3	Phosphoric Acid	194
7.3.3	Sample Preparation	195
7.3.4	Tests conducted	195
7.3.4.1	Specific gravity test	196
7.3.4.2	Atterberg Limits	196
7.3.4.3	pH	197
7.3.4.4	Compaction	197
7.3.4.5	Grain size distribution	197
7.3.4.6	Scanning Electron Microscope (SEM)	198
7.3.4.7	X-Ray Diffraction Analysis	199
7.3.5	Results and Discussions on studies on Phosphoric acid contaminated shedi soil	199
7.3.5.1	Results of X-Ray Diffraction Analysis	199
7.3.5.2	Effect of phosphoric acid contamination on basic geotechnical properties	200
7.3.5.3	SEM images of Pure and Contaminated Shedi Soil	207
7.3.5.4	Soil Resistivity with Moisture Content	210
7.3.5.5	Shrinkage limit assessment of contaminated soils by electrical resistivity measurements	211
7.3.6	Results and Discussions on Bentonite blended shedi soil	217
7.3.6.1	Basic Properties of Bentonite	217
7.3.6.2	Results of X Ray diffraction studies on bentonite	219
7.3.6.3	Effect on basic geotechnical properties of shedi soil on blending with Bentonite	220
7.3.6.4	SEM images of bentonite mixed shedi soil samples	221
7.3.6.5	Variation of Void ratio with increase in Bentonite %	223

7.3.6.6	Variation of Compaction Characteristics with increase in Bentonite %	223
7.3.6.7	Variation of Atterberg Limits with increase in Bentonite %	225
7.3.6.8	Electrical resistivity-moisture content studies on bentonite – shedu soil mix	227
7.3.6.9	Variation of dry density and OMC with Resistivity for Bentonite blended Shedi soil samples	231
7.3.6.10	Variation of Porosity with Resistivity for Bentonite blended Shedi soil	232
7.4	Summary	232
<b>8</b>	<b>SUMMARY AND CONCLUSIONS</b>	<b>235</b>
8.1	Summary and Conclusions	235
8.2	Limitations	237
8.3	Scope for Future Work	238
	<b>REFERENCES</b>	<b>239</b>
	<b>LIST OF PUBLICATIONS</b>	<b>259</b>
	<b>CURRICULUM VITAE</b>	<b>261</b>
	<b>APPENDIX</b>	<b>263</b>



## LIST OF FIGURES

<b>Figure No.</b>	<b>Title</b>	<b>Page No.</b>
2.1	Resistivity ranges for different soil and rock types.	17
2.2	Mineral structure of clay (Sivapullaiah 2015)	18
2.3	Basic Clay minerals	20
2.4	Distribution of ions adjacent to clay surface	21
2.5	Current flow in different soils (Gunn et al. 2015)	22
2.6	Relationship between the volumetric water content and the electrical resistivity for different soil types. Compiled by (Samouelian et al. 2005)	23
2.7	Electrical resistivity by Two probes measurements	27
2.8	Four probes measurements	28
2.9	Potential distribution beneath ground during electrical resistivity measurement.	30
2.10	Wenner and Schlumberger Array configuration	30
3.1	Particle Analysis curve for the six lateritic soil samples	42
3.2	Soil resistivity box	47
3.3	Measurement of conductivity using conductivity meter	47
3.4	Resistivity measurement using resistivity box	47
3.5	Calibration chart for soil resistivity box	47
3.6	Circuit diagram showing the connections for the setup	48
3.7	Soil resistivity measurement	49
3.8	Set up for electrical resistivity measurements for CBR samples.	52
3.9	Results of EDAX conducted on sample S0	54
3.10	Results of EDAX conducted on sample S1	54
3.11	Results of EDAX conducted on sample S2	55
3.12	Results of EDAX conducted on sample S3	55
3.13	Results of EDAX conducted on sample S4	56
3.14	Results of EDAX conducted on sample S5	56
3.15	Variation of moisture content with resistivity for the six soil samples	57

3.16	Comparison of the effect of moisture content and density with soil resistivity for Sample S0	59
3.17	Comparison of the effect of moisture content and density with soil resistivity for Sample-S1	59
3.18	Comparison of the effect of moisture content and density with soil resistivity for Sample-S2	60
3.19	Comparison of the effect of moisture content and density with soil resistivity for Sample-S3	60
3.20	Comparison of the effect of moisture content and density with soil resistivity for Sample-S4	61
3.21	Comparison of the effect of moisture content and density with soil resistivity for Sample-S5	61
3.22	Variation of degree of saturation on soil resistivity	62
3.23	Variation of normalized ER of saturated and partially saturated soil with porosity for all the six soil samples (A to F)	63
3.24	Relationship between $\rho_o/\rho_{sat}$ and degree of saturation	63
3.25	Variation of electrical resistivity of soil with its percentage of fine at saturated and partially saturated states	65
3.26	Variation of resistivity at different points on light compaction curve from dry to wet side for sample S0	66
3.27	Variation of resistivity at different points on light compaction curve from dry to wet side for sample S1	67
3.28	Variation of resistivity at different points on light compaction curve from dry to wet side for sample S2	67
3.29	Variation of resistivity at different points on light compaction curve from dry to wet side for sample S3	68
3.30	Variation of resistivity at different points on light compaction curve from dry to wet side for sample S4	68
3.31	Variation of resistivity at different points on light compaction curve from dry to wet side for sample S5	69
3.32	Variation of resistivity at different points on heavy compaction curve from dry to wet side for sample S0	70

3.33	Variation of resistivity at different points on heavy compaction curve from dry to wet side for sample S1	71
3.34	Variation of resistivity at different points on heavy compaction curve from dry to wet side for sample S2	71
3.35	Variation of resistivity at different points on heavy compaction curve from dry to wet side for sample S3	71
3.36	Variation of resistivity at different points on heavy compaction curve from dry to wet side for sample S4	72
3.37	Variation of resistivity at different points on heavy compaction curve from dry to wet side for sample S5	72
3.38	Comparison of variation of soil resistivity with light and heavy compaction	73
3.39	Variation of electrical resistivity with permeability	74
3.40	Variation of electrical resistivity with cohesion (at OMC and maximum dry density of soil)	75
3.41	Variation of electrical resistivity with internal friction. (at OMC and maximum dry density of soil)	75
3.42	Variation of electrical resistivity with unconfined compressive strength (at OMC and maximum dry density of soil)	76
3.43	Variation of electrical resistivity with CBR (at OMC and maximum dry density of soil)	77
4.1	Lateritic formations (Shivashankar et al. 2016)	81
4.2	Field resistivity measurement setup	83
4.3	Resistivity meter	83
4.4	Borehole and VES locations	83
4.5	Correlation between SPT and ER ( $R_2 > 0.66$ )	85
4.6	Correlation between SPT and ER ( $R_2 < 0.66$ )	85
4.7(a)	Borehole data at location NITK1	86
4.7(b)	VES curve at location NITK1	87
4.7(c)	Variation of SPT and resistivity with depth at location NITK1	87
4.8(a)	Borehole data at location NITK2	88
4.8(b)	VES curve at location NITK2	88

4.8(c)	Variation of SPT and resistivity with depth at location NITK2	89
4.9(a)	Borehole data at location NITK3	89
4.9(b)	VES curve at location NITK3	90
4.9(c)	Variation of SPT and resistivity with depth at location NITK3	90
4.10(a)	Borehole data at location NITK4	91
4.10(b)	VES curve at location NITK4	91
4.10(c)	Variation of SPT and resistivity with depth at location NITK4	92
4.11(a)	Borehole data at location NITK5	92
4.11(b)	VES curve at location NITK5	93
4.11(c)	Variation of SPT and resistivity with depth at location NITK5	93
4.12(a)	Borehole data at location NITK6	94
4.12(b)	VES curve at location NITK6	94
4.12(c)	Variation of SPT and resistivity with depth at location NITK6	95
4.13(a)	Borehole data at location NITK7	95
4.13(b)	VES curve at location NITK7	96
4.13(c)	Variation of SPT and resistivity with depth at location NITK7	96
4.14(a)	Borehole data at location NITK8	97
4.14(b)	VES curve at location NITK8	97
4.14(c)	Variation of SPT and resistivity with depth at location NITK8	98
4.15(a)	Borehole data at location NITK9	98
4.15(b)	VES curve at location NITK9	99
4.15(c)	Variation of SPT and resistivity with depth at location NITK9	99
4.16(a)	Borehole data at location NITK10	100
4.16(b)	VES curve at location NITK10	100
4.16(c)	Variation of SPT and resistivity with depth at location NITK10	101
4.17(a)	Borehole data at location NITK11	101
4.17(b)	VES curve at location NITK11	102
4.17(c)	Variation of SPT and resistivity with depth at location NITK11	102
4.18(a)	Borehole data at location NITK12	103
4.18(b)	VES curve at location NITK12	103
4.18(c)	Variation of SPT and resistivity with depth at location NITK12	104

4.19(a)	Borehole data at location NITK13	104
4.19(b)	VES curve at location NITK13	105
4.19(c)	Variation of SPT and resistivity with depth at location NITK13	105
4.20(a)	Borehole data at location NITK14	106
4.20(b)	VES curve at location NITK14	106
4.20(c)	Variation of SPT and resistivity with depth at location NITK14	114
4.21	Comparison of field and laboratory electrical resistivity	111
4.22	Correlation of field and laboratory electrical resistivity	111
5.1	Sieve Analysis results of Soil Samples	115
5.2	Resistivity measurement	116
5.3	Variation of Electrical Resistivity with time for different compaction conditions (Light) for sample A2	118
5.4	Variation of Electrical Resistivity with time for different compaction conditions (Light) for sample B2	118
5.5	Variation of Electrical Resistivity with time for different compaction conditions (Light) for sample C2	118
5.6	Variation of Electrical Resistivity with time for different compaction conditions (Light) for sample D2	119
5.7	Variation of Electrical Resistivity with time for different compaction conditions (Light) for sample A4	119
5.8	Variation of Electrical Resistivity with time for different compaction conditions (Light) for sample B4	119
5.9	Variation of Electrical Resistivity with time for different compaction conditions (Light) for sample C4	120
5.10	Variation of Electrical Resistivity with time for different compaction conditions (Light) for sample D4	120
5.11	Variation of Electrical Resistivity with time for different compaction conditions (Light) for sample A6	120
5.12	Variation of Electrical Resistivity with time for different compaction conditions (Light) for sample B6	121
5.13	Variation of Electrical Resistivity with time for different compaction conditions (Light) for sample C6	121

5.14	Variation of Electrical Resistivity with time for different compaction conditions (Light) for sample D6	121
5.15	Variation of Electrical Resistivity with time for different compaction conditions (Heavy) for sample A2	122
5.16	Variation of Electrical Resistivity with time for different compaction conditions (Heavy) for sample B2	122
5.17	Variation of Electrical Resistivity with time for different compaction conditions (Heavy) for sample C2	122
5.18	Variation of Electrical Resistivity with time for different compaction conditions (Heavy) for sample D2	123
5.19	Variation of Electrical Resistivity with time for different compaction conditions (Heavy) for sample A4	123
5.20	Variation of Electrical Resistivity with time for different compaction conditions (Heavy) for sample B4	123
5.21	Variation of Electrical Resistivity with time for different compaction conditions (Heavy) for sample C4	124
5.22	Variation of Electrical Resistivity with time for different compaction conditions (Heavy) for sample D4	124
5.23	Variation of Electrical Resistivity with time for different compaction conditions (Heavy) for sample A6	124
5.24	Variation of Electrical Resistivity with time for different compaction conditions (Heavy) for sample B6	125
5.25	Variation of Electrical Resistivity with time for different compaction conditions (Heavy) for sample C6	125
5.26	Variation of Electrical Resistivity with time for different compaction conditions (Heavy) for sample D6	125
5.27	Variation of Resistivity at dry side and wet side points on the standard proctor compaction curve at day zero	126
5.28	Variation of Resistivity at dry side and wet side points on the modified proctor compaction curve at day zero	127
5.29	Variation of Electrical Resistivity at light (LC) and heavy (HC) day zero compaction conditions at OMC and maximum dry density conditions	127

5.30	Variation of Resistivity with cement content at dry side and wet side points on the standard proctor compaction curve at freshly prepared state for sample A	129
5.31	Variation of Resistivity with cement content at dry side and wet side points on the standard proctor compaction curve at freshly prepared state for sample B	129
5.32	Variation of Resistivity with cement content at dry side and wet side points on the standard proctor compaction curve at freshly prepared state for sample C	130
5.33	Variation of Resistivity with cement content at dry side and wet side points on the standard proctor compaction curve at freshly prepared state for sample D	130
5.34	Variation of Resistivity with cement content at dry side and wet side points on the standard proctor compaction curve at after 7 days curing for sample A	131
5.35	Variation of Resistivity with cement content at dry side and wet side points on the standard proctor compaction curve at after 7 days curing for sample B	131
5.36	Variation of Resistivity with cement content at dry side and wet side points on the standard proctor compaction curve at after 7 days curing for sample C	132
5.37	Variation of Resistivity with cement content at dry side and wet side points on the standard proctor compaction curve at after 7 days curing for sample D	132
5.38	Variation of resistivity with porosity for sample A	133
5.39	Variation of resistivity with porosity for sample B	134
5.40	Variation of resistivity with porosity for sample C	134
5.41	Variation of resistivity with porosity for sample D	135
5.42	SEM image of soil cement at freshly prepared state	136
5.43	SEM image of soil cement after 1 day curing	136
5.44	SEM image of soil cement after 2 days curing	137
5.45	SEM image of soil cement after 3 days curing	137

5.46	SEM image of soil cement after 4 days curing	138
5.47	SEM image of soil cement after 5 days curing	138
5.48	SEM image of soil cement after 6 days curing	139
5.49	SEM image of soil cement after 7 days curing	139
5.50	7 day UCS vs Resistivity (at freshly prepared state)	140
5.51	7 day UCS vs Resistivity (after 1 hour curing)	141
5.52	7 day UCS vs Resistivity (after 7 days curing)	141
5.53	7 day cohesion with Resistivity (freshly prepared)	143
5.54	7 day cohesion with Resistivity (after 1 hour curing)	144
5.55	7 day cohesion with Resistivity (after 7 days curing)	144
5.56	7 day angle of internal friction with Resistivity (freshly prepared)	145
5.57	7 day angle of internal friction with Resistivity (after 1 hour curing)	145
5.58	7 day angle of internal friction with Resistivity (after 7 days curing)	146
5.59	7 day split tensile strength with resistivity (freshly prepared)	147
5.60	7 day split tensile strength with resistivity (after 1 hour curing)	147
5.61	7day split tensile strength with resistivity (after 7 days curing)	147
6.1	Grain size analysis curves	150
6.2	Variation of Electrical Resistivity with time for different compaction conditions (Light) for sample L2	153
6.3	Variation of Electrical Resistivity with time for different compaction conditions (Light) for sample M2	153
6.4	Variation of Electrical Resistivity with time for different compaction conditions (Light) for sample N2	153
6.5	Variation of Electrical Resistivity with time for different compaction conditions (Light) for sample O2	154
6.6	Variation of Electrical Resistivity with time for different compaction conditions (Light) for sample L4	154
6.7	Variation of Electrical Resistivity with time for different compaction conditions (Light) for sample M4	154



6.8	Variation of Electrical Resistivity with time for different compaction conditions (Light) for sample N4	155
6.9	Variation of Electrical Resistivity with time for different compaction conditions (Light) for sample O4	155
6.10	Variation of Electrical Resistivity with time for different compaction conditions (Light) for sample L6	155
6.11	Variation of Electrical Resistivity with time for different compaction conditions (Light) for sample M6	156
6.12	Variation of Electrical Resistivity with time for different compaction conditions (Light) for sample N6	156
6.13	Variation of Electrical Resistivity with time for different compaction conditions (Light) for sample O6	156
6.14	Variation of Electrical Resistivity with time for different compaction conditions (Heavy) for sample L2	157
6.15	Variation of Electrical Resistivity with time for different compaction conditions (Heavy) for sample M2	157
6.16	Variation of Electrical Resistivity with time for different compaction conditions (Heavy) for sample N2	157
6.17	Variation of Electrical Resistivity with time for different compaction conditions (Heavy) for sample O2	158
6.18	Variation of Electrical Resistivity with time for different compaction conditions (Heavy) for sample L4	158
6.19	Variation of Electrical Resistivity with time for different compaction conditions (Heavy) for sample M4	158
6.20	Variation of Electrical Resistivity with time for different compaction conditions (Heavy) for sample N4	159
6.21	Variation of Electrical Resistivity with time for different compaction conditions (Heavy) for sample O4	159
6.22	Variation of Electrical Resistivity with time for different compaction conditions (Heavy) for sample L6	159
6.23	Variation of Electrical Resistivity with time for different compaction conditions (Heavy) for sample M6	160

6.24	Variation of Electrical Resistivity with time for different compaction conditions (Heavy) for sample N6	160
6.25	Variation of Electrical Resistivity with time for different compaction conditions (Heavy) for sample O6	160
6.26	Variation of Resistivity with lime content at dry side and wet side points on the standard proctor compaction curve at freshly prepared state for sample L	161
6.27	Variation of Resistivity with lime content at dry side and wet side points on the standard proctor compaction curve at freshly prepared state for sample M	162
6.28	Variation of Resistivity with lime content at dry side and wet side points on the standard proctor compaction curve at freshly prepared state for sample N	162
6.29	Variation of Resistivity with lime content at dry side and wet side points on the standard proctor compaction curve at freshly prepared state for sample O	163
6.30	Variation of Resistivity with lime content at dry side and wet side points on the standard proctor compaction curve after 7 days curing for sample L	163
6.31	Variation of Resistivity with lime content at dry side and wet side points on the standard proctor compaction curve after 7 days curing for sample M	164
6.32	Variation of Resistivity with lime content at dry side and wet side points on the standard proctor compaction curve after 7 days curing for sample N	164
6.33	Variation of Resistivity with lime content at dry side and wet side points on the standard proctor compaction curve after 7 days curing for sample O	165
6.34	Variation of Resistivity at dry side and wet side points on the standard Proctor compaction curve at day zero	166
6.35	Variation of Resistivity at dry side and wet side points on the modified Proctor compaction curve at day zero	166

6.36	Variation of Electrical Resistivity at light (LC) and heavy (HC) day zero compaction conditions at OMC and maximum dry density conditions	167
6.37	Variation of resistivity with porosity for sample L	167
6.38	Variation of resistivity with porosity for sample M	168
6.39	Variation of resistivity with porosity for sample N	168
6.40	Variation of resistivity with porosity for sample O	169
6.41	SEM image of soil lime at freshly prepared state	170
6.42	SEM image of soil lime after 1 day curing	170
6.43	SEM image of soil lime after 2 days curing	171
6.44	SEM image of soil lime after 3 days curing	171
6.45	SEM image of soil lime after 4 days curing	172
6.46	SEM image of soil lime after 5 days curing	172
6.47	SEM image of soil lime after 6 days curing	173
6.48	SEM image of soil lime after 7 days curing	173
6.49	7 day UCS vs Resistivity (at freshly prepared state)	174
6.50	7 day UCS vs Resistivity (after 1 hour curing)	174
6.51	7 day UCS vs Resistivity (after 7 days curing)	175
6.52	7 day angle of friction vs Resistivity (at freshly prepared state)	176
6.53	7 day angle of friction vs Resistivity (after 1 hour curing)	177
6.54	7 day angle of friction vs Resistivity (after 7 days curing)	177
6.55	7 day cohesion vs Resistivity (at freshly prepared state)	178
6.56	7 day angle of friction vs Resistivity (after 1 hour curing)	179
6.57	7 day angle of friction vs Resistivity (after 7 days curing)	179
6.58	7 day Split Tensile Strength vs Resistivity (at freshly prepared state)	180
6.59	7 day Split Tensile Strength vs Resistivity (after 1 hour curing)	180
6.60	7 day Split Tensile Strength vs Resistivity (after 7 days curing)	181
7.1	Resistivity measurement	190
7.2	Relationship between soil moisture & ER (Voronin, 1986)	192
7.3	Resistivity-moisture content profile for soil sample S0	192
7.4	Resistivity-moisture content profile for soil sample S1	194

7.5	Resistivity-moisture content profile for soil sample S2	195
7.6	Resistivity-moisture content profile for soil sample S3	195
7.7	Resistivity-moisture content profile for soil sample S4	196
7.8	Resistivity-moisture content profile for soil sample S5	196
7.9	Comparison of Shrinkage limits of soil samples obtained from traditional shrinkage limit test and moisture content value at the tangential intersection on resistivity-water content profiles	197
7.10(a)	Cone penetration method	200
7.10(b)	Casagrande's apparatus	200
7.11(a)	Hydrometer test for contaminated soil just after mixing	202
7.11(b)	Hydrometer test for contaminated soil, one hour later	202
7.12	SEM equipment	203
7.13	X – ray diffraction pattern for shedi soil with minerals Kaolinite - $Al_2(Si_2O_5)(OH)_4$ and Saponite - $Mg_3(Si\ Al)_4O_{10}(OH)_2.4H_2O$	204
7.14	Variation of liquid limit and plasticity index with acid normality	206
7.15	Variation of specific gravity with acid normality	206
7.16	Variation of pH with acid normality	207
7.17	Combined grain size distribution curve for contaminated soils	207
7.18	Shrinkage limit and Plastic Limit v/s acid normality curve	208
7.19	Acid normality Vs dry density	209
7.20	Acid normality v/s OMC	209
7.21	Acid normality v/s Void ratio	210
7.22	Pore space in sandy soil v/s clay soil	210
7.23	SEM image of Pure Shedi soil	211
7.24	SEM image of 2.5 N acid mixed soil	212
7.25	SEM image of 5 N acid mixed soil	213
7.26	SEM image of 7.5 N acid mixed soil	213
7.27	SEM image of 10 N acid mixed soil	214
7.28	Variation of ER with moisture content for various acid normalities	215
7.29	Soil could be in a plastic state at its water content equal to shrinkage limit value and soil could be partially saturated at its plastic limit	217

7.30	Resistivity-moisture content profile for contaminated soil sample C0	217
7.31	Resistivity-moisture content profile for contaminated soil sample C1	218
7.32	Resistivity-moisture content profile for contaminated soil sample C2	218
7.33	Resistivity-moisture content profile for contaminated soil sample C3	219
7.34	Resistivity-moisture content profile for contaminated soil sample C4	219
7.35	Comparison of Shrinkage limits determined from standard shrinkage limit test and assessed from resistivity-water content profiles	220
7.36	Variation of Plastic limit and Shrinkage limit obtained from ER test data	220
7.37	Bentonite Flakes (Sample B100)	221
7.38	Grain size distribution curve for bentonite	222
7.39	X-ray diffraction pattern for Na - Bentonite with minerals Montmorillonite - $\text{Na}_{0.3}(\text{Al}, \text{Mg})_2 \text{Si}_4\text{O}_{10}(\text{OH})_2 \cdot 8\text{H}_2\text{O}$ and Quartz – $\text{SiO}_2$	223
7.40	SEM- Sample B20	225
7.41	SEM- Sample B40	225
7.42	SEM- Sample B60	226
7.43	SEM- Sample B80	226
7.44	Variation of void ratio with bentonite % in shedi soil	227
7.45	Variation of dry density with bentonite % in blended samples	228
7.46	Variation of optimum moisture content (%) with bentonite % in blended samples	228
7.47	Bentonite% in blended sample v/s lab shrinkage limit	229
7.48	Variation of Atterberg limits with percentage of bentonite in blended sample	229
7.49(a)	Pure bentonite shrinkage pats wet state	230

7.49(b)	Pure bentonite shrinkage pats after air and oven drying	230
7.50	Shrinkage pats prepared with varying % of bentonite in shedi soil (20%, 40%, 60%, 80%, and 100%)	230
7.51	Water content-ER graphs for B20	231
7.52	Water content-ER graphs for B40	232
7.53	Water content-ER graphs for B60	232
7.54	Water content-ER graphs for B80	233
7.55	Water content-ER graphs for B100	233
7.56	Correlation of Shrinkage Limit assessed from ER-m/c relationship with Shrinkage limit obtained from standard laboratory test	234
7.57	Variation of electrical resistivity (at OMC and max dry density) with bentonite percentage	234
7.58	ER v/s Dry density for bentonite mixed soil	235
7.59	ER v/s optimum moisture content for bentonite mixed soil	235
7.60	Porosity v/s electrical resistivity of bentonite mixed soil	236

## LIST OF TABLES

<b>Table No</b>	<b>Title</b>	<b>Page No.</b>
2.1	Applications of Resistivity Measurements in Groundwater Studies	9
3.1	Blended proportion of river sand with shedi soil	43
3.2	Geotechnical properties of the controlled soil samples	52
3.3	Summary of ionic composition present in shedi soil and their blends	57
4.1	Comparison of Electrical resistivity at layers giving rebound	108
4.2	Soil type for laboratory resistivity measurements	109
5.1	Compaction and strength characteristics of the soil cement samples	117
6.1	Compaction and strength characteristics of soil lime samples	152
7.1	Basic Geotechnical parameters of the soil samples	189
7.2	Index properties of shedi soil contaminated with phosphoric acid	204
7.3	Plasticity index and soil properties	208
7.4	Basic properties of bentonite used	222
7.5	Experimental results obtained from laboratory and ER tests on shedi soil blended with bentonite	224

## NOMENCLATURE

### Abbreviations

ER	Electrical Resistivity
ERT	Electrical Resistivity Tomography
UCS	Unconfined Compressive Strength
STS	Split Tensile Strength
CEC	Cation Exchange Capacity
SSA	Specific Surface Area
DDL	Diffused Double Layer
SEM	Scanning Electron Microscope
EDAX	Energy Dispersive X-ray Spectroscopy
MDD	Maximum Dry Density
OMC	Optimum Moisture Content
SBF	Soil Box Geometric Factor
CBR	California Bearing Ratio
PL	Plastic Limit
SL	Shrinkage Limit
LL	Liquid Limit
SPT	Standard Penetration Test
VES	Vertical Electrical Sounding
OPC	Ordinary Portland Cement
LC	Light Compaction
HC	Heavy Compaction

### Notations

$c$	Cohesion
$\phi$	Angle of internal friction
$\rho$	Electrical Resistivity
$\rho_{\text{sat}}$	Electrical Resistivity at saturation
$S$	Degree of Saturation



$R_0$	Resistivity of sand when all pores are filled with brine
$R_w$	Resistivity of brine
AB	Current Electrode Separation
MN	Potential Electrode Separation
F	Formation Factor
$K_h$	Horizontal Permeability
$w_{opt}$	Optimum moisture content
$e_{min}$	Minimum void ratio
n	Porosity
$\gamma_{dmax}$	Maximum dry density
G	Specific Gravity
$\rho_0$	Electrical resistivity of saturated soil
$\rho_w$	Electrical resistivity of pore fluid
$\rho_i$	Electrical resistivity of partially saturated soil
$\rho_a$	Apparent resistivity
C	Percentage of cement
l	Percentage of lime
w/c	Water content

# **CHAPTER 1**

## **INTRODUCTION**

### **1.1 General**

All matters which consists of electrons and ions are essentially electrical in nature. One of the oldest and generally accepted theories that describe the flow of electric current is that the current consists of moving electrons. This is called the electron theory. Soil has been considered as a specific electrolyte with free ions in the pore water and free electrons in the electrical double layer. This electrical nature of the soil was studied, and applied to predict various soil parameters by various researchers.

In this study, Electrical Resistivity (ER) of soils at controlled and natural field conditions are measured and correlated with various engineering properties. A comparison is made on the laboratory and field electrical resistivity for surface soil samples. The electrical response of cement and lime stabilized soils is also studied and is correlated with its geotechnical properties. The main thrust of the work is given to measurement of electrical resistivity of lateritic soil and stabilized soil at the lab and its correlation with unconfined compressive strength. An attempt has been made to study the electrical behaviour of acid contaminated lithomargic soils which shows an anomalous behaviour, in the plasticity states. Studies conducted on electrical and index properties of lithomargic soil blended with various percentages of bentonite are also discussed.

### **1.2 Scope of the study**

The use of ERT methods have been increasing in the field of Geotechnical Engineering. It is a desirable method to study the heterogeneity of soil and the spatial and temporal variation of soil moisture. The correlation of various geotechnical properties with electrical resistivity will be very effective in subsurface investigation and will close the gap that presently exists between geophysical and geotechnical engineering. A geotechnical engineer can utilize the interpretations from the geophysical data for his design works. Being a rapid, less expensive and handy method it saves a lot of labour, time and cost. Proper understanding of the relationships between

the physical factors influencing the engineering and measurable electrical properties of soil provides a methodology by which the engineering behaviour of soils can be predicted non-intrusively.

Previous researches have largely focused on correlations of strength parameters with the electrical resistivity of hardened concrete and soil-cement/lime rather than the fresh uncured mixes. It is found from the literature that there exists very good correlation between the strength parameters and the electrical resistivity of the cured soil-cement/lime samples. The correlations between strength parameters and electrical resistivity for the uncured freshly prepared soil-cement/lime mixes may offer the option of the soil-cement/lime mix to be upgraded (possibly with additional cement or lime) in its fresh state itself, if it does not fulfil the performance criteria, rather than wasting the material after hardening. Hence there is need for research in this regard.

### **1.3 Objectives**

The current study is aimed to

- Conduct electrical resistivity studies on controlled soil samples in laboratory and its correlation with the geotechnical parameters of soils, both index parameters and strength parameters.
- Conduct electrical resistivity studies in field (by conducting Vertical Electrical Soundings), and to correlate resistivity values with the Standard Penetration Test (SPT) blow counts obtained at the same locations and same depth.
- To compare the laboratory electrical resistivity and field electrical resistivity for surface samples.
- Conduct Electrical resistivity studies on controlled soil-cement and soil-lime samples in laboratory and its correlation with the geotechnical parameters.
- To study in detail the electrical resistivity-moisture content relationship for laboratory controlled soil samples and contaminated soil samples.

### **1.4 Organisation of the Thesis**

The scope, objectives, methodology of the research work and organisation of the presentation of the thesis have been described in **Chapter 1**.

In **Chapter 2**, a review of literature regarding the application of electrical resistivity measurements in several civil engineering problems is presented. The thrust is given to discussing the application of electrical resistivity methods in quantification of geotechnical properties. The conventional methods for determination of engineering properties are incursive, expensive and time-consuming. In this context, electrical resistivity measurements serve as an ancillary tool. In this Chapter the fundamental theory behind electrical resistivity and the factors influencing it are explained. Review of literature concerning field and laboratory applications of electrical resistivity techniques have been discussed. Reliable correlations between electrical resistivity and other soil properties will enable us to characterize the subsurface soil without borehole sampling. Recent studies have proved electrical resistivity technique to be a reasonably good method for evaluating swell-shrinkage properties of expansive soil and for measuring the development of surface cracks in soils. Soil characterization by integrating geo- electrical data and geotechnical data is a promising field of research. Several recent applications of electrical resistivity method in concrete technology have also been discussed.

**Chapter 3** discusses the electrical resistivity studies on controlled soil samples in laboratory and its correlation with the geotechnical soil parameters. Six soil samples were prepared by varying their percentage of sand. Factors affecting soil electrical resistivity such as moisture content, dry density, degree of compaction, percentage of fines, presence of ions etc. are studied. Also, ER is correlated with strength properties, such as compressive strength, shear strength parameters and California Bearing Ratio and is discussed in this Chapter.

**Chapter 4** discusses the electrical resistivity studies carried out on natural ground. Standard Penetration tests (SPT) were conducted at 14 locations in NITK campus. Vertical Electrical Resistivity Soundings were also conducted at the same 14 locations. Electrical resistivity at different layers below the surface is interpreted using IGIS inverse slope software. At all 14 locations, SPT numbers at 1.5m depth intervals are correlated with the electrical resistivities at the same depths. The results of this study propose that by properly handling the uncertainties and ubiquitous resistivity measurement errors, Electrical Resistivity tomography can be applied as a pre-

investigation method on sites, antedating to direct testing methods like Standard Penetration Test to reduce labour, cost and time involved. Comparison between electrical resistivity measured in laboratory and in field is also discussed in this Chapter. It was observed that the lab resistivity is generally higher than the field resistivity and generally correlate quite very well with surface measurements.

Researchers have used electrical resistivity of cement paste to predict its 28 day compressive strength. In this study an attempt has been made to study the use of electrical resistivity test as a potential method to predict the 7 day strength properties of cement and lime stabilized soils at the fresh state itself. So that the mix could be upgraded (possibly by mixing with additional cement) at the fresh state itself. This would help in avoiding the wastage of material if it does not meet the strength and performance criteria, after hardening. Twelve samples each, of soil-cement and soil-lime mixes were prepared, by varying the percentage of sand and mixing each with 2%, 4% and 6% cement or lime. The quantitative correlations developed with electrical resistivity and strength properties such as Unconfined Compressive Strength (UCS), cohesion ( $c$ ) and angle of friction ( $\phi$ ) and the influence of various factors like cement content, compaction conditions, degree of compaction and time of curing on electrical resistivity of soil-cement and soil-lime is studied and discussed in **Chapter 5** and **Chapter 6** respectively.

As per our present general understanding, the soil at all the three limits is fully saturated. At liquid state, as the water content in soil is being reduced, the soil begins to show some measurable shearing resistance. Plastic Limit is defined as that water content at which a pat of soil can be rolled into threads of 3mm diameter without crack on the surface. It should break up into segments about 3mm to 10mm (Holtz et al. 2015). At Shrinkage Limit, the soil is just fully saturated. Any further reduction in water content will not cause a reduction in volume of soil mass and will make the soil partially saturated. But, from literature, it is understood that, some soils like lithomargic clays, when contaminated with phosphoric acid, shows an anomalous behaviour. For such contaminated soils, plastic limit is attained at the partially saturated state, due to chemical and structural change in the soil fabric. Researchers have used electrical resistivity method to study the micro structural characteristics and change in structural

behaviour of clayey soils. Though already some researchers have utilized resistivity measurements to predict the geotechnical parameters, perhaps nobody or very few have contemplated the relationship between electrical resistivity of soils and moisture content in estimating shrinkage limit of soils from electrical resistivity-moisture content relationship. **Chapter 7** discusses the electrical resistivity studies on Atterberg limits of the soil. A graphical method developed which estimates the shrinkage limit (point where the soil is just saturated) of the soils, very quickly and accurately is discussed in this Chapter. The study shows that electrical resistivity measurements (ER-moisture content profile) of a well compacted soil can be a useful tool for assessing shrinkage limit of soils. A very good agreement was obtained between Shrinkage limit assessed from standard Shrinkage Limit test and resistivity-water content profile. The assessment is confirmed by testing with the phosphoric contaminated soils and bentonite mixed soils too, where in the Atterberg limits got altered.

The major conclusions of the investigations are summarised in **Chapter 8** of this thesis.



## **CHAPTER 2**

### **LITERATURE REVIEW**

#### **2.1 General**

The need for an improved ability to “see into the earth” has resulted in the use of geophysical techniques, especially the electrical resistivity method, in engineering, geological and environmental investigations (Owusu-Nimo, 2011). The application of electrical resistivity measurements has expanded a great deal in the last decade to various fields of civil engineering. Apart from its applications in mineral exploration, oil and gas exploration, studying aquifer properties, depth to bedrock, etc., it also finds its role in geotechnical, concrete engineering, environmental engineering, transportation engineering etc.

The electrical measurements have been used by geologists for over 200 years because of the wide range of resistivity values in nature. This chapter deals with several studies carried out using electrical resistivity techniques. A review of literature regarding the application of electrical resistivity measurements in several civil engineering problems is presented. The thrust is given to discussing the application of electrical resistivity methods in quantification of geotechnical properties. The conventional methods for determination of engineering properties are incursive, expensive, time-consuming and limited. In this context, electrical resistivity measurements serve as an ancillary tool so that time, labour and cost needed can be reduced.

#### **2.2 Electrical Resistivity and Conductivity**

All matters which consists of electrons and ions are essentially electrical in nature. One of the oldest and generally accepted theories that describe the flow of electric current is that the current consists of moving electrons. This is called the electron theory (Partridge, 1908). Electrical resistivity (otherwise called as resistivity, specific electrical resistance, or volume resistivity) is an intrinsic property that quantifies a material’s ability to resist the flow of electric current. The resistivity of a material is a measure of how well the material retards the flow of



electrical current. Resistivities vary tremendously from one material to another (Herman, 2001). Soil can be considered as a rather specific "electrolyte" having ions in free soil solution and in the electrical double layer. Compared with ions in free solution these ions have different mobilities and other properties (Pozdnyakova, 1999). Electric current flows in earth materials at shallow depths through two main methods. They are electronic conduction and electrolytic conduction. In electronic conduction, the current flow is via free electrons, such as in metals. In electrolytic conduction, the current flow is via the movement of ions in groundwater (Loke, 2004).

Soil electrical properties are the parameters of natural and artificially created electrical fields in soils and influenced by distribution of mobile electrical charges, mostly inorganic ions, in soils (Bery and Saad, 2012). It is an important factor in design of grounding systems in an electrical substation, or for lightning conductors. It can also be a useful measure in agriculture as an intermediary estimation for moisture content. Electrical conductivity or specific conductance is the reciprocal of electrical resistivity which measures how easily the material allow the flow of current.

The working principle of the electrical resistivity method is based on the conductivity of the soil. The presence of moisture is important for the conduction phenomenon of soil and also, it changes its consistency and strength. Conductivity and resistivity also depend on the mineralogy of soil, particle size distribution, index properties, unit weight, porosity, degree of saturation, compaction, shape and orientation, cation exchange capacity, ion composition, ionic strength of soil solution and other parameters. Right understanding of the causes of variance of these parameters with resistivity can be helpful for development of correlations. The measured resistivity values depend on a number of interrelated factors. It is difficult to separate the influence of each individual parameter (Michael, 2012).

### **2.3 Applications of Resistivity Measurements in Groundwater Studies**

In the predominantly crystalline rock terrains of south India, groundwater occurs in two distinct zones, namely the near-surface weathered and decomposed rock material (regolith) and the joints and fractures that may extend to a few hundred metres depth in the underlying bed rock. Shear zones are often found to contain substantial amounts of groundwater, as such zones are generally highly fractured and jointed, a condition

conductive for storage and movement of ground water. The success of a borewell under these conditions depends on the presence of such deep water-bearing zones, and therefore, it is essential that they be identified to successfully locate sites for constructing water wells. Weathering renders such zones electrically more conductive in comparison to the country rock, and hence it is an easy target for exploration through geo-electric techniques (Ballukraya, 1996). Some of the groundwater studies conducted by researchers using electrical resistivity measurements are listed (Table 2.1).

Table 2.1 Applications of Resistivity Measurements in Groundwater Studies

<b>Research</b>	<b>Researchers</b>
For locating zones of groundwater inflow and for estimation of its rate of filtration	Rao et al. (1977), Bose and Ramakrishna (1977), Sabet (1975). Verma et al. (1980), Kelly (1985) Srinivasan et al. (2013), and Gagliano et al. (2010).
For prediction of yield of wells in granite	Patangay et al. (1977), Bhowmick and Baweja (1977), Rao (2002) and Parikh et al. (1990)
For predicting aquifer properties	Kosinsky and Kelly (1981), Kelly (1978) and Arora and Ahmed (2010)
For demarcation of zones of corrosive groundwater  To identify the approximate boundaries of contaminant plumes (hydrocarbons) in groundwater.	Sharma and Jayashree (1998)  Hamzah et al. (2008)
Delineating geohydrology of basin	Sarma (1977)
To determine the depth of the base of water table aquifer	Nolan et al. (1998)

## **2.4 Specific Applications of Resistivity Measurements in Concrete Engineering.**

Electrical measurements have found a remarkable place in concrete technology too. Studies demonstrate that electrical resistivity measurements can be applied for predicting compressive strength of Portland cement paste (Wei et al. 2010). Recently it has been investigated that there exists a linear relation between chemical shrinkage and electrical resistivity of cement pastes. Electrical resistivity was measured by a non-contacting electrical resistivity apparatus (Liao and Wei, 2014). Transformer principle was followed in this apparatus. Wang et al. (2014) proved that electrical resistivity measurements are capable to assess Freezing-Thawing damage of cement pastes. Chung and Jingyao (2004) studied the microstructural effect of shrinkage of cement based materials during hydration, using electrical resistivity measurements. They also investigated that microstructural change induced in cement by shrinkage during hydration is diminished by addition of silica fume and is increased by addition of sand. Setting time for Portland cement paste is determined by using electrical resistivity measurements (Wei and Li, 2006). Different hydration periods were identified from the electrical resistivity curve and differential electrical resistivity curve of Portland cement paste. Quantitative relationships between the setting time of concrete and electrical resistivity was developed (Li et al. 2007). The equations developed by them can be applied to estimate the setting time of concrete as an alternative method. Also, study has proved that electrical resistivity methods can be used for determining the water content ratio in fresh and hardened pastes.

## **2.5 Electrical Resistivity Applications in Soil Mechanics**

The knowledge of soil electrical resistivity has been used to predict various soil parameters, phenomenon and mechanisms occurring in soils, such as for obtaining the soil water content (Samouelian et al. 2005), (Toll et al. 2013), (Bhatt and Jain, 2014), (Gunn et al. 2015), (Asif et al, 2016), and (Castelblanco et al. 2012), degree of compaction (Seladji et al. 2010), (Kibria, 2011) and saturation (Abu-Hassanein, 1996, Sreedeeep et al. 2004), investigating the effects of soil freezing (Seo, 2013), for estimating the soil salinity (Kishore and Bhagat, 2006) and for agricultural activities for describing the details of micro structural characteristics of soils (Fukue et al. 1999)

and (Michot et al. 2010), for monitoring sediment consolidation (Jia et al. 2013) for assessing the coefficient of the earth pressure at rest (Tong et al. 2013). Siddiqui et al. (2012) obtained significant quantitative and qualitative correlations between resistivity and moisture content and angle of internal friction and weaker correlations with the cohesion and unit weight of soil.

Abidin et al., (2014) showed that the electrical resistivity value was greatly influenced by the geotechnical properties, and thus the resistivity surveying technique is applicable to support and enhance the conventional stand-alone anomaly outcome that is traditionally used in ground investigation interpretation. Results of the studies from both the laboratory controlled samples and actual field samples from Petronas, Malaysia by Osman and Siddiqui (2014) shows consistency in the correlation between friction angle and electrical resistivity, while correlations between moisture content and electrical resistivity shows a similar trend of decreasing moisture content with increase of electrical resistivity value. The empirical relationships of electrical resistivity developed by Akinlabi and Adeyemi, (2014) with bulk density, plasticity index, cohesion and coefficient of compressibility gave correlation coefficients of 0.59, -0.92, -0.98 and -0.77 respectively. Piegari and Di Maio (2013) related soil suction to electrical resistivity, which provided a further example of the high potential of geophysical methods in contributing to more effective monitoring of soil stress conditions, which is important in areas where rainfall induced landslides occur periodically. Vita et al. (2006) demonstrated, the better suitability of geoelectrical methods in characterizing and differentiating pyroclastic series, which are spatially variable along the slopes.

Kahraman and Yeken (2010) used electrical resistivity measurement to predict uniaxial compressive and tensile strength of igneous rocks. Benefits of application of new combined geophysical and geotechnical techniques is relevant for assessing the condition of the subgrade, and thus, the potential performance of the embankment infrastructure under future projected traffic loads and schedules (Gunn et al. 2007). Adebisi et al. (2016) used VES (Vertical Electrical Soundings) along with geotechnical tests to assess the stable and unstable locations of the Ago-Iwoye/Ishara highway, Southwestern Nigeria. Piegari et al. (2012) proposed, a semi-empirical approach based

on the use of geophysical methods and the employment of a geophysical Factor of Safety in terms of local resistivities and slope angles. The study shows a comparison between the values of the geophysical and geotechnical Factor of Safety (FOS) with advantages and disadvantages of the proposed approach. Qazi et al. (2016) developed a conceptual model for the assessment of slope stability and FOS using electrical resistivity values of the insitu soil at controlled moisture content (30%). The studies by Piegari et al. (2014) suggested possible critical rates of resistivity changes for triggering instability in the investigated area and pointed out the crucial role of resistivity variations in prediction of larger rainfall induced landslide events. Bery (2016) studied the application of the time-lapse electrical resistivity tomography (4-D) method using an optimized Wenner-Schlumberger array, coupled with appropriate inversion constraint parameters, and has successfully produced good correlations between electrical resistivity values and soil mechanics properties during the slope monitoring period.

The usage of resistivity methods is also very straightforward for the air-filled underground voids, which should have theoretically infinite resistivity in the ERT image (Putiska et al. 2012). Hen-Jones et al. (2017) proposed a new system based on integrated geophysical–geotechnical sensors to monitor groundwater conditions via electrical resistivity tomography.

### **2.5.1 Electrical resistivity tomography for characterizing cracks in soils.**

Hassan and Toll (2013) investigated the potential of ERT method for characterizing cracking of soils. As the crack is filled with air that is infinitely resistant, model blocks containing a crack were simulated by setting their resistivity to 10000  $\Omega$ .m. Different cracks scenarios (e.g. vertical, oblique, hexagonal, and multi cracks) in dry and wet soil have been tested. Sentenac et al. (2009) described a miniaturised electrical imaging (resistivity tomography) technique to map the cracking pattern of a clay model. Samouelian et al. (2003) performed electrical resistivity measurements at high resolution (1.5-cm electrode spacing) to detect, from the soil surface, small cracks developing within the soil. The process of crack propagation in expansive soils due to moisture change was investigated by Jun-hua et al. (2012). Resistivity measurements

may be useful for identifying desiccation cracking or poor interlift bonding in compacted clay liners (Kalinski and Kelly, 1994).

### **2.5.2 Electrical resistivity measurements for evaluation of swell-shrinkage properties of expansive soils.**

The axial swell, axial shrinkage and swelling pressure of the compacted expansive soils are found to have a good relationship with the electrical resistivity of the soils, indicating that the electrical resistivity method can be used as a reasonable method to evaluate the swell-shrinkage properties of expansive soils. (Zha et al. 2006). Zha (2007) performed swelling tests on the undisturbed expansive soil samples with a modified oedometer consolidation cell. The experimental results showed the effectiveness of electrical resistivity method in quantitative study on the microstructure change of expansive soils during swelling.

### **2.5.3 Electrical resistivity measurements for quantifying soil hydraulic parameters**

Cosentini (2012) used electrical resistivity tomography (ERT) to monitor local water content changes during transient wetting processes in sand and silt laboratory samples. Sreedeeep (2005) proposed a methodology to determine unsaturated soil hydraulic conductivity of a fine-grained soil by knowing the electrical resistivities corresponding to different compaction states.

### **2.5.4 Correlations of Electrical Resistivity with Strength Properties by previous researchers**

Kahraman and Yeken (2010) performed UCS, tensile strength, electrical resistivity, density, and porosity measurements on twelve igneous rocks. The results were evaluated using simple and multiple regression analysis. UCS and tensile strength values were linearly correlated with electrical resistivity. Compared to the simple regression, multiple regression analysis produced regression models having high correlation coefficients. The highest correlation coefficients were obtained when resistivity, density and porosity values were included in the models. The cohesion of clayey sand soils can influence the resistivity values of tropical clayey sandy soils. Bery

and Saad (2012) performed laboratory tests to determine 32 clayey sand soil's engineering characterization. The empirical correlations between electrical parameter, percentage of liquid limit, plastic limit, plasticity index, moisture content, internal friction angle and effective soil cohesion were obtained via curvilinear models. The results showed that internal friction angle is inversely proportional to the resistivity of samples and effective cohesion is directly proportional to the resistivity. Regression coefficient,  $R^2$  was approximately 0.647 for internal friction angle and for effective cohesion it was 0.664. Liquid limit, plastic limit, plasticity index showed inverse relation with resistivity with regression coefficient 0.645, 0.433, 0.475 respectively. Osman et al. (2016) correlated angle of friction and cohesion with electrical resistivity for sandy clay loam soil.

### **2.5.5 Electrical Resistivity Measurements and SPT**

The standard penetration test (SPT) is very widely used for subsurface investigation in many parts of the world. It measures the resistance of a hollow core being hammered with a 63.5kg weight. Field test such as SPT does not depend on undisturbed samples because it is carried out on original field soil (Mahmoud, 2013).

An attempt has been made by Syed and Siddiqui (2014), Gautam and Sastry (2013) and Osman et al. (2016) to predict SPT profile using correlation of geoelectric and point geotechnical data (SPT). Abidin et al. (2012) used geoelectrical survey and geotechnical SPT to investigate the stability of a slope together with the influence of heterogeneous geomaterials in wet tropical region. The analysis shows that the zone with high resistivity value generally has a high  $N$  value, which stand for high stiffness and vice versa. However, some zones with low resistivity value are not accompanied by a decrease of its  $N$  value and sometimes even showing a higher  $N$  value. A low resistivity zone may be weak status due to a result of water conductivity or/and heterogeneous geomaterials condition. It may be erroneous to say that the low resistivity value always means the unstable or troubled status of material to shield against seepage if the core zone shows the proper range of resistivity value considering the retained water in the fine particles. In the region where fine particles are deficient

due to the piping condition or other causes, the resistivity value may increase because the clay component, which is the factor for decreasing the resistivity value, would flow out, accompanied by a decrease of the N value. (Seokhoon et al. 2008). Sudha et al. (2009) integrated SPT, DCPT and grain size analysis data with the ERT results of two different soil types at Aligarh and Jhansi site, in Uttar Pradesh, India. Oh and Sun (2008) interpreted the results of resistivity survey and borehole test to infer the condition of the core material of an earth dam against the piping or leakage condition and to understand the relation between the two properties.

Standard penetration test (SPT) is a widely used method of sub-surface soil investigation for foundation design or other engineering applications. Another common source of interpretive error in the SPT procedure is when the sampler encounters rocks slightly larger than the sample barrel's sleeve diameter, very high blow counts can be recorded, and these horizons can easily be misinterpreted to be "bedrock" or "drilling refusal" when, in fact, the object may be a "floater" within the colluviums. A less recognized problem is the influence of strata thickness and changes in stiffness. As the sample barrel approaches an appreciably stiffer horizon, the penetration resistance will increase, even though the sampled material remains more or less constant throughout the softer horizon. This can lead to overestimates of strength, density, and compressibility based solely on blow-count values (Rogers, 2006).

ERT measurements work well in both resistive sediments, such as gravels and sands, as well as conductive sediments like silt and clay (Smith and Sjogren, 2006). Kabir et al. (2011) used electrical resistivity imaging tools to differentiate silty clay and sandy clay soils in Madhupur tract, Bangladesh. Giao et al. (2003) used Electric imaging and laboratory resistivity testing for geotechnical investigation of Pusan clay deposits. Cosenza et al. (2006) based on the geoelectrical model proposed by them and with the comparison of geotechnical data, confirms that ERT is a relevant method to determine clay cover in a subsurface context.

#### **2.5.6 Cone penetration and vane shear test with ER measurements**

Cosenza et al. (2006) tried to establish qualitative and quantitative correlations between electrical and geotechnical data. In situ vane shear test and dynamic cone



penetration test were performed. In order to compare electrical properties and the data provided by the geotechnical tests, two geophysical methods were used: Electrical Resistivity Tomography (ERT) and Ground Penetrating Radar (GPR) profiling technique. Both methods suggested a three-layer model in which a fine soil with a significant clay fraction was sandwiched between an unsaturated sandy soil with gravels and the top of oolitic limestones. The study confirmed that ERT is a relevant method to determine clay cover in a subsurface context. Moreover, despite of the low number of data, a satisfactory quantitative correlation between inverted resistivity values and water content values had been obtained. This result demonstrates once more that resistivity is a good indirect predictor of water content.

## **2.6 Factors Affecting Soil Resistivity**

### **2.6.1 Effects of Soil Type**

Bhat et al. (2007) reported that the dielectric constant of a material is dependent on its type (i.e., fine-grained or coarse-grained and mineralogy), volumetric moisture content and the frequency of ac used for its measurement. The flow of electricity through soils comprises of three paths: a) flow through the pore fluid and conducting soil particles in series, b) flow through soil particles in contact with each other, and c) flow through the pore fluid. Thus, the total electrical flow is defined by soil type, soil structure (i.e. related to the tortuosity of the flow paths), and degree of saturation and pore fluid characteristics (Drnevich et al. 2008). In coarse granular soils, electrical resistivity is affected by the soil porosity/tortuosity and also by the nature of the pore fluid. Soil structure can influence electrical flow because the arrangement of the pores can provide different paths for the current. In fine grained soils, however, it depends also on the minerals present because electrical current may flow through the charged surfaces of the clay minerals (Gingine, 2016). For fine sands, the matrix solids resistivity is the result of electron conductance through the grain-to-grain contacts of contiguous sand grains of the media. Electrical conduction in clean sands and gravels occurs almost exclusively in the pore fluid, because quartz sand is virtually a non-conducting material and matrix solids resistivity is considered infinitely large. In clays and clay-rich soils, electrical conduction occurs in the pores and on the surfaces of electrically charged clay minerals. For these soils, surface conductance can be a

significant factor affecting the bulk electrical resistivity of the soil (Bryson, 2005). The study of the soil electric properties for different layers of soil is needed to obtain reliable information on the soil characteristics (Islam et al. 2012). The range of resistivities for various rocks and soils are shown in Fig 2.1. There is considerable overlap between different rock and soil types.

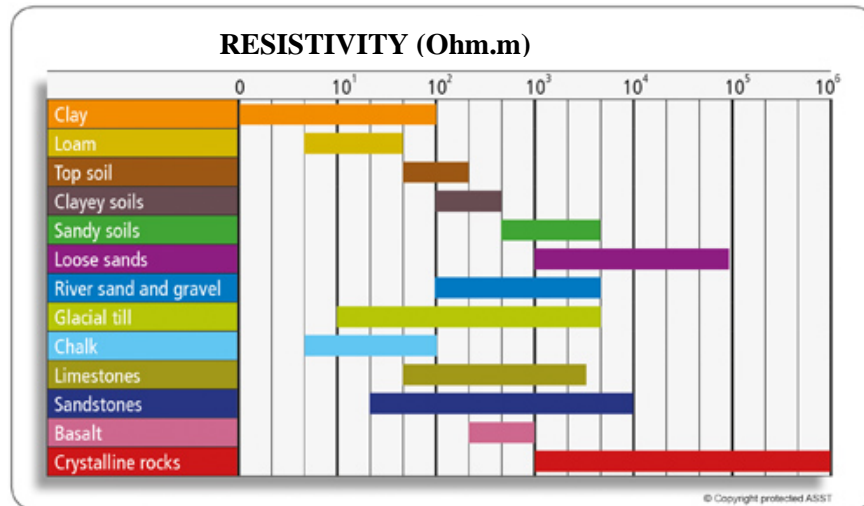


Figure 2.1 Resistivity ranges for different soil and rock types  
(source:asstgroup.com)

The surface electrical conductivity is a major parameter describing structure of electrical double layer and its ion composition. Only limited research has been carried out with experimental measurements of surface electrical conductivity in soils (Ozcep et al. 2010). Electrical resistivity permits the delineation of the main soil types and when performed repeatedly over time, also provides information on soil functioning. The information collected is usually very useful for agronomists, soil scientists, waste management, civil and environmental engineers (Samouelian, 2005).

### 2.6.1(a) Basic Structure of Clay

Kibria and Hossain (2016) studied that activity, cation exchange capacity and mineralogical factors significantly affect the resistivity. Therefore, a proper understanding of the dominant mineral of clay materials is important to interpret resistivity results. The behaviour of fine grained soils depends to a large extent on the type of minerals present. These minerals impart cohesion and plasticity to clay. For

clays, the gravitational forces are insignificant compared to surface forces. Clay mineralogy, cation exchange capacity (CEC), specific surface area (SSA), and clay fraction are the dominant factors in controlling the behavior of fine-grained soils.



Figure 2.2 Mineral structure of clay (Sivapullaiah 2015)

Clays have the greatest surface area of any of the mineral constituents of soil, but it varies within different types of clay minerals. For example, swelling clays such as montmorillonite have specific surface areas up to  $810 \text{ m}^2/\text{g}$  whereas for nonexpanding soils like kaolinite surface area ranges from  $10$  to  $40 \text{ m}^2/\text{g}$ . Clay mineral platelets carry a residual negative charge and attract cations present in the pore water to form a cloud around the particle, which is termed as the double layer. The net negative charge may be due to the following reasons:

- Isomorphous substitution of one atom by another atom of low valency
- $\text{OH}^-$  ions dissociated into hydrogen ions
- Adsorption of anions on clay surface
- Absence of cations on the crystal lattice
- Presence of organic matter

Magnitude of negative charge is more on small particles having larger surface area. Clay particles have a tendency to change the cation adsorbed on the surface, which is known as base – exchange capacity or cation – exchange capacity (CEC). Higher resistivity clays, such as kaolinite have a low CEC ( $4 \text{ meq per } 100\text{gm}$ ), lower resistivity clays, such as chlorite and illite have a medium CEC ( $40 \text{ meq per } 100\text{gm}$ ), and the lowest resistivity clays like smectite have a high CEC ( $70 - 100 \text{ meq per } 100 \text{ gm}$ ) (Gunn, 2015).

Adjacent clay particles attract each other by short-range Van der Waals forces. As the distance between the particles increases, this attraction decreases rapidly. On the other hand, repulsion occurs between the like charges of the double layers. If attractive Van der Waals forces dominate over the repulsive forces between cations, then the particles will orientate themselves with edge-to-face orientation (positive to negative). This is termed flocculation and the soil is said to exhibit a flocculent structure as shown in Fig. 2.2. On the other hand, if there is a high concentration of cations, (in the marine environment) adsorbed layers are thin and the clay minerals tend to settle out of suspension with this structure. This is in contrast to lacustrine clays deposited in a freshwater environment which settles in a face-to-face orientation because of a net repulsion. This is termed a dispersed structure (Fig. 2.2). Natural clays invariably contain a mixture of various types of clay minerals and larger particles of more inert minerals such as quartz, leading to very complex structural arrangements. (Sivapullaiah, 2015).

At the molecular level, clay is composed of alternating layers of silica, alumina, and water. The silica molecule has a tetrahedral shape, a triangle-based pyramid, with a silicon atom in the center and four oxygen atoms, one at each corner. Kaolinite clay mineral is the weathering product of feldspar. Kaolinite molecules are bonded together strongly within the sheet, but they are only weakly bonded to the sheets above and below as shown in Fig. 2.3. This enables them to slide easily over each other. However, because of the strong bonds within the sheet, the kaolinite particles are relatively large and the plasticity of pure kaolinite is low. Kaolinite is the main constituent of china clay, ball clays, and fireclays.

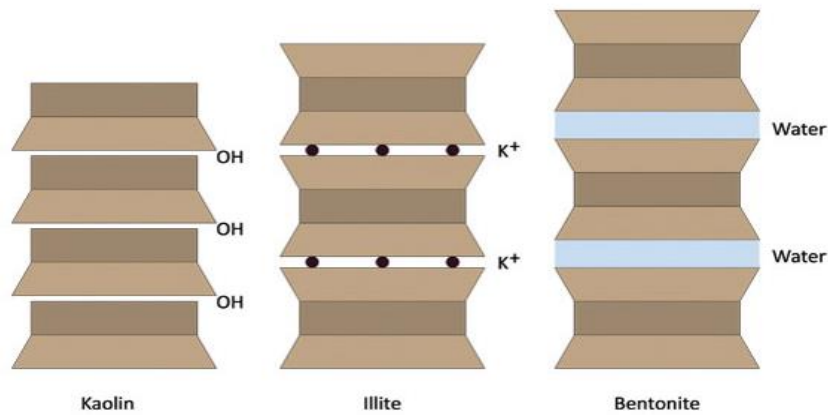


Figure 2.3 Basic Clay minerals

Montmorillonite (bentonite), has three repeating layers, but with water in between. The formula for bentonite is  $\text{Al}_2\text{O}_3 \cdot 4\text{SiO}_2 \cdot 2\text{H}_2\text{O}$ , which has twice as much silica as kaolinite, as there are two layers of silica for every layer of alumina. Because the three-layer sheets are only weakly bonded together, with oxygen atoms at the top and bottom, additional water can easily get in between (Fig. 2.3). Some of the silicon atoms in bentonite are replaced by Aluminium, and these, in turn, can be exchanged for magnesium and iron, which create an overall negative charge. Positively charged sodium or calcium ions are therefore attracted to balance the charge. Sodium bentonite can absorb a large amount of water, which causes it to expand greatly when added to water. It is used in small amounts to increase plasticity in clay bodies, however, as some of the Aluminium atoms are substituted by iron or magnesium, bentonite usually has more impurities than kaolinite.

Illite (like mica) has three repeating layers: silica, alumina, then an inverted layer of silica, with potassium ions bonding together each group of three layers (Fig. 2.3). At the top and bottom of each group is a layer of oxygen atoms, into which the potassium ions,  $\text{K}^+$  fits. The layers in illite are therefore bonded together more strongly than in kaolinite, which only has weak hydroxyl bonds between its layers. The potassium ions are attracted by an overall charge deficiency caused by substitution of some of the silicon atoms for Aluminium and some of the Aluminium atoms for magnesium or iron. Illite clays often contain a large amount of iron oxide and are used by potters as red.

### 2.6.1(b) Clay Water Interaction

Diffused double layer (DDL) is the result of clay-water-electrolyte interaction. Because of the net negative charge on the surface, the clay particles attract cations, such as potassium, calcium and sodium from surrounding soil moisture to attain an electrically balanced state. These adsorbed cations, in turn, attract particles with negative charges and dipolar water molecules. The adsorbed cations would try to diffuse away from the clay surface and tries to equalize the concentration throughout pore water. The diffusion tendency of adsorbed cations and electrostatic attraction together would result in cation distribution adjacent to each clay particle in suspension. The net force of attraction decreases exponentially with an increase in distance from the clay surface. Thus, close to the surface there is a high concentration of ions which decreases outwards.

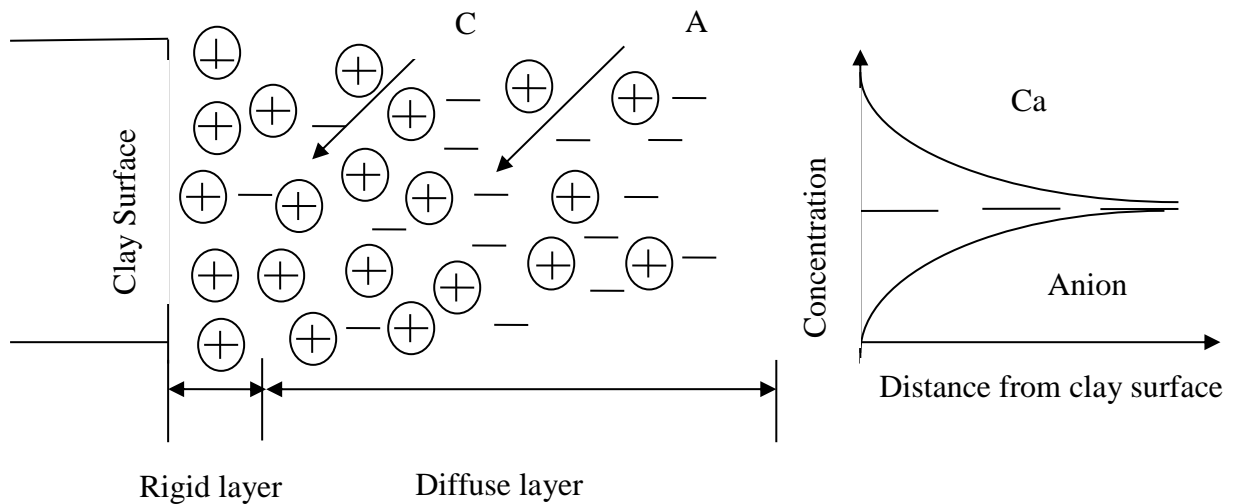


Figure 2.4 Distribution of ions adjacent to clay surface

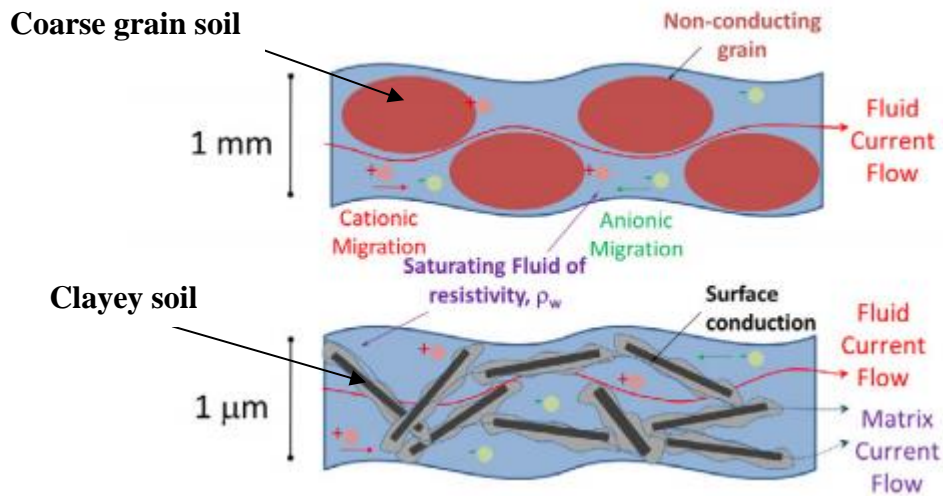


Figure 2.5 Current flow in different soils (Gunn et al. 2015)

Figure 2.4 presents such a distribution of ions adjacent to a single clay particle. The layer extending from clay surface to the limit of attraction is termed as diffused double layer (DDL). The water held in DDL is known as adsorbed water (oriented water). Outside the DDL, the water molecules are non-oriented. Monovalent cations such as  $\text{Na}^+$  leads to a thicker layer, compared to that by divalent cations, such as  $\text{Ca}^{2+}$ . In sands and gravels, the current flows around non-conducting grains via ionic migration within the saturating fluid (Fig.2.5).

### 2.6.2 Effect of temperature

Electrical resistivity surveys may be useful for analysing the structure and behaviour of soils during freezing- thawing cycles (Seo, 2013). The electrical conductivity increases when the temperature increases. On the contrary, the electrical resistivity decreases when the temperature decreases. Robertson and Macdonald (1962) studied the relation between resistivity and ground temperature at different depths. The results of the study showed that the best fit was obtained at a depth of 0.61m and the best relation between resistivity ( $\rho$ ) and ground temperature ( $t$ ) is given by  $\rho=395e^{-0.182t}$ . An increase in the temperature of the soil sample results in an increase in the mobility of the ions in the pore solution and a decrease in measured resistivity (Spragg et al.

2013). Mostafa et al. (2003) studied the temperature dependence of the electrical resistivity of basalt and granite samples.

### 2.6.3 Effect of water content

Prior to field surveys, preliminary calibration of the volumetric water content related to the electrical resistivity is usually performed in the laboratory. Fig. 2.6 shows examples of laboratory calibration between the electrical resistivity and the volumetric water content (Samouelian et al. 2005).

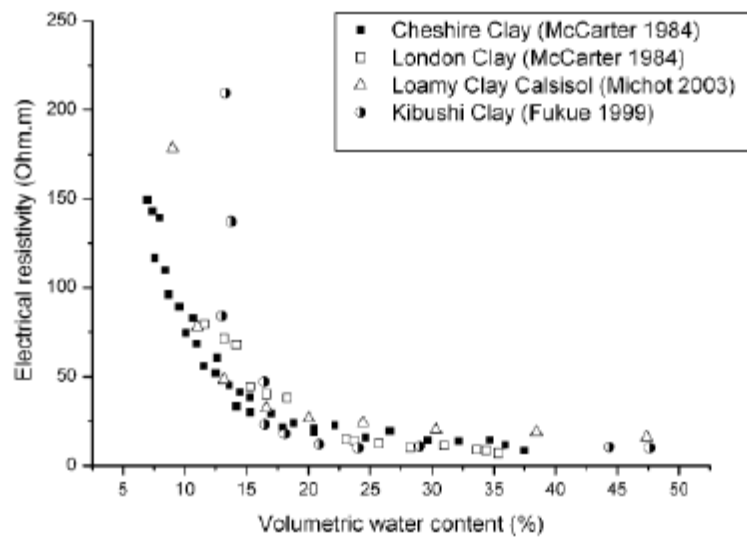


Figure 2.6 Relationship between the volumetric water content and the electrical resistivity for different soil types. Compiled by (Samouelian et al. 2005)].

In unsaturated soils, the resistivity changes widely with the water content. The discontinuity of pore water causes an extremely high resistivity in the materials. The continuity of pore water can be obtained for water content higher than the plastic limit which is almost 'adsorbed water content'. Soil structure is dispersive for the highest water contents and/or larger dry volumetric weights studied. For this reason, even if the size of the macropores is small there is the contribution of the water in the micropores and of adsorbed water. The contribution of the latter increases conductivity. For the smallest water contents and low densities, soil structure is flocculated and therefore electrons flow mechanism is expected to occur mainly through the water in the macropores, like in granular soils (Gingine et al. 2016). It is possible to use the



resistivity of soils for describing the details of micro structural characteristics of soils (Fukue et al. 1999). Soil with high surface area required more water for the formation of water film and bridging between the particles (Kibria and Hossain, 2012). Within the context of preventative geotechnical asset maintenance, ERT imaging can provide a monitoring framework to manage moisture movement and identify failure trigger conditions within embankments, thus supporting on demand inspection scheduling and low cost early interventions (Gunn et al. 2015).

#### **2.6.4 Effect of degree of saturation**

Electrical resistivity also depends on the degree of saturation. As the soil goes from partially to fully saturated conditions, non-conducting air voids gets replaced with electrolytic pore fluid (Bryson, 2005). The electrical resistivity of unsaturated soil  $\rho$  can be related to that of saturated soil  $\rho_{sat}$  as follows (Abu-Hassanein, 1996).

$$\frac{\rho}{\rho_{sat}} = S^B \quad (2.1)$$

where,  $S$ = degree of saturation,  $B$ = an empirical parameter. From above relationship, it is evident that increasing the degree of saturation results in lower electrical resistivity. The equation (2.1) is applicable when the degree of saturation is above a critical value  $S_{cr}$ , which corresponds to the minimum amount of water required to sustain a continuous film of water surrounding the solid particles. And when the degree of saturation falls below  $S_{cr}$ , there will be an abrupt increase in electrical resistivity. Measurement of resistivity is, in general, a measure of water saturation and connectivity of pore space (Ogungbe et al. 2012).

#### **2.6.5 Effect of hydraulic conductivity**

The correlation between electrical resistivity and hydraulic conductivity of different types of soils had been made by many researchers. These relationships are empirical and confined to a few locations. For clay, sand and silt the relationship between electrical resistivity and hydraulic conductivity are direct, with coarse grained soils generally having the highest electrical resistivity and highest hydraulic conductivity. The direct relationship between electrical resistivity and hydraulic conductivity for soils of different type is primarily due to alterations in surface

conductance (Abu-Hassanein, 1996). That is, surface conductance decreases as soils become increasingly coarse grained. More often than not, for coarse grained soils, having the highest resistivity has the highest hydraulic conductivity. But the relationship between hydraulic conductivity and electrical resistivity is the inverse for soils of a particular type. For example, saturated dense sands have lower porosity, lower hydraulic conductivity and greater electrical resistivity than loose clean sands. Huntley (1986) showed that at low groundwater salinities, surface conduction substantially affects the relation between resistivity and hydraulic conductivity. It is worth mentioning that all these relations are site specific and have no potentially physical law. In addition, the physical relation between hydraulic conductivity and aquifer resistivity is not completely understood. It has a direct correlation in some studies and inverse in others (Khalil et al. 2009).

#### **2.6.6 Effect of void ratio/porosity**

Archie (1942), formulated a simple relation that exists for porosity and salinity with resistivity for brine saturated sand cores from the Gulf Coast Region.

$$R_o = FR_w \quad (2.2)$$

Where  $R_o$ = resistivity of the sand when all the pores were filled with brine,  $R_w$ = resistivity of the brine, and  $F$ = formation resistivity factor. The Formation factor  $F$ , defined as the ratio of the conductivity of the fluid which saturates a sand aggregate to the conductivity of the mixture, is shown theoretically to depend on the basic features of the sand structure (Arulanandan, 1991). Kim et al. (2011) conducted a study for the determination of void ratio from a sea shore soil. He measured electrical resistivity using a newly designed Electrical Resistivity Cone Probe (ERCP). The resistivity-based void ratio matched well with the volume-based void ratio at various depths. The void ratio profile thus obtained was inversely proportional to the SPT  $N$ -value or CPT cone-tip resistance. Sediment resistivity plays an important role in the consolidation process. Porosity is the primary factor affecting the resistivity behaviour during the consolidation process of silty sediments. As porosity and water content decrease, resistivity increases with time. Hence resistivity is a good indirect predictor of porosity (Jia et al. 2013).

### **2.6.7 Effect of pore fluid composition**

The resistivity of rocks and minerals can vary with the mobility, concentration, and ion dissociation. Dissolved chlorides and sulphates in water can result in different conductivities (Dafalla et al. 2012). In general, in order to fully understand the mechanisms that control resistivity in soils, it is vital to include also soil mineralogy and pore water chemistry in the analysis of soil's physical properties (Montafia et al. 2013). Kishore and Bhagat (2006) studied the soil resistivity variation with salinity.

### **2.6.8 Effect of dry density and degree of compaction**

Among the geophysical tools used in soil science, electrical methods are considered as potentially useful to characterize soil compaction intensity (Seladji et al. 2010). Kibria (2011) in his study, showed that resistivity was high when compacted at dry optimum. With the increase of moisture content and unit weight, resistivity decreased significantly. Air, with naturally high resistivity, results in the opposite response compared to water when filling voids (Cardimona, 2002). In the studies conducted by Yamasaki et al. (2013) on tropical compacted sandy soil, the moist portion of the same compaction curve shows a decrease in resistivity as the voids ratio increases, tending towards equilibrium because, unlike the case at the dry points, the soil's voids are filled with air, instead of water. Cabalar (2007) described relationship of compacted soils and electrical resistance by a geometric model

## **2.7 Laboratory Electrical Resistivity Measurement Methods**

### **2.7.1 Two probes measurements**

This is the simplest method of resistivity measurement and is depicted in Fig. 2.7. In this method, voltage drop  $V$  across the sample and current through the sample  $I$  are measured.

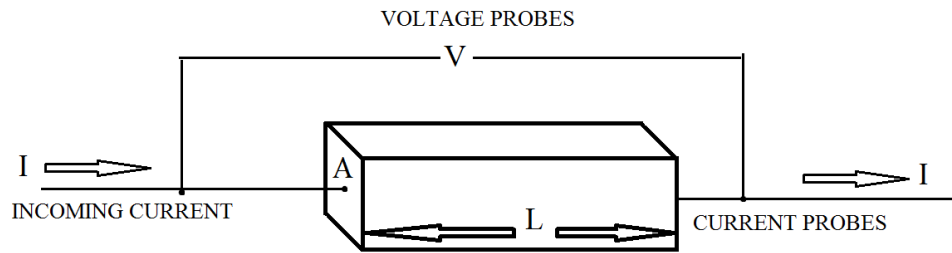


Figure 2.7 Electrical resistivity measurement by Two probes method

Then the resistivity is given as

$$\rho = \frac{VA}{IL} \quad (2.3)$$

Where ‘A’ is the area of specimen and ‘L’ is the distance between the potential probes. (Which is same as the length of specimen). This method is useful for the samples with large electrical resistance. The disadvantages of this method are:

- i) Error due to contact resistance of measuring leads
- ii) This method cannot be used for materials of random shape

These drawbacks of two probes method can be resolved by four probes method.

### 2.7.2 Four probes measurements

The potential probe is the most broadly used method for electrical resistivity measurements on the comparatively low resistive samples. Four probe method (Fig 2.8) can be used to determine the resistance of the single crystal as well as the bulk specimen also. This method can eliminate the effects of contact resistance between the sample and electrical contacts and therefore is most suitable for low and accurate resistance measurements. Contact and lead resistances are cancelled out by the four point method, however the contact resistance can still cause error if these produce enough heat.

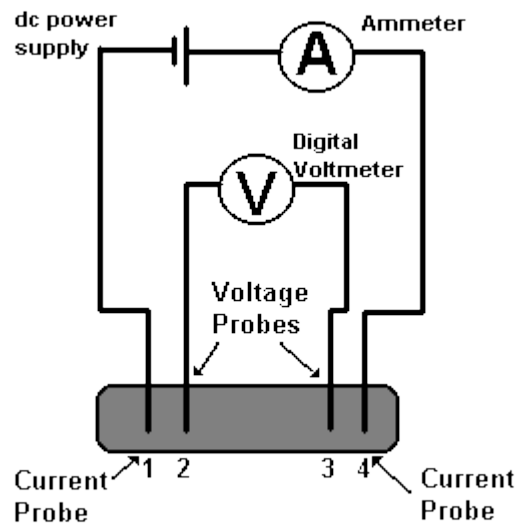


Figure 2.8 Electrical resistivity measurement by Four probes method

Instrumental dc offsets also contributes to the error, but this can be easily corrected by subtraction. Self-induced voltage offsets in the circuit further add to the error. This problem can be corrected by reversing the flow of current through the sample. When the low level of the voltage (in the range of  $\mu\text{V}$ ) is produced across the sample, signal noise also adds to the error. The use of thoroughly shielded cables and low thermal contactors, as well as making single point grounding, noise problem can be reduced (Singh, 2013).

## 2.8 Field Electrical Resistivity Measurements

A pre investigation of a site with geophysical methods can help to plan an efficient drilling program, minimizing costs and efforts. An efficient drilling program eliminates the "chance" encounter of features by drilling and confirming the anomalies (Anderson et al, 2003). The economy of any project depends upon the quantum and the quality of the preliminary investigations carried out. The data thus gathered and generated through these studies undertaken increases the confidence level in the interpretation of the foundation conditions and facilitates the design of appropriate foundation systems (Meshram et al. 2013).

Electrical resistivity method of exploration, could be used to detect the boulders. If the boulders are present in the soft soils, boulders can be the resistive target around the electrically conductive conditions (Jee et al. 2007). Gardi (2014) employed

electrical resistivity techniques for identifying pollution zones in areas of quaternary sediments, (gravel, sand, silt and clay).

It should be noted that alternating current is used in these studies to avoid macroscopic polarization of the subsurface material. Such macroscopic polarization would result from the bulk migration of charges in the subsurface in response to a constant applied field. This would create an artificial DC potential that would interfere with the resistivity measurements. An AC frequency in the range 1–100 Hz is sufficient to avoid this problem (Herman, 2001).

### **2.8.1 Survey Methods and Electrode Configurations**

Resistivity surveys are conducted as either soundings or profiles. A sounding is used to determine changes in resistivity with depth. The electrode spacing is varied for each measurement, but the centre point of the array is constant. There are various electrode configurations which can be used in resistivity surveying.

### **2.8.2 True resistivity and apparent resistivity**

The ratio between the potential difference (V) and the current (I) gives the apparent resistance, which depends on the electrode arrangement and on the resistivities of the subsurface formations.

There are several types of electrode arrangements (configurations) of which Wenner and Schlumberger configurations are more popular. Where the ground is uniform, the resistivity should be constant and independent of both electrode spacing and surface location. The true resistivity of the subsurface is obtained if it is homogeneous. When subsurface inhomogeneities exist, the resistivity will vary with the relative positions of the electrodes. The calculated value is called apparent resistivity. The apparent resistivity measured by the array depends on the geometry of the electrodes. In general, all field data are apparent resistivity. They are interpreted to obtain the true resistivities of the layers in the ground.

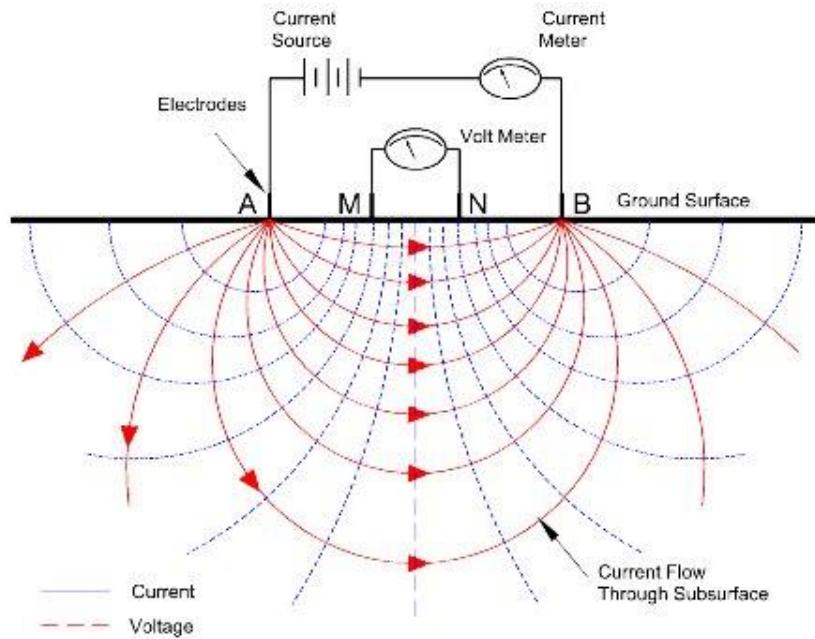


Figure 2.9 Potential distribution beneath ground during electrical resistivity measurement. (Source: <http://www.geocities.ws/>)

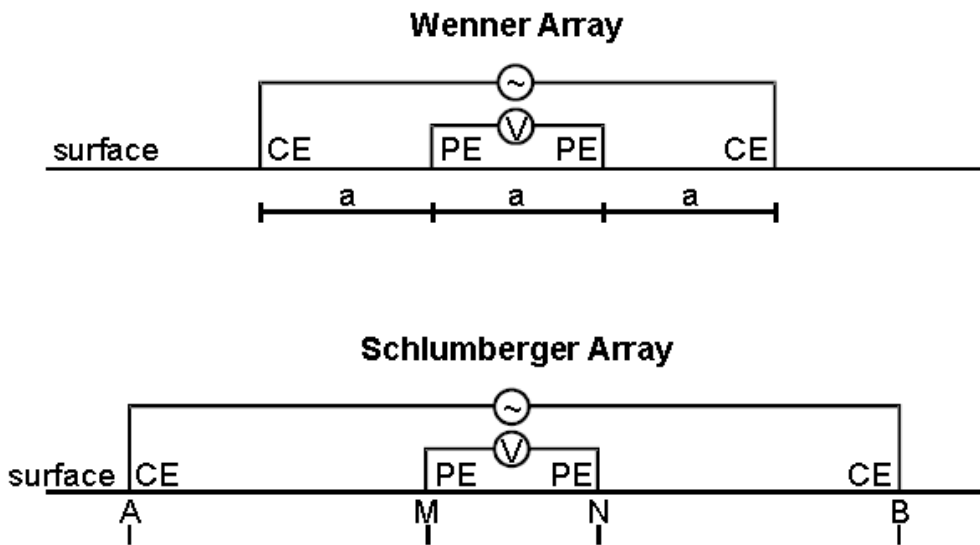


Figure 2.10 Wenner and Schlumberger Array configuration

The majority of resistivity surveys use two current electrodes and two potential electrodes (Fig 2.9). The two main array configurations are the Wenner array and the Schlumberger array (Fig. 2.10). The Wenner array has the simplest geometry, with all of the electrodes equally spaced. The Schlumberger array is more complex with the

spacing between the current electrodes not equal to the spacing between the potential electrodes. In general, the potential electrode spacing is negligible compared to the current electrode spacing for this type of array.

Four electrodes are used at certain spacing depending on the type of array used. To conduct the test, the four electrodes, which are usually in the form of metal stakes, are driven in to the ground. The two outer electrodes are known as current electrodes. The two inner electrodes are called potential electrodes. The mean resistivity of the strata is determined by applying D.C. current to the outer electrodes and by measuring the voltage drop between the electrodes. In usual practice the current used is direct electric current (D.C.), commutated direct current (i.e. a square wave alternating current), or AC of low frequency (typically about 20Hz).

### **2.8.3 Interpretation of electrical resistivity sounding data**

The interpretation of electrical resistivity sounding data is the process of deriving the values of true resistivities ( $\rho$ ) and thicknesses ( $t$ ) of various subsurface strata from the values of recorded resistance ( $R$ ) or apparent resistivity ( $\rho_a$ ) at electrode separations ( $a$ ). There are a number of interpretation techniques for evaluating  $\rho$  and  $t$  of each of the stratum as proposed by many investigators. These can be grouped as analytical, numerical, empirical, graphical, computer (software) based etc. and several amongst each category (Ramaiah et al. 2010). Electrical resistivity data acquired using either the Wenner or Schlumberger array, can be modelled using master curves or computer modelling algorithms. When using master curves, the interpreter attempts to match overlapping segments of the apparent electrical resistivity versus electrode separation plots with a succession of two-layer master curves. This modelling method provides coarse estimates of the model parameters. This is time consuming, and requires skill on the part of the interpreter. An alternative method of modelling sounding mode electrical resistivity data is to use readily available computer modelling software packages. There are a variety of different types of algorithms; some assume discrete electrical resistivity layers while others assume that electrical resistivity is a smooth function of depth. The discrete layer algorithms require interaction on the part of the interpreter, but allow for constraining model parameters to adequately reflect known geologic conditions. The continuous electrical resistivity algorithms are automatic, that is, they require no



interaction on the part of the operator, and therefore geologic constraints cannot be incorporated into the models. The modelling of profiling and profiling-sounding mode data is much more involved than in the case of sounding data. The profiling-sounding data reflect electrical resistivity variations in the lateral and vertical directions, resulting in a much more complicated computer simulation of the potential fields. The computer techniques capable of simulating these fields are finite difference, finite elements and integral equation algorithms. PC based software is available to interpret these data, but caution should be exercised when using automatic interpretation routines: the inexperienced interpreter can make assumptions that will lead to a statistically accurate result, but not (necessarily) a correct geological interpretation. Generally, most profiling-sounding mode data is interpreted in a qualitative manner, with the accuracy of the interpretation being based solely on the experience of the geophysicist.

The Vertical Electrical Sounding (VES) is the most widely used geophysical technique for subsurface exploration. It can be interpreted by different technique to get subsurface profile, their layer thickness and true resistivity. However, confusion occurs during the selection of suitable methods of interpretation, as the accuracy of result largely depends on interpretation technique (Bhoi, 2012).

#### **2.8.4 Inverse Slope Method**

In Schlumberger system, all the four electrodes are placed in a line and the distance between current electrodes (AB) is kept equal to or more than five times the distance between the potential electrodes (MN). According to this approach, the inverse of resistance measured ( $1/R$ ) is plotted against the electrode separation 'a' in wenner configuration and the distance  $AB/2$  in schlumberger configuration on a linear graph. Points are plotted with best fitting straight lines such that a minimum of 3 points fall on each line. Each line segment represents a layer and the intersections of the line segments correspond to the depths to the particular layers for wenner configuration and  $2/3^{\text{rd}}$  of the abscissa of intersection corresponds to depths for schlumberger configuration. The resistivity of the layers are obtained by the inverse slope of the particular line segment multiplied with ' $2\pi$ '.

The resolution of the conventional approaches by Curve matching and inverse techniques is poor and thin layers buried at depths more than 5-times their thickness cannot be identified because of the logarithmic plotting. In conventional interpretation methods, a middle layer with resistivity intermediate between enclosing beds will have practically no influence on the resistivity curve as long as its thickness is small in comparison to its depth. Hence the layers with small thickness cannot be recognized. Also, a conductive layer sandwiched between two layers of higher resistivities will have the same influence on the curve as long as the ratio of its thickness to resistivity ( $h/\rho$ ) remains the same and similarly (ii) a resistive layer sandwiched between two conducting layers will have the same influence on the curve as long as the product of its resistivity and thickness. Hence the thicknesses and resistivities of sandwiched layers of small thickness cannot be determined uniquely. The linear plotting of the data and analysing will be able to decipher thin layers even if they are buried at great depths, provided the data density is adequate enough to get the signals from the target layers.

### **2.9 Laboratory Resistivity vs Field Resistivity**

Studies conducted by Adli et al. (2010) showed that laboratory measured resistivity value of rock samples differ from field measurement by less than 50%, a relatively small difference in resistivity survey application. This study suggested that field measurement which gives generally lower resistivity than laboratory analysis could be attributed to the presence of underground water in pores and cracks of subsurface rock or unknown near-surface strata. Siddiqui et al. (2012) studied the correlation of field and laboratory electrical resistivity which showed a good linear correlation. Relationship indicated that laboratory resistivity values are 1.306 times higher than the resistivity values obtained in the field.

### **2.10 Lateritic Soils**

Laterite is derived from Greek word 'later' meaning brick. From the geological point of view laterite can be defined as, "a kind of vesicular rock composed essentially of mixture of hydrated oxides of Aluminium and iron with small percentage of other oxides such as manganese or Titanium" (Gidigas 1976). It is defined as soil layer that is rich in iron oxide and derived from a wide variety of rock weathering under strongly

oxidizing and leaching conditions. It forms in tropical and subtropical regions where the climate is humid. Lateritic soils may contain clay minerals; but they tend to be silica-poor, for silica is leached out by waters passing through the soil. Typical laterite is porous and claylike. The term laterite is often substituted for ferricrete but technically refers to a soil rich in iron oxides and aluminium. In fields of extensive leaching, many plant nutrients are lost, leaving quartz and hydroxides of iron, manganese, and aluminium. This remainder forms a typical type of soil, called laterite or latosol. Laterite beds/deposits forms at the top mainly due to chemical weathering of rocks laterisation with high content of iron hydroxides. Later on their formation laterites are either denuded by erosion, or covered below younger deposits.

Tropical weathering (lateritization) is a prolonged process of chemical weathering which produces a wide variety in the thickness, grade, chemistry and ore mineralogy of the resulting soils (Elarabi and Ali, 2013). According to Aleva and Creutzberg (1994) laterite (or rather some varieties of it) is formed by a process, by which certain rocks undergo superficial decomposition, with the removal in solution of combined silica, lime, magnesia, soda, potash, and with the residual accumulation, assisted, no doubt, by capillary action, metasomatic replacement, and segregative changes of a hydrated mixture of oxides of iron, aluminium, and titanium, with more rarely, manganese. These oxides and hydroxides of iron, aluminium, titanium, and manganese are designated as the lateritic constituents. This residual rock is true laterite, and the presence of any considerable proportion (> 10 percent) of non-lateritic constituents requires expression in the name, as it always indicates want of completion in the process of lateritisation. True laterite contains, then, 90 to 100 percent of lateritic constituents. There is often a gradation in composition between true laterite as defined above and lithomarge which is taken as the amorphous compound of composition  $2\text{H}_2\text{O} \cdot \text{Al}_2\text{O}_3 \cdot 2\text{SiO}_2$ , corresponding to the crystalline mineral kaolinite of the same composition. For rocks intermediate between laterite and lithomarge the terms 'lithomargic laterite' and 'lateritic lithomarge' are available, the former being applied to forms containing 50-90 percent of lateritic constituents, and the latter to forms containing only 25 to 50 percent of lateritic constituents.

### **2.10.1 Electrical resistivity studies on laterites**

Bai et al. (2013) investigated the electrical properties of lateritic soil using electrical conductivity measurements on a self-developed testing device. An increment in the conductivity value of laterite soil has been reported with the increase in water content, degree of saturation and dry density and subsequently tends to be constant if there is a certain increase made in the values of above mentioned soil properties. It was also found that electrical conductivity increases with the increase of temperature and decreases with the increase of the number of wetting drying cycles. Asif et al. (2016) successfully correlated electrical resistivity values with index properties of sandy and silty soils in the study area, Wattar, Pakistan. Very limited study has been conducted so far to assess the relationship between electrical resistivity and strength properties for compacted laterite soil such as cohesion and internal angle of friction. Bai *et al.*, (2013) recommends to examine the effects of shear strength properties of compacted lateritic soil in relation with electrical resistivity which would enable electrical resistivity to eliminate the physical parameters in calculations and designing for the foundation and construction purposes.

### **2.11 Electrical resistivity of contaminated soils**

Due to population growth, a progressive living standards, and industrial progress, much of land is polluted. Soil-pollutant interactions occur altering the geotechnical behaviour of the soils. Soil-pollutant interactions can affect almost all properties of the soil which in turn may lead to various geotechnical problems such as landslides, ground subsidence, settlement, erosion, progressive failure, underground structural stability, foundation failures. In order to take remedial measures, it is necessary to understand the soil-pollutant interaction.

#### **2.11.1 Case study on heaving of soil due to acid contamination**

Investigations were carried out to find out the causes for distress to the floors, beams and upheaval of foundations at many places in a fertilizer plant (Sridharan et al. 1981). Extensive chemical tests showed presence of high phosphate content in acidic environment in the soil. This could be connected up with phosphoric acid as the source of soil pollution, which resulted in heaving of soil. Also, tilting of phosphoric acid

storage tanks was reported in the chemical fertilizer factory in Aqaba, Jordan, due to chemical reaction taking place between the acid that leaked and the subgrade soil (Assa'ad, 1998). Many other cases of ground heave are reported, due to prolonged spillage of concentrated solution of caustic soda and expansive reactions between lime and sulphate bearing clays (Ramakrishnegowda, 2005). Unexpected heave can occur in swelling and non-swelling soils due to contamination with acid, contamination induces swelling in soils due to gradual changes in the mineralogy of soils (Sivapullaiah, 2009). The large amounts of phosphate fertilizers which are used in agriculture activities in Egypt lead to the contamination of large quantities of soil surrounding the agricultural area. The compaction characteristics, hydraulic conductivity and shear strength parameters of sandy soils and the hydraulic conductivity, Atterberg limits, and shear strength parameters of silty clay soil got altered due to chemical reaction (Eltarabily, 2015).

Since electrical resistivity measurement method is sensitive to changes in chemical binding of the soil, this method can be a useful tool for detecting areas of contamination in the surface and subsurface. Ahmed and Sulaiman (2001) used electrical resistivity imaging survey to investigate the leachate production within the landfill of Seri Petaling located in the State of Selangor, Malaysia. The study conducted by Arrubarrena-Moreno and Arango-Galvan, (2013) proved that electrical resistivity tomography have substantial impact on identifying soils contaminated by hydrocarbons since it gives valuable information on the spatial distribution of pollutants in the subsoil. Sirhan and Hamidi (2013) employed electrical resistivity tomography (ERT) technique in determining lateral and vertical electrical resistivity variations of possible infiltration zones of waste water. Furthermore, the extracted vertical electrical soundings (VES) provided indications about the nature of the geological features that can affect the behaviour of leakage.

## **2.12 Electrical Resistivity Studies on Engineering Properties of Soil-Cement/Lime**

Soil electrical resistivity testing has been gaining importance in geotechnical and geo-environmental fields due to its non-destructive nature, cost and time efficiency. To gather a thorough awareness of the subject, it is important to review, compile, and

organize the current state of research that identifies the various progresses that are being made in the area.

### **2.12.1 Stabilisation of soils**

Nayak and Sarvade (2012) studied the effect of cement and quarry dust on characteristics of the Lithomargic clay after stabilisation. Microfabric and mineralogical studies were carried out to find out the reason for the strength development of the stabilized soil using SEM and XRD analysis. Stabilisation with additives helps to increase strength, reduce deformability, provide volume stability, reduce permeability and reduce erodibility (Hausmann, 1990).

The results showed a decrease in liquid limit and plasticity index, and an increase in cohesion and internal friction with increase of cement content. With addition of quarry dust, liquid limit, plasticity index and cohesion decreased while angle of internal friction and maximum dry density increased. As the percentage of the quarry dust and cement increased, the liquid limit decreased. But with the increase in the percentage of cement on different percentages of quarry dust there is increase in the plastic limit, decrease in plasticity index, increase in the angle of internal friction and cohesion, provide volume stability, reduce permeability and reduce erodibility (Hausmann 1990).

### **2.12.2 Electrical resistivity of stabilised soils**

Electrical resistivity is one of the most sensitive indicators of changes in the nature of the chemical binding (Singh, 2013). Liu et al. (2008) conducted a study for investigating the factors controlling the electrical resistivity of soil-cement admixture. Electrical resistivity method was identified to be a non-destructive and cost effective method against Standard Penetration Test (SPT) for checking the quality of soil-cement columns. The following results were given:-

- Effect of cement content on electrical resistivity- With the increase in cement content, water content and void ratio of the soil–cement admixture decreased due to the hydration reaction and pozzolanic reaction. Therefore, the conduction path for the electrical current became more tortuous. As a result, the electrical resistivity of the soil–cement admixture increased.

- Effect of degree of saturation on electrical resistivity- Electrical resistivity increased with the decrease in degree of saturation because less pore spaces were filled with pore water and thereby the path for the electrical current became less tortuous in the soil–cement.
- Effect of water content on electrical resistivity- With decrease in water content, the conduction path for the electrical current became more tortuous resulting in increase of electrical resistivity.
- Effect of curing time on electrical resistivity- With the increase in the curing time, the chemical reaction products such as calcium silicate hydrate (CSH) and calcium aluminate hydrate (CAH) formed binds more fine soil particles together resulting in a denser soil structure. Hence electrical resistivity is increased.

It was also found that with the increase in the unconfined compressive strength the electrical resistivity increased.

Dong et al (2016) established a linear relation between the standard compressive strength and the resistivity of the cement pastes at 24 hours, which can demonstrate the resistivity and the standard compressive strength have a close corresponding relationship, and the resistivity curve of cement and the strength development curve has the same trend. Bhangale and Bhosale (2010) made correlations of UCS and CBR with electrical resistivity for Black Cotton soil stabilised with lime. It was found that resistivity decreased with increase of water content. The resistivity value was high when soil had water content less than optimum and then decreased and attained constant value after optimum which was independent of curing period. UCS values increased rapidly to a certain resistivity value and then became almost a constant. It was further noted that the peak value of UCS increased with resistivity and curing period. Also the CBR value of treated soil increased with the curing period.

Zhang et al. (2012) worked on quantifying the effect of cement content, porosity, and curing period on the electrical resistivity and UCS of cement treated soil. The general Archie's law, which includes the effect of water content and porosity, was modified to evaluate the effect of cement content and curing periods on the electrical resistivity of cement stabilized soil. Archie (1942) developed an empirical relationship

that relates the electrical resistivity of saturated sand ( $\rho$ ) to the electrical resistivity of its pore fluid ( $\rho_w$ ), and the porosity ( $n$ ) of the soil.

$$\frac{\rho}{\rho_w} = n^{-m} \quad (2.4)$$

Where  $m$  is the material-dependent empirical exponent, which is a measure of pore tortuosity and the interconnectivity of the pore network.

From the study it was found that for a given curing time, higher cement content yields greater amount of hydration compounds such as calcium silicate hydrate and calcium aluminate hydrates gels as a result of hydration processes. The hydration compounds fill in pore spaces and intersect each other to form solid networking resulting in a denser structure. The free water space and porosity decrease, and tortuosity increases with electric current. Consequently, electrical resistivity increases more significantly. A new parameter, termed as after-curing porosity/cement content-curing time ratio,  $n_t/(a_w \cdot T)$ , was proposed to relate the electrical resistivity values and those factors as given by:

$$\rho = A \left( \frac{nt}{a_w T} \right)^{-B} \quad (2.5)$$

Where  $A$  and  $B$  are dimensionless constants.

### 2.13 Summary

The role of geophysical testing in geotechnical studies is sometimes looked at as a more probable rather than certain approach when it comes to making a precise subsurface soil profile. However, it can be possible to employ the electrical resistivity soil profiling techniques combined with few boreholes data to make a true and correct subsurface profile, which can be used confidently by geotechnical engineers.

Review of literature concerning field and laboratory applications of electrical resistivity techniques have been showcased in this Chapter. Reliable correlations between electrical resistivity and other soil properties will enable us to characterize the subsurface soil without borehole sampling. Recent studies have proved electrical resistivity technique to be a reasonably good method for evaluating swell- shrinkage properties of expansive soil and for characterization of cracks in soils. Soil



characterization by integrating geo- electrical data and geotechnical data is a promising field of research.

## CHAPTER 3

### LABORATORY EXPERIMENTAL INVESTIGATIONS ON LATERITIC SOILS

#### 3.1 Introduction

Proper understanding of the relationships between the physical factors influencing the engineering properties of soils and their measurable electrical parameters provides a methodology by which the engineering behaviour of soils can be predicted non-intrusively. This Chapter discusses the results of electrical and geotechnical tests performed on controlled soil samples in the laboratory, and correlation of the influence of the index and engineering properties of soil on its electrical response.

#### 3.2 Sample Preparation

Lithomargic clays are present at depths of 1-3 meters below the top laterite caps throughout the Konkan area that extends along the western coast from Cochin to Bombay. These soils are classified as silty sand or sandy silt with higher percentage of silt content and low strengths (George et al. 2012). These are formed by tropical or subtropical weathering, and contain hydrated alumina, primary silicates, and kaolinite. These soils have an amorphous blend of  $\text{Al}_2\text{Si}_2\text{O}_5(\text{OH})_4$ . Soils with 50-90% lateritic constituents are known as lithomargic laterites, while soils with 25-50% laterite content are known as lateritic lithomarge. Shedi soil is the local name given to the locally available whitish, pinkish or yellowish lithomargic soils.

In the present study, soil samples were collected and were studied for geotechnical and electrical resistivity measurements by adding different percentage of river sand to them. The percentages of river sand added were 0, 10, 20, 30, 40 and 50% by weight of dry soil. This is done to prepare controlled lateritic soil samples which are comprised of silt, sand and clay to conduct parametric studies. The samples are designated as S0, S1, S2, S3, S4 and S5 respectively. The particle size distribution of the samples are shown in Fig. 3.1.

Sieve analysis was done on the sand used in the experiment, and found that sand was well graded and was clean with little or no fines. For the experimental work, river sand which was passing through IS 4.75 mm sieve and retained on IS 75 micron sieve is considered. The samples were kept for air drying for 24 hrs. After air drying, the samples were kept in oven for 24 hrs. These oven dried samples were mixed in different proportions by dry weight as per the study interest.

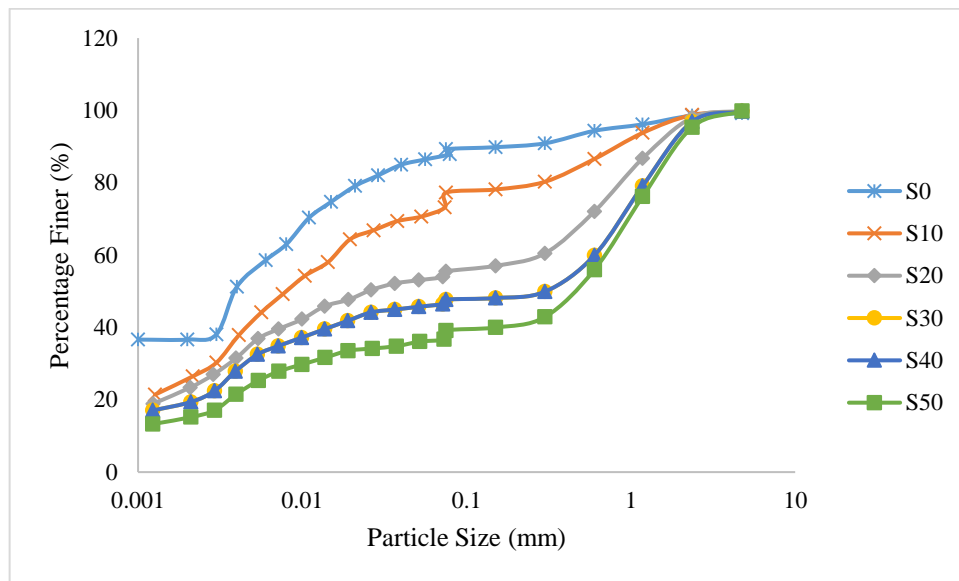


Figure 3.1 Particle Analysis curve for the six lateritic soil samples

### 3.3 Geotechnical Properties of Soil

An extensive laboratory experimental program is undertaken to achieve the objectives of the study. The collected soil samples were classified according to the IS Classification using sieve analysis, liquid limits and plastic limits test results. Moreover, ionic composition of the soil samples and fabric structures are analysed by Scanning Electron Microscope (SEM) and Energy Dispersive X-ray Spectroscopy (EDAX). After that, soil resistivity of the samples was determined at different condition. Preliminary tests like sieve analysis and specific gravity were done on coarse and fine fraction. Blended proportion of river sand with shedi soil is shown in Table 3.1.

Table 3.1. Blended proportion of river sand with shedi soil

Soil sample	Fine fraction (%)	Coarse fraction (%)
S0	100	0
S1	90	10
S2	80	20
S3	70	30
S4	60	40
S5	50	50

Laboratory testing on the prepared samples were conducted to determine grain size distribution, compaction characteristics, specific gravity, index properties, cohesion, angle of internal friction, and unconfined compressive strength. Electrical resistivity measurements were also carried out on these samples in the laboratory to bring out the correlation between geotechnical properties and soil electrical resistivity.

### **3.4 Test Procedures**

#### **3.4.1 Water content**

Water content of soil was obtained by oven dry method. This is the most accurate method of determining the water content and is, therefore, used in this investigation and done as per IS:2720 (Part II)1973 description.

#### **3.4.2 Specific gravity test**

Specific gravity of soils finds application in finding out the degree of saturation and unit weight of moist soil. The procedure for the test is as per IS:2720 (Part 3/ Section I)- 1980. While doing experiment for finding out specific gravity, extra care was taken to expel all the air entrapped inside the soils.

#### **3.4.3 Liquid limit and Plastic limit**

Liquid limit of soil sample is determined by equipment conforming to IS: 2720 (Part 5) – 1985. Soil passing through IS 425 micron sieve is used for the test. The procedure for the determination of liquid limit conforms to IS: 2720 (Part 5) - 1985. The liquid limit and plastic limits of soils are both dependent on the amount and type

of the clay present in the soil. They form the basis for soil classification system for cohesive soils based on the plasticity tests and plasticity charts. Plasticity test gives information concerning the cohesion properties and of the soil and the amount of the capillary water it can hold. The index properties have also been related to various other properties of the soil. The test results are shown in the Table 3.2

#### **3.4.4 Shrinkage limit**

The shrinkage limit (SL) is the water content where further loss of moisture will not result in any more volume reduction in soil. At shrinkage limit, the soil is just fully saturated. Shrinkage limit tests were conducted as per IS: 2720 (part VI)- 1972. The test results are shown in the Table 3.2 The shrinkage limits of the soil samples ranged from 19.09 to 26.10.

#### **3.4.5 Compaction characteristics**

The Standard Proctor compaction tests and Modified Proctor compaction tests are conducted on the soil samples passing through 4.75mm sieve to determine the maximum dry density (MDD) and optimum moisture content (OMC). The procedure given by IS: 2720 (Part 7)-1980 & IS 2720- (Part 8)1983 is followed. The test results are shown in the Table 3.2

#### **3.4.6 Sieve analysis and Hydrometer analysis**

The grading of soil sample, apart from mechanical strength, is the most important factor assessing the sample as construction material. For the determination of the grain size analysis, wet sieve analysis is done, where the soil sample is washed through IS 75 micron sieve and the soil retained in the sieve is oven dried. The dried out sample is again sieved through the sieve set specified by the standards and another 50 grams of dried sample from the washout ( $<75\mu$ ) is used for hydrometer analysis. The whole procedure for the grain size analysis is done as per IS:2720 (Part 4)- 1985.

#### **3.4.7 Falling Head Permeability test**

A Falling head permeability test was conducted to find the horizontal permeability of the soil samples. The water is allowed to flow horizontally through a saturated soil sample so that any drop in volume of water in the stand pipe is equal to

the discharge that comes out of the soil sample. This forms the basis behind the falling head permeameters commonly used in the laboratories for finding the coefficient of permeability of fine grained soils of intermediate and low permeability consisting mainly of silt and clay.

A mould of 82mm inner diameter and 81.5mm length was specially prepared for conducting this test. The samples were first prepared at their maximum dry density and optimum moisture content using this mould. It was then put to saturation for 1 or 2 days till some water comes out at the other end. It is then connected to a main stand pipe which is under observation. The permeability value in this test is given by the following equation.

$$k = (aL/At) * \ln (h_1/h_2) \quad (3.1)$$

Here 'a' and 'A' refers to the cross sectional area of stand pipe and soil specimen respectively. 'L' is the length of the soil specimen and 't' is the time taken for head to drop from a water level of  $h_1$  to  $h_2$ . Both these water levels  $h_1$  and  $h_2$  are measured from the reference datum which corresponds here to the central longitudinal axis of the specimen. Before starting the experiment, it is important to ensure that the soil specimen is fully saturated. To attain saturation at a faster rate higher head is provided. The time for the water level to drop from  $h_1$  to  $h_2$ , differing by exactly 1mm was noted against the usual convention of measuring the head drops for a fixed time interval. However, the time for dropping from  $h_1$  to  $(h_1 h_2)^{1/2}$  and  $(h_1 h_2)^{1/2}$  to  $h_2$  was observed and found to be the same as suggested by IS 2720 (part 17) – 1986. Consistent values of coefficient of permeability, k is obtained and presented in Table 3.2.

#### **3.4.8 Unconfined compression tests**

Unconfined Compression (UCS) tests are done to obtain unconfined compressive strength as well as stress-strain behaviour. UCS tests are performed according to IS: 2720 (Part 10)- 1991. Tests are performed on statically compacted samples prepared at optimum moisture content and maximum dry density corresponding to Standard Proctor Test.

### **3.4.9 Triaxial compression test**

Undrained unconsolidated triaxial compression test was conducted on all the six soil samples. The test is conducted as per IS 2720 (Part 11): 1993. The values of cohesion,  $c$  and angle of internal friction,  $\phi$  were found out.

### **3.4.10 Energy-dispersive X-ray spectroscopy (EDAX)**

Energy-dispersive X-ray spectroscopy (EDS or EDX) is an analytical technique used for the elemental analysis or chemical characterization of a sample. It relies on the investigation of an interaction of some source of X-ray excitation and a sample. The thin sections were examined under scanning electron microscope (SEM) and Energy-dispersive X-ray spectroscopy (EDX) was also conducted to know the chemical composition of soil samples.

Its characterization capabilities are based on the fundamental principle that each element has a unique atomic structure allowing unique set of peaks on its X-ray spectrum. To stimulate the emission of characteristic X-rays from a specimen, a high-energy beam of charged particles such as electrons or protons, or a beam of X-rays, is focused into the sample being studied. At rest, an atom within the sample contains ground state (or unexcited) electrons in discrete energy levels or electron shells bound to the nucleus. The incident beam may excite an electron in an inner shell, ejecting it from the shell while creating an electron hole where the electron was. As the energy of the X-rays are characteristic of the difference in energy between the two shells, and of the atomic structure of the element from which they were emitted, this allows the elemental composition of the specimen to be measured.

### **3.4.11 Electrical Resistivity of Soil**

#### **3.4.11(a) Fabrication of Soil Resistivity Box**

Soil resistivity box is made of Nylon Delrin, that is strong, rigid, and have good moisture, heat and solvent resistance. Good mechanical properties and resistance to heat and fuels make these materials suitable for mechanical and electrical hardware. Dimensions of the resistivity box are given in Fig. 3.1. Stainless steel current electrodes

are placed at the 2 ends of the box and potential electrodes are placed at 1/3<sup>rd</sup> distance from the corresponding ends of the box, as shown in fig.3.2.

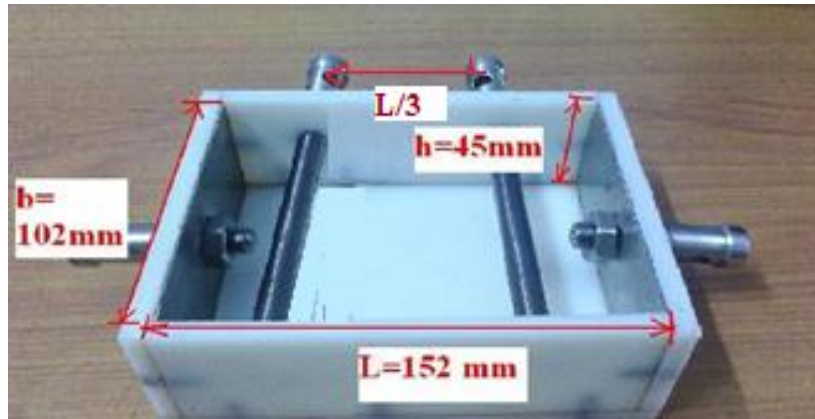


Figure 3.2. Soil resistivity box

The geometric dimension factor of soil resistivity box is obtained as 9.06 as given below:

$$SBF = \frac{A}{D} \quad (3.2)$$

Where, SBF= Soil box geometric factor, A = cross sectional area of a current electrode, cm<sup>2</sup>, D = distance between potential electrodes, cm

Hence, SBF = (4.5\*10.2)/(15.2/3) = 9.06

#### 3.4.11(b) Calibration of soil resistivity box



Figure 3.3 Measurement of conductivity using conductivity meter

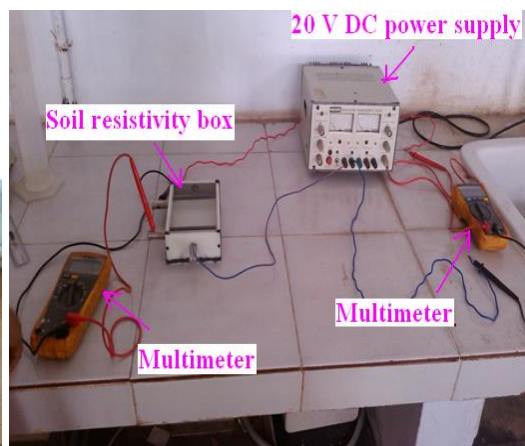


Figure 3.4 Resistivity measurement using resistivity box



Conductivity of standard solutions of NaCl and KCl is measured using Conductivity meter (Fig. 3.3). Standard solutions of NaCl and KCl, with different molarities and known electrical conductivity, shall be used for standardizing the test setup (fig. 3.4) The calibration factor is determined (fig. 3.5) before measurement of soil resistivity.

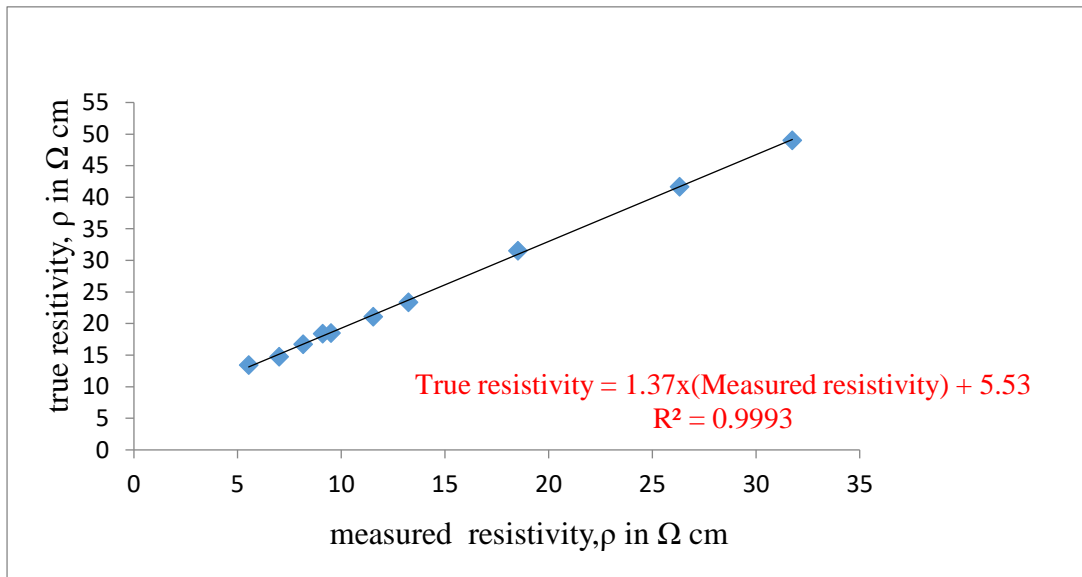


Figure 3.5 Calibration chart for soil resistivity box

### 3.4.11(c) Test procedure for soil resistivity measurement

- a) Remove the two stainless steel potential pins. After removing the pins fill the soil box with the soil at the required moisture content and dry density. Compaction is very crucial for obtaining accurate results. Replace the stainless steel pins. Pour or tamp material to be tested into soil box until flush with top of box.
- b) Connect power supply and DC multimeter so as to pass current between the two end terminals of the soil box (Fig 3.6).
- c) Connect DC multimeter between the two stainless steel potential pins, which are located near the center of the soil box.

- d) Using appropriate Milliammeter and Voltmeter ranges, measure the potential between the two steel pins with no current applied and again with measured current passed between the end terminals of the soil box (Fig 3.7).
- e) During the experiment room temperature was around  $27\pm 1^\circ\text{C}$ .

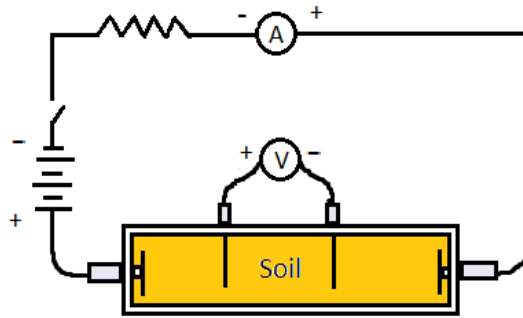


Figure 3.6 Circuit diagram showing the connections for the setup



Figure 3.7 Soil resistivity measurement

$$\text{Resistance(Ohm)} = \text{Change in Potential (mV)} / \text{Current (mA)} \quad (3.3)$$

It is usually more convenient to express the current in mA and the change in potential in mV.

Assuming that a change in the current passing through the sample ( $\Delta I$ ) causes a change in voltage dropped across the pins of  $\Delta V$ , the resistance of the sample would be  $\Delta V/\Delta I$  and the units would be  $\Omega$ , assuming that the current is in Amps and the voltage is in Volts (or that the current is in milliamperes and the voltage is in millivolts). Measured resistance is multiplied by calibration factor (Fig 3.5) and geometric dimension factor (equal to 9.06) to get the true resistivity.

$$\text{Resistivity (ohm - cm)} = \text{Resistance(ohm)} \times \left(\frac{A}{L}\right) \quad (3.4)$$

where A= cross sectional area of resistivity box (cm<sup>2</sup>), L= pin separation (cm).

Soil resistivity tests were conducted at different conditions such as

- At fixed unit weight with different moisture content.
- At fixed moisture content with different unit weight.
- At unit weight and moisture content corresponding to Standard Proctor compaction.
- At fixed unit weight and moisture content.

To identify the variation of soil resistivity with different geotechnical parameters, the adopted procedure can be summarized below:

- (a) One of the primary objectives of this study was to determine the variation of soil resistivity with gravimetric moisture content. To achieve this objective, soil resistivity tests were conducted at fixed unit weight with different moisture condition in order to bring out the variation of electrical resistivity with moisture content. Moisture content was varied from 10% to 50%. Soil samples were compacted at 95% of maximum dry unit weight of the soil in the soil resistivity box. The samples were then compacted in the resistivity box after thorough mixing with moisture.
- (b) To obtain soil resistivity and unit weight correlation, dry unit weight was varied from 1.3 g/cc to maximum dry density in each sample. Test was repeated for three moisture conditions such as 9%, 18% and 30% in each sample.
- (c) Standard Proctor compaction test was conducted at different moisture contents and dry unit weights. From the test results, a compaction curve was generated for each sample. Soil resistivity was determined for the moisture condition and unit weight corresponding to Standard Proctor compaction. Therefore, soil resistivity was correlated with compaction condition and state of strength at that condition.
- (d) Degree of saturation, a physical index, can be obtained by

$$S_r = \frac{wG_s\rho_d}{G_s\rho_w - \rho_d} \quad (3.5)$$

where  $S_r$  is the degree of saturation,  $\rho_d$  is the dry density,  $\rho_w$  is the density of water and  $G_s$  is the specific gravity of the soil sample. Soil resistivity is then correlated with degree of saturation making use of the values of  $w$  and  $\rho_d$  obtained in step (a).

- (e) Soil resistivity tests were conducted at 95%  $\gamma_{dmax}$ . Tests were repeated for three moisture contents 9%, 18% and 30% water content to determine the effects of fine fraction, ionic composition and pore space on soil resistivity
- (f) To bring out the variation of soil resistivity with liquid limit and plastic limit, soil resistivity tests were conducted at corresponding limits keeping dry density equal to 95%  $\gamma_{dmax}$ .
- (g) Unconfined compression strength was determined at moisture content and unit weight as that of Standard Proctor compaction. Soil resistivity tests were determined at optimum moisture content ( $w_{opt}$ ) and maximum dry density ( $\gamma_{dmax}$ ) corresponding to each soil sample in order to deduce the correlation that exists between unconfined compressive strength and the electrical resistivity values.
- (h) Triaxial tests were carried out at OMC and  $\gamma_{dmax}$  corresponding to Standard Proctor compaction to determine the shear strength parameters, and electrical resistivity values of the samples at the same compaction conditions were correlated with it.

#### **3.4.11(d) Measurement of California Bearing Ratio (CBR) and Electrical Resistivity**

The soil samples were compacted at the same conditions as for CBR test and was extracted from the mould. Electrical resistivity was measured using circular stainless steel current electrodes of 15cm diameter, and stainless steel potential electrode pins of 1cm diameter. Thus the electrical resistivity for all the 6 soil samples which are 12.5cm high and with 15cm diameter, was measured as shown in the Fig. 3.8. The resistivity values measured on the above described cylindrical soil samples were found similar to that measured on the soil samples using the resistivity box at same compaction conditions. Resistivity is a unit parameter depending on the material rather than size and shape of the samples.

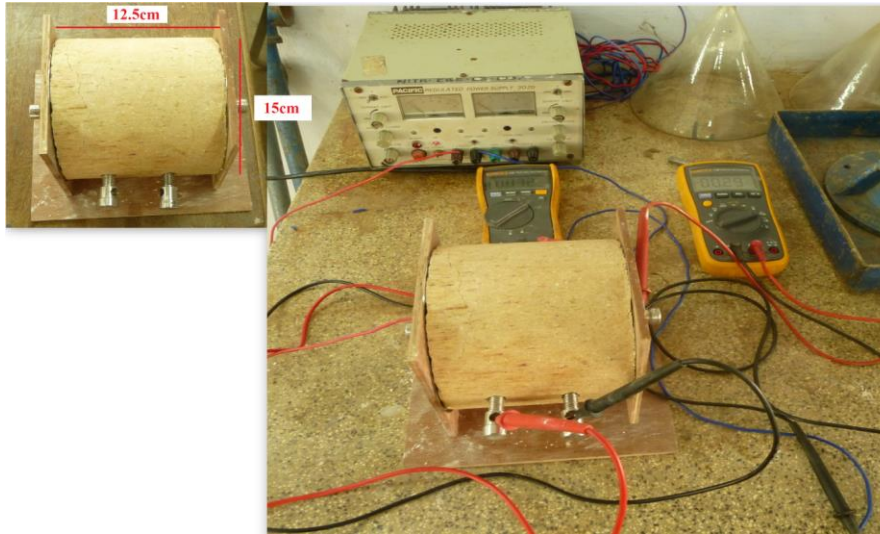


Figure 3.8 Set up for electrical resistivity measurements for CBR samples

### 3.5 Results and Discussions

#### 3.5.1 Basic Geotechnical parameters of the soil samples

Table 3.2 Geotechnical properties of the controlled soil samples

The summary of basic Geotechnical properties of the six lateritic soil samples are shown in Table 3.2.

Parameter	Soil sample					
	S0	S1	S2	S4	S5	S6
G	2.58	2.58	2.60	2.61	2.61	2.62
PL (%)	33.90	31.42	30.50	29.90	27.10	25.30
LL (%)	47.0	44.5	40.6	39.4	37.7	34.4
SL (%)	26.10	24.13	23.70	21.50	20.15	19.09
OMC (%)	28.0	25.0	23.0	21.0	18.0	17.0
$\gamma_{dmax}$ (g/cc)	1.45	1.56	1.59	1.64	1.74	1.77

$e_{min}$	0.78	0.65	0.64	0.59	0.50	0.48
n (at $e_{min}$ )	0.44	0.39	0.39	0.38	0.33	0.32
S (%) at OMC	92.70	98.65	94.14	92.67	93.00	93.00
K (cm/s)	2.22	2.29	2.41	3.17	4.93	5.08
Clay Size (%)	36.60	26.90	28.90	23.40	19.40	15.20
Silt Size (%)	52.60	50.80	39.60	32.10	28.30	24.00
Sand Size (%)	10.80	22.30	31.50	44.50	52.30	60.80
Gravel Size (%)	0	0	0	0	0	0

**Note: G- Specific Gravity, PL- Plastic Limit, LL- Liquid Limit, SL- Shrinkage Limit, OMC- Optimum Moisture Content,  $\gamma_{dmax}$ - maximum dry density,  $e_{min}$ - void ratio, n- porosity at  $e_{min}$ , S- degree of Saturation,  $K_h$ - Horizontal Permeability of soil**

### **3.5.2 Energy-dispersive X-ray spectroscopy (EDAX )**

The results from Energy Dispersive X Ray Spectroscopy (EDAX) are shown from Fig. 3.9 to Fig. 3.14 and the summary of percentage of ions present in the 6 soil samples are shown in Table 3.3.

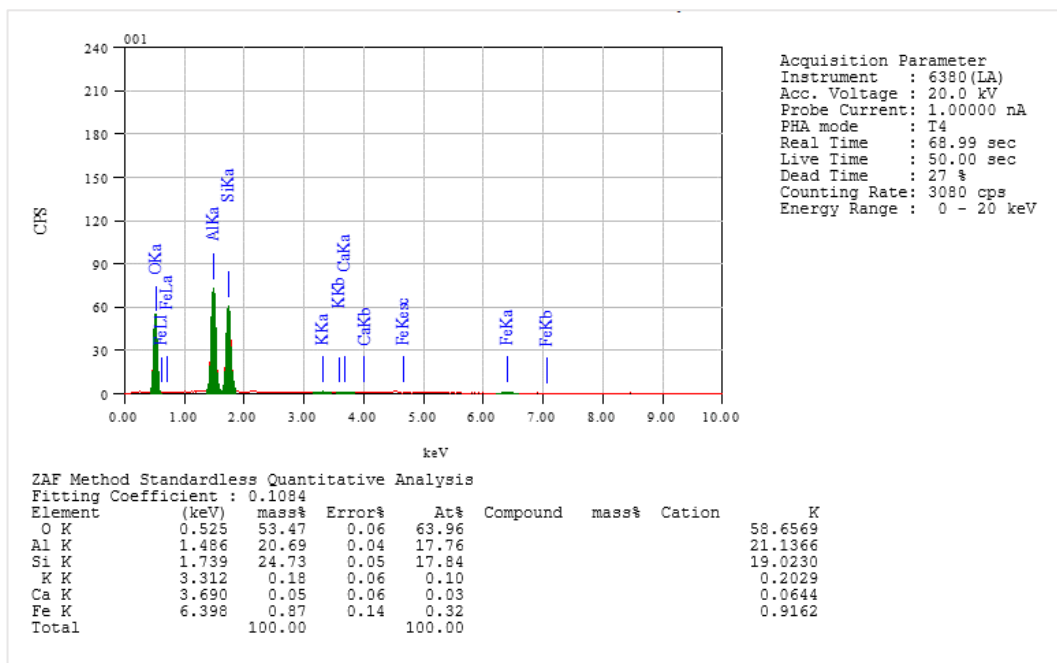


Figure 3.9 Results of EDAX conducted on sample S0

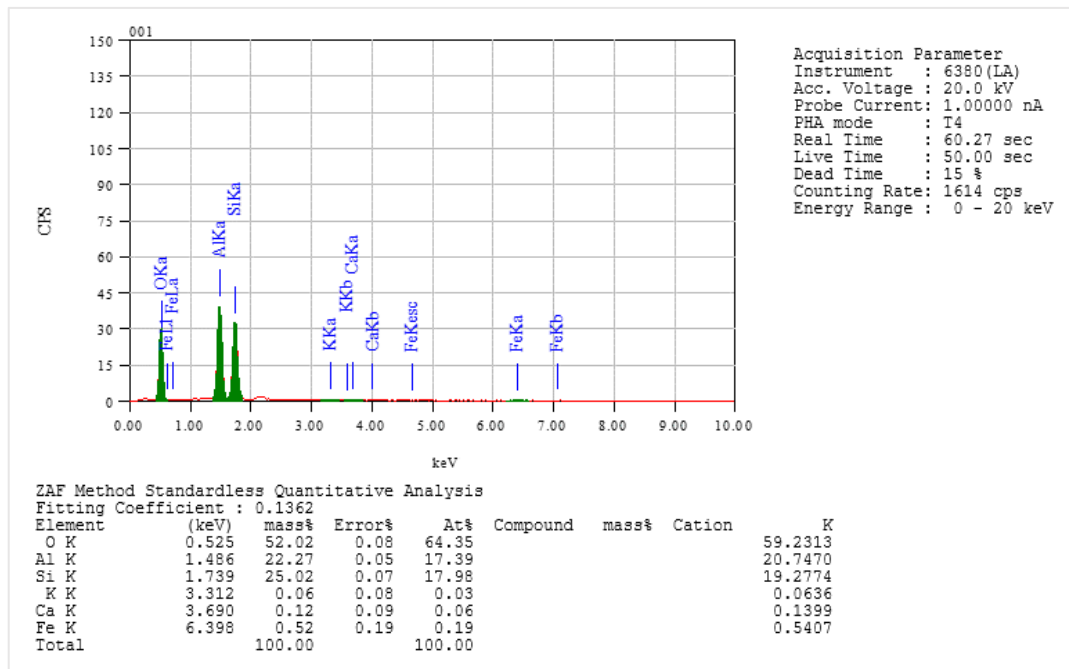


Figure 3.10 Results of EDAX conducted on sample S1

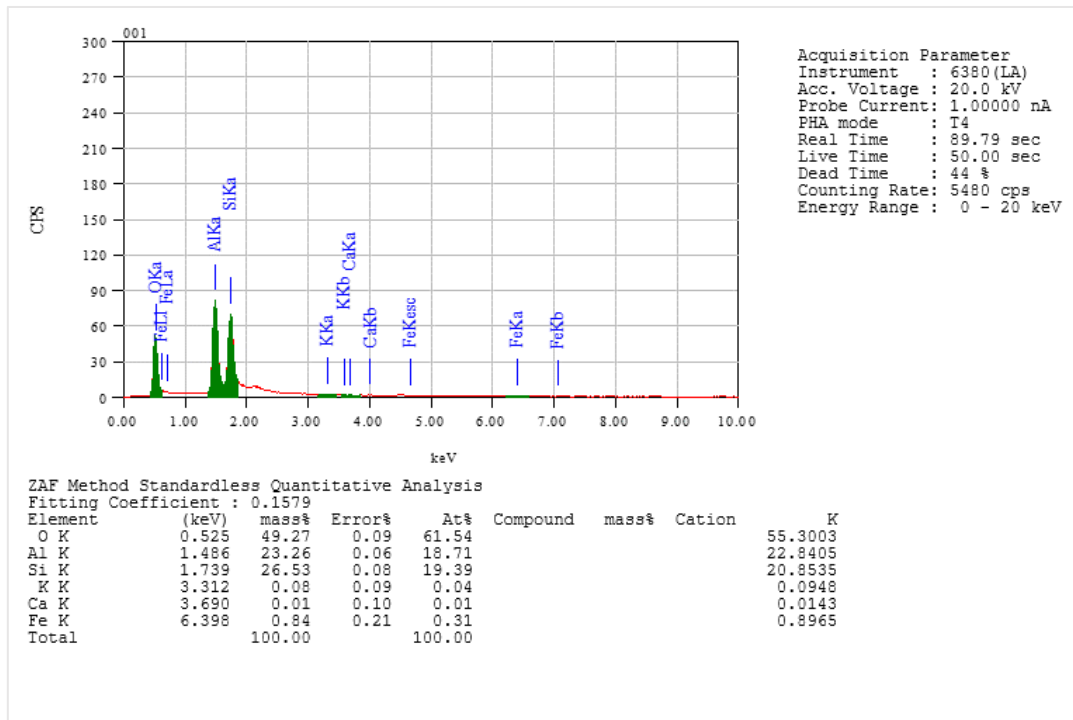


Figure 3.11 Results of EDAX conducted on sample S2

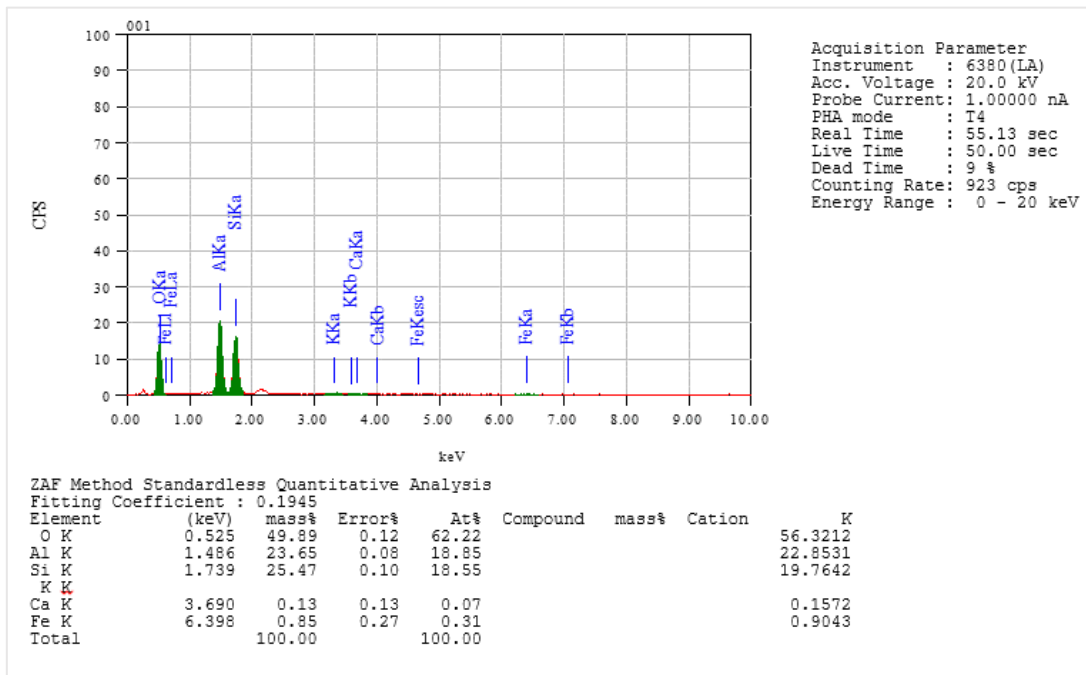


Figure 3.12 Results of EDAX conducted on sample S3



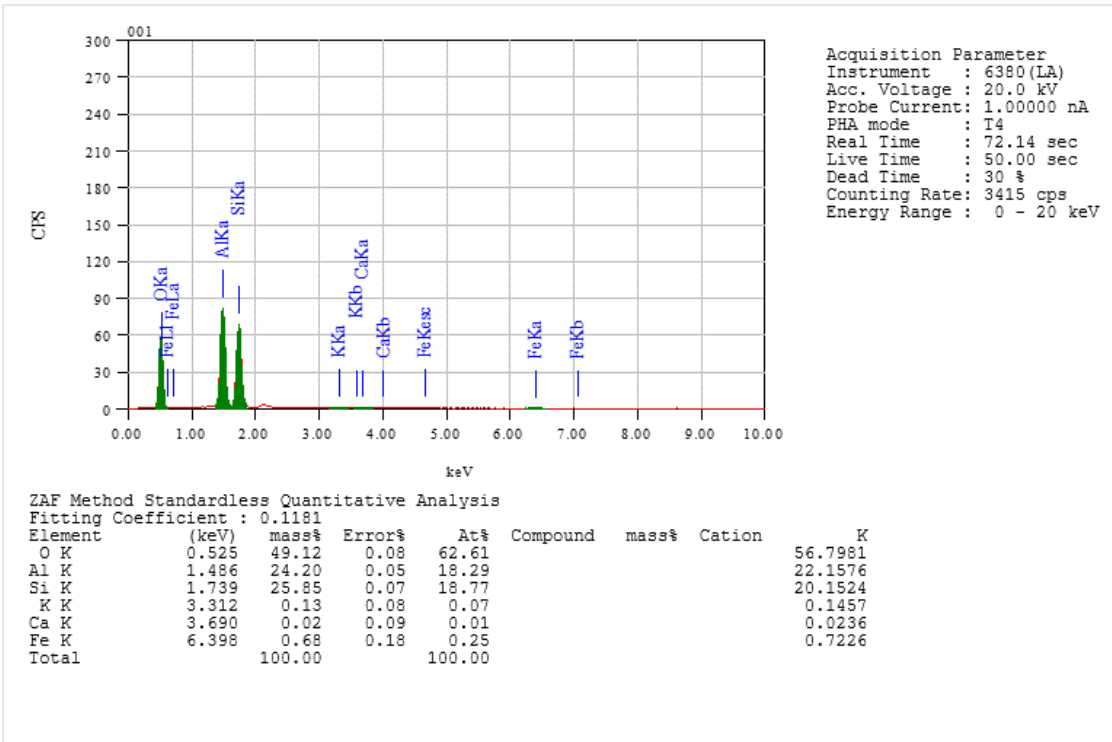


Figure 3.13 Results of EDAX conducted on sample S4

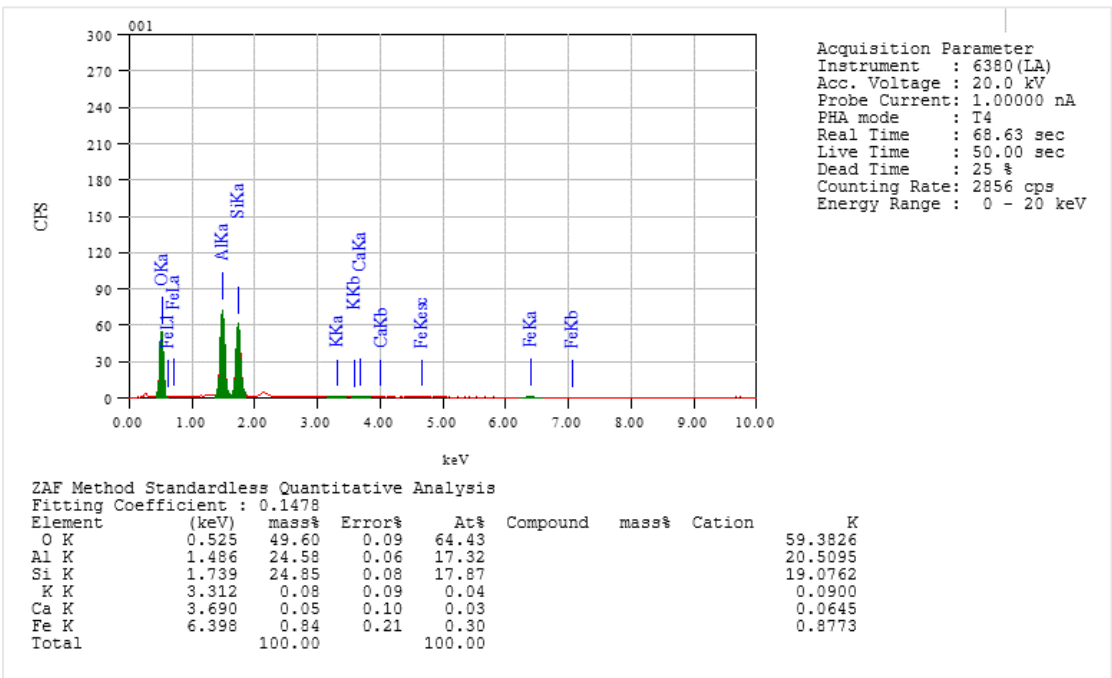


Figure 3.14 Results of EDAX conducted on sample S5

Table 3.3 Summary of elemental composition present in shedi soil and their blends

Sample designation	Al ions (mass %)	Si ions (mass %)	K ions (mass %)	Ferric ions (mass %)	Ca ions (mass %)
S0	19.02	18.13	0	0.64	0.10
S1	22.73	26.08	0.09	0.63	0.09
S2	23.26	25.02	0.06	0.52	0.12
S3	22.27	24.43	0.13	0.38	0
S4	23.65	24.73	0.18	0.87	0.05
S5	24.87	25.47	0	0.85	0.13

### 3.5.3 Correlations of Geotechnical Parameters with Soil Electrical Resistivity

#### 3.5.3(a) Soil Resistivity with Moisture Content

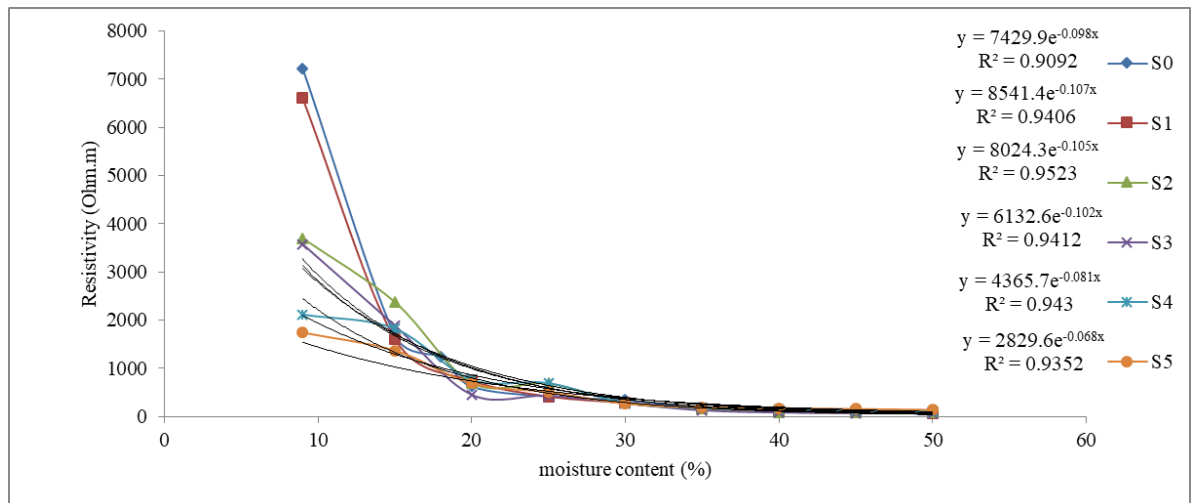


Figure 3.15 Variation of moisture content with resistivity for the six soil samples

The variations of resistivity with moisture content for the six different soil samples are presented in Fig 3.15. The  $R^2$  values vary from 0.86 to 0.9915. It is seen that the rate of reduction in resistivity is very high at lower water contents, and it decreases with increase in water content. It reaches to a saturation phase of resistivity, from where further increase in water content cause negligible reduction in resistivity. The

discontinuity of pore water causes an extremely high resistivity in the materials on the dry side of optimum. The continuity of pore water can be obtained for water content higher than the plastic limit which is almost 'adsorbed water content'. This results in a relatively lower resistivity value at higher water content (Bhatt and Jain, 2014). Beyond 30% moisture content, all samples have almost same low resistivity. Resistivity-moisture content relationship is discussed in detail in Chapter 8.

### **3.5.3(b) Resistivity- dry density relationships**

The variation of resistivity with dry density at fixed moisture content of studied soil samples are presented in Figs. 3.16 to 3.21. It was found that soil resistivity decreased with increase of density for all types of soil samples. Soil resistivity decreased almost linearly with an average reduction of 897.35 ohm-m for an increase of dry density from 1.3 to 1.45 g/cc at 9% moisture content for the six samples. The least variation in soil resistivity was observed in soil sample F with 50% river sand for the same condition. Soil resistivity decreased at an average reduction of 296.88 Ohm-m at 18% moisture content with an increase of dry density from 1.3g/cc to 1.45g/cc. Whereas, the average reduction in soil resistivity was only 27.27Ohm-m at 30% moisture content. Therefore, the variation in soil resistivity with density was not substantial at high moisture content. However, soil resistivity did not show remarkable changes for further increase in dry density at the three moisture contents for any of the samples.

An increase in degree of saturation is associated with the increase in density. More pronounced bridging occurs between the particles at high degree of saturation. In addition, increase of density is associated with remoulding of clay clods, elimination of interclod voids and reorientation of particle. Therefore, soil resistivity decreases with the increase of density (Abu Hassanein et al., 1996).

However, test results showed that soil resistivity was more sensitive to moisture content compared to density. The average rate of reduction in soil resistivity with the increase of dry density from 1.3 to 1.45 g/cc is presented in Table 3.4.

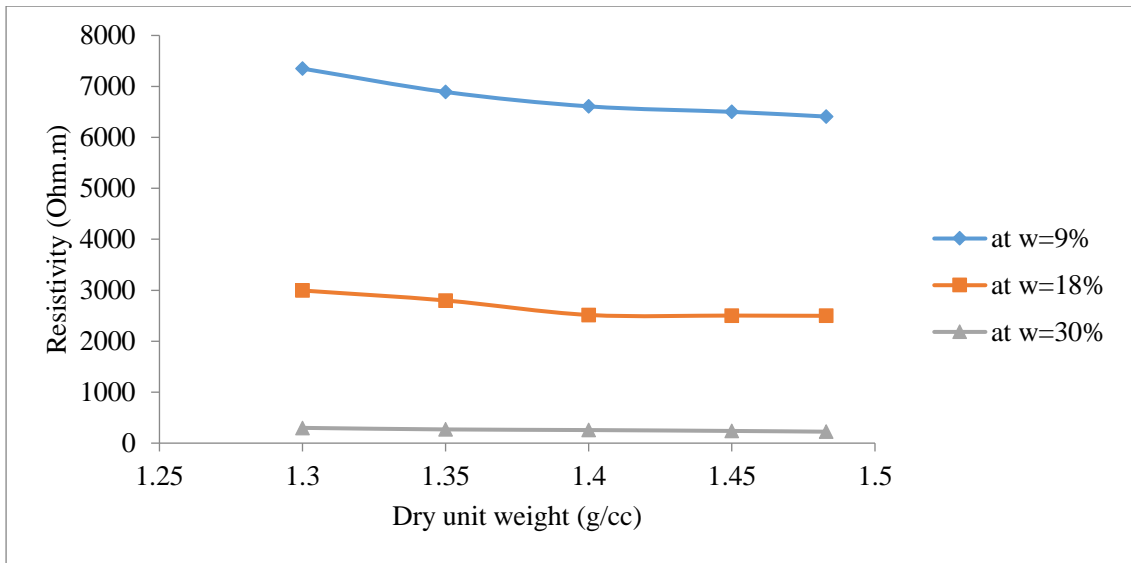


Figure 3.16 Comparison of the effect of moisture content and density with soil resistivity for Sample S0

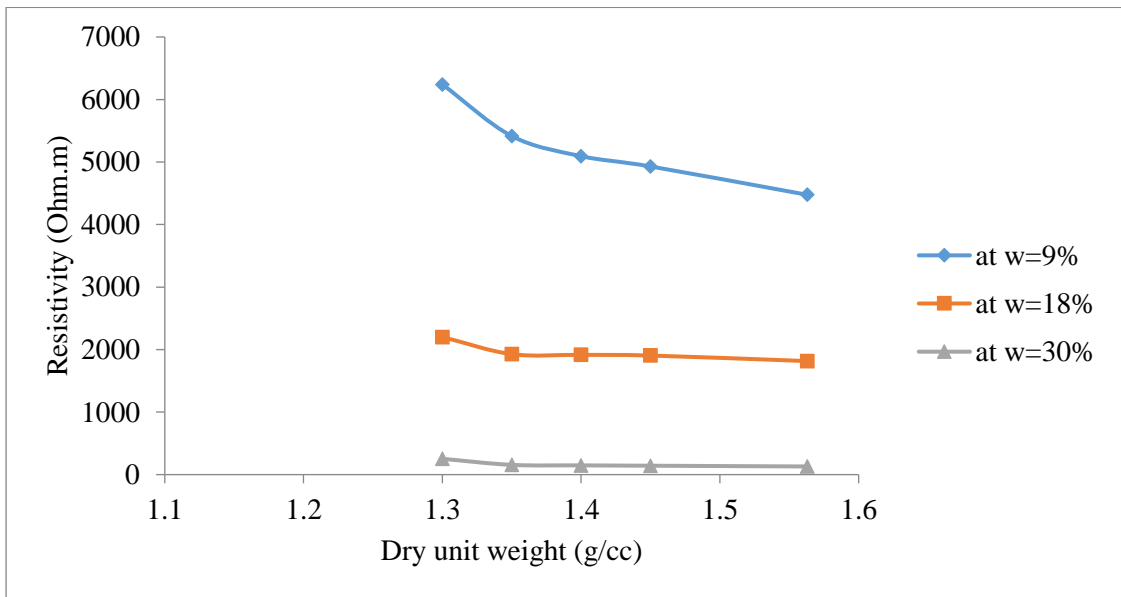


Figure 3.17 Comparison of the effect of moisture content and density with soil resistivity for Sample-S1

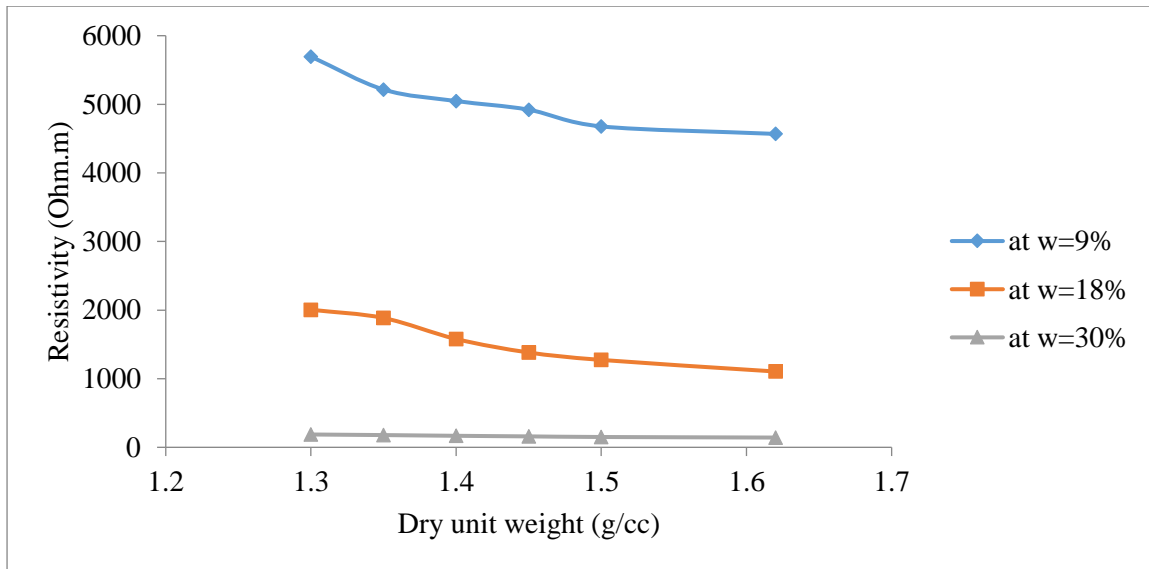


Figure 3.18 Comparison of the effect of moisture content and density with soil resistivity for Sample-S2

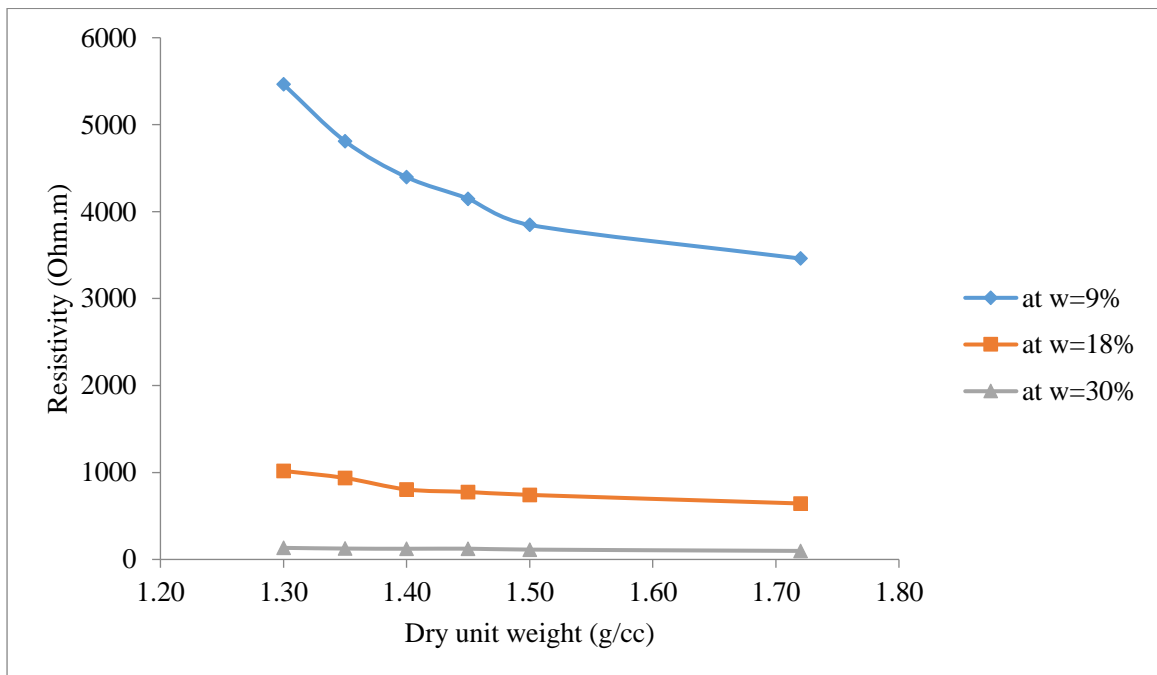


Figure 3.19 Comparison of the effect of moisture content and density with soil resistivity for Sample-S3

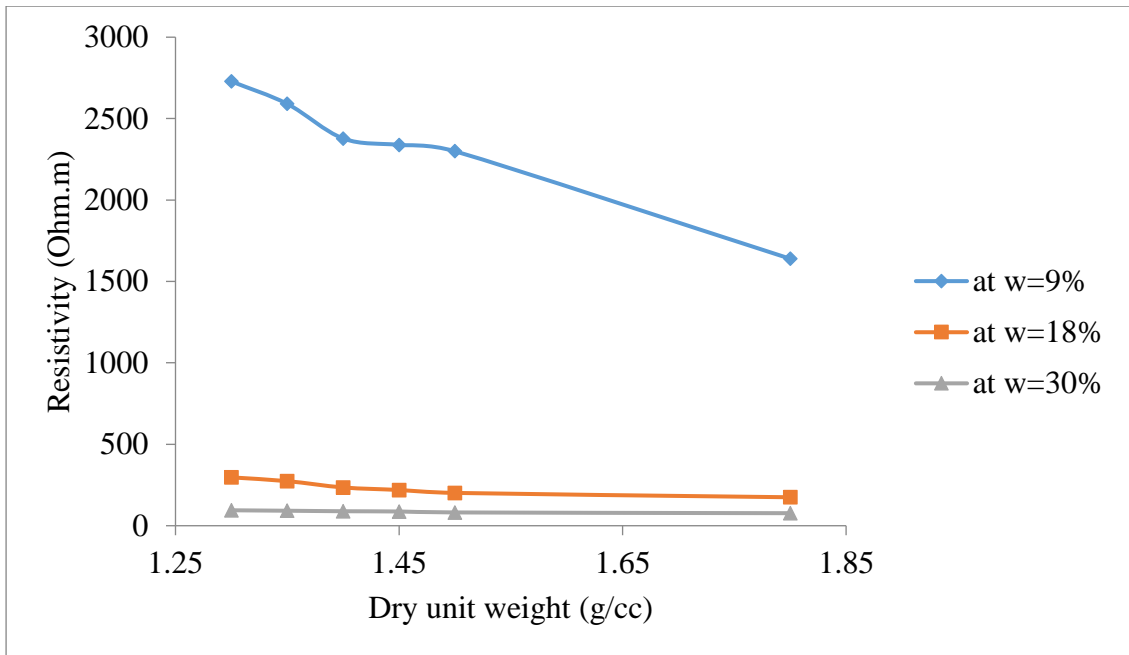


Figure 3.20 Comparison of the effect of moisture content and density with soil resistivity for Sample-S4

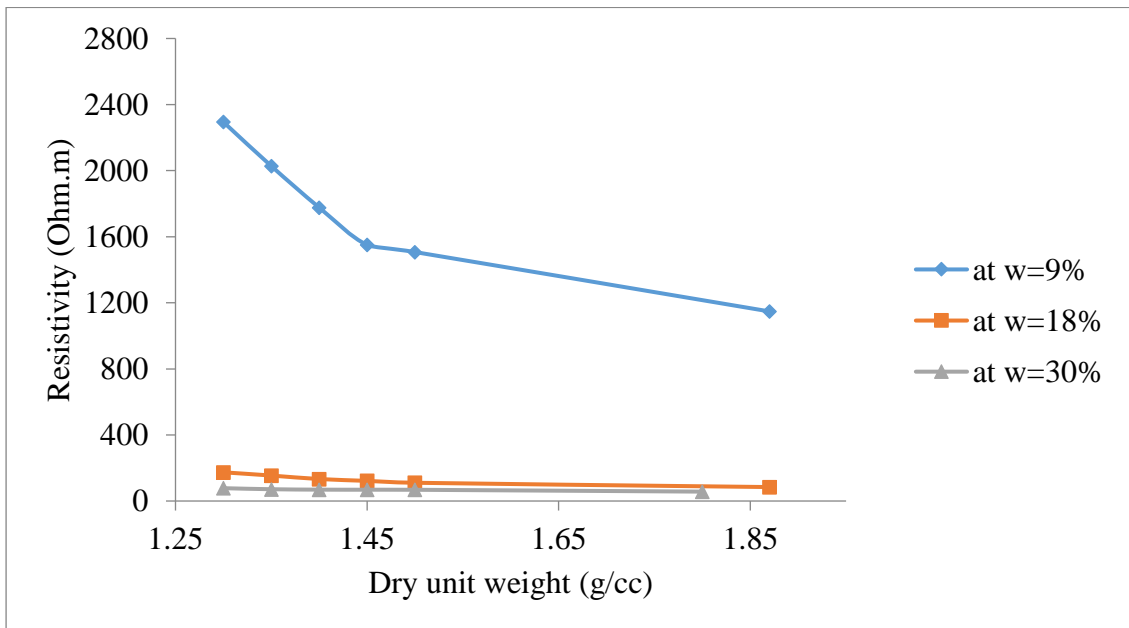


Figure 3.21 Comparison of the effect of moisture content and density with soil resistivity for Sample-S5

### 3.5.3(c) Effect of degree of saturation on soil resistivity

The water content and density of soil can be combined to a single geotechnical parameter called degree of saturation. The variation of soil resistivity with degree of saturation is presented in Fig. 3.22 for all the soil samples. It was observed that soil resistivity decreased with increase of degree of saturation with  $R^2$  value ranging from 0.89 to 0.97 when fitted with polynomial regression model. Degree of saturation increases with the increase of water content or dry density (Abu-Hassanein, 1996).

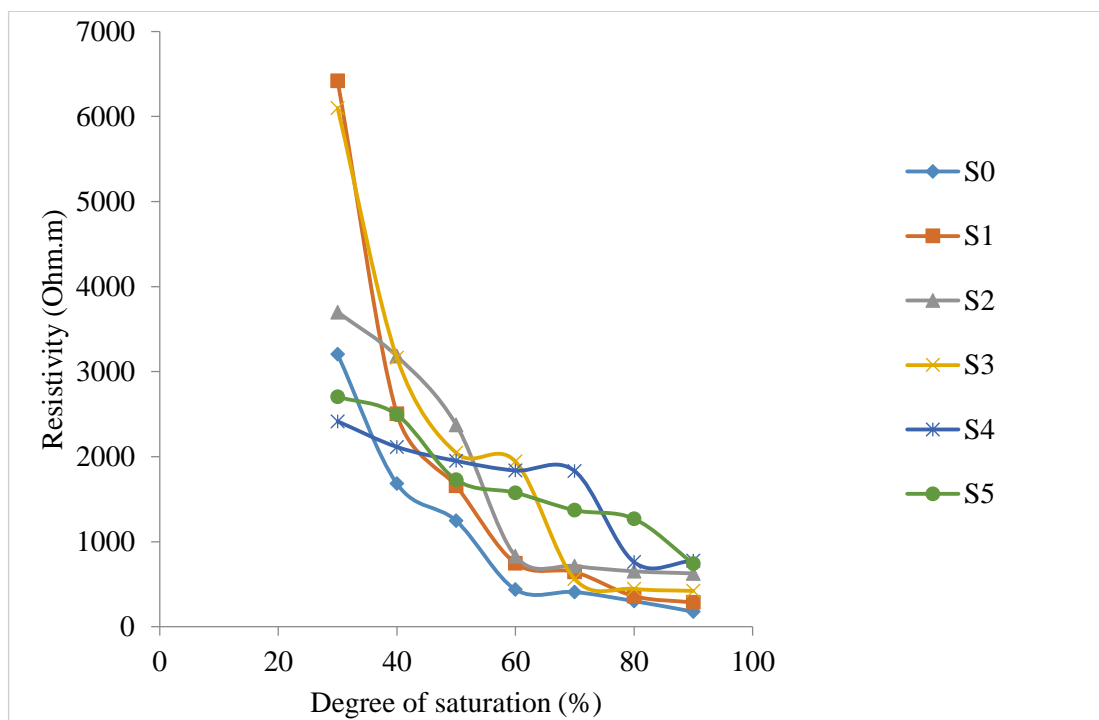


Figure 3.22 Variation of degree of saturation on soil resistivity

Average soil resistivity was 4089.9 Ohm-m at 30% degree of saturation. However, average soil resistivity decreased to 505.62 Ohm-m at 90% degree of saturation. Increase in degree of saturation yields changes in clay clods, reduction in interclod macro voids and orientation of clay particles. Therefore, soil resistivity decreased with the increase in degree of saturation.

### 3.5.3(d) Correlation of Electrical resistivity with Porosity

The relationship between electrical resistivity of saturated and partially saturated soil and porosity were studied and are shown in Fig. 3.23. The following relation was obtained for the saturated soil, which agrees very well with the Archie's law (1).

$$\rho_o/\rho_w=an^{-m} \quad (3.6)$$

where  $\rho_o$ , is the electrical resistivity of saturated soil and  $\rho_w$  is the electrical resistivity of pore fluid. As proposed by Archie (1942),  $m$  and  $n$  are constants which depend on the type of soil or rock.  $\rho_o/\rho_w$  is the called the formation factor, which is the normalized ER of saturated soil, normalized with ER of pore fluid. For the current study with lateritic soils, i.e. lithomargic clay blended with different percentages of river sand, the cementation factor ‘ $m$ ’, is about 1.642 and ‘ $a$ ’ is 0.0099.

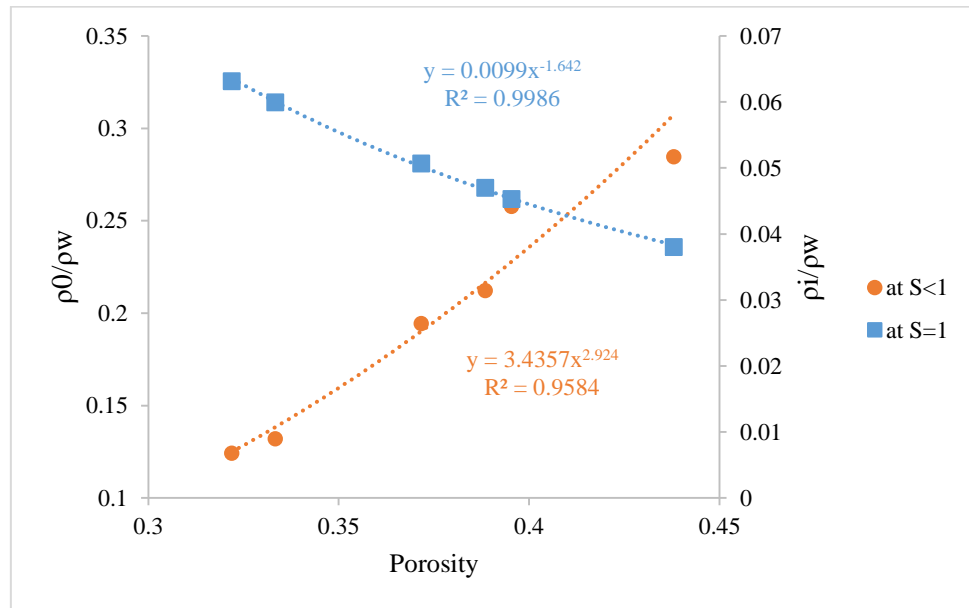


Figure 3.23 Variation of normalized ER of saturated and partially saturated soil with porosity for all the six soil samples (S0 to S5)

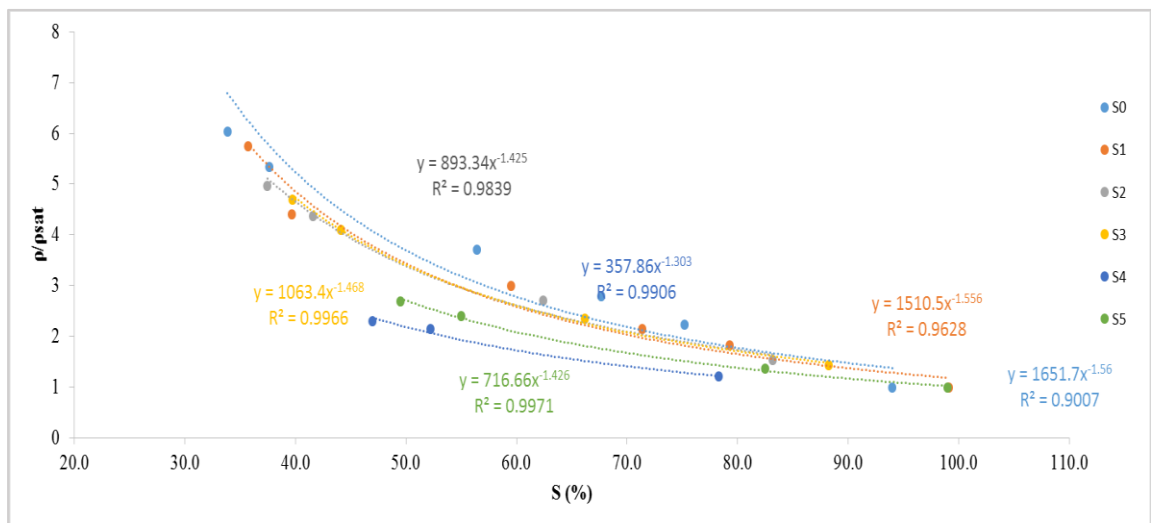


Figure 3.24 Relationship between  $\rho_o/\rho_{sat}$  and degree of saturation



From Fig. 3.23, for partially saturated soil, as the porosity increases, more air will be entrapped in the soil pores, which attribute to higher electrical resistance. Hence  $\rho_i/\rho_w$ , (which is the normalized ER of the unsaturated soil, normalized with ER of pore fluid) bears a direct positive relation with partially saturated soil porosity. The following relation was obtained for the partially saturated soil.

$$\rho_i/\rho_w = an^m \quad (3.7)$$

where  $\rho_i$  is the partially saturated soil electrical resistivity,  $\rho_w$  is the pore fluid electrical resistivity. 'a' in case of partially saturated soils is about 3.4357 and 'm' is 2.924.

The electrical resistivity of unsaturated soil  $\rho$  can be related to that of saturated soil  $\rho_{sat}$  as follows: (Archie, 1942)

$$\rho/\rho_{sat} = S^{-n} \quad (3.8)$$

where 'n' is an empirical parameter, close to 2, for clean unconsolidated sands and for consolidated sands.

Abu-Hassanein et al. (1996) proposed that the above equation (3.8) is applicable when the degree of saturation is above a critical value  $S_{cr}$  which corresponds to the minimum amount of water required to maintain a continuous film of water surrounding the solid particles. An abrupt increase in electrical resistivity occurs when the degree of saturation falls below  $S_{cr}$ .

The relationship between electrical resistivity of unsaturated soil to that of saturated soil was also studied and plotted (Fig 3.24). The following empirical relation was developed.

$$\rho/\rho_{sat} = AS^{-B} \quad (3.8)$$

where A and B are empirical constants which depend on the soil type. 'A' is between 300 and 1600 and 'B' is close to 1.5.

### **3.5.3(e) Effect of percentage of fine fraction on electrical resistivity at saturated and partially saturated states**

Soil resistivity tests were conducted on all the soil samples at 9%, 18% (partially saturated) and 30% moisture content (fully saturated) and 1.3 g/cc dry density for the different soil samples. Test results showed that soil resistivity was dependent on

fine fraction for the soil samples as seen in Fig. 3.25. It is observed that soil resistivity increases significantly with increase of percent fines especially at 9% moisture content for a dry density of 1.3 g/cc.

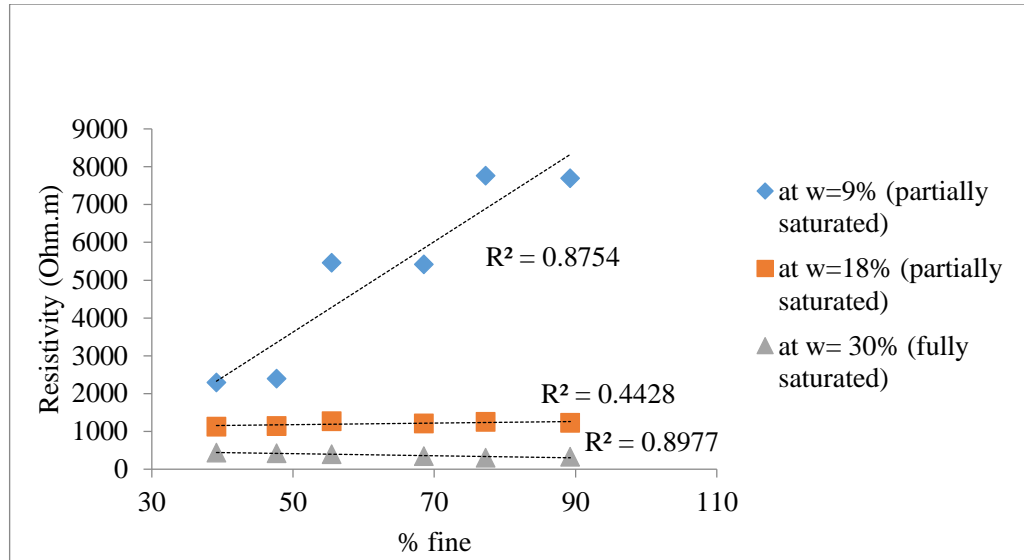


Figure 3.25 Variation of electrical resistivity of soil with its percentage of fine at saturated and partially saturated states

Specific surface area of soil particles increases as percentage of fines increases. As the surface area increases, more water is required for the formation of continuous water film around fine particles. In the absence of continuous water film, bridging between soil particles is not possible to occur. In addition, even though conductive clay content is present, ionic conduction does not take place without proper water bridging between soil particles. Hence at undersaturated conditions, the increase of percentage of fines would result in increase in electrical resistivity in lateritic soils as a result of greater specific surface area.

However, there is a decrease in soil resistivity at 30% moisture content and 1.3 g/cc dry density with an increase in percent fines (Fig. 3.24). At this stage all the soil samples are fully saturated. Soils with high percentage of fine content are often composed of more conductive clay particles (Abu-Hassanein et al. 1996). Therefore, soil resistivity may decrease with increase in fine content at fully saturated conditions, since continuous film of water will be maintained along the inter-aggregate voids which facilitate ionic conduction. Thus, the most influential factors for soil resistivity are moisture content and density.

### 3.5.3(f) Resistivity vs Light Compaction

Standard Proctor compaction tests were conducted to generate compaction curve. Parallely, resistivity of the soil samples was measured at corresponding moisture content and dry density (Figs. 3.26 to 3.31). Optimum moisture content and dry density of different soil samples are presented in Table 3.2.

Soil resistivity tests were conducted at moisture content and dry density corresponding to compaction curve in each sample. Test results showed that resistivity was high when compacted at dry side of optimum. With increase of moisture content and dry density, resistivity decreased significantly. At wet side, soil resistivity was low. The test results are presented in Fig. 3.25 to Fig. 3.30. Therefore, soil resistivity was independent of moulding water content and dry density at wet of optimum. High dry density and near saturated pores increases electrical conductance (Abu Hassanein et al., 1996).

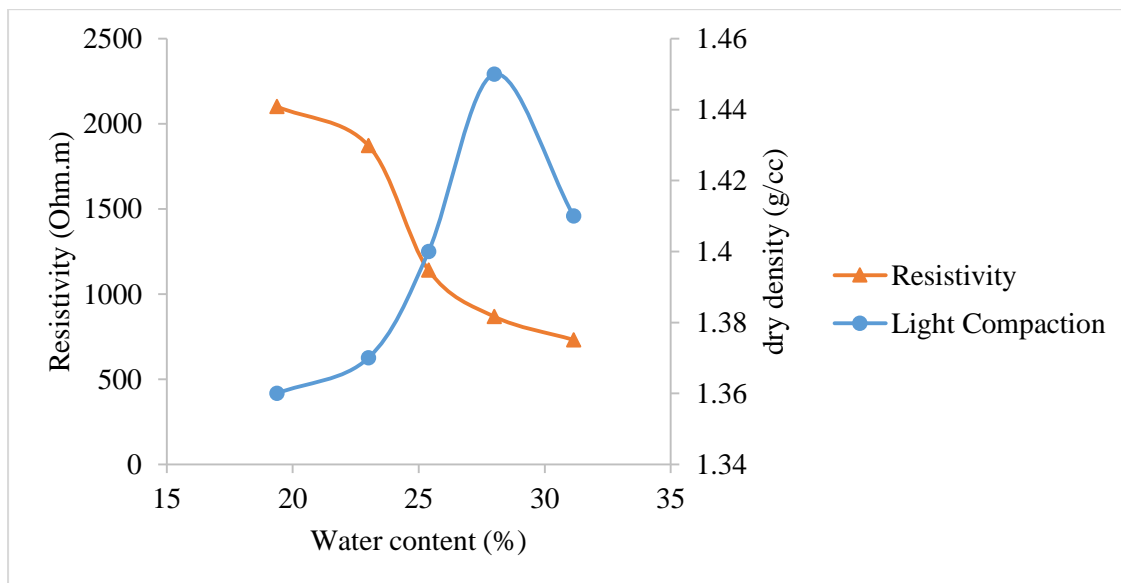


Figure 3.26 Variation of resistivity at different points on light compaction curve from dry to wet side for sample S0

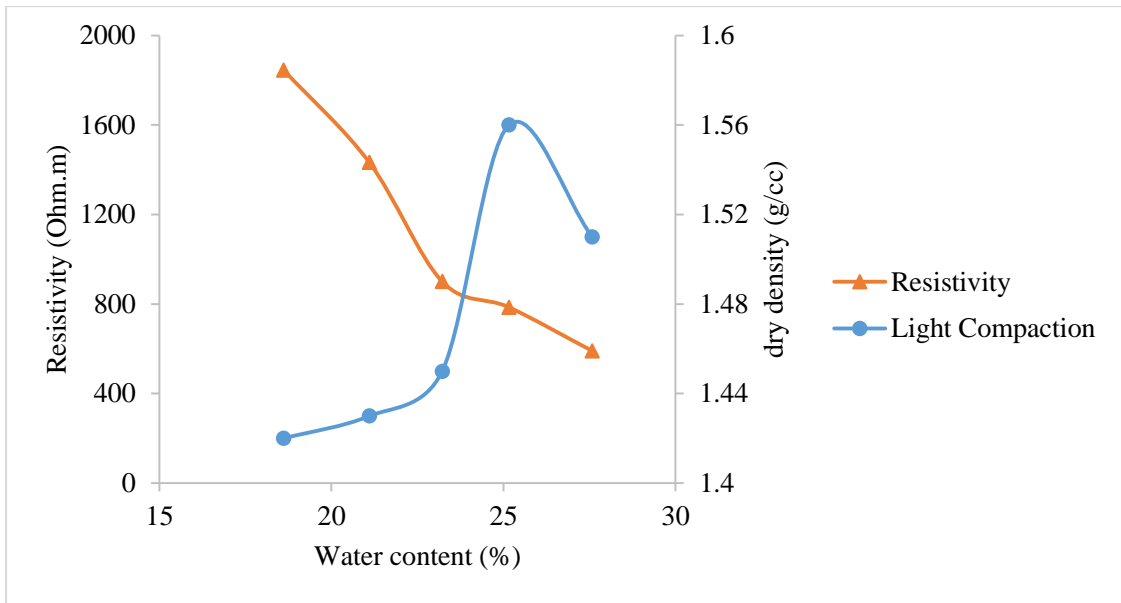


Figure 3.27 Variation of resistivity at different points on light compaction curve from dry to wet side for sample S1

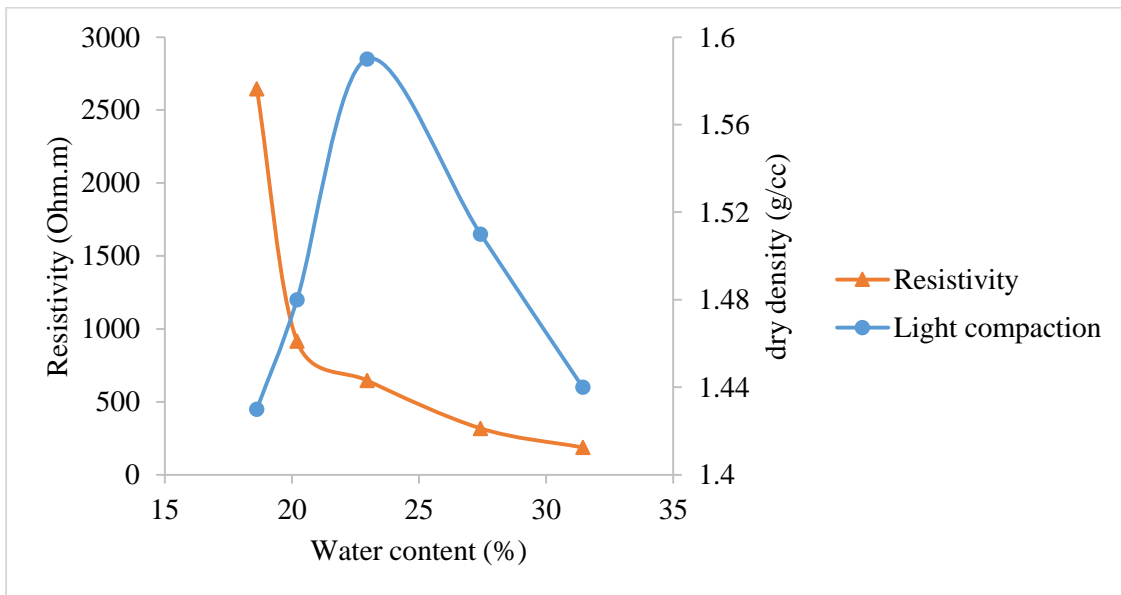


Figure 3.28 Variation of resistivity at different points on light compaction curve from dry to wet side for sample S2

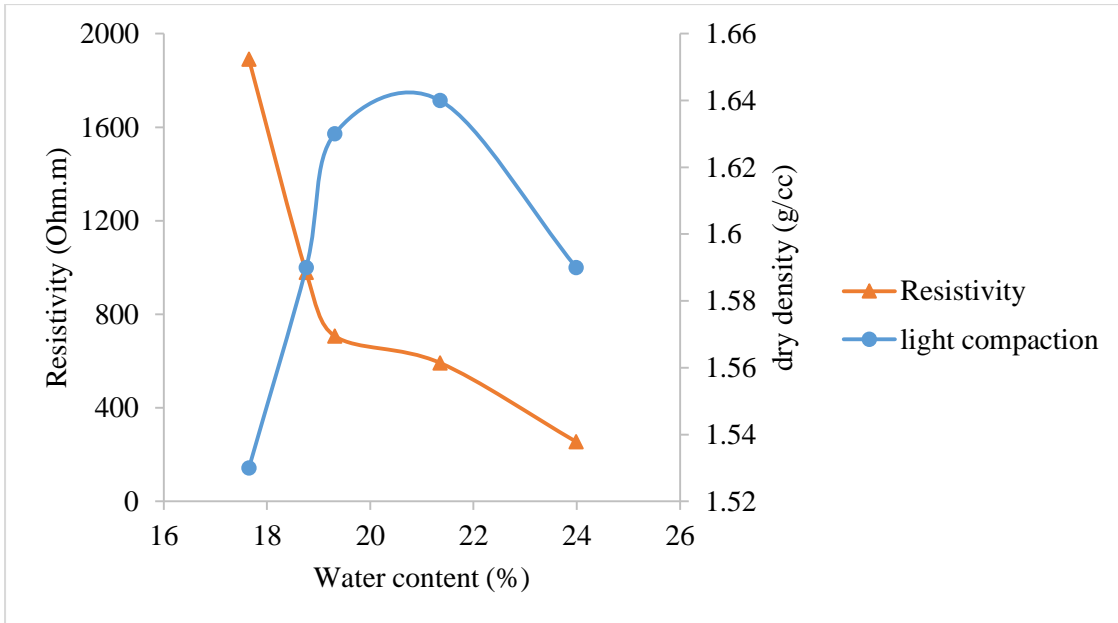


Figure 3.29 Variation of resistivity at different points on light compaction curve from dry to wet side for sample S3

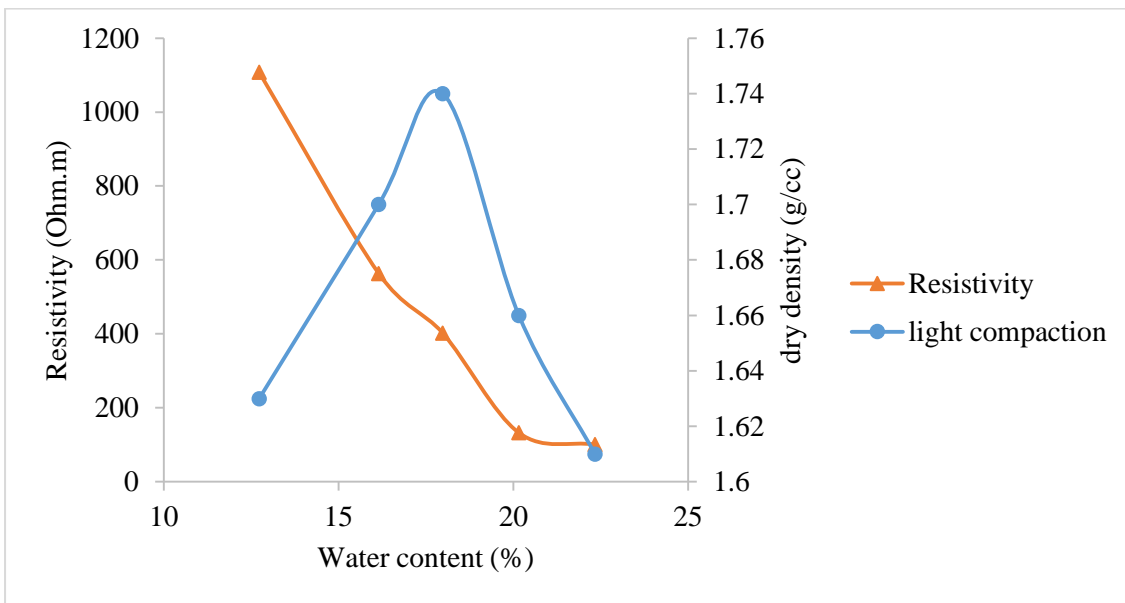


Figure 3.30 Variation of resistivity at different points on light compaction curve from dry to wet side for sample S4

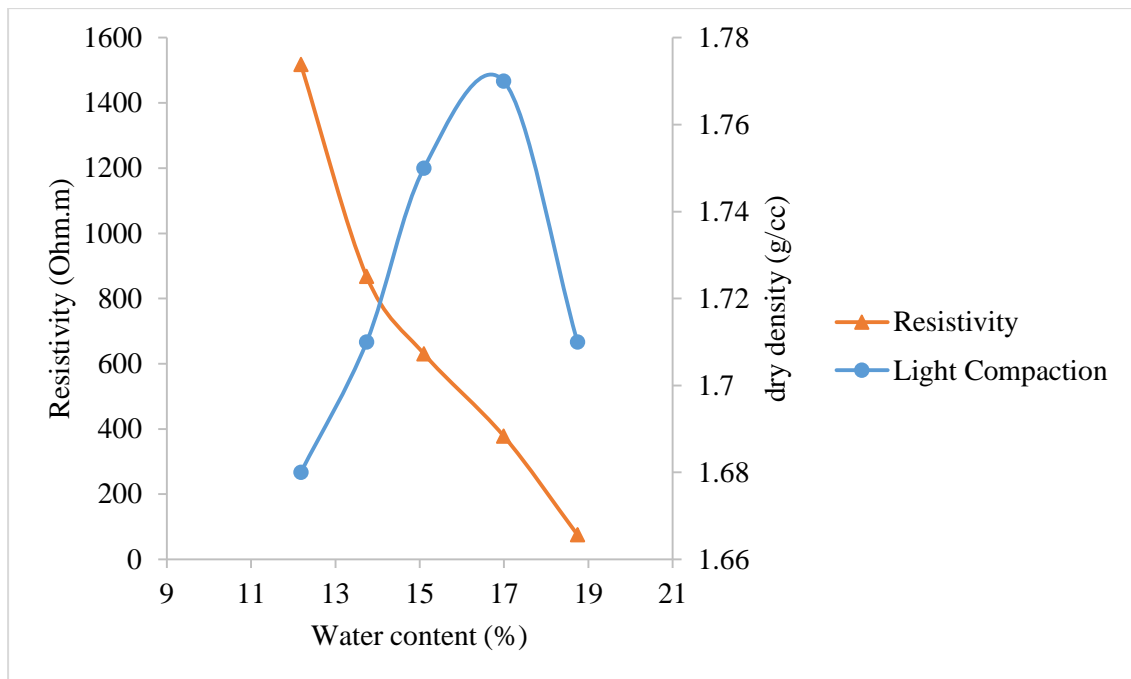


Figure 3.31 Variation of resistivity at different points on light compaction curve from dry to wet side for sample S5

### 3.5.3(g) Variation of Resistivity with heavy compaction

Modified Proctor compaction tests were conducted to generate compaction curve. Parallely, resistivity of the soil samples was measured at corresponding moisture content and dry density. Optimum moisture content and dry density of different soil samples are presented in Table 3.2.

Soil resistivity tests were conducted at moisture content and dry density corresponding to compaction curve in each sample (Figs. 3.32 to 3.37). Test results showed that similar to light compaction, resistivity was higher when compacted at dry side of optimum. With the increase of moisture content and dry density, resistivity decreased significantly. At wet side, soil resistivity was low. But as shown in Figs. 3.31 to 3.40 as the degree of compaction increases, the soil become less resistive to the electric flow as it attains a denser arrangement such that soil grains are in better contact and provides continuous water film for conduction.

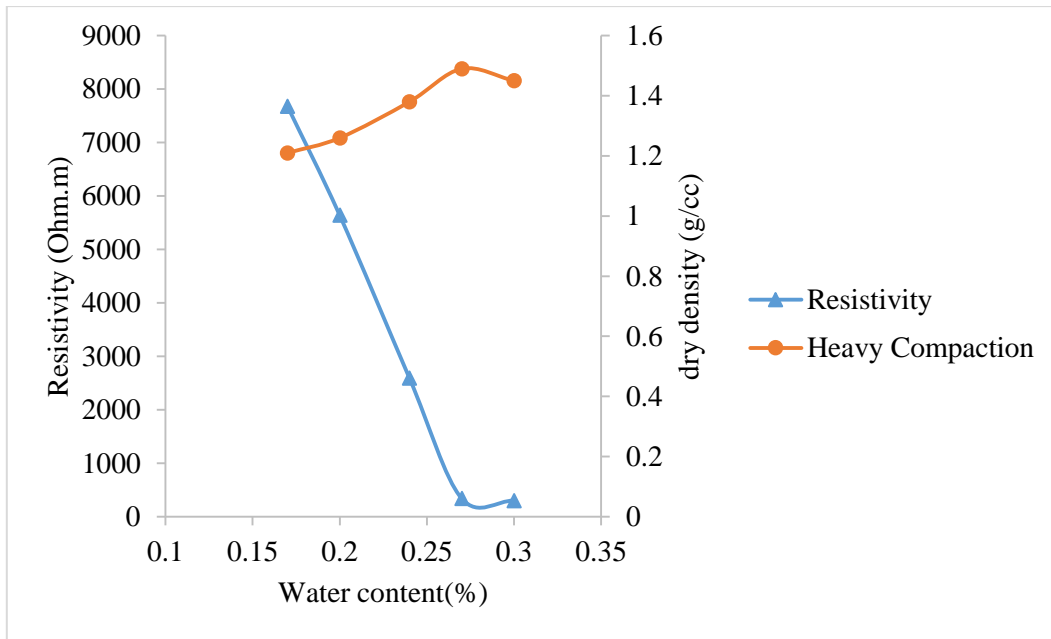


Figure 3.32 Variation of resistivity at different points on heavy compaction curve from dry to wet side for sample S0

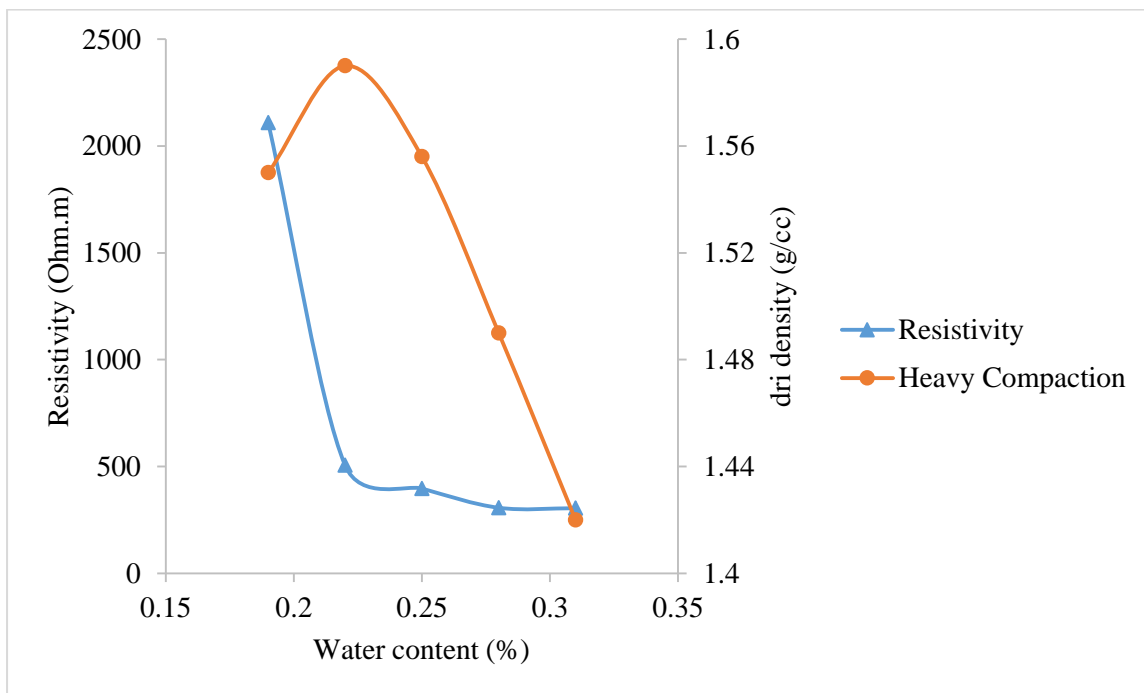


Figure 3.33 Variation of resistivity at different points on heavy compaction curve from dry to wet side for sample S1

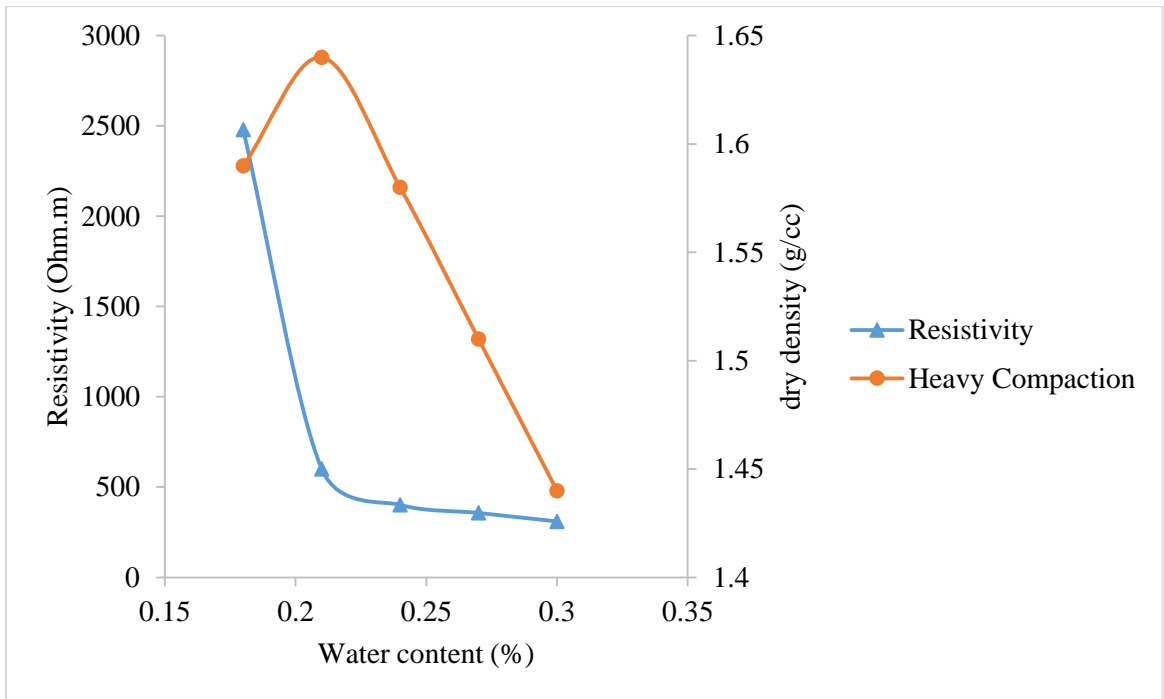


Figure 3.34 Variation of resistivity at different points on heavy compaction curve from dry to wet side for sample S2

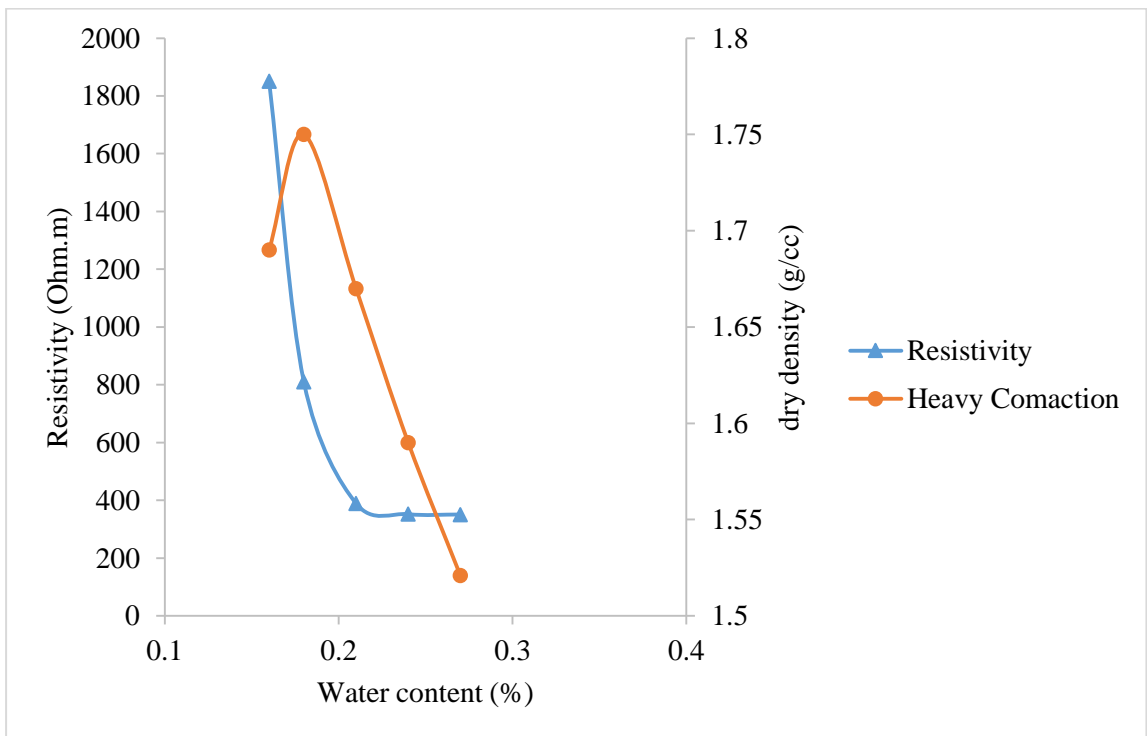


Figure 3.35 Variation of resistivity at different points on heavy compaction curve from dry to wet side for sample S3



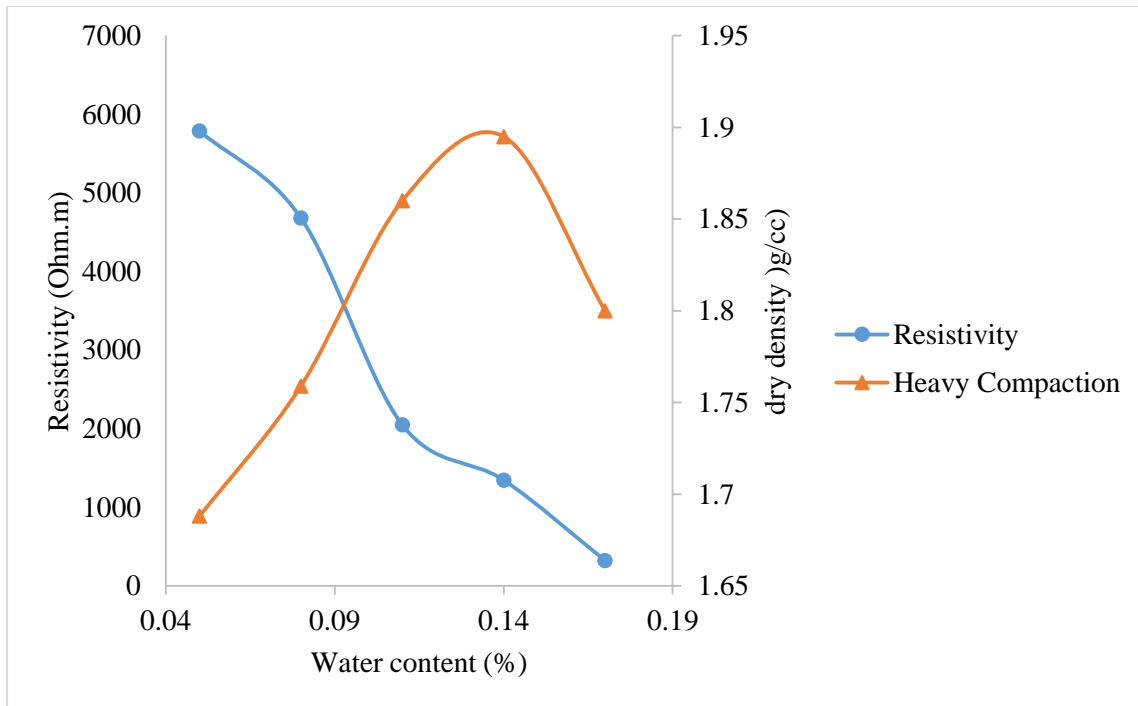


Figure 3.36 Variation of resistivity at different points on heavy compaction curve from dry to wet side for sample S4

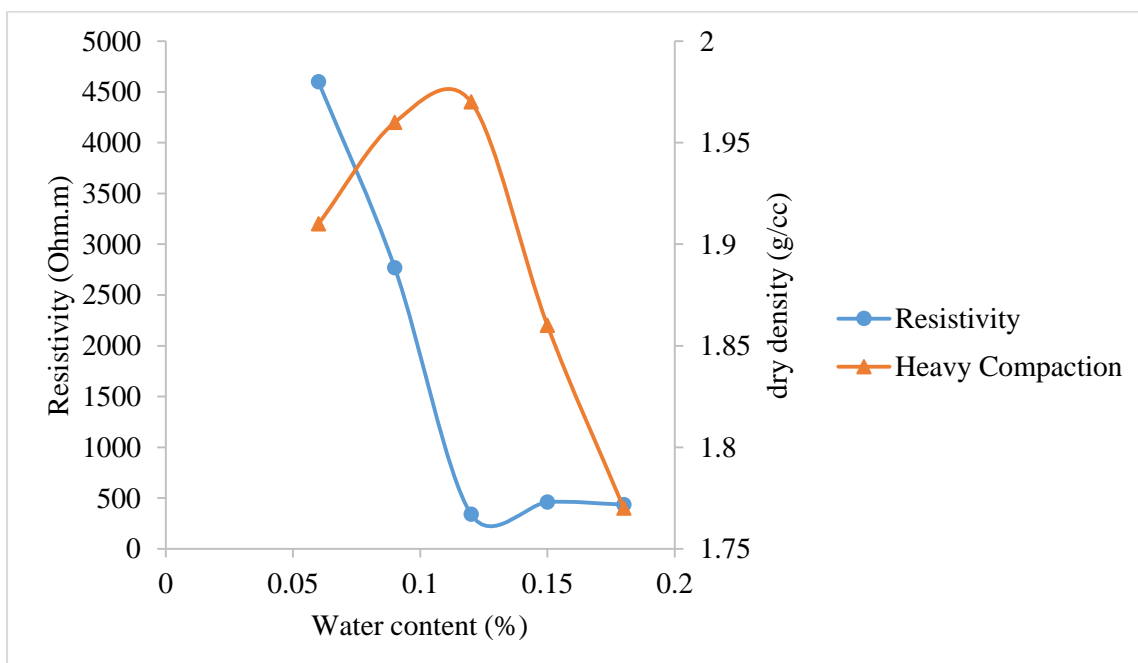


Figure 3.37 Variation of resistivity at different points on heavy compaction curve from dry to wet side for sample S5

### 3.5.3(h) Resistivity with compaction effort

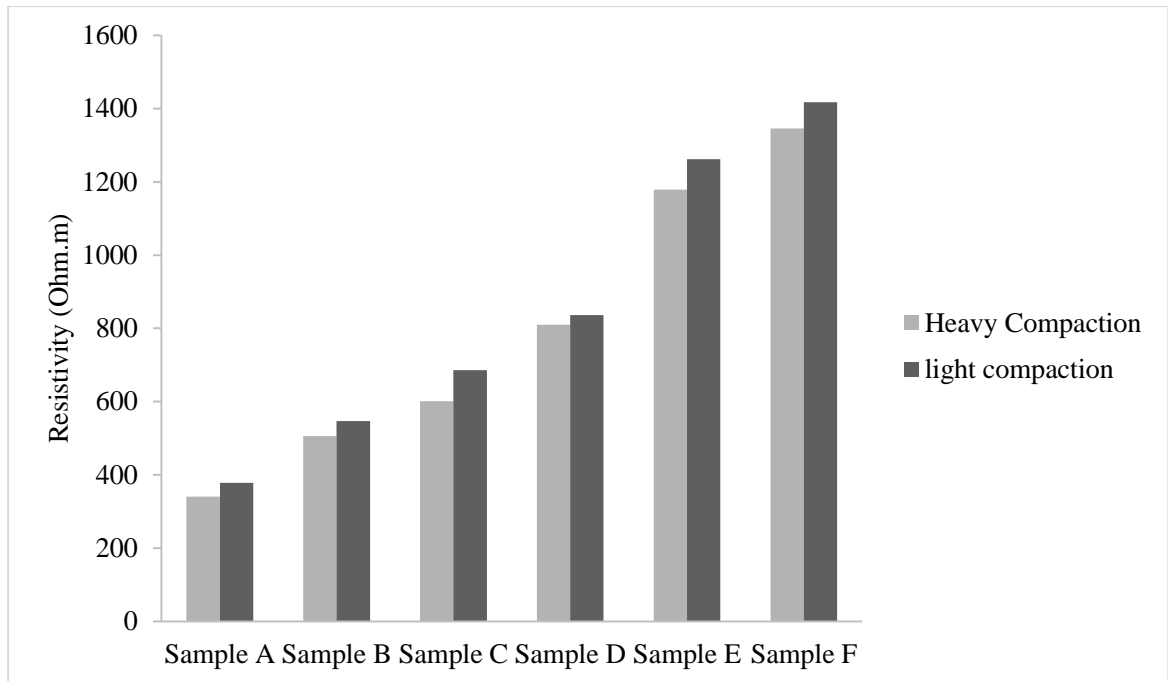


Figure 3.38 Comparison of variation of soil resistivity with light and heavy compaction

From Fig. 3.38, it is observed that the resistivities are comparatively lower for the soil samples compacted at heavy compaction conditions than those compacted at light compaction conditions. At heavy compaction conditions, soil attain a denser state with higher degree of saturation and lesser air voids, which results in a lower apparent resistivity of the soils.

### 3.5.3(i) Soil Resistivity with Elemental Composition

Summary of ionic composition in all the six soil samples is presented in Table 3.3. In order to study the cumulative effect of ion concentration on resistivity, multiple regression analysis was done on elemental concentration and resistivity of soil samples at 9%, 18%, 30% moisture content. The results showed perfect correlation of  $R^2=1$ . The multiple regression equation are as follows:

$$\text{Resistivity } (\rho_{30,9}) = 61.97Al - 29.98Si - 225.15K - 928.05Ca + 12.55Fe - 220.72$$

$$\text{Resistivity } (\rho_{18}) = -43.14Al + 24.08Si - 225.15K - 205.62Ca + 120.83Fe - 1713.91$$

### 3.5.3(j) Correlation of permeability with resistivity

Falling head permeability test was conducted to determine the permeability of the soil samples. The permeability thus measured is correlated with electrical resistivity (Fig.3.39). In ER test conducted in the laboratory, current was allowed to pass through the soil sample in horizontal direction. It is seen that as permeability increases i.e. as connectivity of pores increases, electrical conductivity increases and hence, the electrical resistivity decreases.

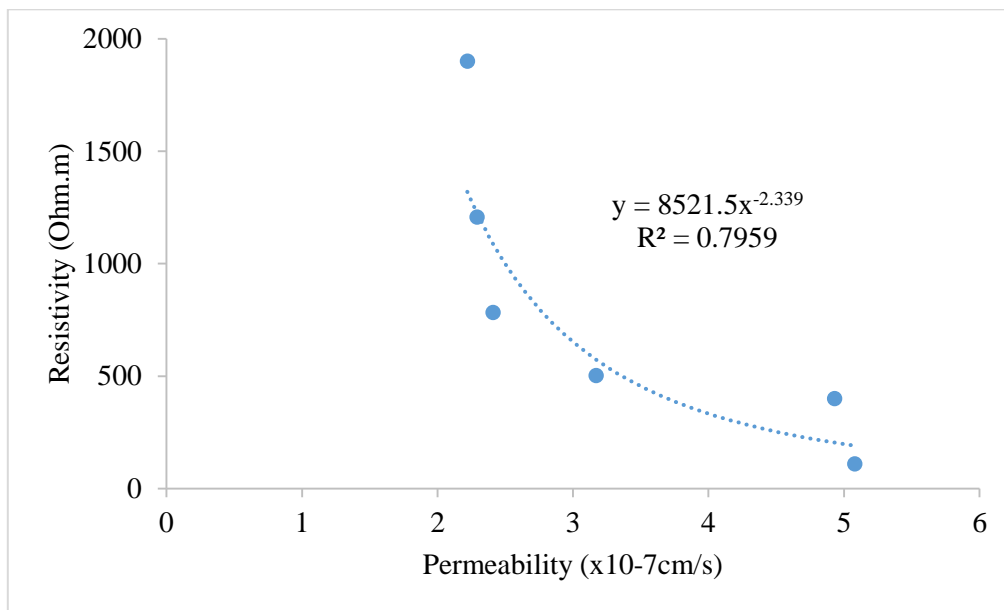


Figure 3.39 Variation of electrical resistivity with permeability

### 3.5.3(k) Correlation of Resistivity with Shear Strength parameters

Figures 3.40 and 3.41 show the correlation of electrical resistivity with the shear strength parameters of soil i.e. cohesion and angle of friction of soil respectively. The cohesion and friction angle were measured under total stress conditions. The results show that resistivity has got a direct positive relation with cohesion, ie, resistivity value increases with increasing cohesion (Fig. 3.40). This correlation is similar to the results of the resistivity study obtained by Razali and Osman (2011) with sand, silt and clay. Cohesion is a component of shear strength of soil, which is independent of interparticle friction and probably caused by electrostatic forces and/or cementation (bonding) at particle contacts.

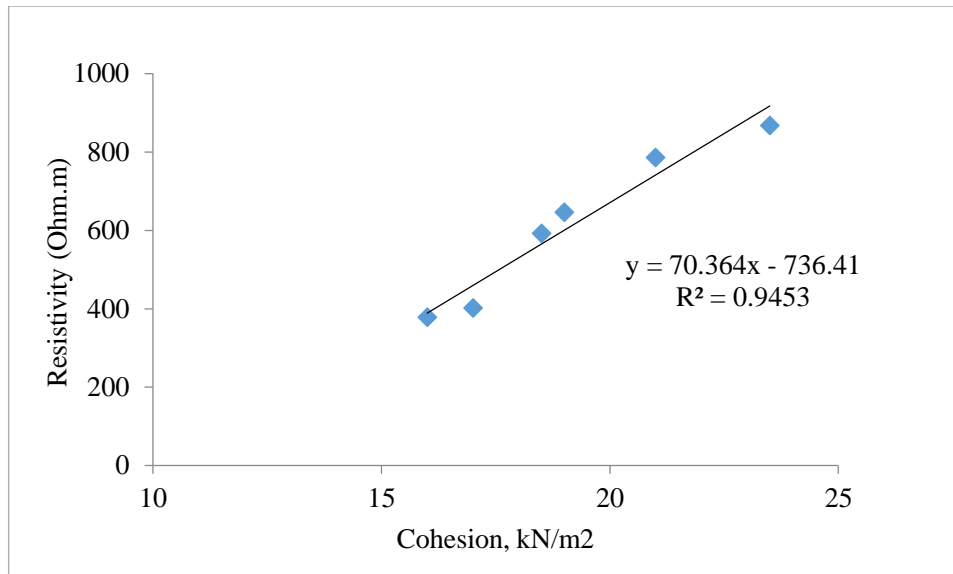


Figure 3.40 Variation of electrical resistivity with cohesion (at OMC and maximum dry density of soil)

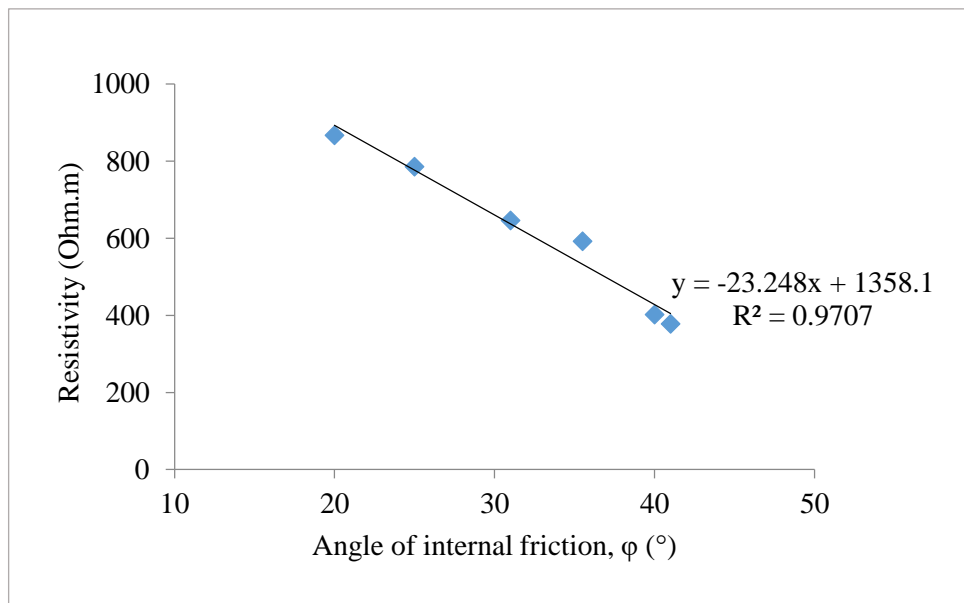


Figure 3.41 Variation of electrical resistivity with internal friction. (at OMC and maximum dry density of soil)

ER is found to have inverse correlation with angle of friction (Fig 3.41). This can be explained in following manner. It is seen from Fig.3.14 that, as percentage of sand increases ER values are found to decrease in the moisture content range of 10 to 25%. As percentage of sand content increases in the soil sample, its maximum dry density

increases (Table 3.2) and obviously compacted and denser soils will have a higher angle of internal friction. Optimum Moisture content of sample 'F' is 17%. In Fig. 3.40, the increase in angle of internal friction of soil samples is due to increase in sand content (decreasing porosity of soil at OMC i.e.  $S < 1$ ) resulting in increased maximum dry density. Therefore resistivity tends to decrease with increase in angle of internal friction ( $\phi$ ). Seladji et al (2010) also observed that soil resistivity decreases significantly with increase in density especially in drier soils. Increased density means higher compaction and higher angle of internal friction.

### 3.5.3(l) Correlation of Resistivity with Unconfined Compressive Strength (UCS)

Variation of soil resistivity with unconfined compressive strength is shown in Fig. 3.42.

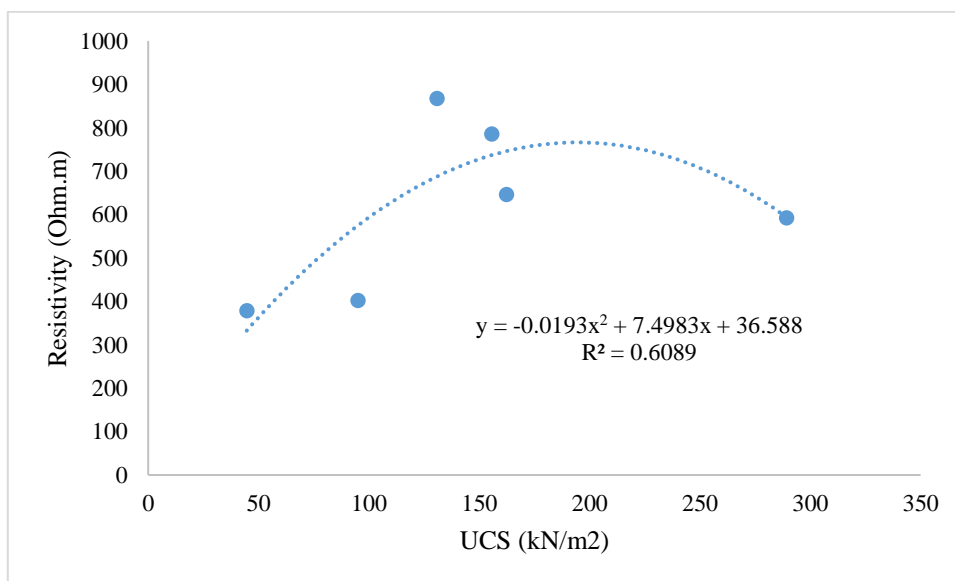


Figure 3.42 Variation of electrical resistivity with unconfined compressive strength (at OMC and maximum dry density of soil)

It can be seen that there does not exist a good correlation between them as  $R^2$  value is only 0.6089. As the percentage of sand increases, compressive strength increases initially. But beyond a certain percentage of sand (in this case, 30%) UCS will decrease. This is because soil being a particulate material, will tend to bulge

laterally due to lack of confinement (barreling and fragmentation will occur) during compressive loading in the unconfined compression test.

### 3.5.3(m) Correlation of Resistivity with CBR

California Bearing Ratio (CBR) test is a penetration test, commonly used for evaluation of strength of soil subgrades, in which the soil sample is confined. Figure 3.43 shows a very good correlation of ( $R^2=0.9649$ ) between California Bearing Ratio (CBR) and electrical resistivity. The relation is inverse, similar to relation of ER with  $\phi$ . Increase in percentage of sand increases CBR and decreases resistivity (as also seen in Fig. 3.42). The soil sample is confined on all sides while penetration loading.

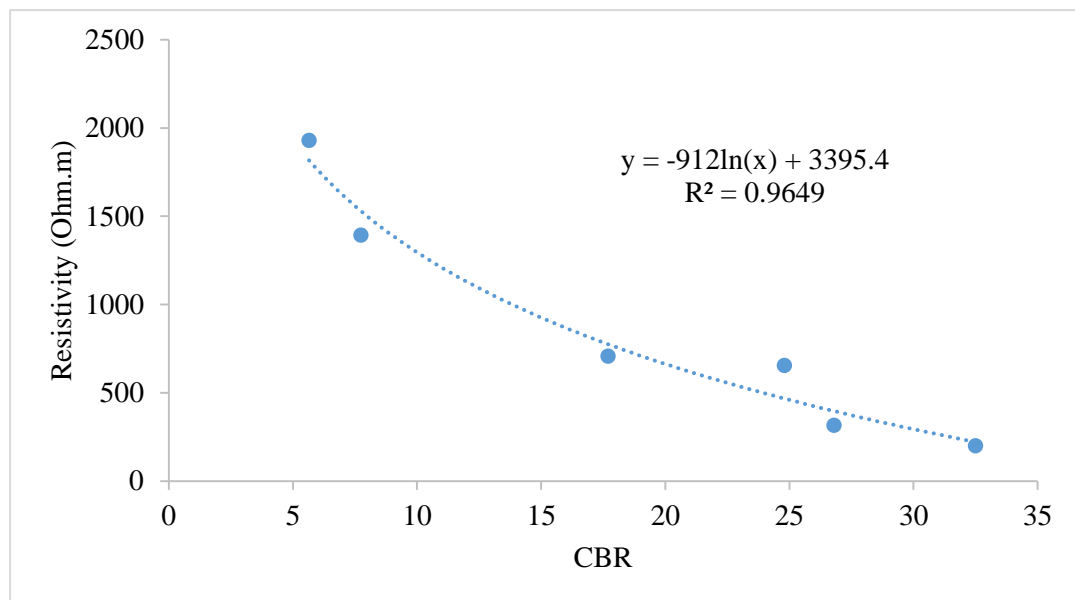


Figure 3.43 Variation of electrical resistivity with CBR (at OMC and maximum dry density of soil)

### 3.6 Summary

- The effect of various geotechnical parameters such as water content, dry density, porosity, degree of saturation, elemental composition and degree of compaction, in controlling the soil electrical resistivity is studied.
- Quantitative correlations between geotechnical and geo-electrical properties of lateritic soils, in regulated laboratory conditions are obtained. It is found that electrical resistivity bears positive correlation with cohesion and an inverse

correlation with angle of internal friction and CBR. Due to fragmentation of soil samples on compressive loading as the percentage of sand increase, UCS and ER are less correlated for the soil samples studied.

## **CHAPTER 4**

### **FIELD EXPERIMENTAL INVESTIGATIONS**

#### **4.1 Introduction**

Proper design and successful construction of any structure requires an accurate determination of the engineering properties of the soil at the site. Conventional laboratory experimental testing can be very costly and take a long time when dealing with large number of soil samples. Geotechnical engineers have realized the importance of geophysical methods for subsurface explorations. Geophysical method involving electrical resistivity, seismic, ground penetrating radar, etc have been increasingly applied in site investigation. Geophysical method applies the principles of physics in studying the earth such as resistivity, velocity, density, magnetic susceptibility, etc. Geophysical method has been able to produce good efficiency due to the cost, time and data coverage. The electrical measurement method is one of the non-destructive geophysical methods which can be applied both in the laboratory and in the field. Investigators and engineers working in various fields such as mining, geotechnical, civil and underground engineering have commonly used the electrical measurement technique.

From among all the geophysical methods that could be used to characterise soils, electrical resistivity method is chosen because the resistivity of soil materials ranges over several orders of magnitude allowing them to be distinguished optimally. For each type of material, however, the resistivity can vary considerably. It depends on several parameters that are not homogeneous like, the geological characteristics of the site (depth and nature of the bedrock), the physical characteristics of the soil materials (particle size, porosity and intrinsic resistivity of minerals) and the water content. Thus, geophysical techniques need to be carefully adapted and developed for this purpose. In order to obtain the sub-surface profile (bore hole logs), it is imperative to interpret field vertical electrical soundings (VES) data to derive true resistivities and thicknesses of various subsurface strata. Identification of the different soil materials is not possible on the basis of resistivity data alone, However, correlation with outcrops and/or pits is essential.



The soils and rocks are essentially nonconductive, except some metallic ores. The electrical conduction in electrolytic solutions, moist soil and water bearing rocks takes place as a result of the movement of ions. The ability to transmit ions is governed by the electrical resistivity property of the materials and has been demonstrated to be an effective predictor of various soil properties including salinity, porosity and water content. For soils, as we have seen in the previous Chapter, electrical resistivity depends on many factors such as porosity, electrical resistivity of the pore fluid, composition of the solids, degree of saturation, particle shape, orientation, and pore structure. The basic principle of the soil investigation with electrical resistivity is that when a constant voltage is applied to one of the two probes placed in the soil the current that flows between the probes is inversely related to the resistance of the soil. Electrical resistivity shows strong variations that principally depend on soil water content variations.

#### **4.2 Laterites and Lateritic Soils**

The study area is National Institute of Technology (NITK) campus, Surathkal which lies in the coastal belt of Karnataka in India. The lateritic formations in the area, consists of the top hard and porous lateritic crust (typically 1 to 3m thick), underlain by lateritic soils (typically 5 to 8m thick) underlain by the parent rock which is generally hard granitic gneiss. Figure 4.1 shows a typical lateritic formation. The top lateritic crust, being porous, has less water retention capacity and considerable strength (compared to strength of general soils). Strength-wise they fall under category of hard soils or soft rocks. The compressive strength of top laterite in this area varies from about 0.45 MPa to about 2.2 MPa in soaked condition, and from about 0.6 MPa to about 4.0 MPa in dry condition when loaded perpendicular to the rift (Shivashankar et al. 2016). Lateritic soils are generally lithomargic clays which are products of tropical weathering or lateritization. These soils (called locally as shedi soils) behave like dispersive soils. They are generally classified as silty sands or sandy silts, with very little or no cohesion, and are also highly erosive by nature when not confined. Lateritic soils can be either lateritic lithomarges having a larger percentage of lithomargic clays or lithomargic laterites with a larger percentage of gravelly laterites and less of lithomargic clays. Lateritic lithomarges and lithomargic clays are very sensitive to moisture variations, some chemical effluents and lack of confinement (Shivashankar et al. 2015). With such

varied differences in their texture, porosity and strength, these laterites and lateritic soils make an interesting subject for studying their electrical resistivity variations and correlating with their geotechnical parameters.



Figure 4.1 Lateritic formations (Shivashankar et al. 2016)

### 4.3 Electrical Resistivity Method

The electrical resistivity measurement is done by applying a direct or alternating current between two electrodes and the difference of potential between two other electrodes implanted in the ground that do not carry current is measured (Fig 4.2). Usually the potential electrodes are in line between the current electrodes but in principle they can be located anywhere. The theory and field methods used for resistivity surveys are based on the use of direct current, because it allows greater depth of investigation than alternating current (AC) and it avoids the complexities caused by effects of ground inductance and capacitance and resulting frequency dependence of resistivity. The electrical resistivity measurements work well in both resistive sediments, such as gravels and sands, as well as conductive sediments like silt and clay. Figure 4.2 shows the potential distribution beneath ground for the resistivity setup.

Resistivity surveys are conducted as either soundings or profiles. A sounding is used to determine changes in resistivity with depth while profiling method is employed for investigating its change up to a depth involved in longitudinal direction. The

electrode spacing is varied for each measurement, but the centre point of the array is kept constant. There are various electrode configurations which can be used in resistivity surveying. Where the ground is uniform, the resistivity should be constant and independent of both electrode spacing and surface location. The true resistivity of the subsurface is obtained if it is homogeneous. When subsurface inhomogeneities exist, the resistivity will vary with the relative positions of the electrodes. The calculated value is called apparent resistivity. The apparent resistivity measured by the array depends on the geometry of the electrodes. In general, all field data are apparent resistivity. They are interpreted to obtain the true resistivities of the layers in the ground.

#### **4.4 Vertical Electrical Soundings (VES)**

Signal Stacking Resistivity meter manufactured by Integrated Geo Instruments Services Ltd. (IGIS), Hyderabad was used to measure the electrical resistivity (Fig 4.2 and 4.3). In the present investigation Schlumberger electrode arrangement was employed and the following electrode separations ( $AB/2=L$ ) were used 0.5, 1, 1.5, 2, 2.5, 3, 3.5, 4, 4.5, 5, 6, 7, 8, 9, 10, 12, 14, 16, 18, 20, 25, 30, 40, 50m. Care was taken such that the potential electrode distance is not more than one-fifth the current electrode distance (Eve et al. 1954).

Electrodes were driven into the ground vertically. The apparent resistivity and the corresponding apparent depth was given by the resistivity meter for each electrode separations. The potential electrode separation was increased when the signal became too feeble to be detected. The apparent resistivities were interpreted using inverse slope software in which true resistivity is given by the inverse slopes of line segments formed in graph plotted between  $AB/2$  and  $(AB/2)/\rho_a$ . The x-coordinates of the intersection points in the curve gave depth of the interface.

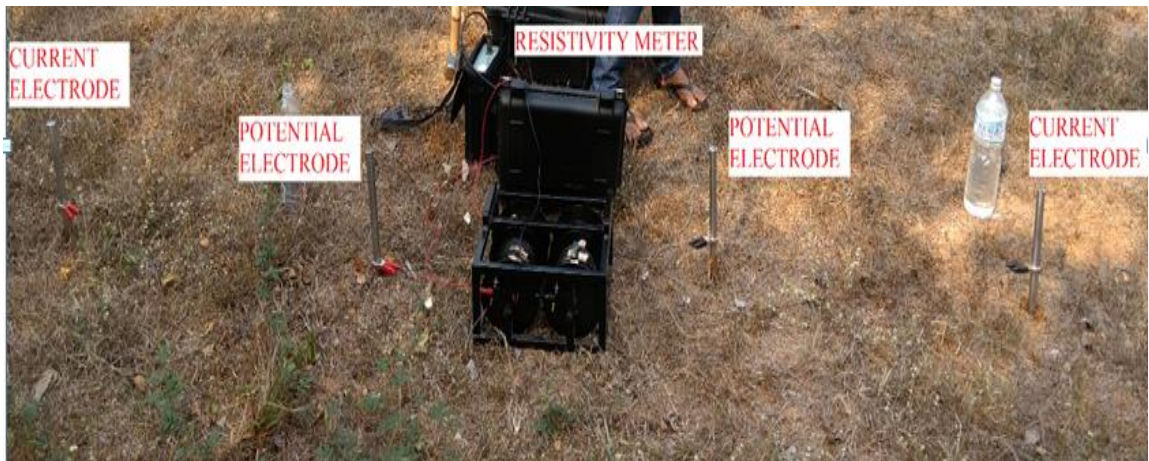


Figure 4.2 Field resistivity measurement setup



Figure 4.3 Resistivity meter

#### **4.5 Interpretation of the Apparent Resistivity data**

The interpretation of the apparent resistivity data at each location was made using Inverse Slope Software developed by IGIS.

#### **4.6 Standard Penetration Test (SPT) and Borehole sampling**

SPT tests were conducted at 14 selected locations in the NITK campus on eastern and western side of the campus. The borehole locations are shown in Fig. 4.6. Disturbed soil samples were collected and visual identification of soil type was done (as shown in Fig 4.7(b) to 4.20(b)).

## 4.7 Results and Discussions

Vertical electrical soundings were conducted at the same 14 locations where SPT was conducted (Fig 4.4). Schlumberger arrangement of electrodes was used. Apparent Electrical Resistivity values were measured using high precision Signal Stacking Resistivity meter (given in Appendix). The apparent resistivity values thus measured were interpreted using IGIS “inverse slope” software. Thus true resistivity, thickness and depth of each soil layer were obtained at all these 14 locations.

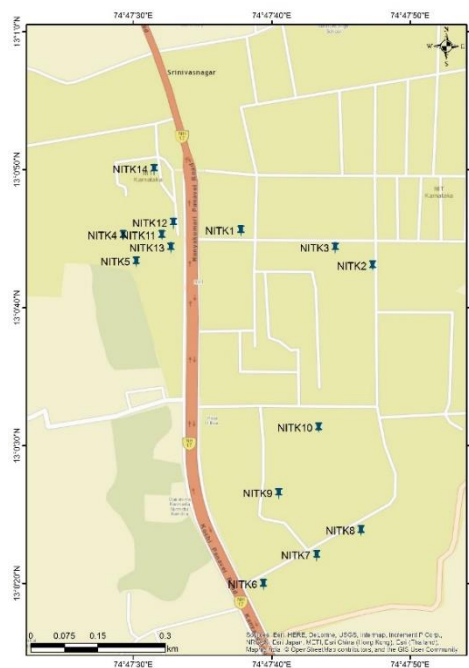


Figure 4.4 Borehole and VES locations

### 4.7.1 Correlation of SPT (N) with Electrical Resistivity(ER)

The SPT numbers (N) and the resistivity values in ohm.m. were plotted and correlation was checked. The results are presented in Fig. 4.5 and Fig. 4.6.

It is seen that at 10 of the 14 borehole locations (Fig. 4.5), there exists good correlation between SPT and Electrical Resistivity. Considering the unexplained uncertainties and complexities of nature in field investigations, the correlations obtained are relatively good and are consistent with the results from previous studies. Electrical resistivity of soil primarily depends on ions concentration in pore fluid, mineral composition of the soil, pore tortuosity (the continuity of the electrical

current path), bulk density, state of compaction of the soil strata, degree of saturation and the surface charges of the soil solid particles.

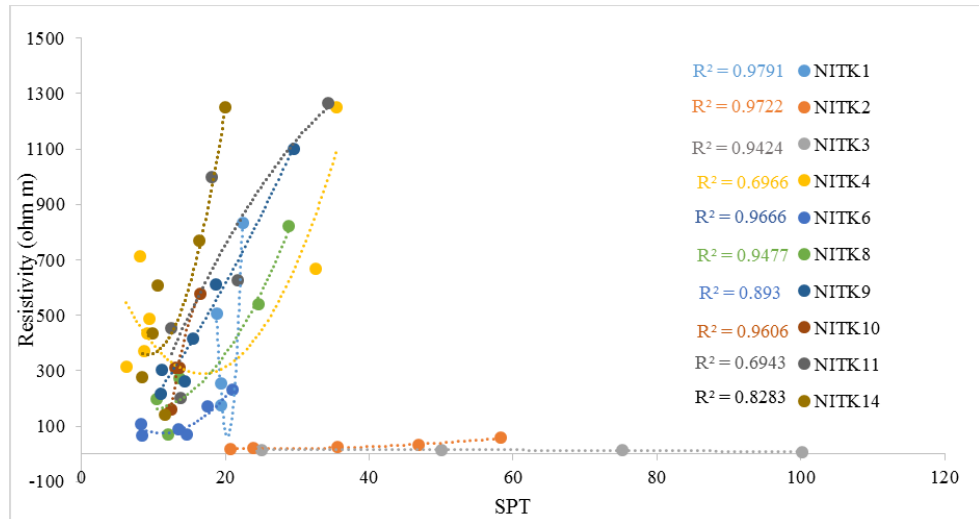


Figure 4.5 Correlation between SPT and ER ( $R^2 > 0.66$ )

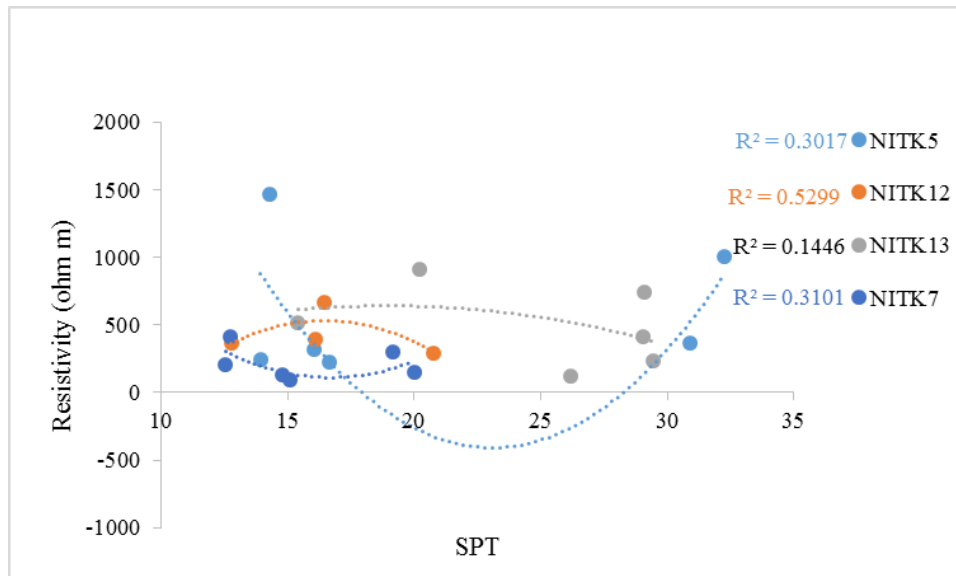


Figure 4.6 Correlation between SPT and ER ( $R^2 < 0.66$ )

The value of SPT number (N) depends upon the relative density of the cohesionless soil and the compactness or stiffness of the cohesive soil. Natural water content affects both resistivity and SPT number. The differences in controlling factors of the electrical resistivity and the strength could be the cause behind the nonlinear relationship between electrical resistivity and SPT. The results

include positive, negative and some inconsistent correlations too (Figs. 4.5 and 4.6). The results of borehole sampling and SPT test conducted is presented from Fig. 4.7(a) to Fig. 4.18(a). The results of interpretation of apparent resistivity into true resistivity of soil layers, layer thickness and depth are shown in Figs. 4.7(b) to 4.18(b). The variation of SPT and ER with depth at each of above ten locations is shown. (Fig. 4.7(c) to Fig. 4.18(c)).

depth (m)	LEGEND	Observed N	DESCRIPTION OF STRATA
0.5			DARK BROWN SILTY SAND
1			
1.5		53	BROWN SILTY GRAVELLY SAND
2.5			
3		58	WHITISH BROWN SILTY SAND
4			
4.5		29	BROWNISH WHITE SANDY SILT
6		30	
7.5		26	
9		24	
10.5		31	
12		34	BROWNISH WHITE SANDY SILT
12.5			

Figure 4.7(a) Borehole data at location NITK1

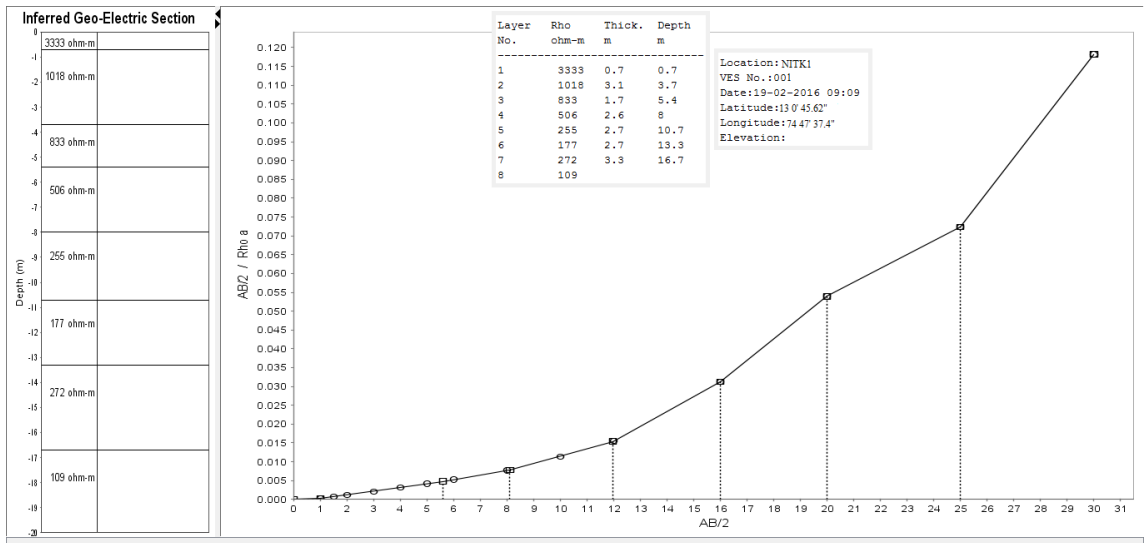


Figure 4.7(b) VES curve at location NITK1

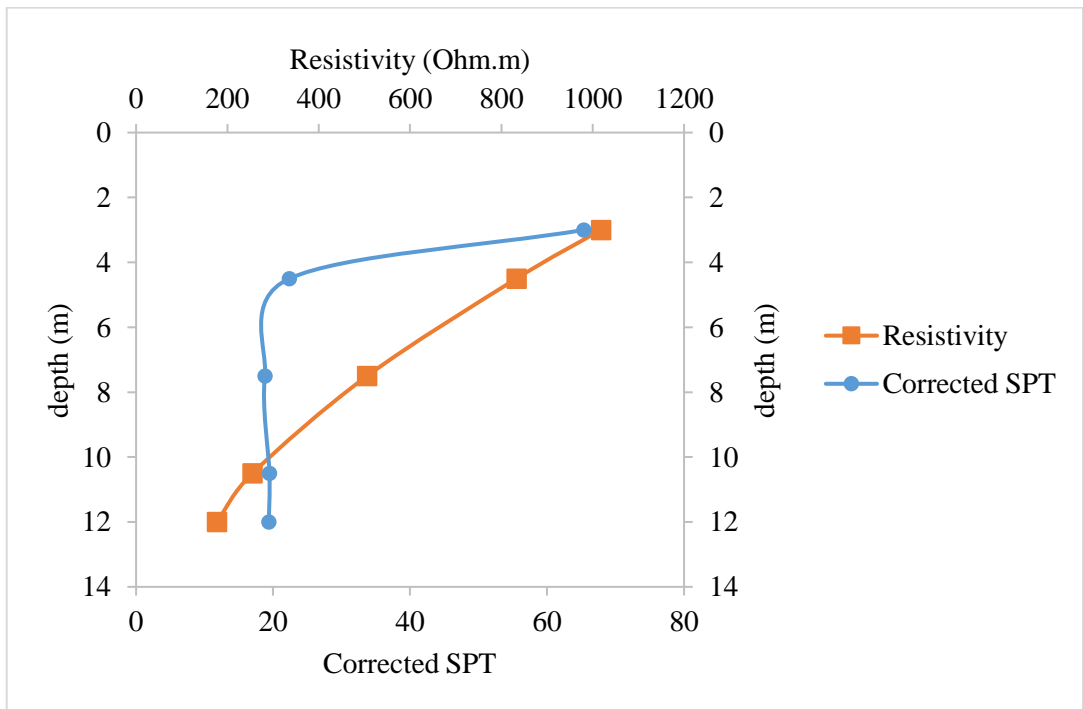


Figure 4.7(c) Variation of SPT and resistivity with depth at location NITK1



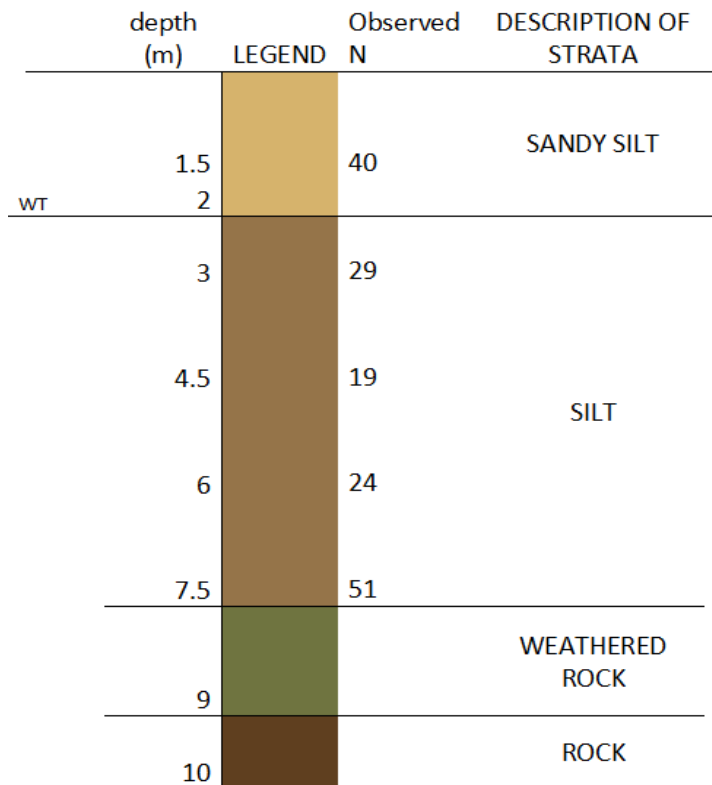


Figure 4.8(a) Borehole data at location NITK2

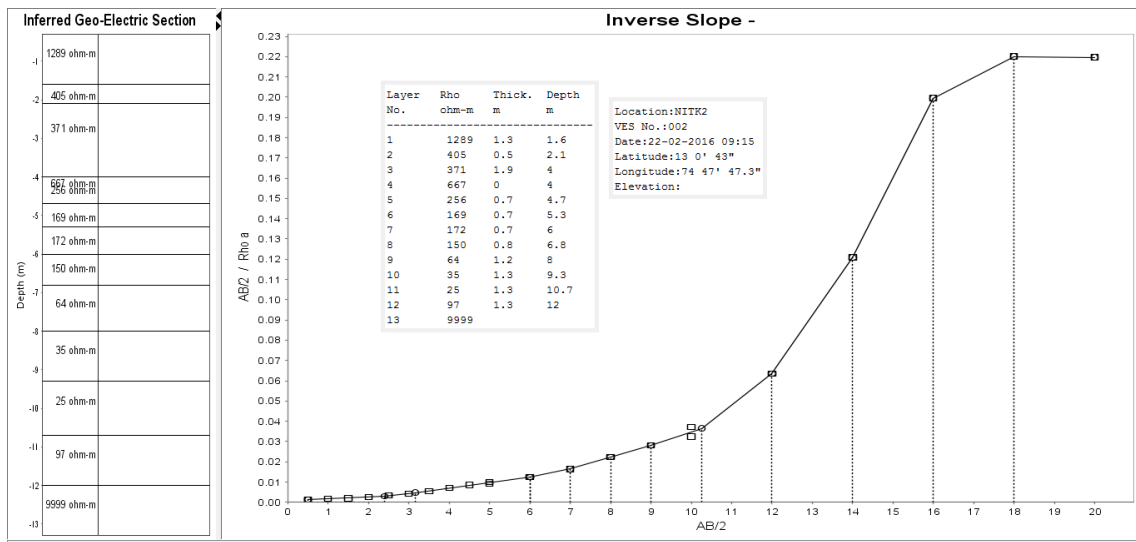


Figure 4.8(b) VES curve at location NITK 2

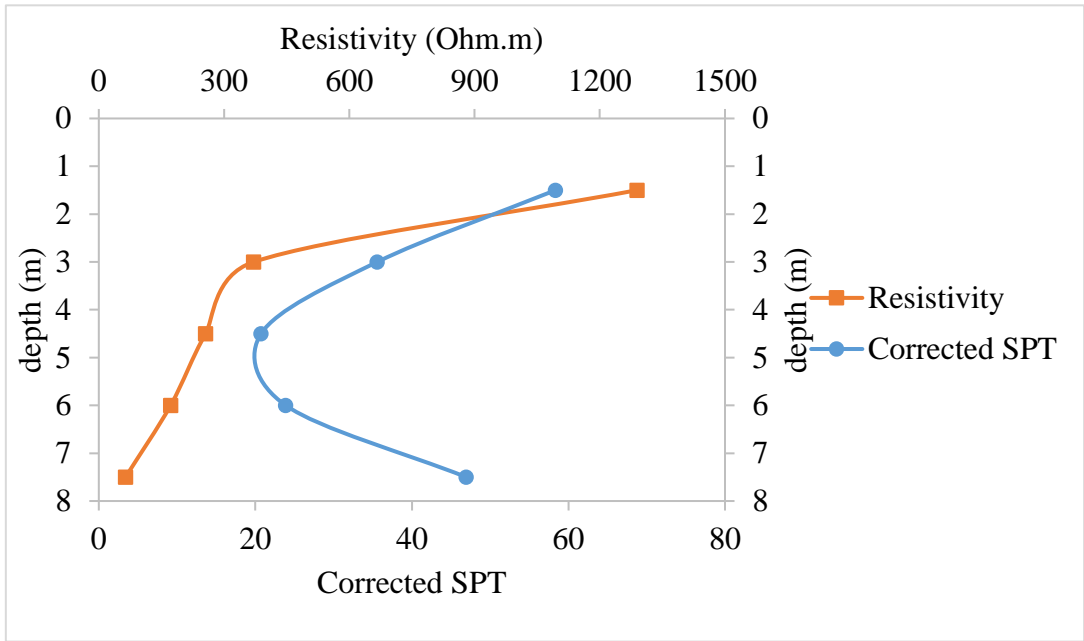


Figure 4.8(c) Variation of SPT and resistivity with depth at location NITK2

depth (m)	LEGEND	Observed N	DESCRIPTION OF STRATA
1.5	[Light Brown Box]	10	SANDY SILT
2			
3	[Dark Brown Box]	11	SILT
4.5		12	
6		7	
7.5		Rebound	
8	[Green Box]		WEATHERED ROCK
10	[Dark Brown Box]		ROCK

Figure 4.9(a) Borehole data at location NITK3

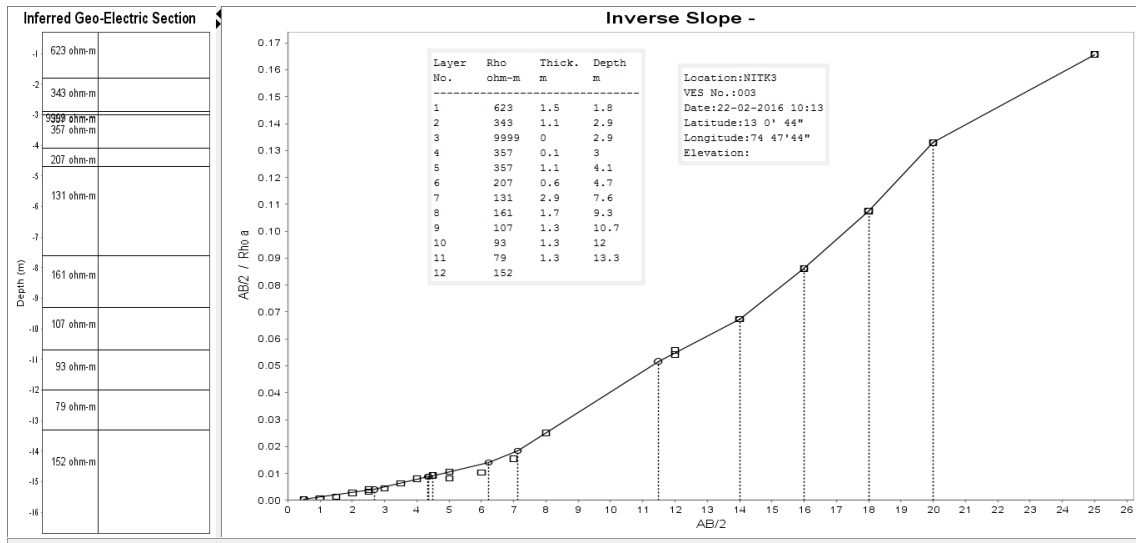


Figure 4.9(b) VES curve at location NITK 3

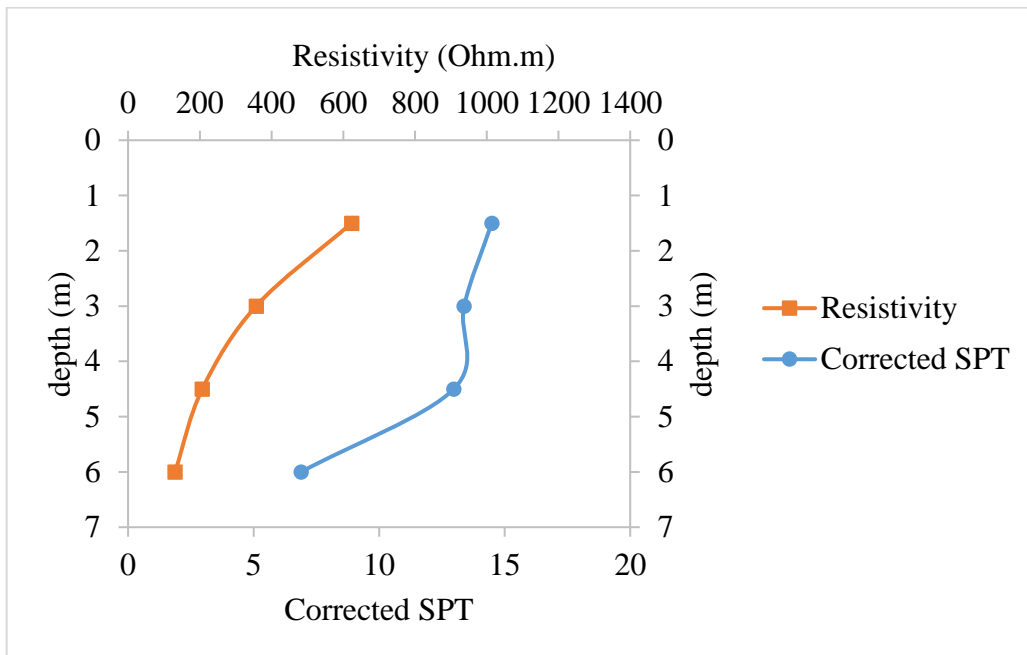


Figure 4.9(c) Variation of SPT and resistivity with depth at location NITK3

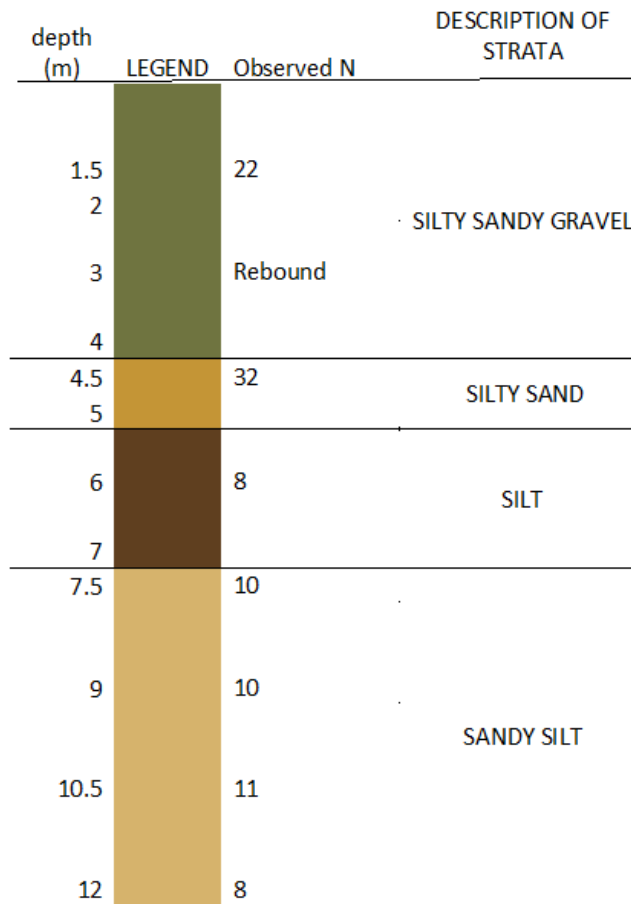


Figure 4.10(a) Borehole data at location NITK4

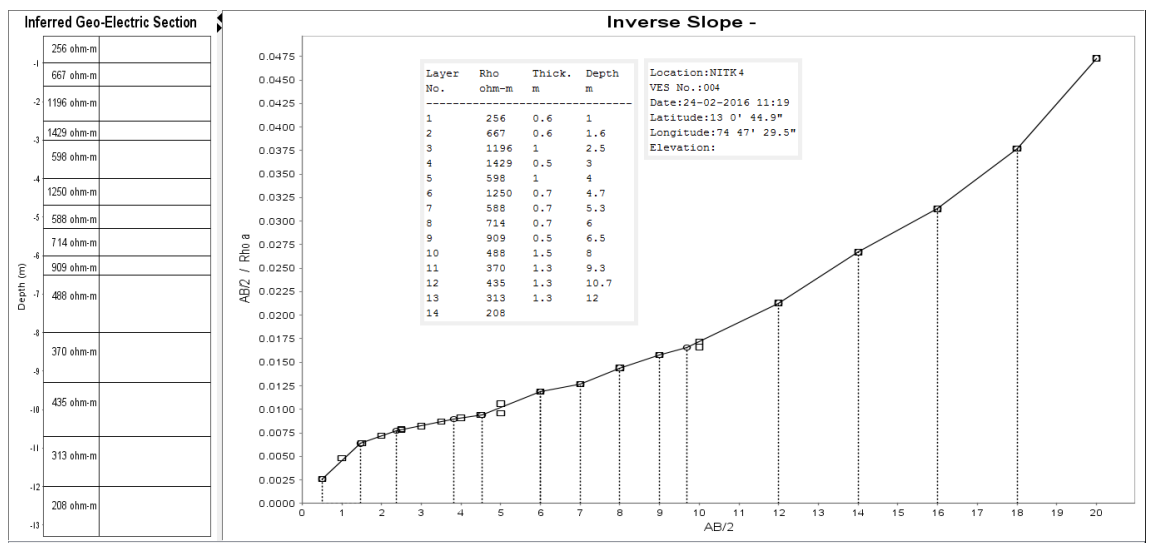


Figure 4.10(b) VES curve at location NITK 4

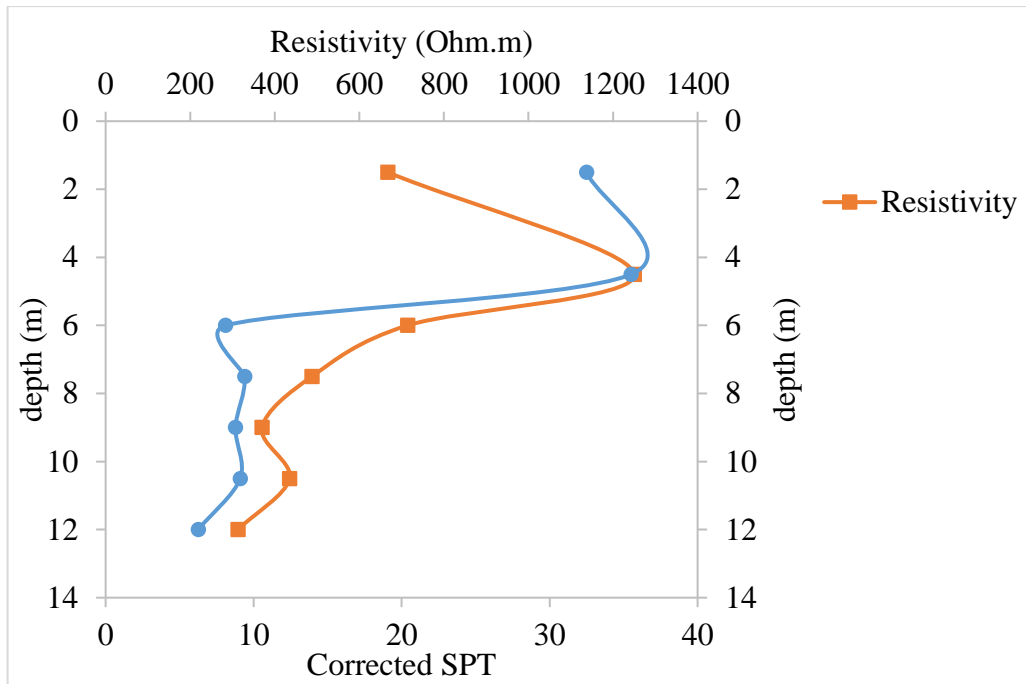


Figure 4.10(c) Variation of SPT and resistivity with depth at location NITK4

depth (m)	LEGEND	Observed N	DESCRIPTION OF STRATA
1.5	[Dark Brown Box]	22	SILTY SAND
3		25	
4			
4.5	[Light Brown Box]	13	SANDY SILT
6		16	
7.5		15	
10		20	

Figure 4.11(a) Borehole data at location NITK5

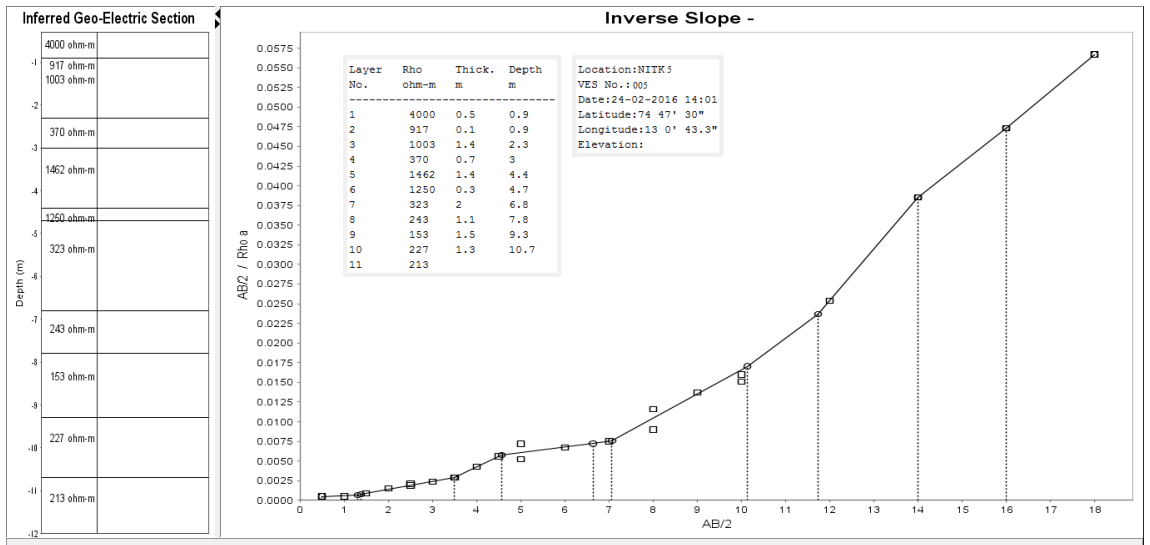


Figure 4.11(b) VES curve at location NITK 5

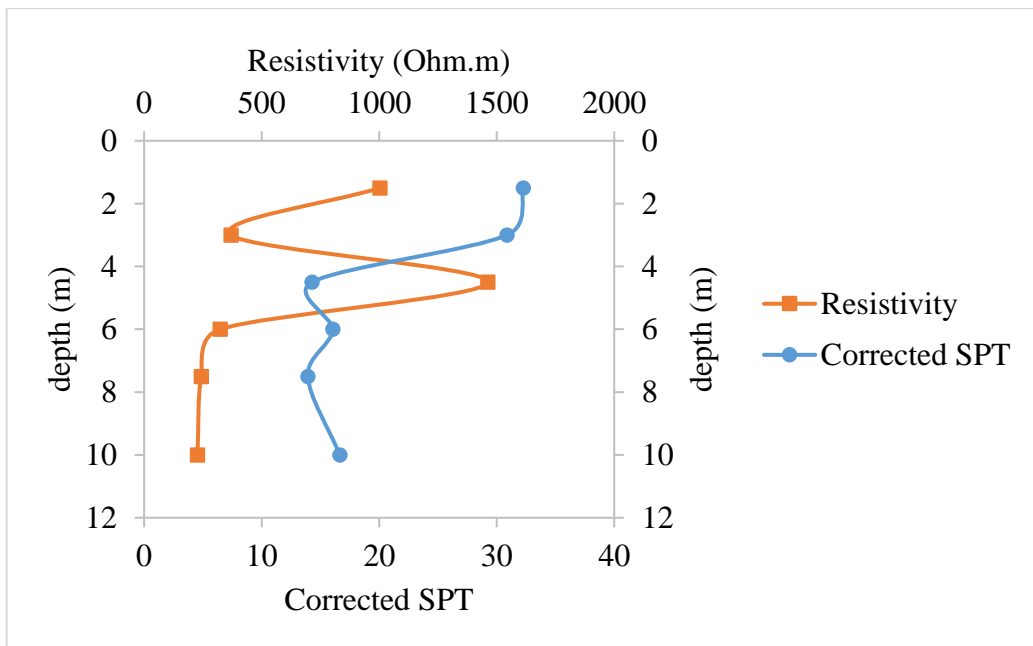


Figure 4.11(c) Variation of SPT and resistivity with depth at location NITK5

depth (m)	LEGEND	Observed N	DESCRIPTION OF STRATA
1.5	[Light Brown Bar]	15	SANDY SILT
3		15	
4		15	
4.5	[Dark Brown Bar]	8	SILT
6		9	
8		16	
10		19	

Figure 4.12(a) Borehole data at location NITK6

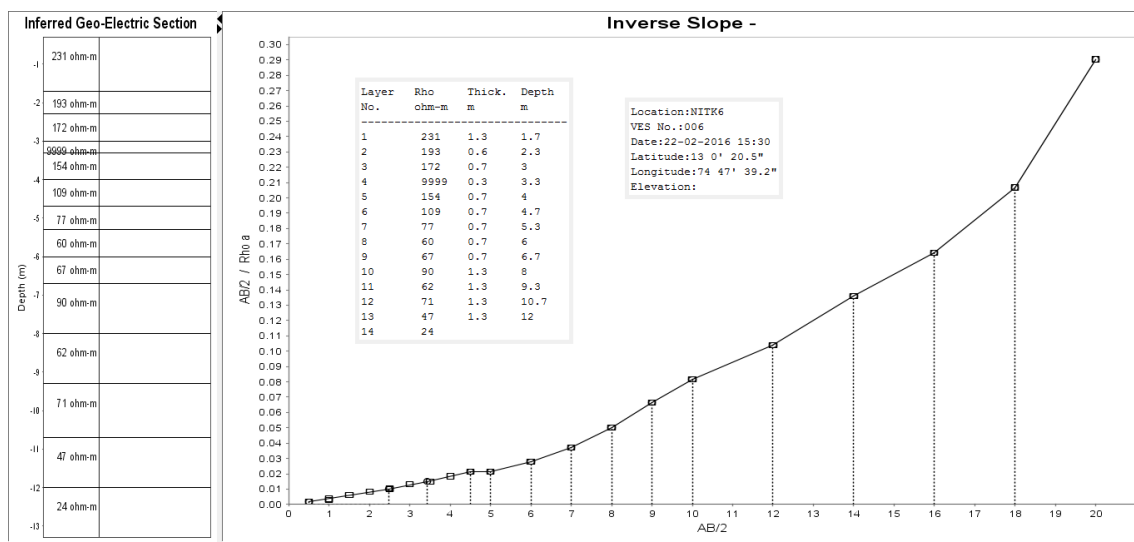


Figure 4.12(b) VES curve at location NITK 6

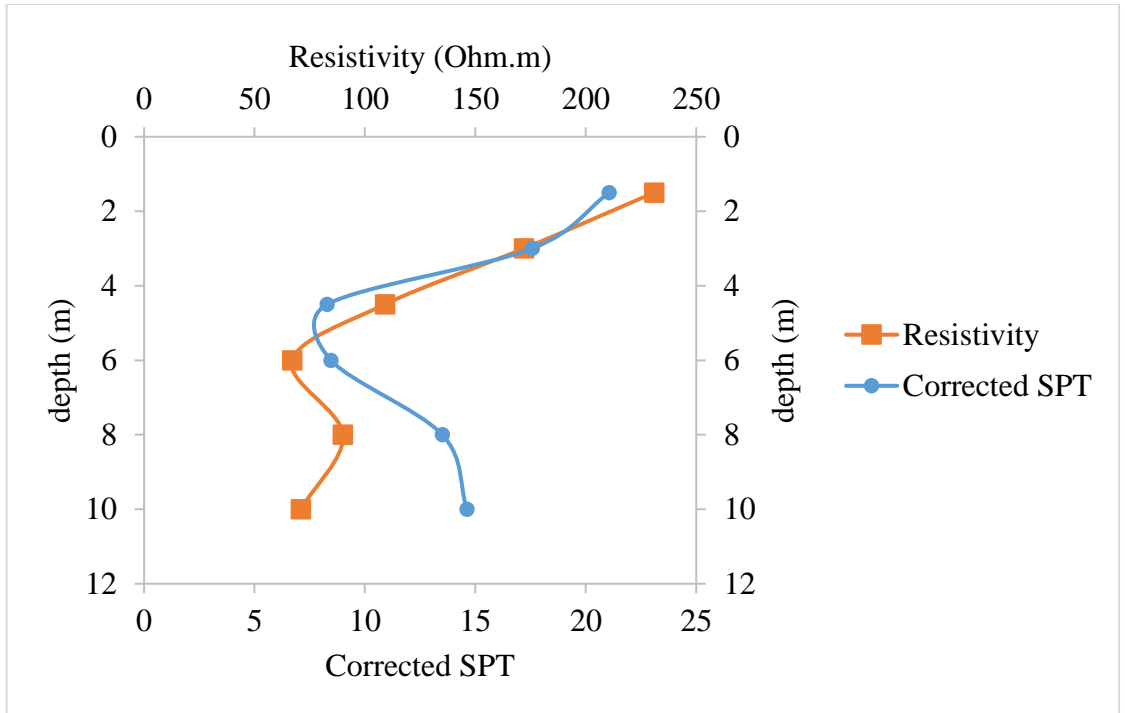


Figure 4.12(c) Variation of SPT and resistivity with depth at location NITK6

depth (m)	LEGEND	Observed N	DESCRIPTION OF STRATA
1.5		14	SANDY SILT
3		16	
4.5		12	
6		13	
8		17	
10		19	

Figure 4.13(a) Borehole data at location NITK7



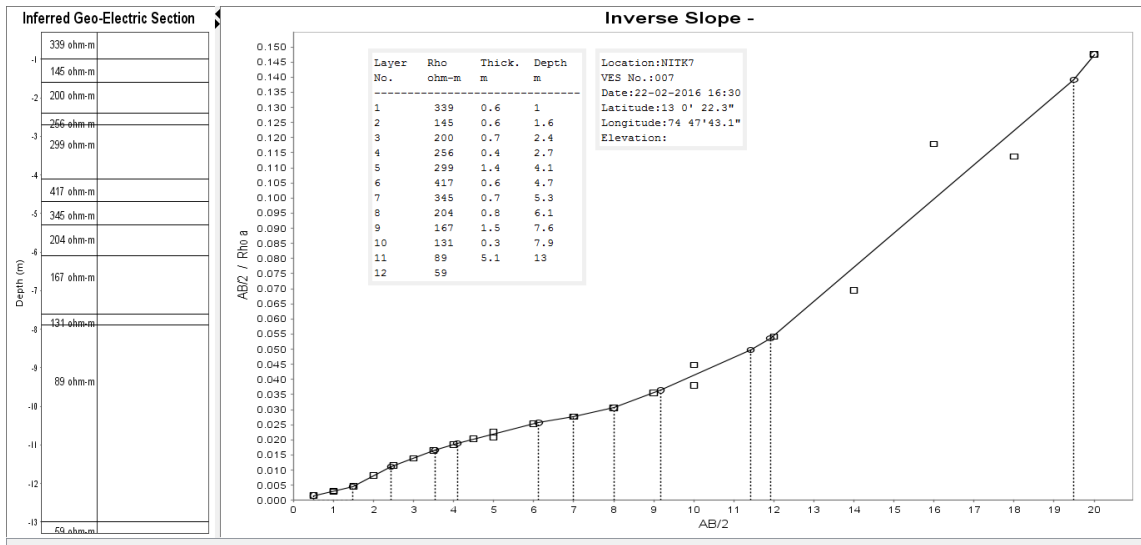


Figure 4.13(a) VES curve at location NITK 7

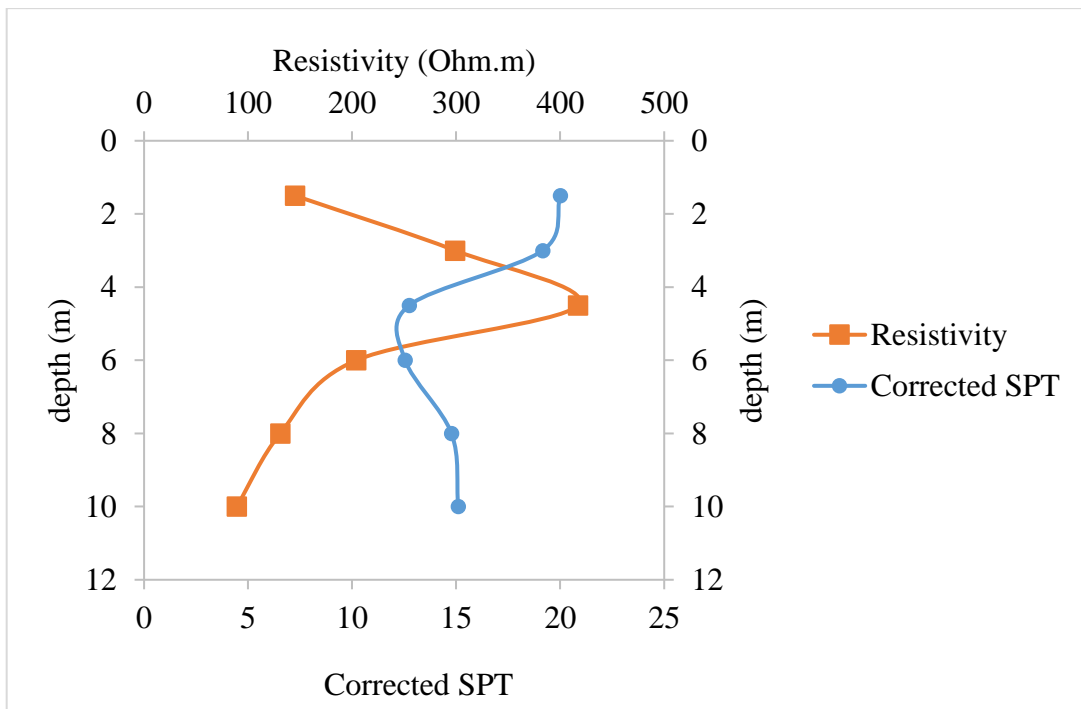


Figure 4.13(c) Variation of SPT and resistivity with depth at location NITK7

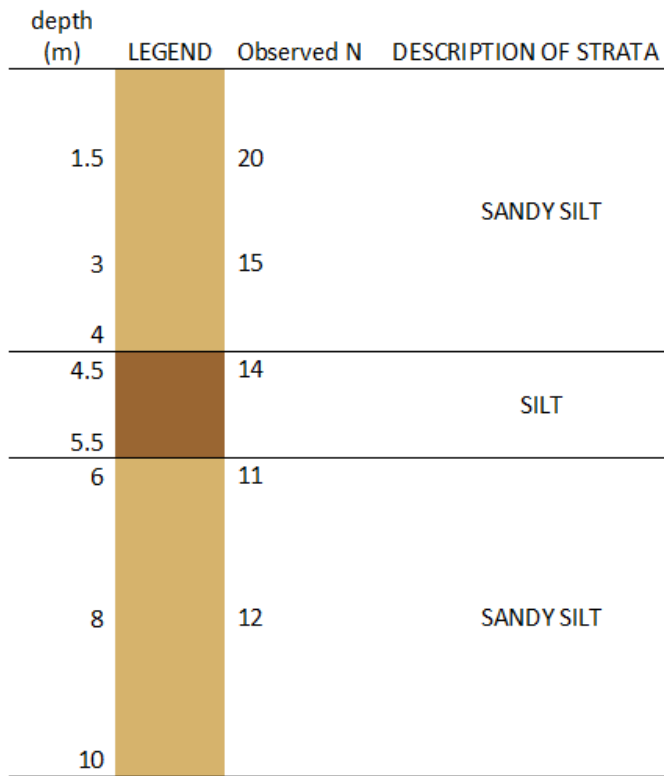


Figure 4.14(a) Borehole data at location NITK 8

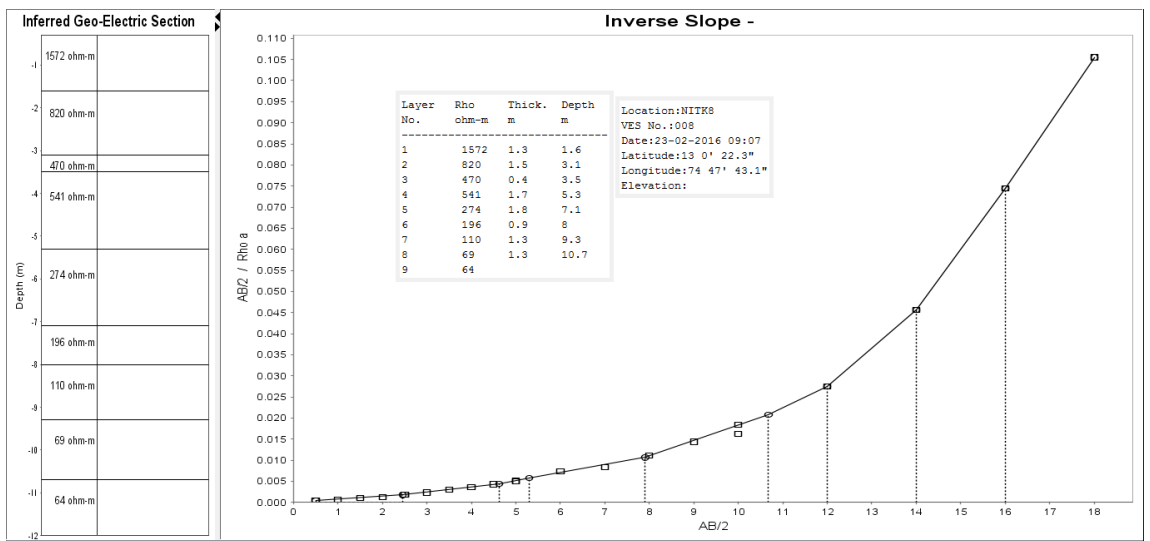


Figure 4.14(b) VES curve at location NITK 8

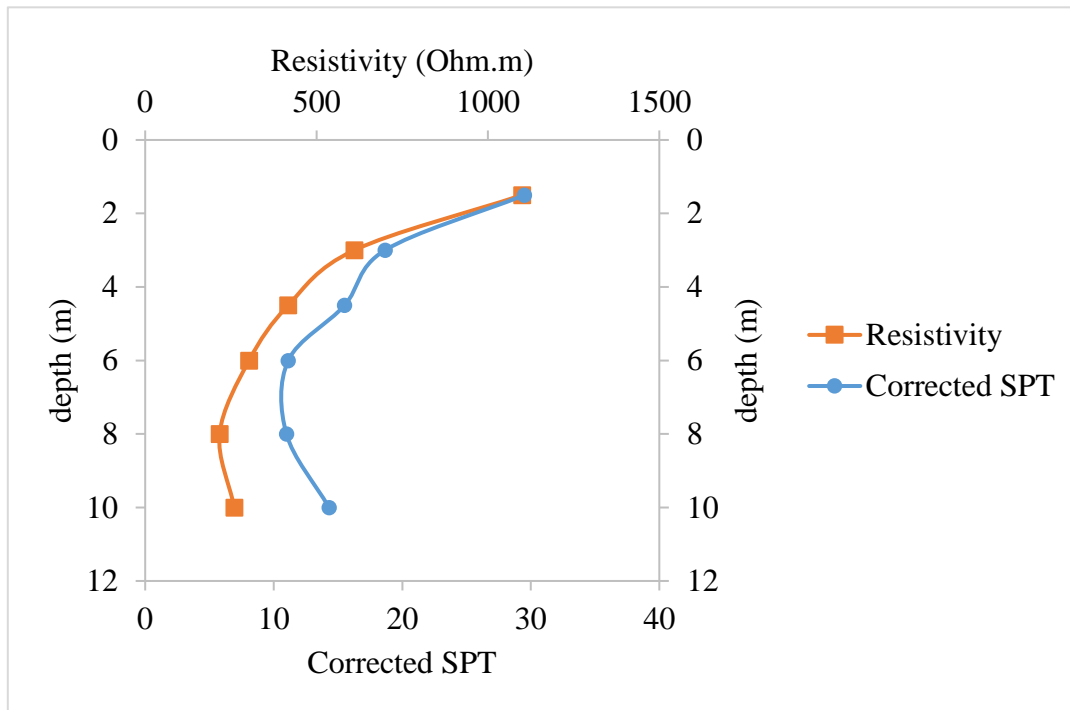


Figure 4.14(c) Variation of SPT and resistivity with depth at location NITK8

depth (m)	LEGEND	Observed N	DESCRIPTION OF STRATA
1.5	[Reddish-brown box]	Rebound	LATERITIC SOIL
2.5			
3	[Dark brown box]	24	SILT
4.5		23	
6		14	
8		12	
10		15	

Figure 4.15(a) Borehole data at location NITK9

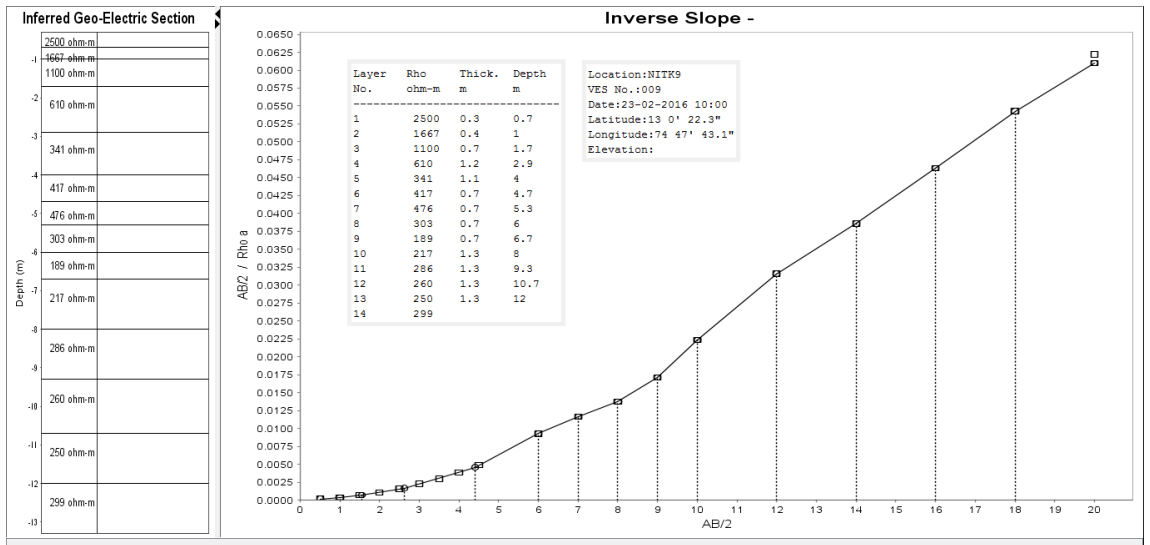


Figure 4.15(b) VES curve at location NITK9

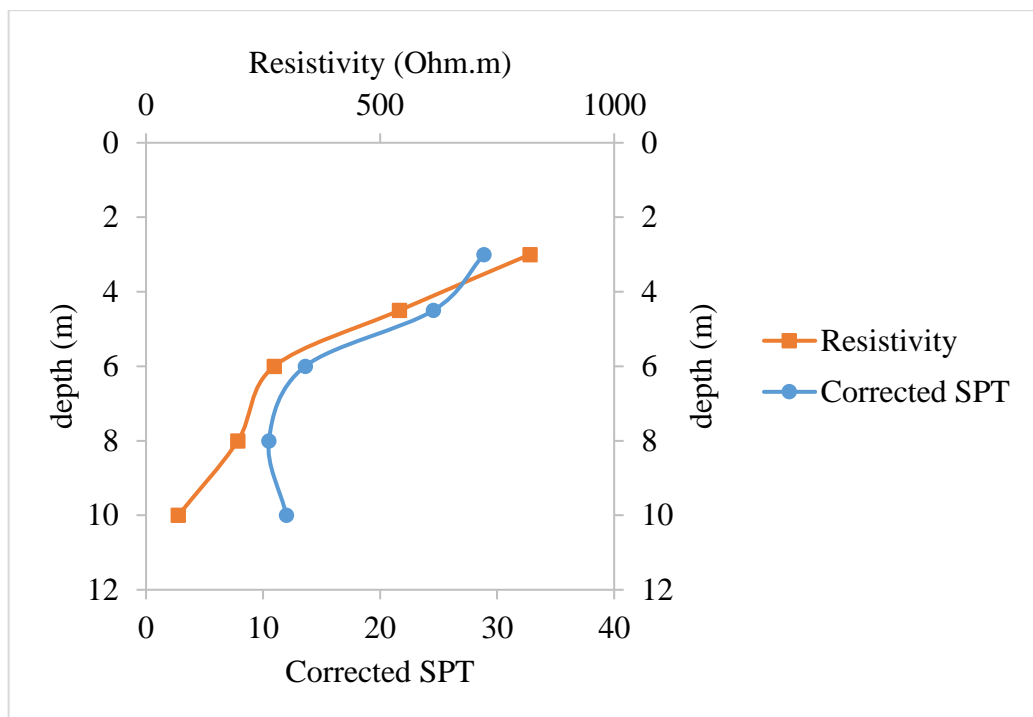


Figure 4.15(c) Variation of SPT and resistivity with depth at location NITK9

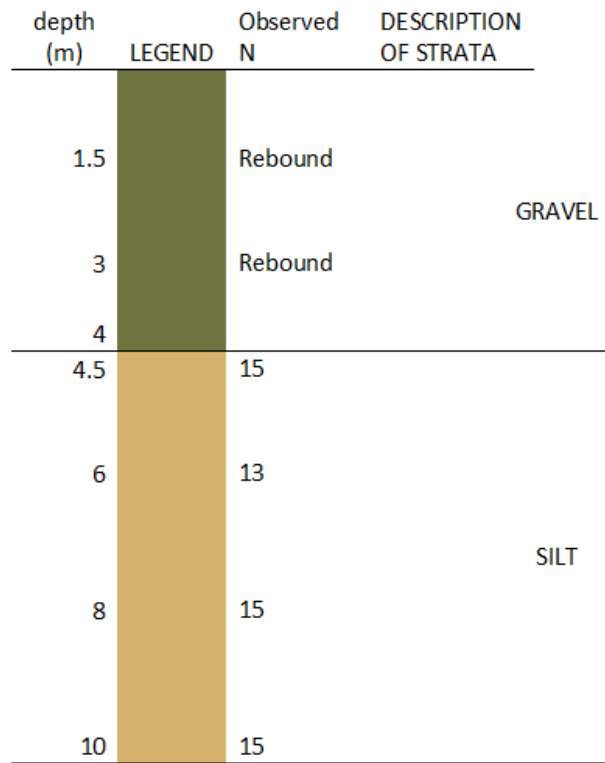


Figure 4.16(a) Borehole data at location NITK10

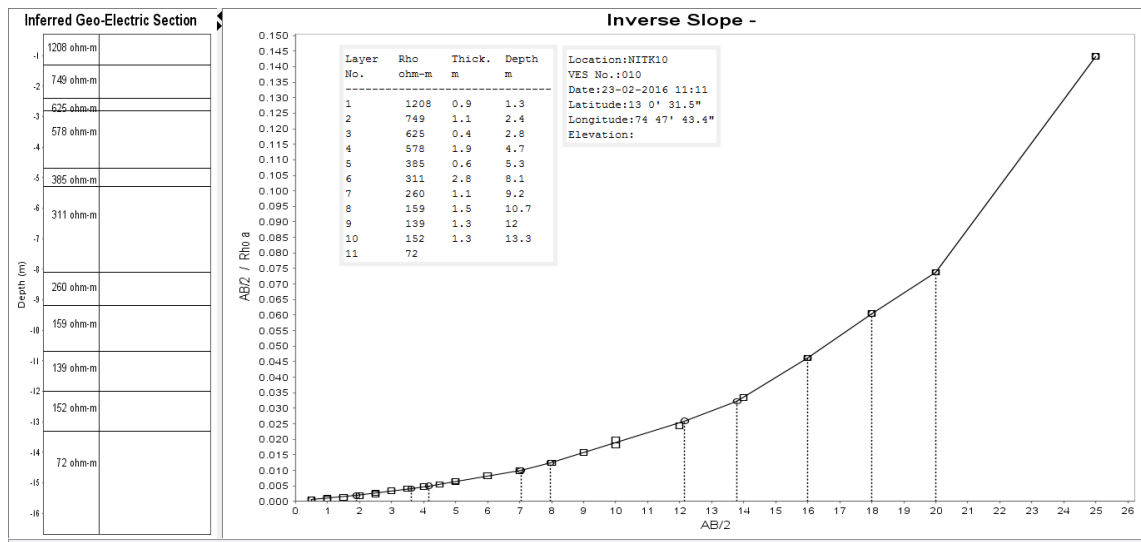


Figure 4.16(b) VES curve at location NITK 10

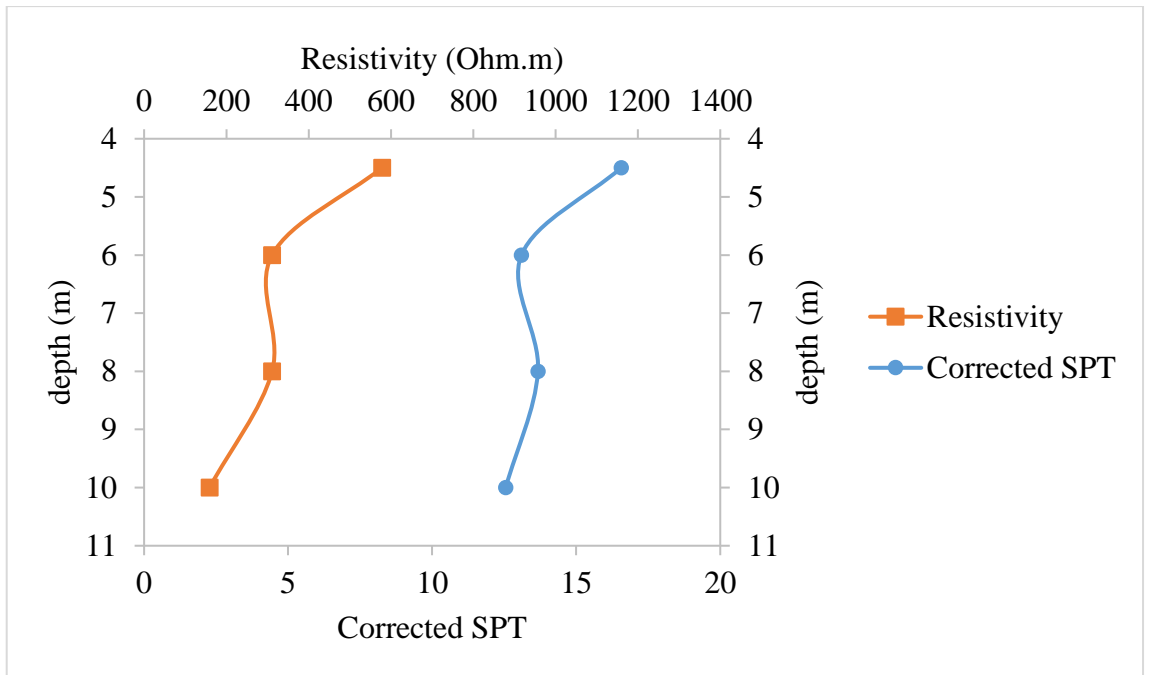


Figure 4.16(c) Variation of SPT and resistivity with depth at location NITK10

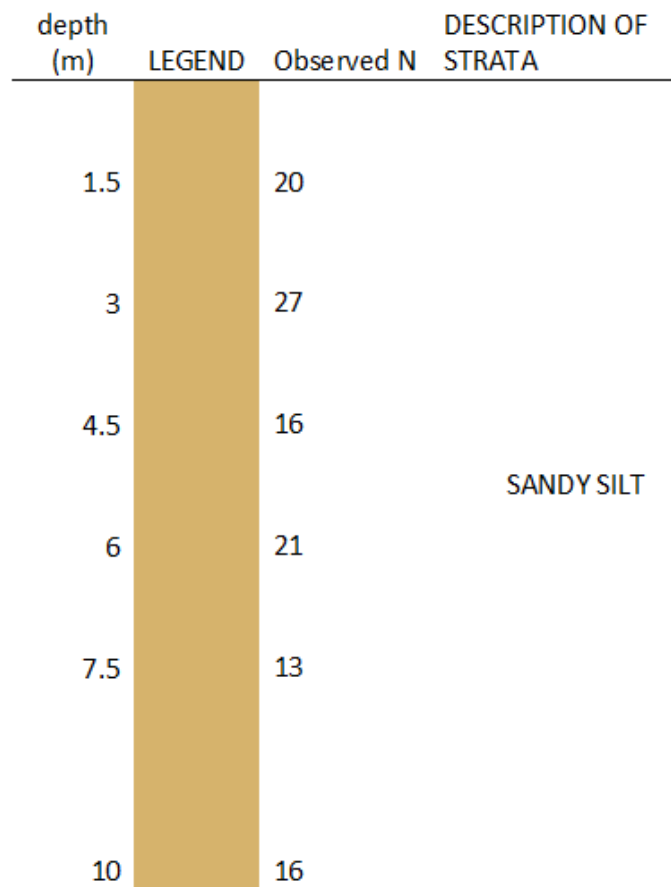


Figure 4.16(a) Borehole data at location NITK11

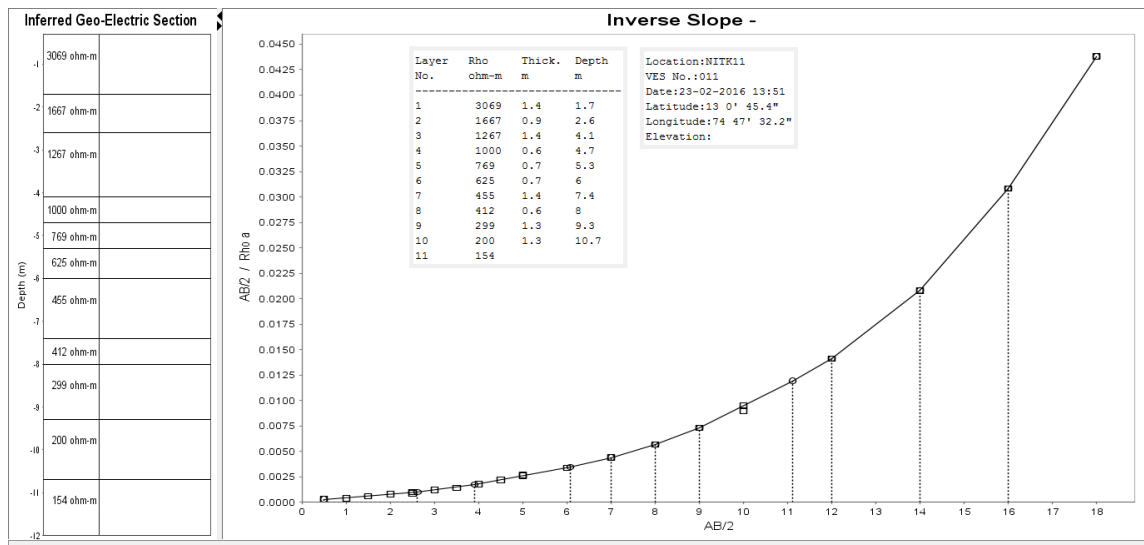


Figure 4.16(b) VES curve at location NITK11

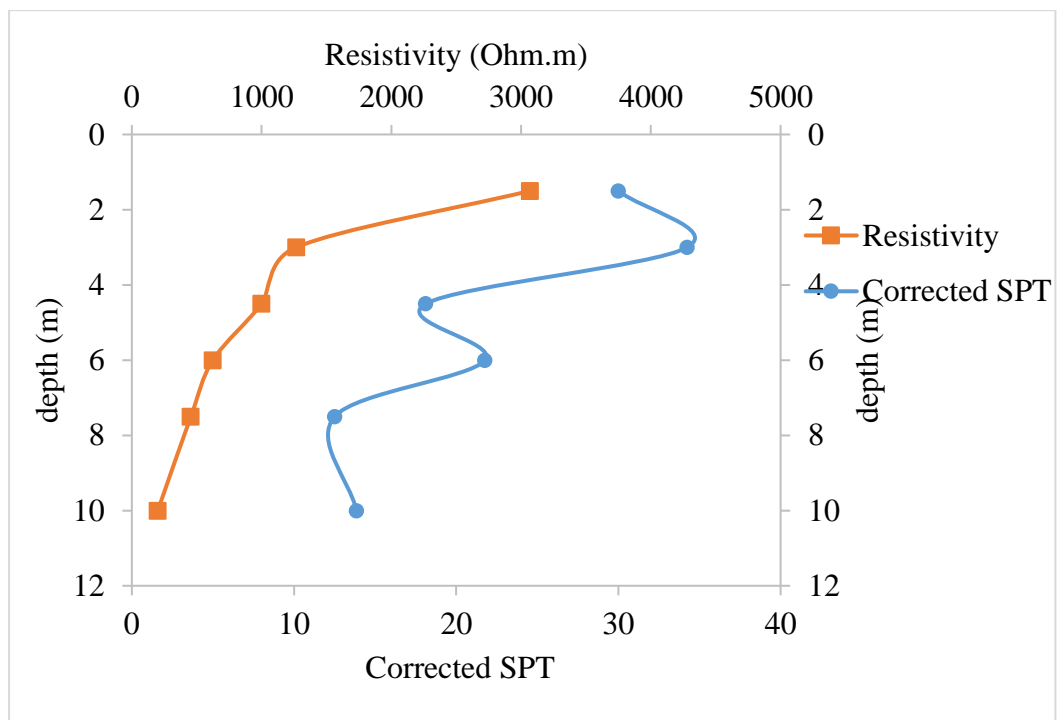


Figure 4.16(c) Variation of SPT and resistivity with depth at location NITK11

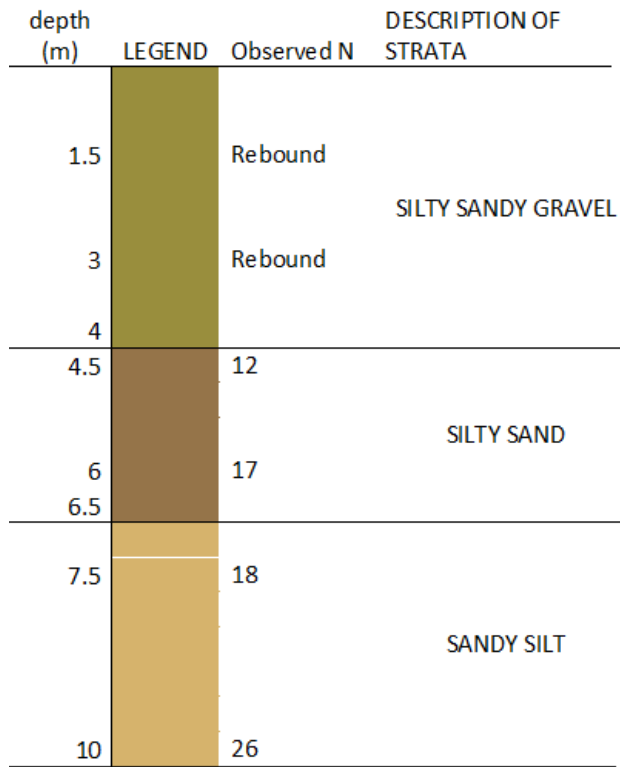


Figure 4.17(a) Borehole data at location NITK12

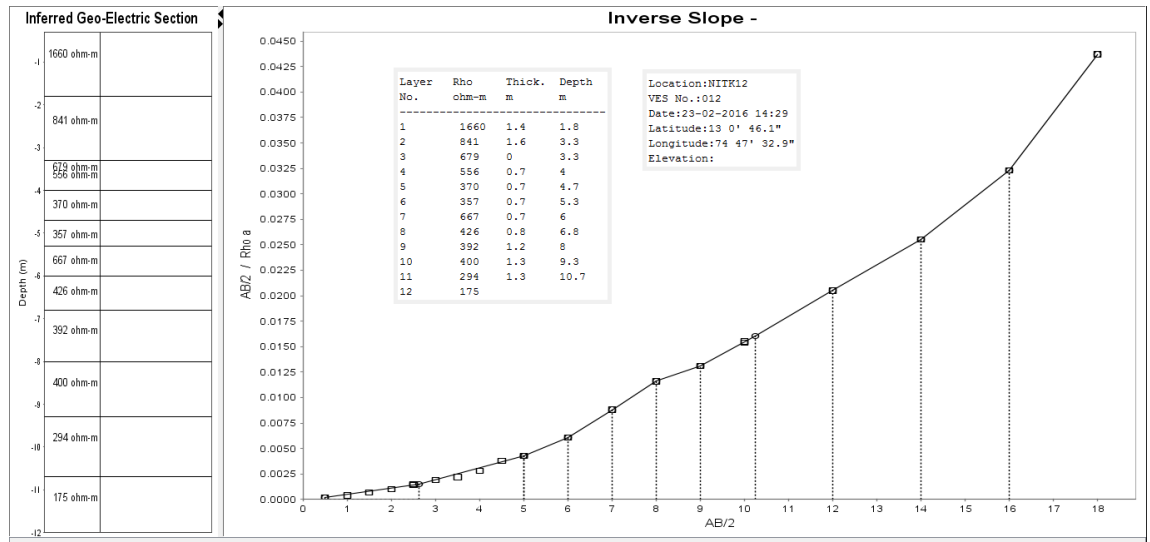


Figure 4.17(b) VES curve at location NITK12



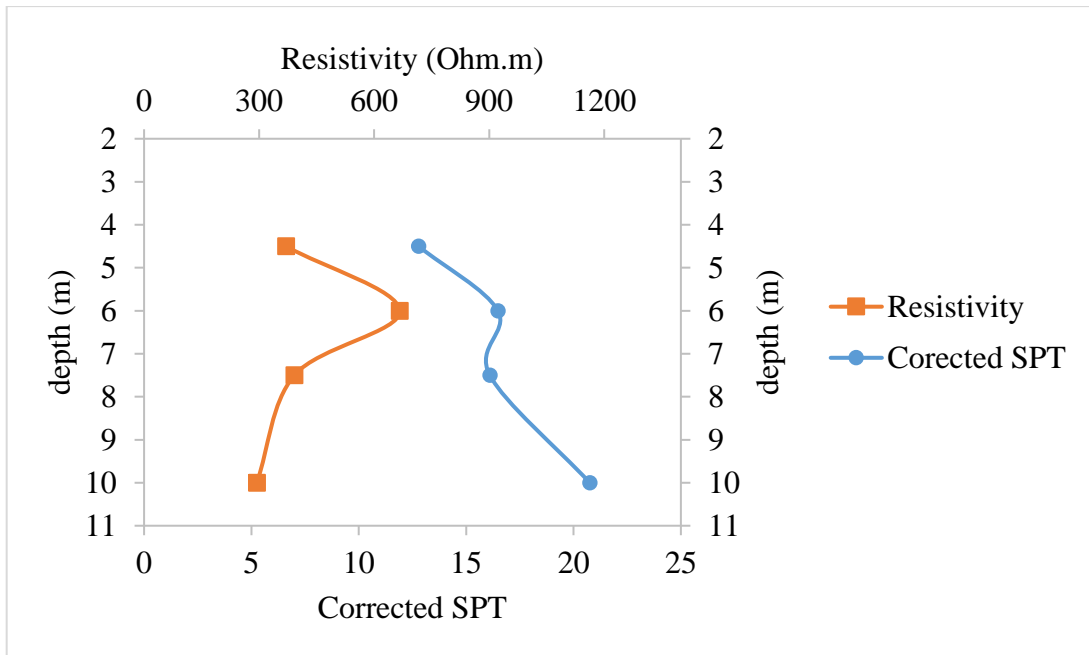


Figure. 4.17(c) Variation of SPT and resistivity with depth at location NITK12

depth (m)	LEGEND	Observed N	DESCRIPTION OF STRATA
1.5	[Light Brown Box]	14	SANDY SILT
3		24	
3.5	[Dark Brown Box]	26	
4			SILTY SAND
6		30	
7	[Light Brown Box]	17	
7.5			SANDY SILT
8.5	[Dark Brown Box]	31	
9			SILT
10.5		30	
11	[Light Brown Box]		
12		33	SANDY SILT

Figure 4.19(a) Borehole data at location NITK13

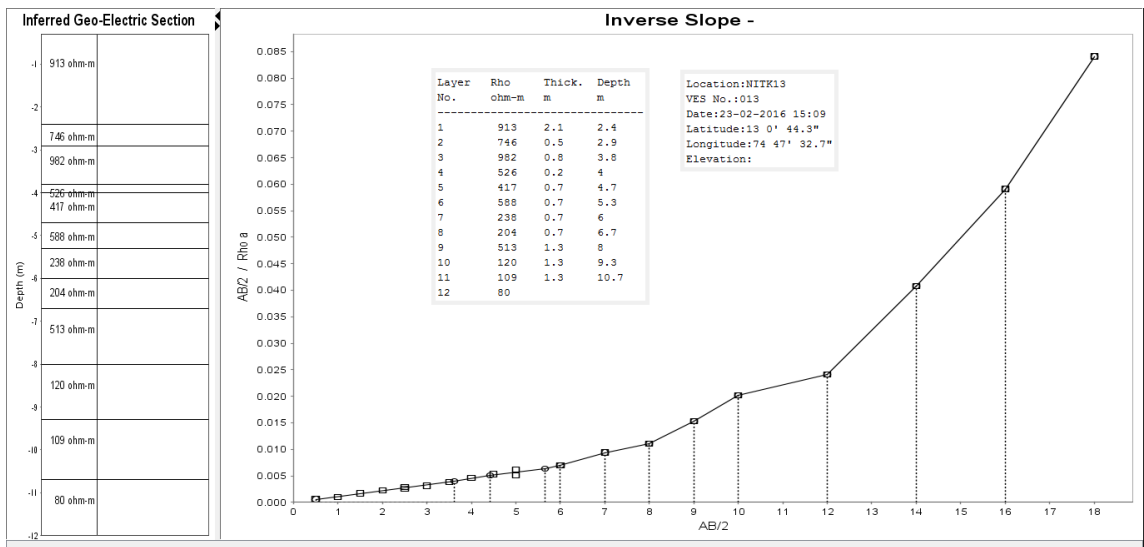


Figure 4.18(b) VES curve at location NITK13

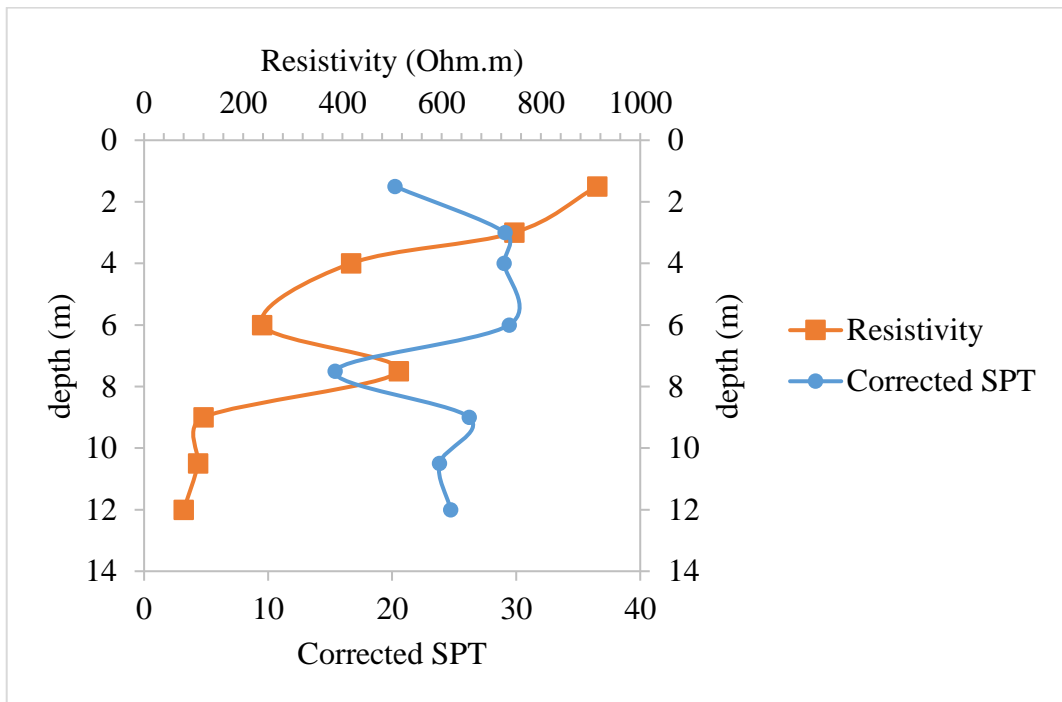


Figure 4.19(c) Variation of SPT and resistivity with depth at location NITK13

depth (m)	LEGEND	Observed N	DESCRIPTION OF STRATA
1.5	[Olive Green Box]	Rebound	SILTY SANDY GRAVEL
3		Rebound	
4			
4.5	[Brown Box]	19	SILTY SAND
6		17	
7.5		12	
9	[Yellow-Gold Box]	12	SANDY SILT
10.5		11	
12		16	

Figure 4.20(a) Borehole data at location NITK14

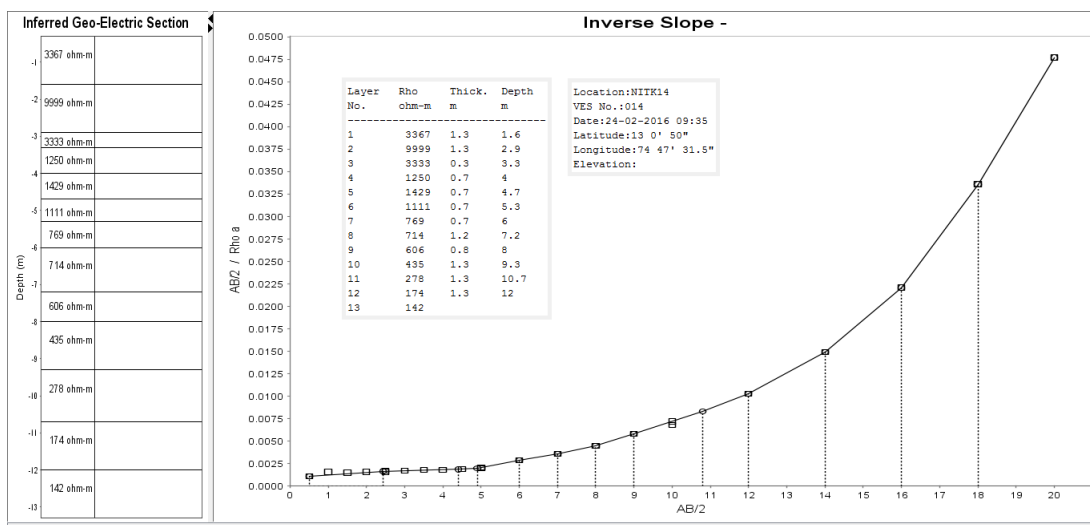


Figure 4.20(b) VES curve at location NITK14

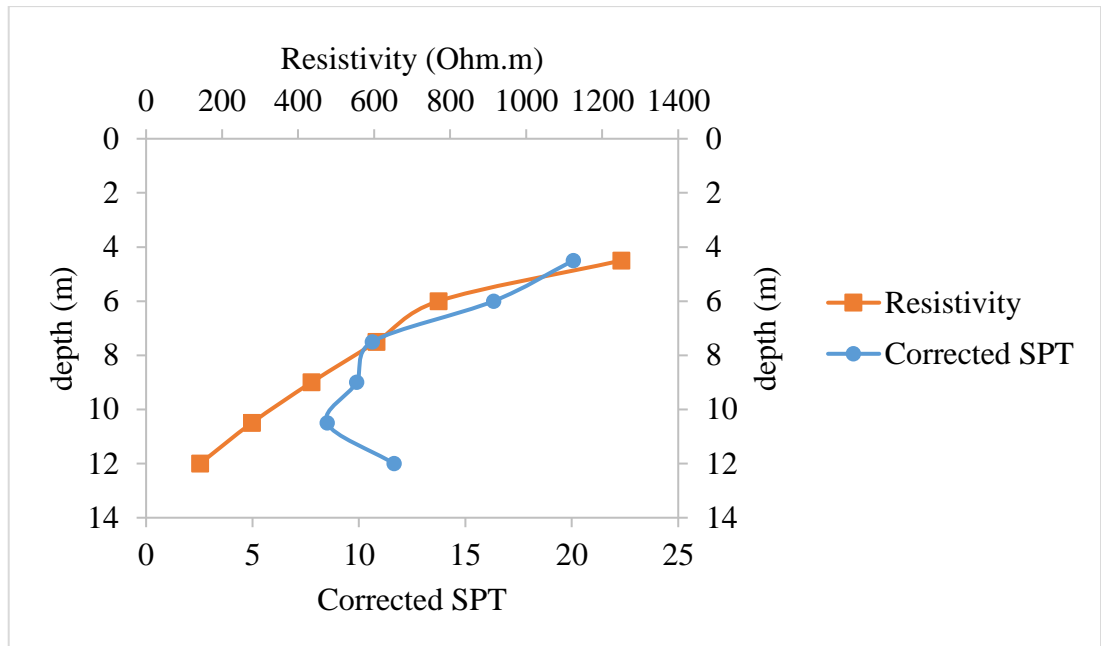


Figure 4.20(c) Variation of SPT and resistivity with depth at location NITK14

At Borehole Location NITK1, the correlation between ER and SPT is good (Fig. 4.7(c)). The presence of water table at 4m depth resulted in decrease of electrical resistivity, while SPT is not very much affected. At borehole NITK2 (Fig. 4.8(c)) and NITK3 (Fig. 4.9(c)), below water table, when weathered rock was encountered, SPT was high, but resistivity was low. Generally in field, the soil electrical resistivity data is observed to be very sensitive to the quantitative proportion of water and geomaterial particle fractions (Abidin et al. 2013). At some locations, Borehole NITK4 (Fig. 4.10(c)), NITK10 (Fig. 4.16(c)), NITK12 (Fig. 4.18(c)), NITK14 (Fig. 4.20(c)), gravelly soil possess higher SPT and higher resistivity compared to finer soils at higher depths. At location NITK 9 (Fig. 4.15(c)), top layer was dry laterite which gave higher SPT and Resistivity, below which was silt, which gave comparatively lesser resistivity and SPT.

At some locations it is seen that, the correlation between SPT and ER is inverse. Soil resistivity decreases significantly with increase in density, and the decrease was more pronounced for the drier soils (Seladji et al. 2010). The dry density reflects the soil particle compactness to some degree: the higher the dry density is, the better the connectivity of pore fluid pathway is the reason by which the electrical resistivity decreases with increasing dry density (Bai, 2013). However, once the dry density

approaches the maximum, the decrement rate of the resistivity slows down and tends to be stable. At borehole locations NITK5 (Fig. 4.11(c)), NITK 7 (Fig. 4.13(c)) water table is deep and of the several factors governing resistivity of the soil, bulk density was predominant. SPT increased with increase in density while the resistivity decreased. The rate of reduction in resistivity with increase in dry density decreases with increase in moisture content. Resistivity and SPT have got positive correlation with stiffness and water content. Hence at sites where soil stiffness and water content become the influential factors, resistivity maintains direct relation with SPT. At NITK6 (Fig. 4.12(c)), NITK8 (Fig. 4.14(c)), and NITK 11 (Fig. 4.17(c)), increase of water content in the soil layers might have influenced SPT as well as ER. Very poor correlation was obtained at borehole location NITK13 (Fig. 4.19(c)), with a regression coefficient of about,  $R^2=0.1446$ . It is because the multiple factors influencing SPT and ER contradict each other, resulting in inconsistency. Presence of metal pipes, cables, fences and electrical grounds can distort the resistivity measured and complicate the interpretation, which could also be the reason for the inconsistent correlations.

Rebound was obtained in some of the boreholes. Resistivity values at depths of rebound were very high and are presented in the Table 4.1. At location NITK3 (Fig. 4.11(c)) at 7.5m depth weathered rock was encountered below water table which gave rebound. Lesser resistivity can be attributed to the very porous texture and being submerged in water.

Table 4.1 Comparison of Electrical resistivity at layers giving rebound

SPT (N)	Resistivity (Ohm.m)	Depth (m)	Borehole location	Type of strata	Remarks
Rebound	131	7.5	NITK3	Weathered Rock	Below Water table
Rebound	1250	3	NITK4	Gravelly	Above Water table
Rebound	1208	1.5	NITK10	Gravelly	Above Water table
Rebound	625	3	NITK10	Gravelly	Above Water table
Rebound	1660	1.5	NITK12	Gravelly	Above Water table
Rebound	845	3	NITK12	Gravelly	Above Water table

Rebound	3367	1.5	NITK14	Gravelly	Above Water table
Rebound	3333	3	NITK14	Gravelly	Above Water table

From the overall results, resistivity generally bears a positive correlation with SPT. However, at some depths some inverse correlations are also noticed. Some factors like presence of water table, presence of weathered rocks submerged in water at depths, higher degree of saturation etc. cause inverse relation between SPT and ER. Also when the water table is deep and the same soil type is present in different compaction conditions, the densely packed partially saturated soil layer is more conductive than the loosely packed soil layer. This is somewhat in conformity with the relationship obtained from laboratory test results between ER and porosity ‘n’ (Fig. 3.22) in case of partially saturated soils. This is because pore water film is more continuous in the denser layer. At the same time, SPT will be higher for the former, which results in an inverse correlation.

#### 4.7.2 Correlation between field and laboratory electrical resistivity of soil samples at shallow depths

Table 4.2 Soil type for laboratory resistivity measurements

Borehole	Soil Type
NITK1	Silty Sand
NITK2	Sandy Silt
NITK3	Sandy Silt
NITK4	Silty Sandy
NITK5	Silty Sand
NITK6	Sandy Silt
NITK7	Sandy Silt
NITK8	Sandy Silt
NITK9	Lateritic Soil
NITK10	Gravel
NITK11	Sandy Silt
NITK12	Silty Sandy
NITK13	Sandy Silt
NITK14	Silty Sandy

Disturbed Soil Samples were collected from a depth of 1m, using auger and classification of soil type was done. The field density and moisture content were measured at each borehole locations. Field density was determined by sand replacement

method and water content by oven drying method. These locations are shown in the Fig. 4.6. The samples were taken from same locations where field electrical survey was carried out. Fourteen soil samples (Table 4.2) taken from these borehole locations were subjected to laboratory resistivity measurement in order to determine electrical resistivity of different samples under laboratory conditions.

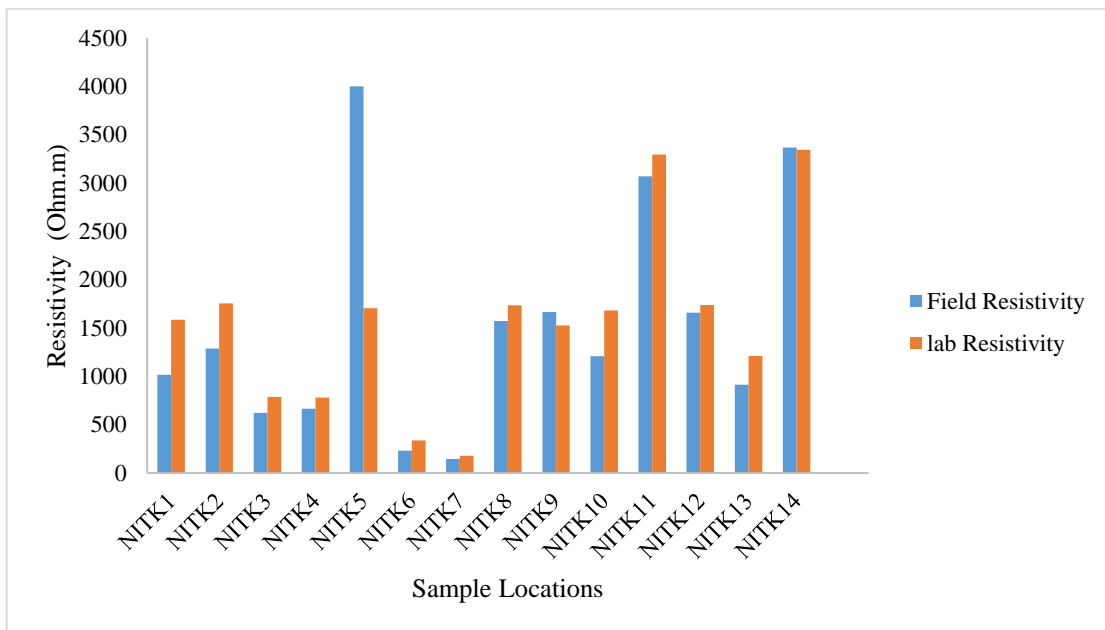


Figure 4.21 Comparison of field and laboratory electrical resistivity

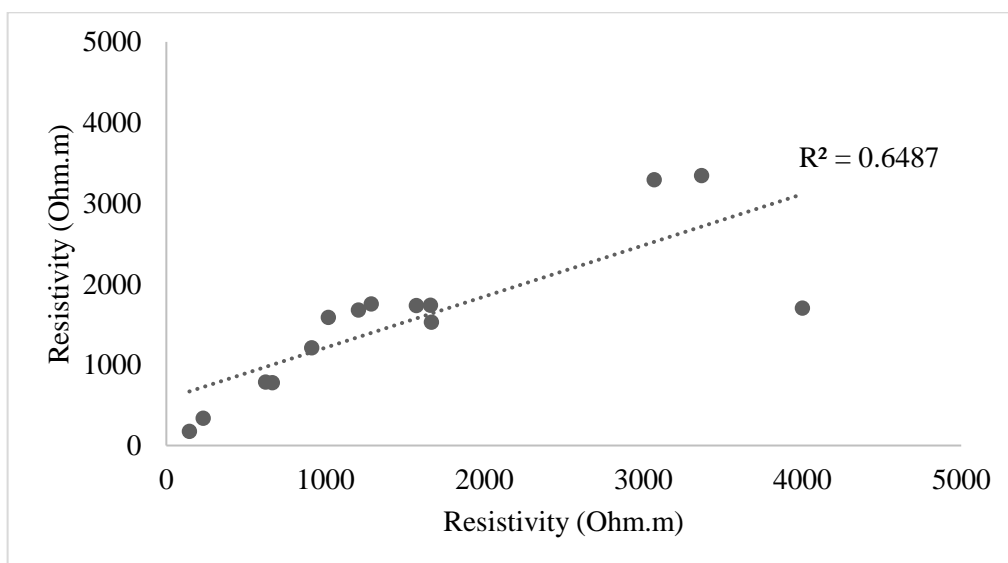


Figure 4.22 Correlation of field and laboratory electrical resistivity

The soil was oven dried and mixed with the pre-determined field moisture content and filled in the resistivity box at field density. Then the soil samples were measured for their electrical resistance, and the true resistivity was obtained by multiplying with the multiplication and calibration factors. The resistivity measured by laboratory and field measurements are plotted and the correlation factor thus obtained is about 0.6487(Figs. 4.23 and 4.24). Laboratory measurements on small soil samples are much more representative of the macroscopic induced-polarization responses, and generally correlate quite well with surface measurements. It is also noted that the laboratory resistivities are generally higher than the field resistivities.

Since it is not possible to reproduce the exact field condition in the laboratory, it may be the reason behind the differences in resistivity. It is also vital to consider that in laboratory assessment, impact of inhomogeneities in the samples does not represent the entire geological formation due to the small size of samples being tested. Results show that values from field and laboratory measurement, although do not match perfectly, are still comparable.

#### **4.8 Summary**

- The primary objective of this study is to obtain quantitative and qualitative correlations between geotechnical and geo-electrical properties of laterites and lateritic soils, in natural field conditions.
- The results of this study suggest that by properly handling the uncertainties and ubiquitous resistivity measurement errors, Electrical Resistivity tomography can be used as a pre investigation method on sites, prior to direct testing methods like SPT in order to reduce labour, cost and time involved. Overall, there exists a good correlation between SPT and ER. In that direct and inverse relations are investigated. However, a few inconsistent relations also exists between SPT and ER. Water content, soil type, stiffness of the soil layers, develop a direct relation between SPT and ER. However, compaction/bulk density, soil layers submerged under the water table, salt concentration ensue inverse relation between ER and SPT. Gravelly soils and hard laterites gave higher SPT and higher ER values. Fine grained soils, even at large depths, gave lower SPT and



lower ER values. Dry soil, at locations where water table was very low showed higher resistivity values.

- Comparisons made on laboratory and field electrical resistivity data showed fairly good correlations. The difference in resistivity could be due to the difficulty to produce the exact field conditions in the laboratory. It is also noted that the lab resistivity is generally higher than the field resistivity and generally correlate quite well with surface measurements.
- The correlations are site-specific and require a detailed study to establish its validity and restrictions. More field tests have to be conducted in various flat and sloping geological environments for getting more summed up conclusions.

## CHAPTER 5

### LABORATORY ELECTRICAL RESISTIVITY STUDIES ON CEMENT STABILIZED SOIL

#### 5.1 Introduction

Electrical resistivity measurement of freshly prepared uncured and cured soil cement materials are done and the correlation between the factors controlling the performance of soil cement and electrical resistivity are discussed in this Chapter. Conventional quality control of soil-cement quite often, involves wastage of a lot of material, if it does not meet the strength criteria. In this study, it is observed that in soil cement, resistivity follows a similar trend as unconfined compressive strength, with increase in cement content and time of curing. Quantitative relations developed for predicting 7 day strength of soil-cement mix, using resistivity of the soil-cement samples at freshly prepared state, after 1 hour curing help to decide whether the soil-cement mix meets the desired strength and performance criteria at the freshly prepared state itself. This offers the option of the soil-cement mix to be upgraded (possibly with additional cement) in its fresh state itself, if it does not fulfil the performance criteria, rather than wasting the material after hardening.

Stabilisation of soils with additives helps to increase strength, reduce deformability, provide volume stability, reduce permeability and reduce erodibility. Chen et al. (2011) observed that apparent electrical resistivity increases with the increase of curing time and decreases porosity and degree of saturation as a result of cement hydration development. Wei et al. (2012) established a linear relationship between 28 day compressive strength and resistivity of cement paste after 24 hours. The compressive strength of cement paste at 28 day could be predicted easily using a quantitative relation developed with resistivity of cement paste at 24 hours. In this study, electrical resistivity measurements of freshly prepared uncured and cured soil cement materials are carried out and the correlation between the factors controlling the performance of soil cement and electrical resistivity are being studied. Simple regression equations are developed between electrical resistivity and compressive, tensile and the shear strength parameters. Multiple regression equations are developed

between unconfined compressive strength and electrical resistivity of the soil-cement mix at freshly prepared state and after 1 hour curing, in an attempt to predict the performance of soil cement mixtures in the fresh state itself without having to wait for 7 days. Moreover, predicting the strength parameters at the freshly prepared state could be advantageous and a necessity in many cases. If the soil-cement material does not meet the strength requirement as per the resistivity models developed, additional cement constituents could be added in the fresh state itself and used. This will prevent wasting of the materials after hardening. The additional advantages of the technique are that it is quick and non-destructive.

## **5.2 Electrical Resistivity of Stabilised Soils**

Liu et al. (2008) conducted a study for investigating the factors controlling the electrical resistivity of soil-cement admixtures.

**5.2.1 Effect of cement content:** With the increase in cement content, water content and void ratio of the soil-cement admixture get decreased due to the hydration reaction and pozzolanic reaction. As a result, the path for the conduction of electrical current becomes more tortuous. Therefore, the electrical resistivity of the soil-cement admixture increased. Higher the cement content, higher will be the hydration compounds formed.

**5.2.2 Effect of degree of saturation:** Electrical resistivity increased with the decrease in degree of saturation because less pore spaces were filled with pore water, as water get utilized for hydration reaction and thus a continuous water bridging is not available for electrical conduction.

**5.2.3 Effect of water content on electrical resistivity:** With decrease in water content, the tortuosity of the conduction path for the electrical current increases, resulting in increase of electrical resistivity.

**5.2.4 Effect of curing time on electrical resistivity:** with the increase in the curing time, the chemical reaction products such as calcium silicate hydrate (CSH) and calcium aluminate hydrate (CAH) formed binds finer soil particles together resulting in a denser soil structure. Hence electrical resistivity is increased.

### 5.3 Materials used

The soils used in the present study are lithomargic soils, which are products of lateritization. These soils are locally called as ‘Shedi soils’ and are available in varied colours. These soils are characterized by high silt content and low strengths (George et al., 2012). In order to vary the percentage of fines, in the different test samples, controlled soil samples were prepared. River sand was used for blending the shedu soil. All these soil samples were used to study the geotechnical and electrical properties. The percentages of river sand used were 0, 10, 20 and 30 % by weight of dry soil. The samples are designated as A, B, C, and D respectively. For the experimental investigations, river sand passing IS 4.75 mm sieve and retained on IS 75 micron sieve was considered. The sieve analysis curves of the samples are shown in Fig 5.1.

### 5.4 Cement

Ordinary Portland Cement (OPC) 43 grade was used in the study. The percentages of cement used were 2%, 4% and 6% in each of the four soil samples, A, B, C and D. These samples are designated as A2, A4, A6, B2, B4, B6, C2, C4, C6, D2, D4 and D6 respectively.

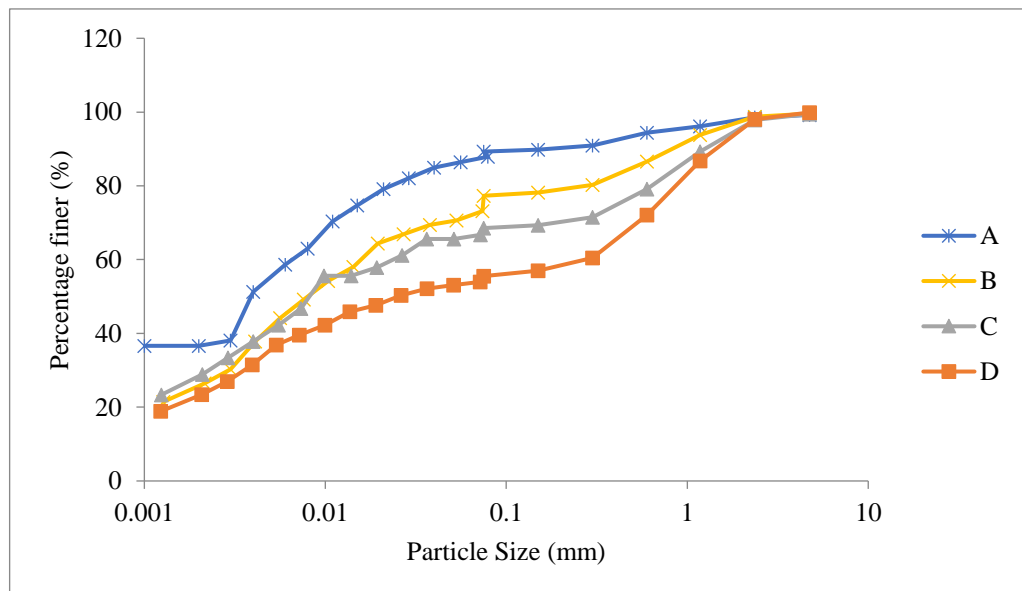


Figure 5.1 Sieve Analysis results of Soil Samples

## 5.5 Test method

Electrical resistivity measurement of all the controlled samples were done by making cylindrical samples of size 7.6 cm height and 3.8 cm diameter. For each combination, in addition to the point of maximum dry density and optimum moisture content obtained from Standard Proctor and Modified Proctor tests, two points each were selected on the dry side and wet side of the compaction curve to study resistivity variation for different compaction conditions (Figs. 5.3 to 5.26). The resistivity measurements were taken for all the seven curing days. Electrical resistivity was measured by using a circuit consisting of a 30 V DC power supply, two high precision multimeters serving as ammeter and voltmeter and electrodes connecting to the sample as seen in Fig. 5.2. Two circular steel plates are placed touching the two ends of the sample which acts as current electrodes and two steel pins at one-third length from both ends act as voltage electrodes. The stainless steel electrodes were arranged in Wenner  $\alpha$  configuration. Wenner  $\alpha$  array is less affected by the electrode position error compared to dipole-dipole array (Clement and Moreau 2016).

Resistivity was measured in the freshly prepared state, after one hour curing and after one to seven days of curing.

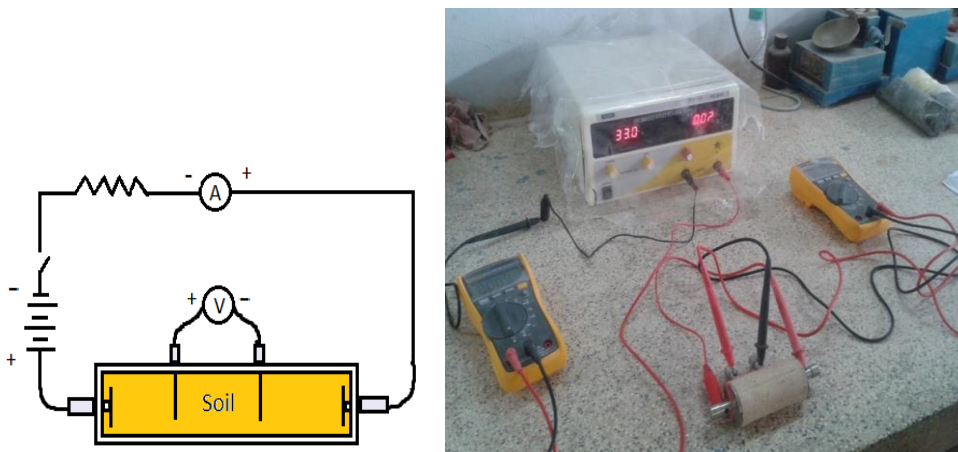


Figure 5.2 Resistivity measurement

## 5.6 Results and Discussions

The basic geotechnical properties of the soil stabilized with different percentages of cement are given in Table 5.1.

Table 5.1 Compaction and strength characteristics of the soil cement samples.

Parameter	Soil-cement samples															
	A0	A2	A4	A6	B0	B2	B4	B6	C0	C2	C4	C6	D0	D2	D4	D6
$\gamma_{dmax}$ , kN/m <sup>3</sup> (LC)	14.5	14.6	14.8	14.6	15.6	15.6	15.0	15.4	15.9	15.7	15.6	15.6	16.4	16.6	16.7	16.6
<b>OMC (%)</b> (LC)	28.0	28.3	26.8	25.6	25.0	22.4	25.2	24	23.2	22.8	23.4	23.2	21.0	20.6	18.8	20.4
$\gamma_{dmax}$ , (kN/m <sup>3</sup> ) (HC)	14.9	16.4	16.4	16.5	15.9	17.3	17.3	17.7	16.4	18.3	18.4	18.2	17.5	18.8	18.4	18.4
<b>OMC (%)</b> (HC)	27.0	22.1	21.9	21.6	22.0	19.0	19.0	17.2	21.0	14.4	16.0	16.5	18.0	14.9	15.4	16.0
<b>7 day</b> <b>UCS (kPa)</b> (LC)	130.8	478.8	814.8	991.7	155.6	733.0	863.6	1691.8	162.2	769.3	1307.3	1703.5	289.2	1080.8	1507.5	2130.2
<b>C (kPa)</b> (LC)	23.5	290.0	340.0	480.0	21.0	265.0	280.0	390.0	19.0	190.0	245.0	320.0	18.5	140.0	180.0	260.0
<b>Φ</b> (degrees) (LC)	20.0	31.0	35.0	40.0	25.0	34.0	36.0	41.0	31.0	37.0	41.0	43.0	31.0	38.0	46.0	51.0
<b>STS</b> (kPa) (LC)	-	75.52	109.9	112.8	-	64.1	104.2	107.03	-	52.6	101.3	104.2	-	55.5	98.4	101.3

NOTE:  $\gamma_{dmax}$ - max dry density, OMC- Optimum Moisture Content, LC- Light Compaction, HC- Heavy Compaction, UCS- Unconfined Compressive Strength, C- Cohesion,  $\Phi$ - Angle of internal friction, STS- Split Tensile Strength.

### 5.6.1 Variation of resistivity with time of curing

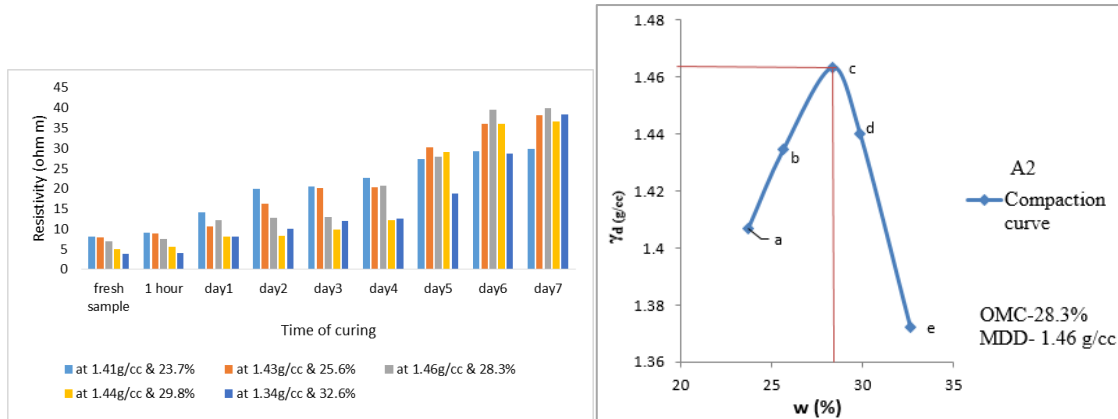


Figure 5.3 Variation of Electrical Resistivity with time for different compaction conditions (Light) for sample A2

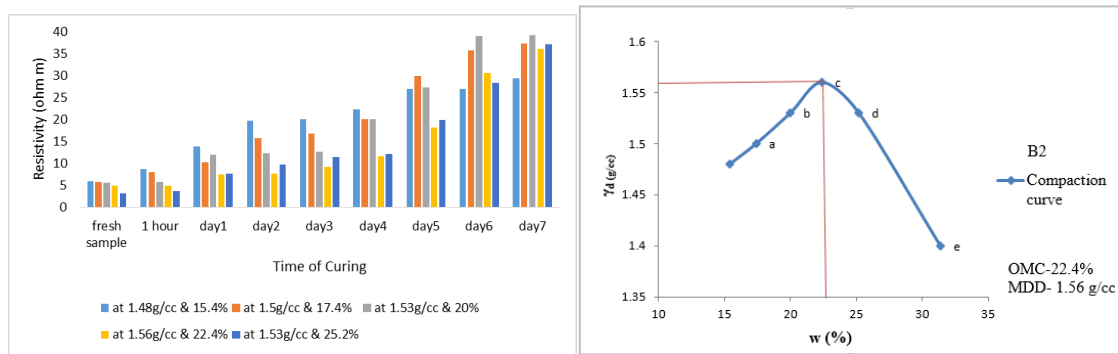


Figure 5.4 Variation of Electrical Resistivity with time for different compaction conditions (Light) for sample B2

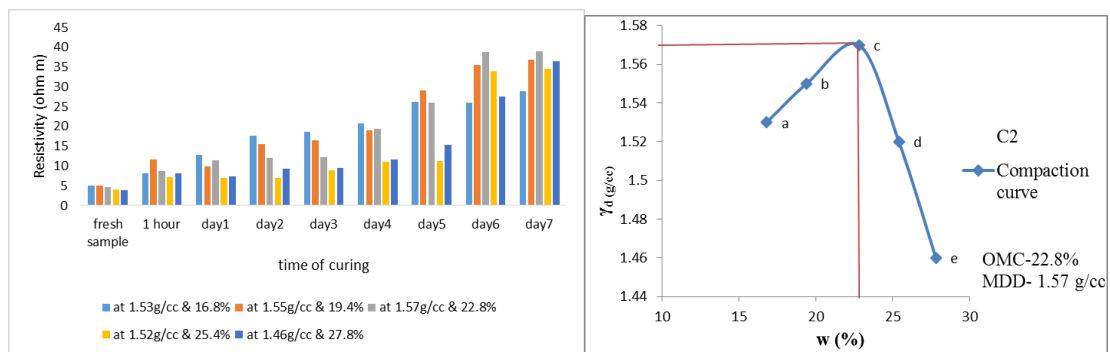


Figure 5.5 Variation of Electrical Resistivity with time for different compaction conditions (Light) for sample C2

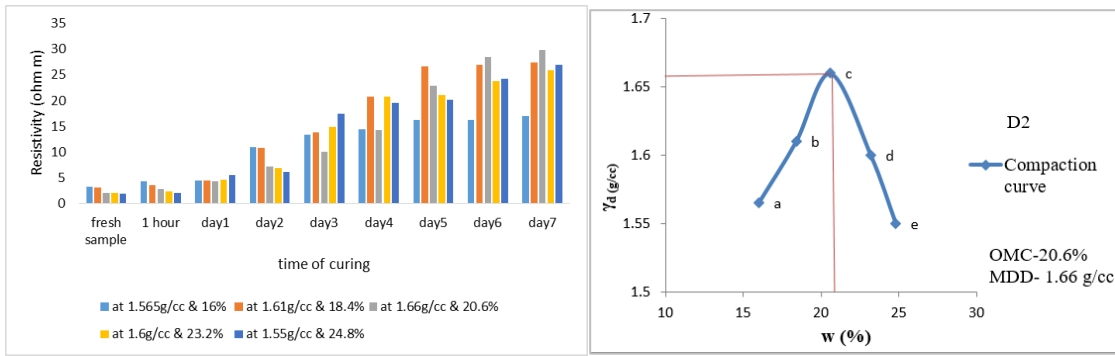


Figure 5.6. Variation of Electrical Resistivity with time for different compaction conditions (Light) for sample D2

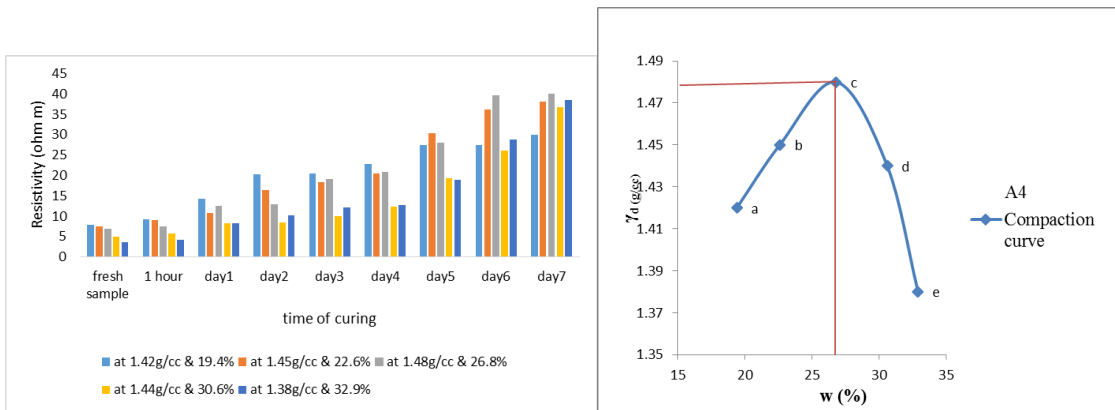


Figure 5.7 Variation of Electrical Resistivity with time for different compaction conditions (Light) for sample A4

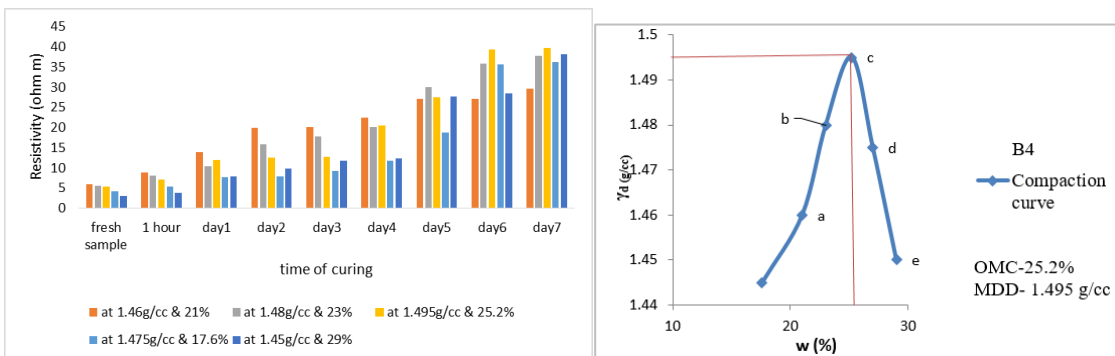


Figure 5.8 Variation of Electrical Resistivity with time for different compaction conditions (Light) for sample B4



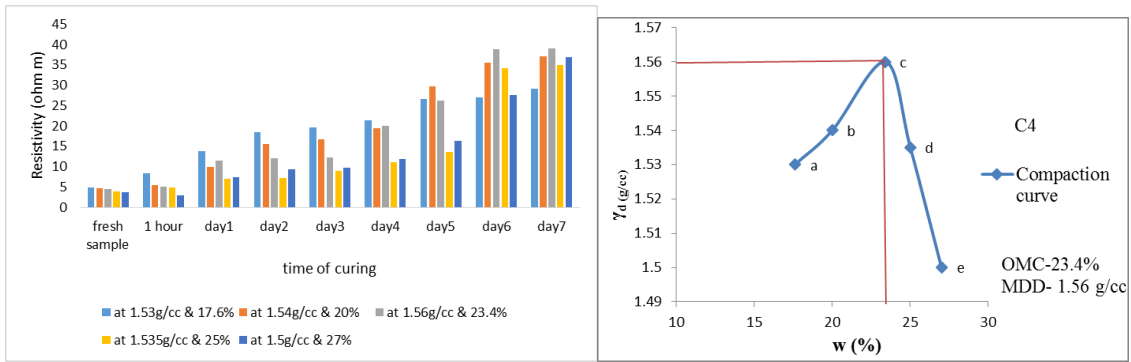


Figure 5.9 Variation of Electrical Resistivity with time for different compaction conditions (Light) for sample C4

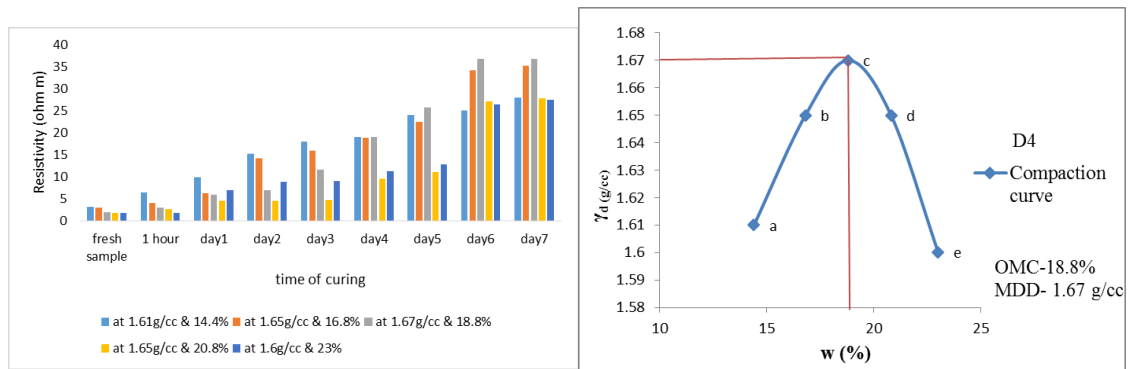


Figure 5.10 Variation of Electrical Resistivity with time for different compaction conditions (Light) for sample D4

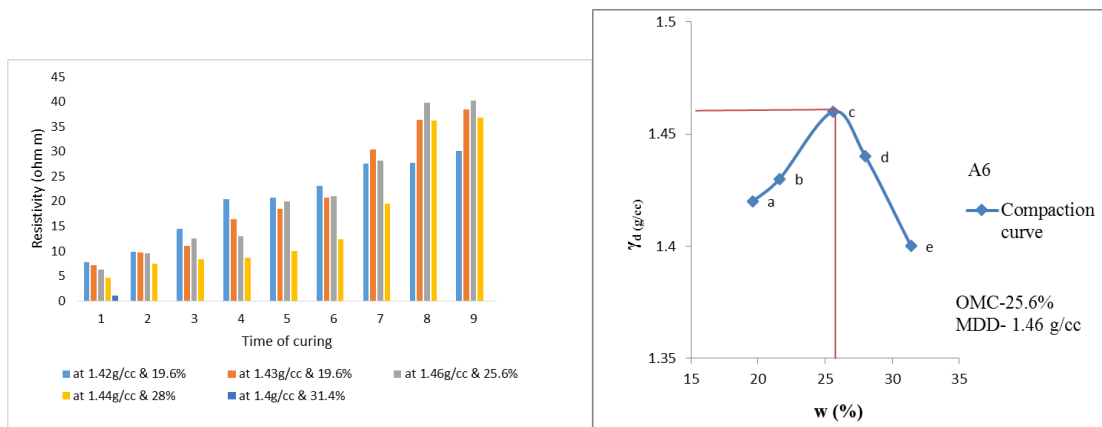


Figure 5.11 Variation of Electrical Resistivity with time for different compaction conditions (Light) for sample A6

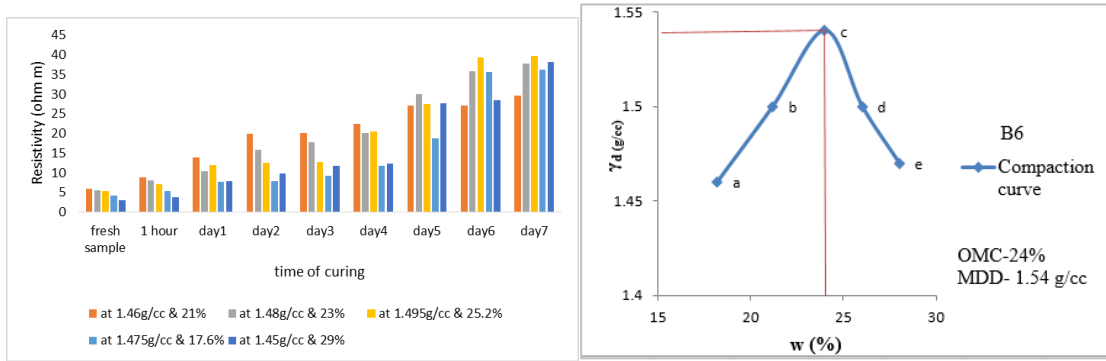


Figure 5.12 Variation of Electrical Resistivity with time for different compaction conditions (Light) for sample B6

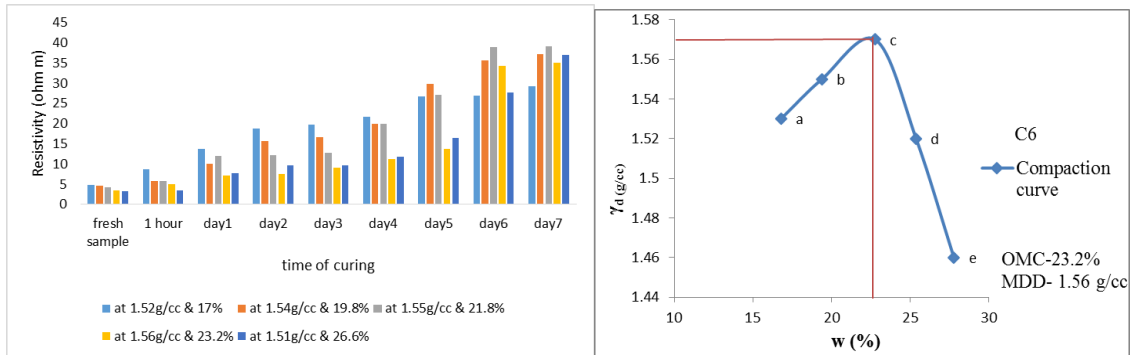


Figure 5.13 Variation of Electrical Resistivity with time for different compaction conditions (Light) for sample C6

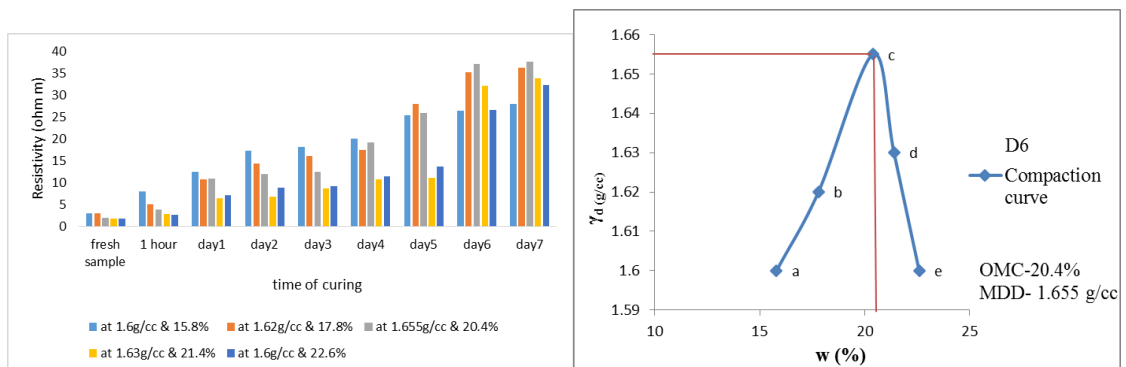


Figure 5.14 Variation of Electrical Resistivity with time for different compaction conditions (Light) for sample D6

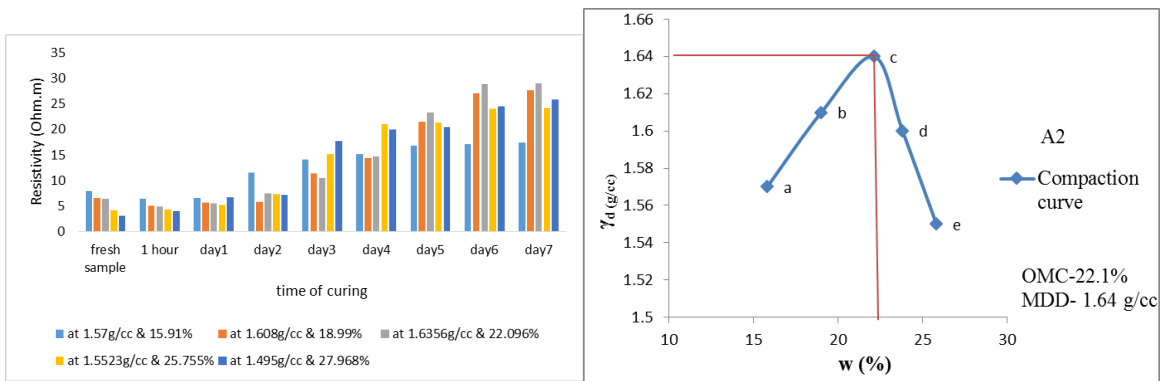


Figure 5.15 Variation of Electrical Resistivity with time for different compaction conditions (Heavy) for sample A2

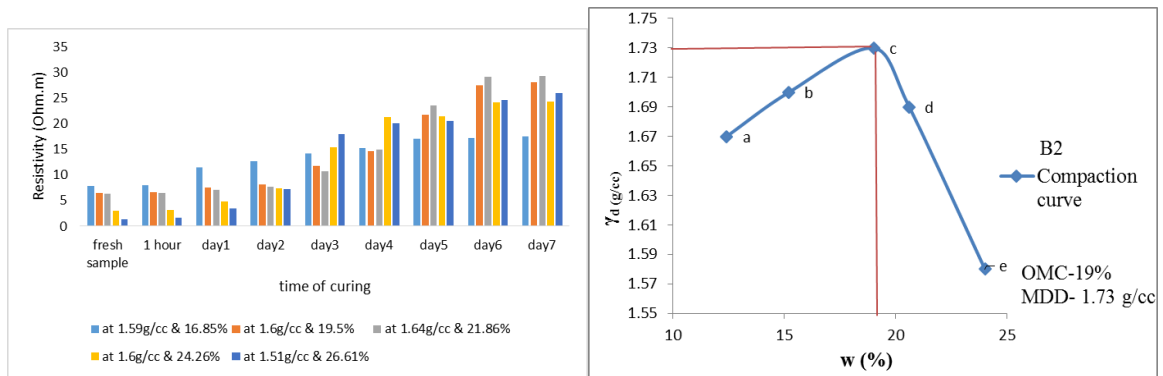


Figure 5.16 Variation of Electrical Resistivity with time for different compaction conditions (Heavy) for sample B2

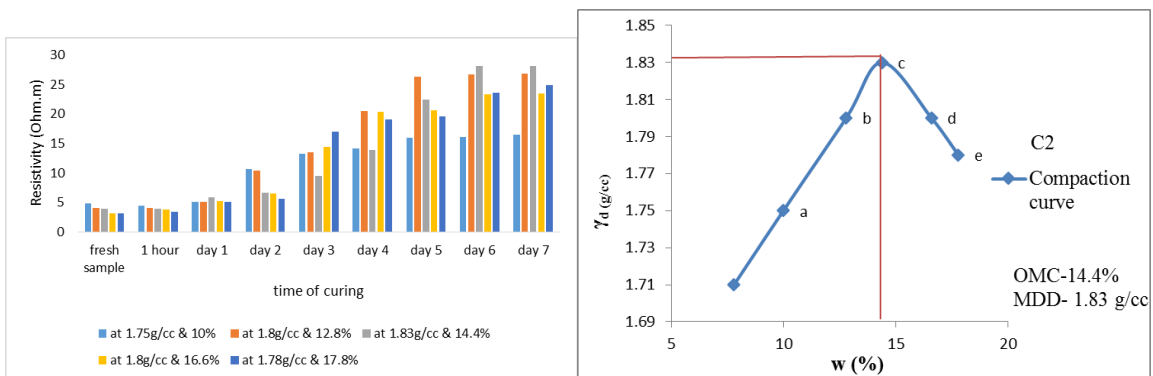


Figure 5.17 Variation of Electrical Resistivity with time for different compaction conditions (Heavy) for sample C2

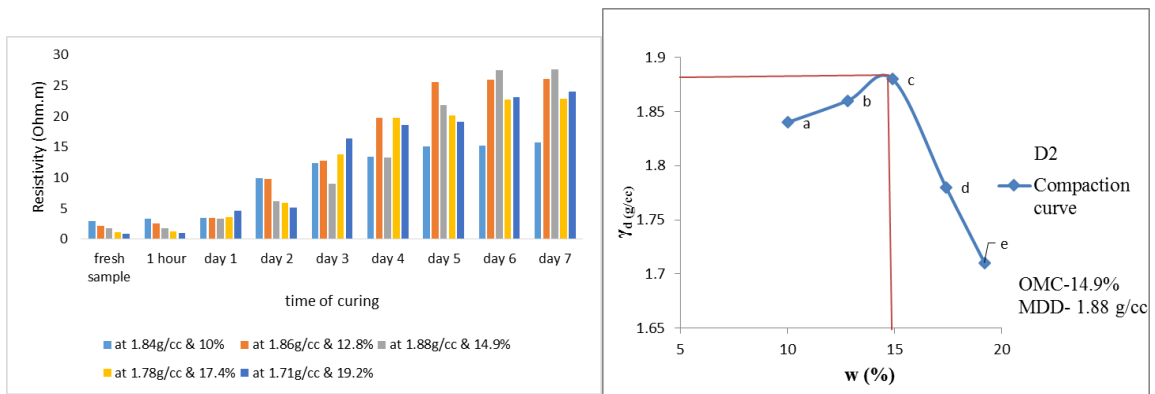


Figure 5.18 Variation of Electrical Resistivity with time for different compaction conditions (Heavy) for sample D2

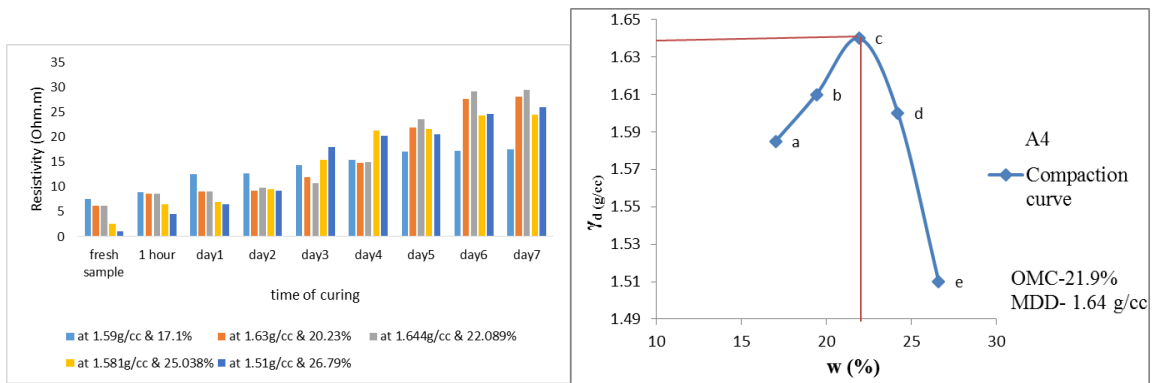


Figure 5.19 Variation of Electrical Resistivity with time for different compaction conditions (Heavy) for sample A4

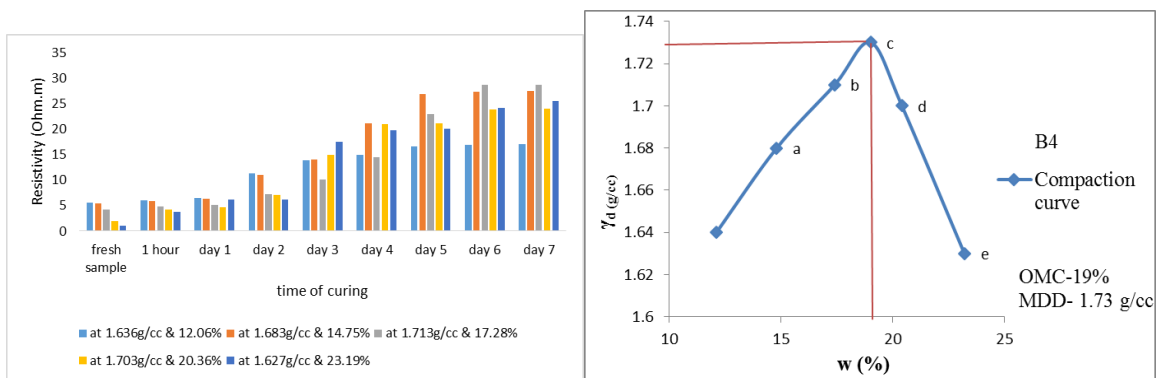


Figure 5.20 Variation of Electrical Resistivity with time for different compaction conditions (Heavy) for sample B4

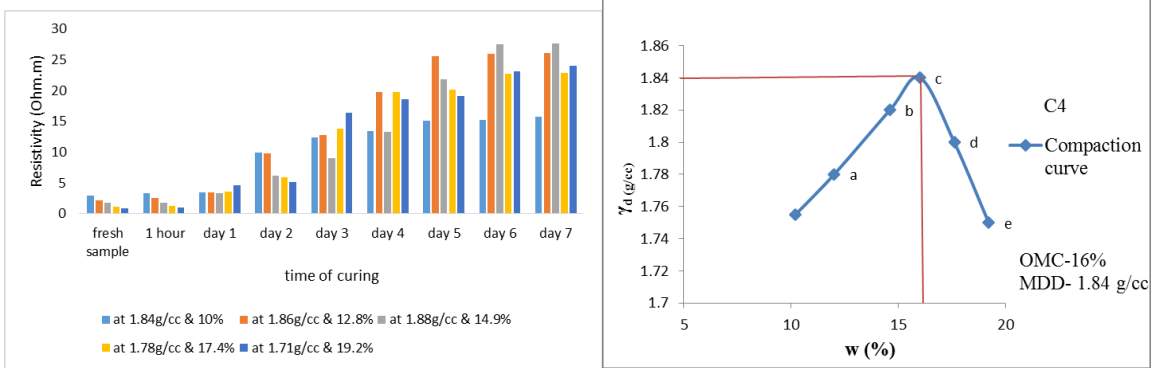


Figure 5.21 Variation of Electrical Resistivity with time for different compaction conditions (Heavy) for sample C4

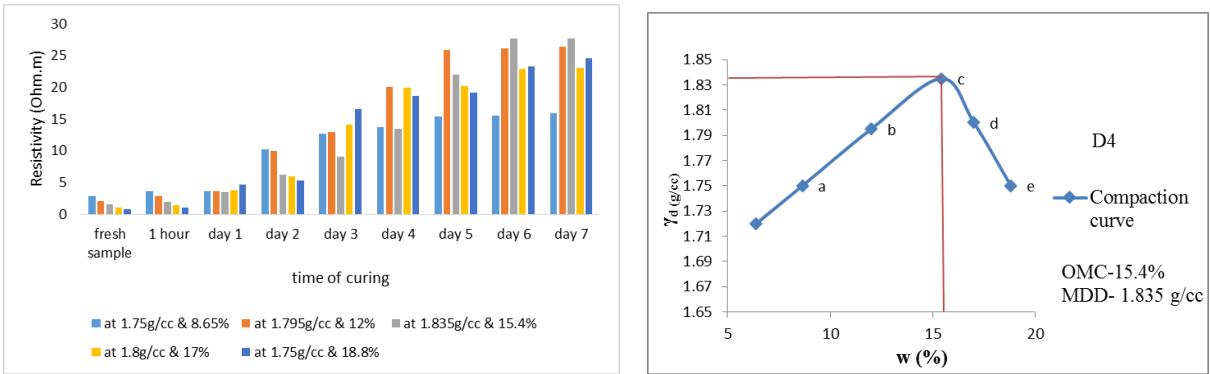


Figure 5.22 Variation of Electrical Resistivity with time for different compaction conditions (Heavy) for sample D4

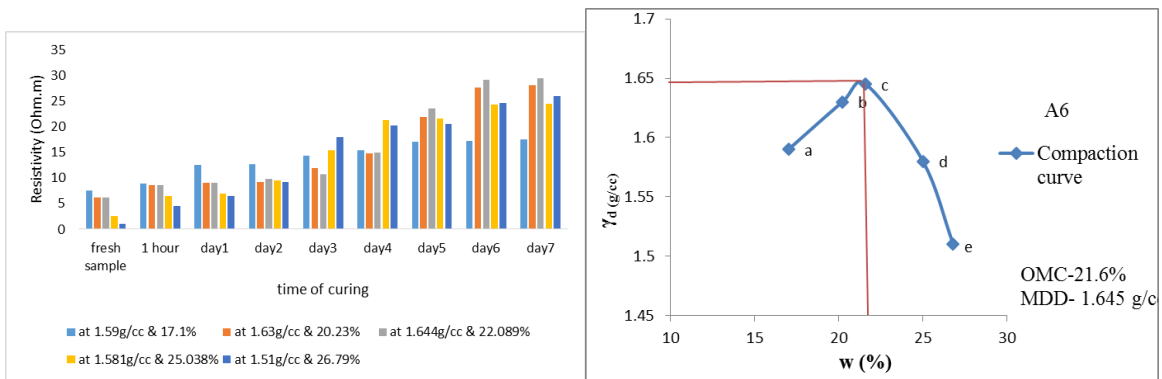


Figure 5.23 Variation of Electrical Resistivity with time for different compaction conditions (Heavy) for sample A6

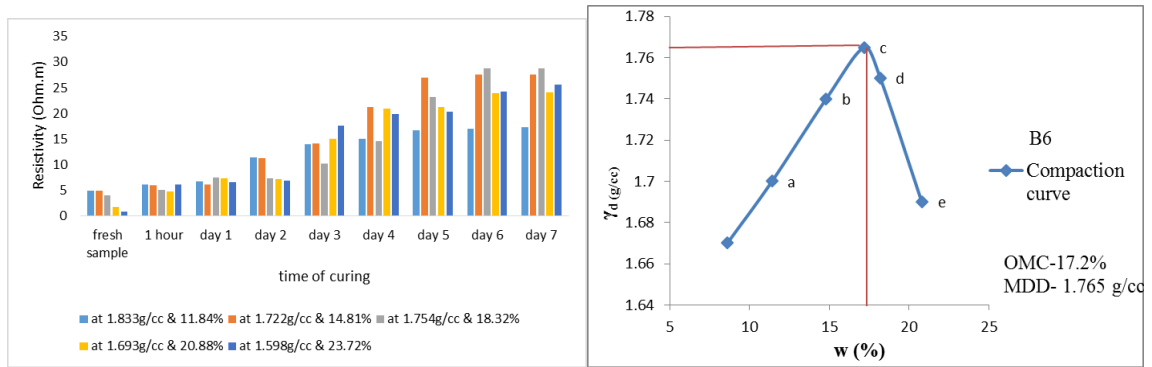


Figure 5.24 Variation of Electrical Resistivity with time for different compaction conditions (Heavy) for sample B6

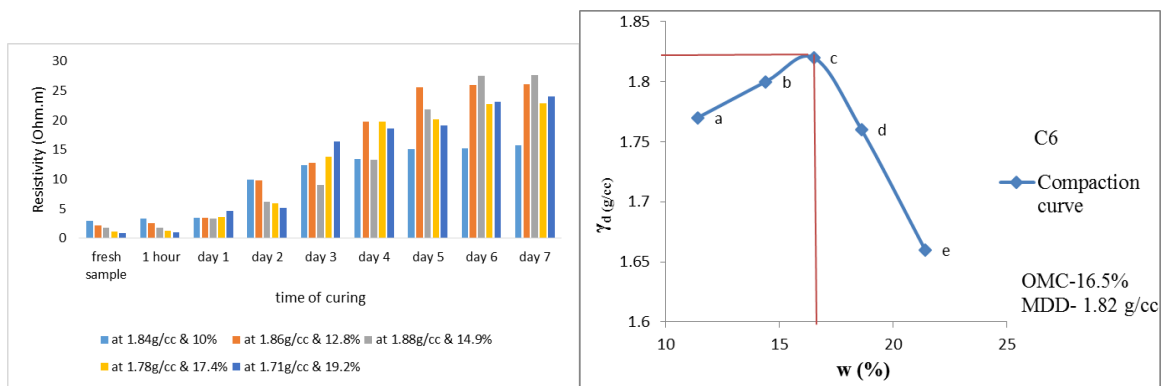


Figure 5.25 Variation of Electrical Resistivity with time for different compaction conditions (Heavy) for sample C6

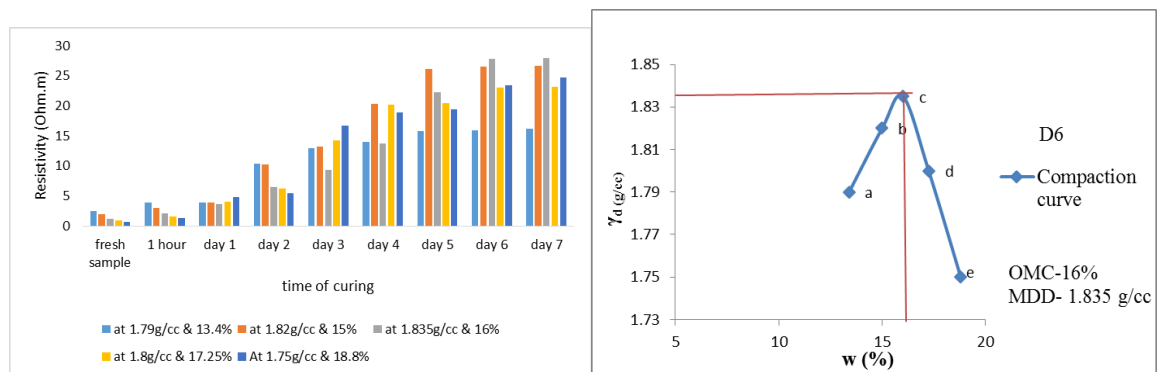


Figure 5.26 Variation of Electrical Resistivity with time for different compaction conditions (Heavy) for sample D6

From Fig 5.3 to 5.26, which shows variation of resistivity at wet side to dry side of the compaction curve, with time of curing, it is seen that resistivity increases with curing period. The resistivity results show that for all the soil cement samples, at freshly prepared state and after one hour of curing time, resistivities are high when compacted on dry side

of optimum. With increase of moisture content, resistivity decreases significantly. In the wet side, soil resistivity is low. The moulding water content which was available for electrical conduction at freshly prepared state gets utilized for hydration of cement, which depletes the free water film available for conduction, with time of curing.

### 5.6.2 Resistivity with compaction effort

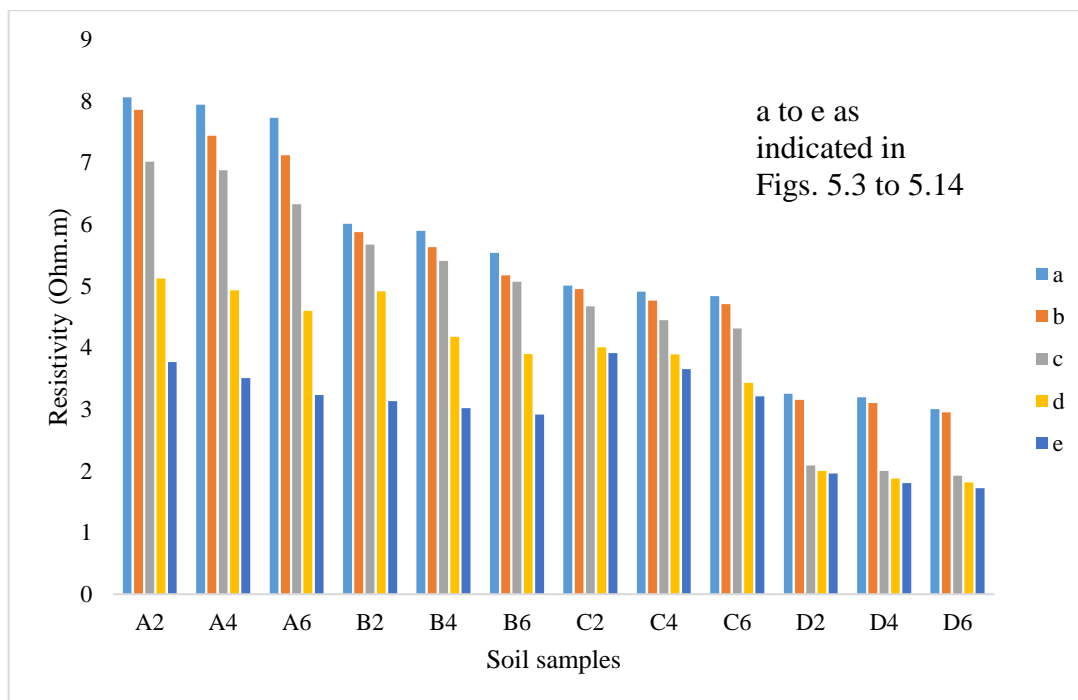


Figure 5.27 Variation of Resistivity at dry side and wet side points on the standard proctor compaction curve at day zero

The electrical response of soil when the soil samples are compacted with different degree of compaction is also looked into. Light and heavy mechanical compaction were performed on the soil samples and the resistivity variation on these samples at different compaction condition is being studied. In the bar graphs (Figs. 5.27 and 5.28), 'a' and 'b' represents the dry side of optimum compaction points. The point 'c' represents the maximum compaction condition. The points 'd' and 'e' represent the wet side of compaction points (as shown in Figs. 5.3 to 5.26). It is seen from Figs. 5.27 and 5.28 that resistivity decreases with increase in water content and dry density on the dry side, but is dependent only on water content in the wet side of the compaction curve.

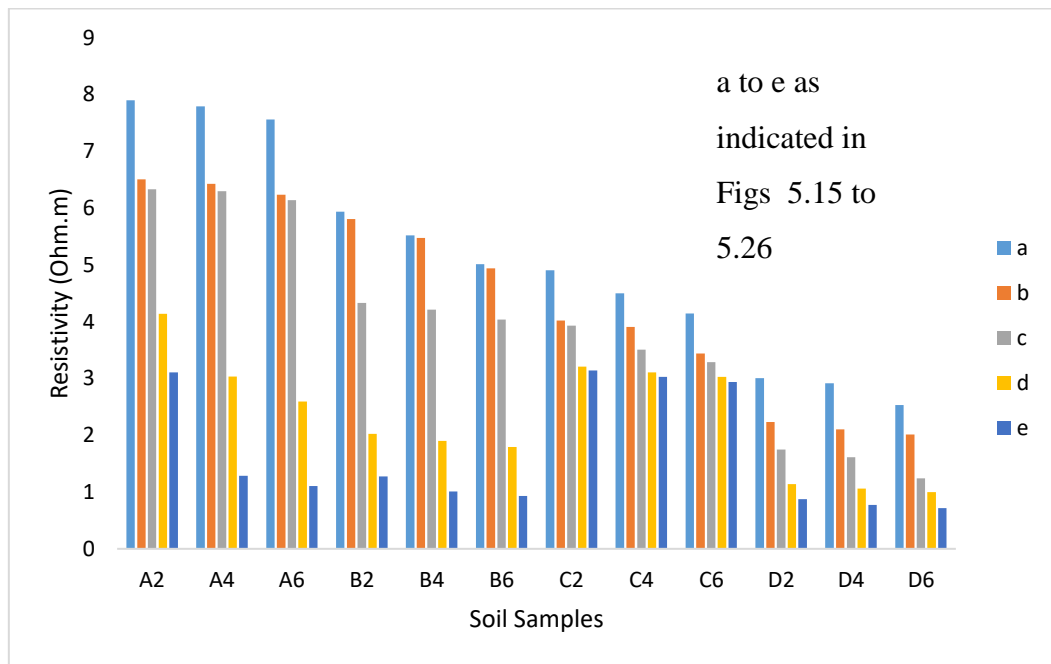


Figure 5.28 Variation of Resistivity at dry side and wet side points on the modified proctor compaction curve at day zero

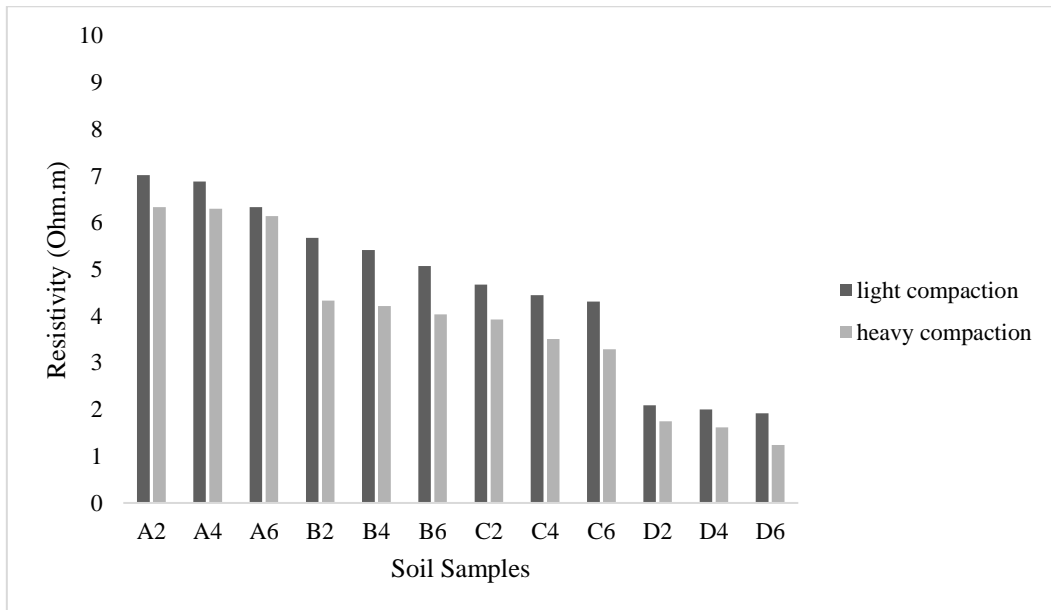


Figure 5.29. Variation of Electrical Resistivity at light compaction (LC) and heavy compaction (HC) day zero compaction conditions at OMC and maximum dry density conditions

From Fig. 5.29, it is observed that the resistivities are comparatively lower for the samples compacted at heavy compaction conditions than those compacted at light compaction



conditions for all curing periods. The solid particles of non-cohesive soils are poor conductive while electrical current flow occurs only in intergranular spaces filled with mineralized water. As a consequence, the electrical conductivity of rocks and soils is clearly dependent on the amount of water in the medium, the conductivity of water and how the water is spread (porosity, the degree of saturation, cementation factor, fracturing). At heavy compaction conditions, soil attain a denser state with higher degree of saturation and lesser air voids, which results in a lower apparent resistivity of the soils. At freshly prepared state and after one hour of curing, the ions present in the saturated and continuous micropores slightly exhibit higher electrical conduction and hence a lower resistivity in heavily compacted soil-cement samples compared to lightly compacted samples.

After 7 days of curing, the soil-cement samples harden and less water and ions will be available for conduction. The lightly compacted samples are more porous than heavily compacted dense samples. After 7 days of curing, water in these pores is utilized for hydration of cement, and is replaced with air which offers infinite electrical resistance. Hence, after a period of seven days of curing also, the lightly compacted soil-cement samples exhibit higher resistivity than the heavily compacted ones.

### **5.6.3 Variation of resistivity with cement content**

It is observed that in freshly prepared state, resistivity decreases slightly with cement content for all the soil-cement samples (Figs 5.30 to 5.33). But on the other hand, resistivity is slightly increasing with cement content when measured after curing (Figs. 5.34 to 5.37).

Cement reduces the plasticity and water-retention capacity of the soil and improves its strength. Immediately after mixing, calcium (Ca) and hydroxyl (OH) ions go into solution. Then after a few minutes a slow precipitation of semi-crystalline calcium silicate hydrate gel (C-S-H) occurs while the Ca and OH ions concentrations continue to increase slowly. Hence, initially the freshly prepared soil-cement samples show some conductivity, which diminishes with time. The Ca ion concentration reaches the saturation level, and the hydration reactions begin, with the crystallization of solid calcium hydroxide and the deposition of C-S-H gel in voids. While the structure is progressing up, the pore spaces decreases and the availability of ions and water will be lesser, which results in a higher electrical resistivity. The hydration compounds fill in pore spaces and intersect with each other to form a denser structure. In the meantime, the free water space and porosity

decreases and tortuosity increases. Consequently, electrical resistivity increases more significantly (Zhang et al., 2012).

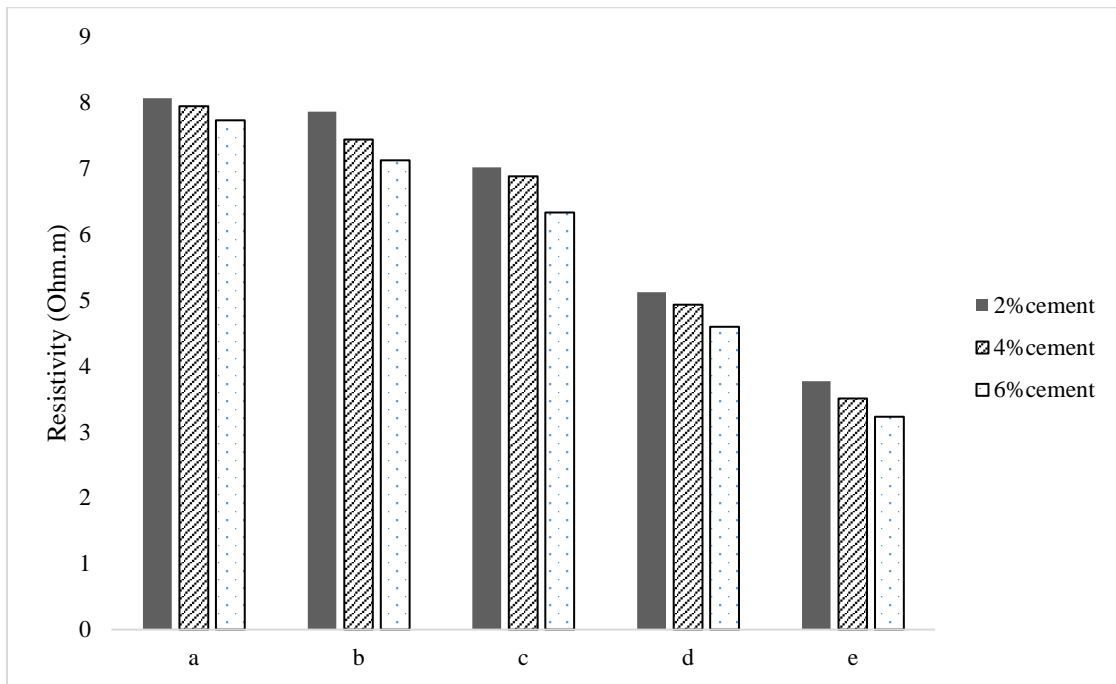


Figure 5.30 Variation of Resistivity with cement content at dry side and wet side points on the standard proctor compaction curve at freshly prepared state for sample A

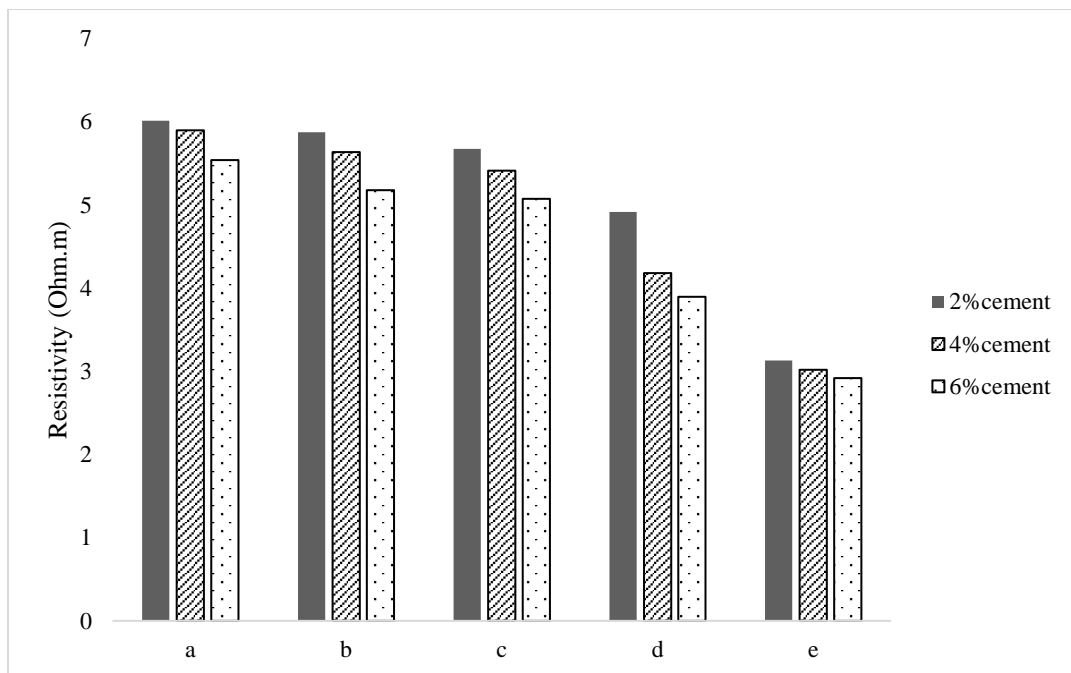


Figure 5.31 Variation of Resistivity with cement content at dry side and wet side points on the standard proctor compaction curve at freshly prepared state for sample B

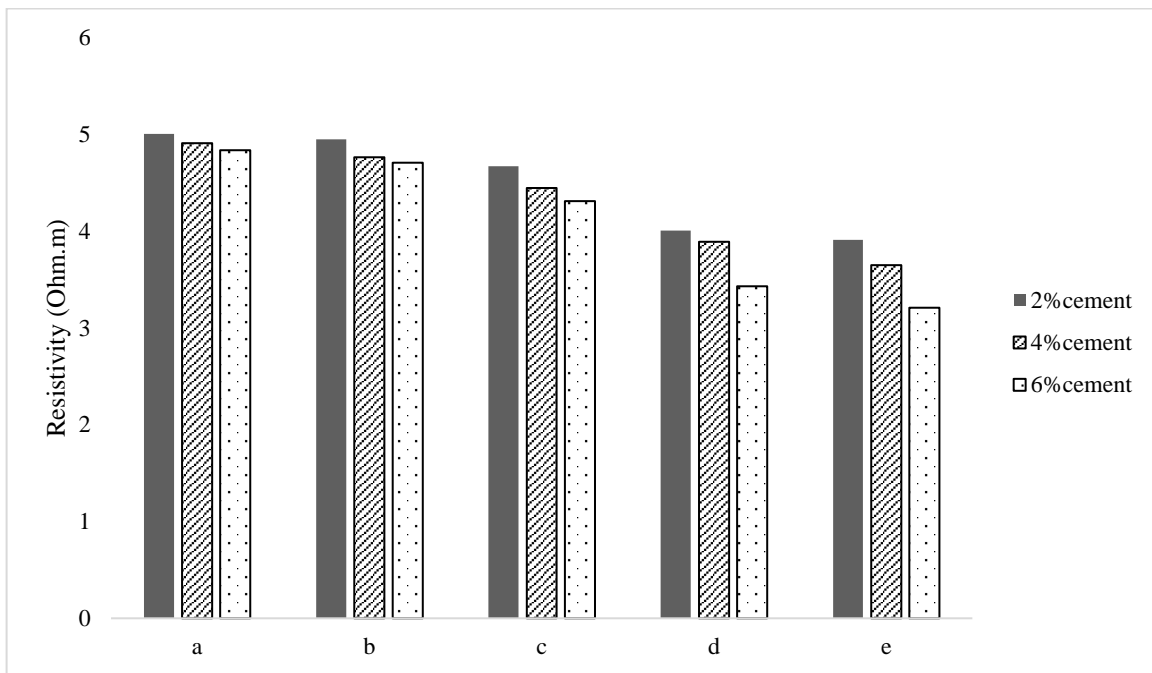


Figure 5.32 Variation of Resistivity with cement content at dry side and wet side points on the standard proctor compaction curve at freshly prepared state for sample C

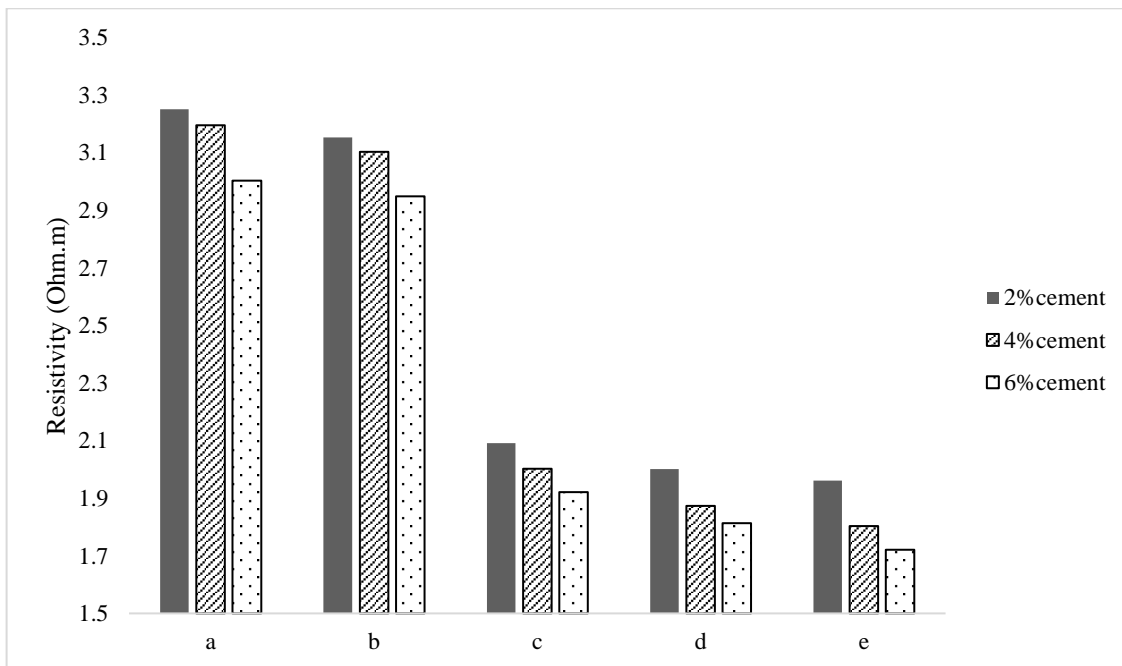


Figure 5.33 Variation of Resistivity with cement content at dry side and wet side points on the standard proctor compaction curve at freshly prepared state for sample D

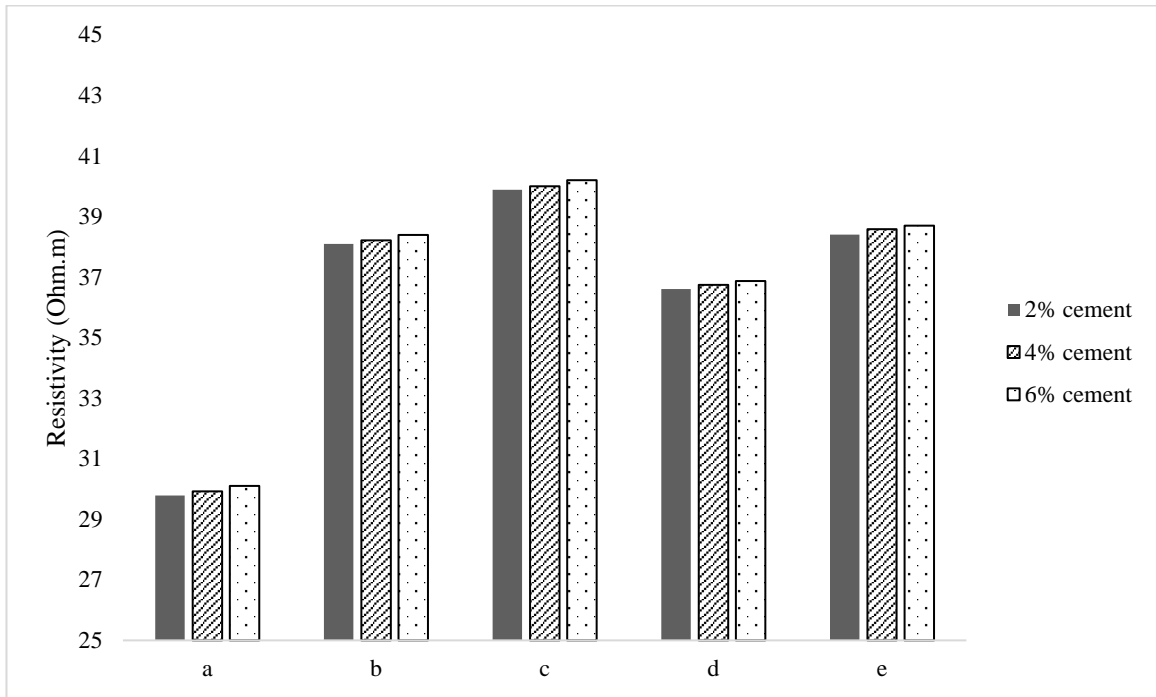


Figure 5.34 Variation of Resistivity with cement content at dry side and wet side points on the standard proctor compaction curve at after 7 days curing for sample A

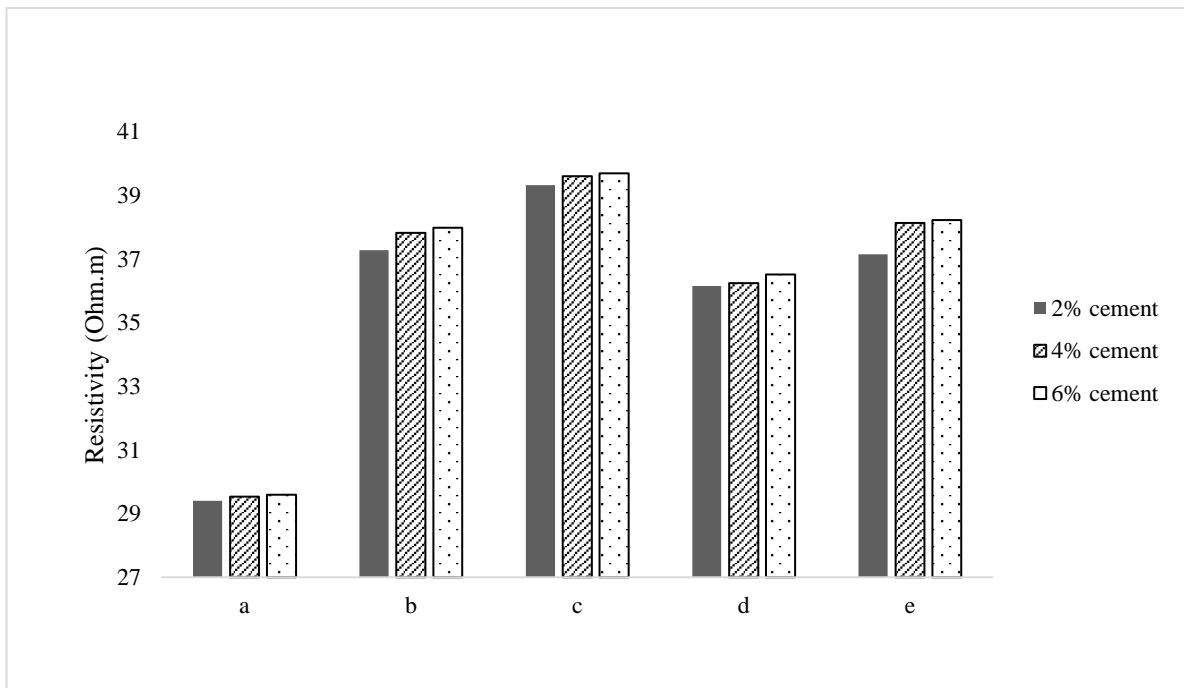


Figure 5.35 Variation of Resistivity with cement content at dry side and wet side points on the standard proctor compaction curve after 7 days curing for sample B

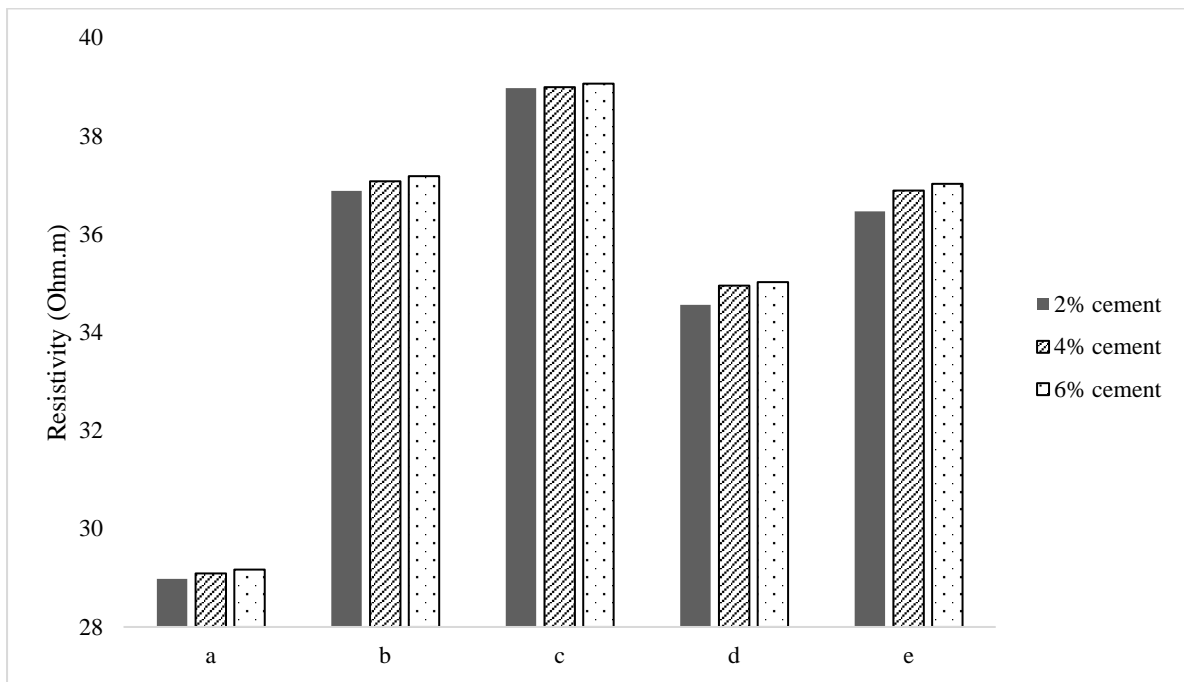


Figure 5.36 Variation of Resistivity with cement content at dry side and wet side points on the standard proctor compaction curve after 7 days curing for sample C

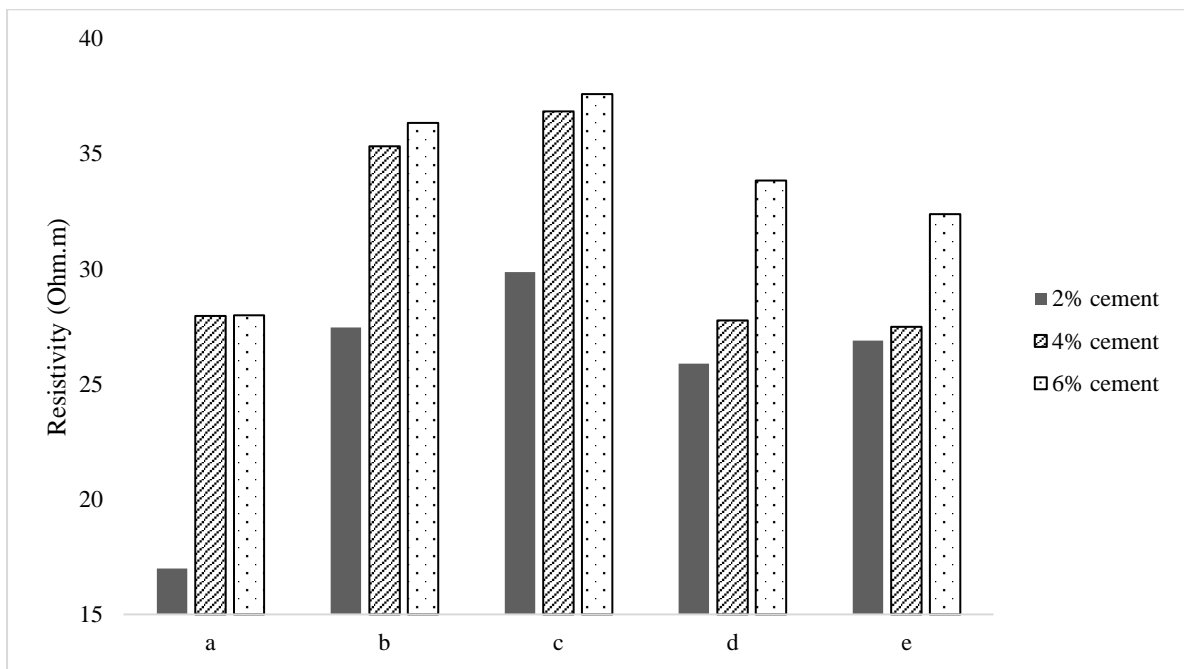


Figure 5.37 Variation of Resistivity with cement content at dry side and wet side points on the standard proctor compaction curve after 7 days curing for sample D

### 5.6.4 Resistivity with porosity

Porosity of all the sample combinations was found for all the curing days. Cement content has a great effect on electrical resistivity of soil-cement. The measured electrical resistivity of cement treated soils increases with the increase of cement content (Zhang et al., 2012). For a given curing time, higher cement content yields higher amount of hydration products resulting in a denser structure. As a result, free water space and porosity decreases and tortuosity increases resulting in increase of electrical resistivity.

Figures 5.38 to 5.41 to show the variation of electrical resistivity with porosity for varying percentages of river sand. It can be observed that as cement content increases, porosity decreases. With curing time, for each percentage of cement, porosity decreases and the denser structure results in increase of resistivity.

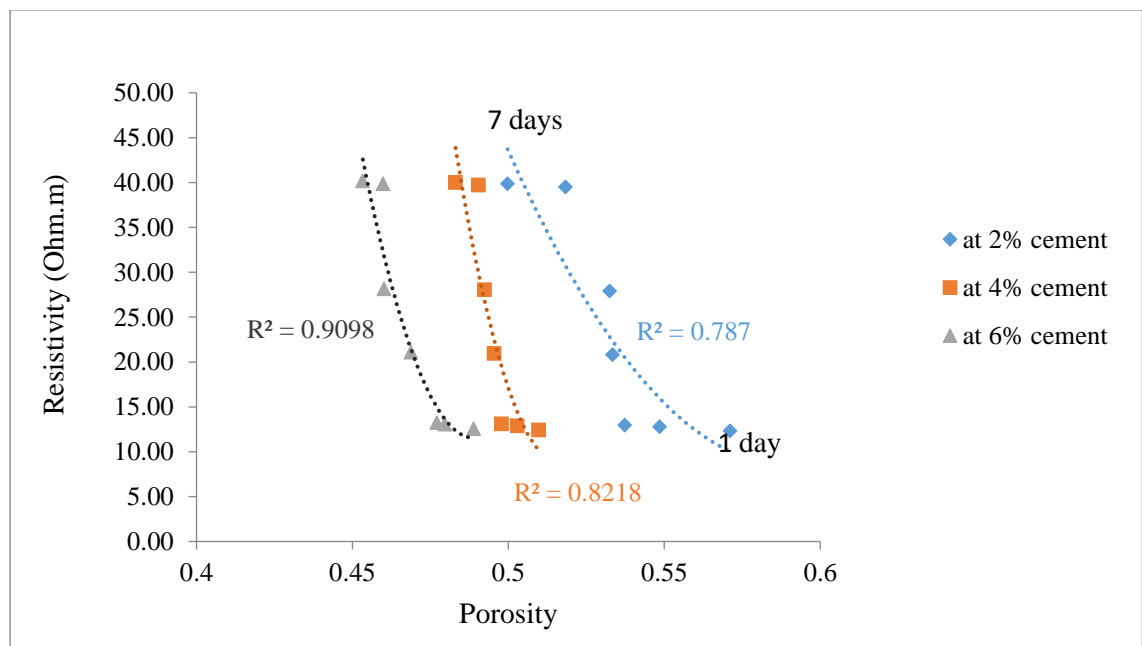


Figure 5.38 Variation of resistivity with porosity for sample A

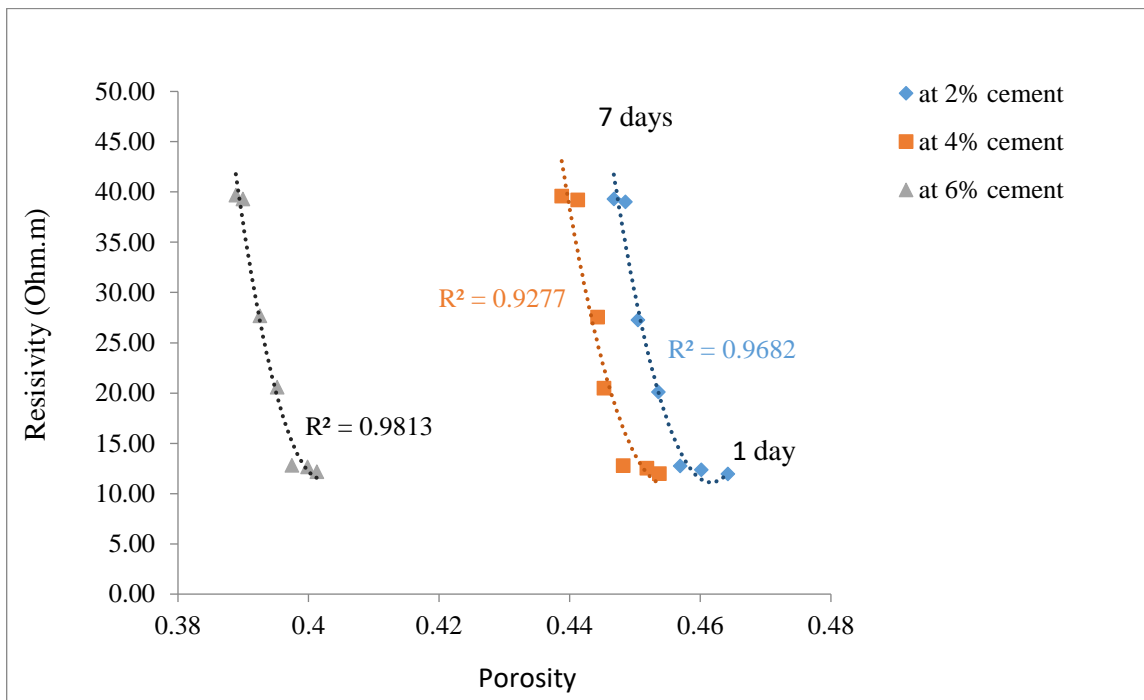


Figure 5.39 Variation of resistivity with porosity for sample B

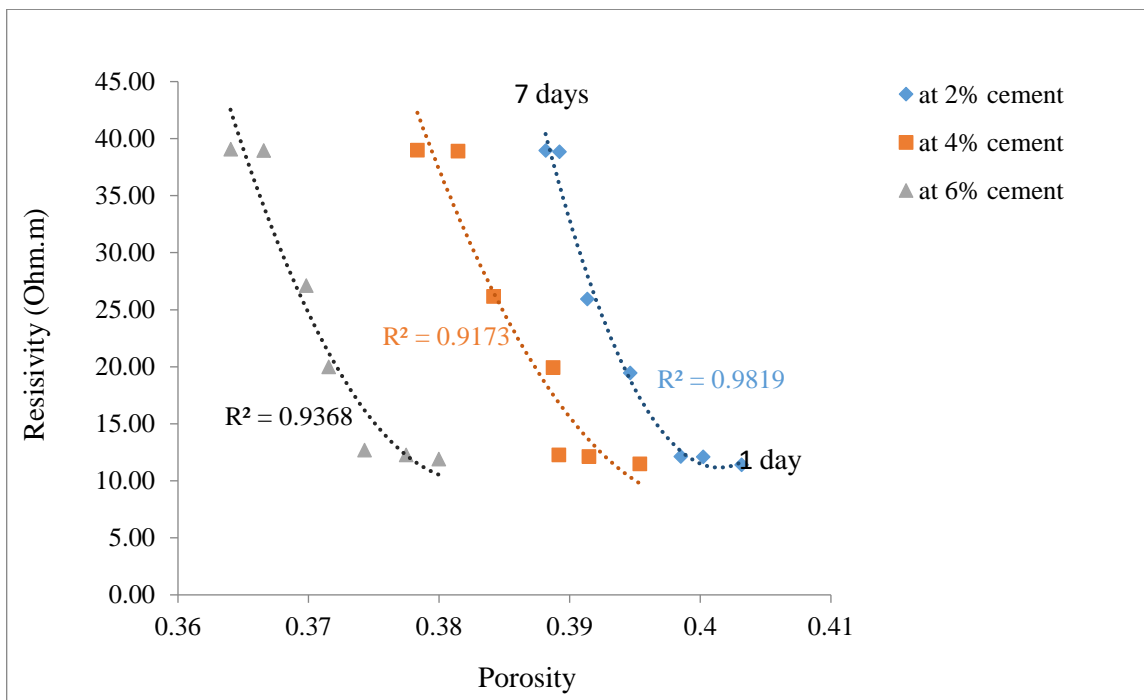


Figure 5.40 Variation of resistivity with porosity for sample C

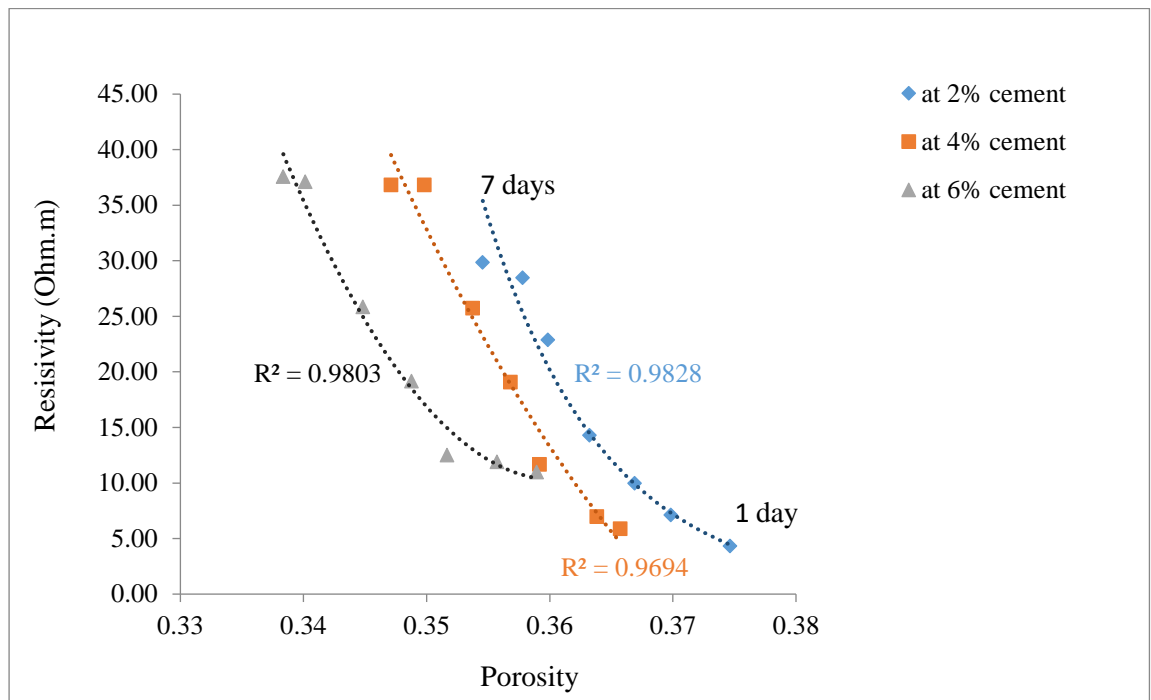


Figure 5.41 Variation of resistivity with porosity for sample D

### 5.6.5 Scanning Electron Microscope (SEM) Analysis

The micro fabric (geometric arrangement of platelets) and mineralogical aspects of the lithomargic clay combined with cement and river sand was studied using Scanning Electron Microscope (SEM). The Scanning Electron Microscope (SEM) is a type of electron microscope that images the sample surface by scanning it with a high-energy beam of electrons in a raster scan pattern. The electrons interact with the atoms that make up the sample producing signals that contain information about the sample's surface topography, composition and other properties such as electrical conductivity. In this case the secondary electrons are reflected only from the surface of the sample. Thus, SEM can identify the micro fabric of only topmost surface of the sample. Sample preparation included mounting samples on carbon double-stick tape on aluminum stubs. The samples were then coated with gold sputter coater. First the entire surface is scanned under low magnification and then, the chosen areas are magnified to get the clear picture of the micro fabric arrangement. Scanning Electron Microscope Analysis is explained in detail in Chapter 7.



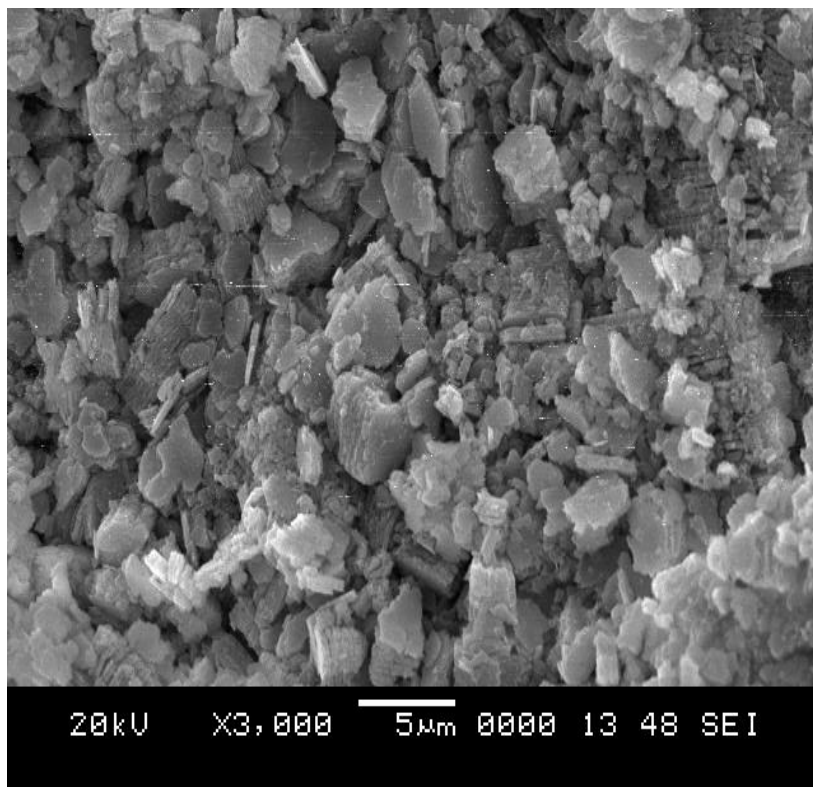


Figure 5.42 SEM image of soil cement at freshly prepared state

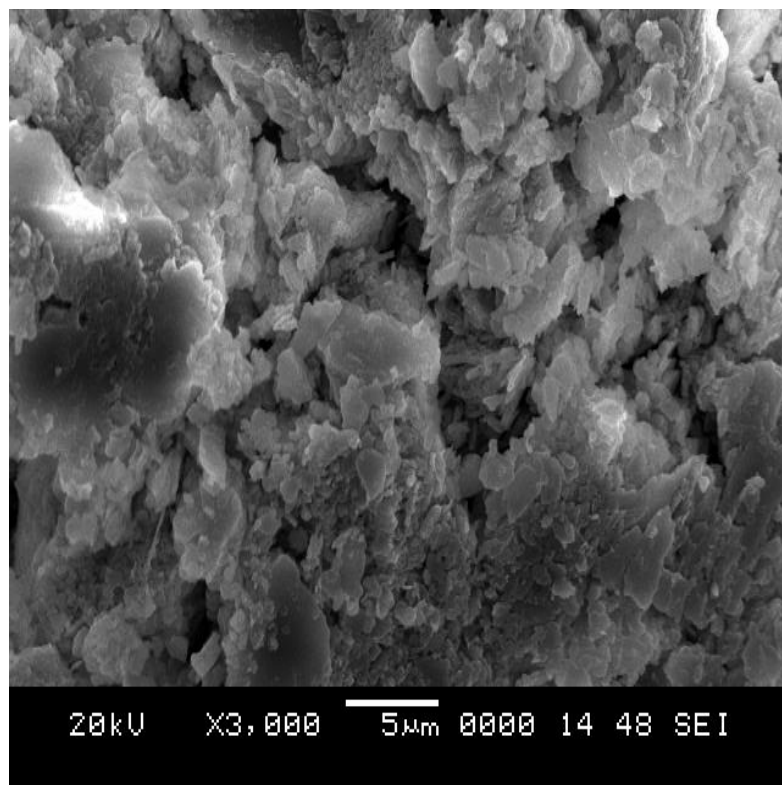


Figure 5.43 SEM image of soil cement after 1 day curing

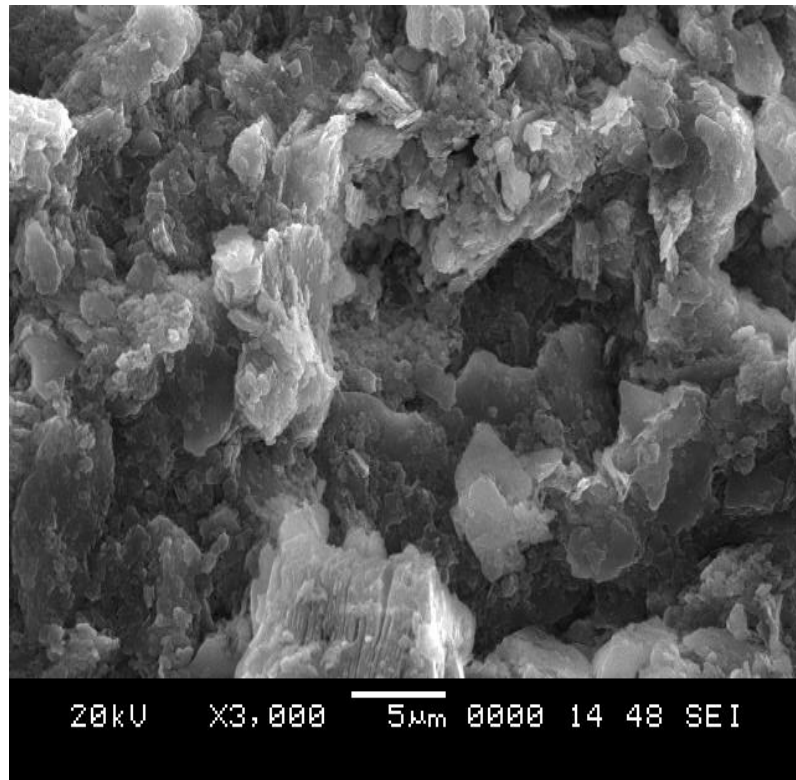


Figure 5.44 SEM image of soil cement after 2 days curing

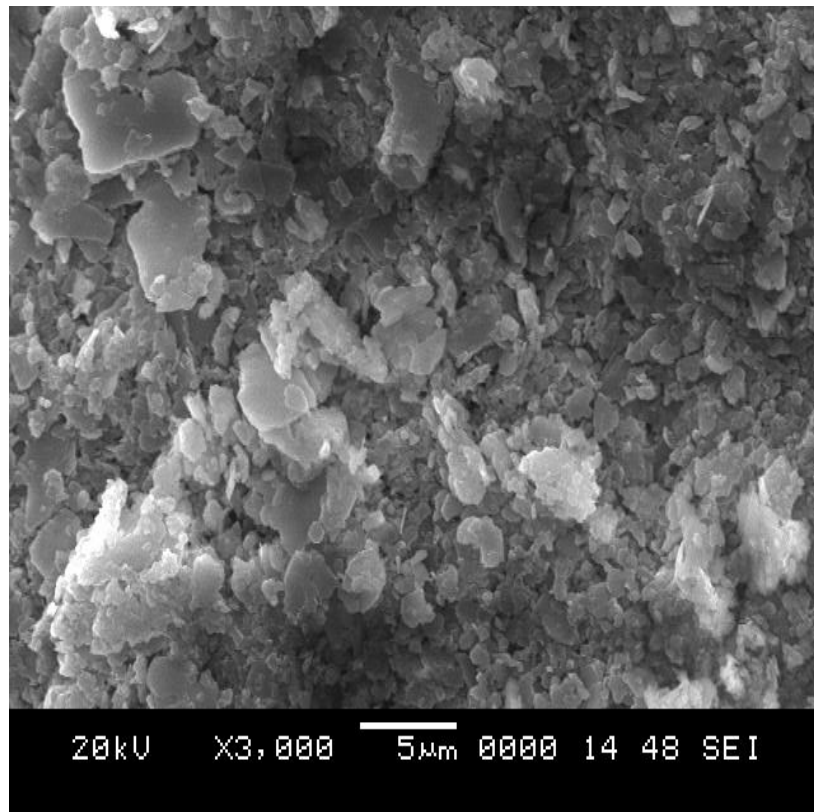


Figure 5.45 SEM image of soil cement after 3 days curing

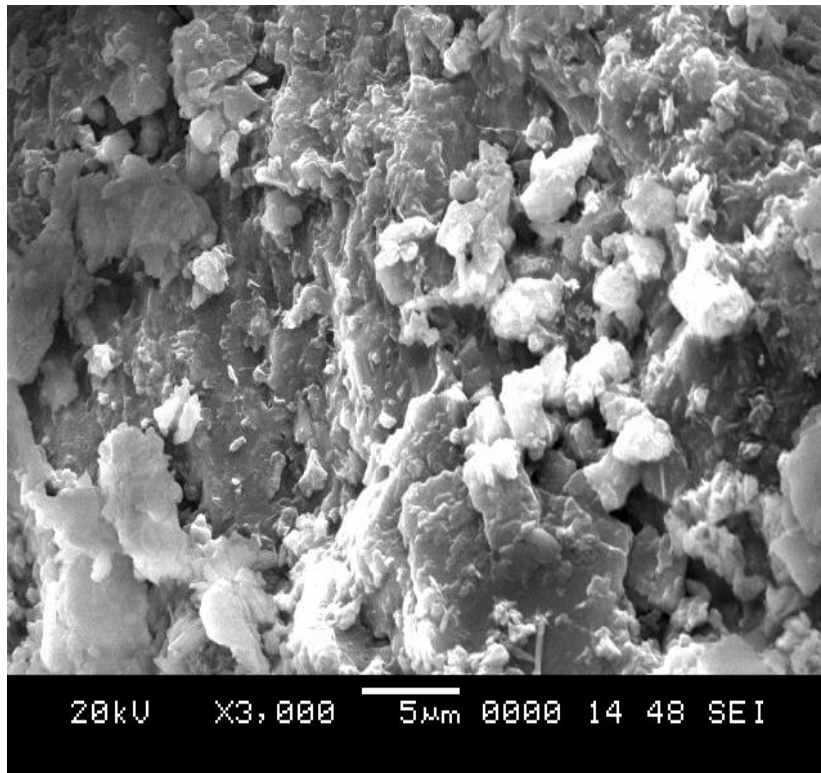


Figure 5.46 SEM image of soil cement after 4 days curing

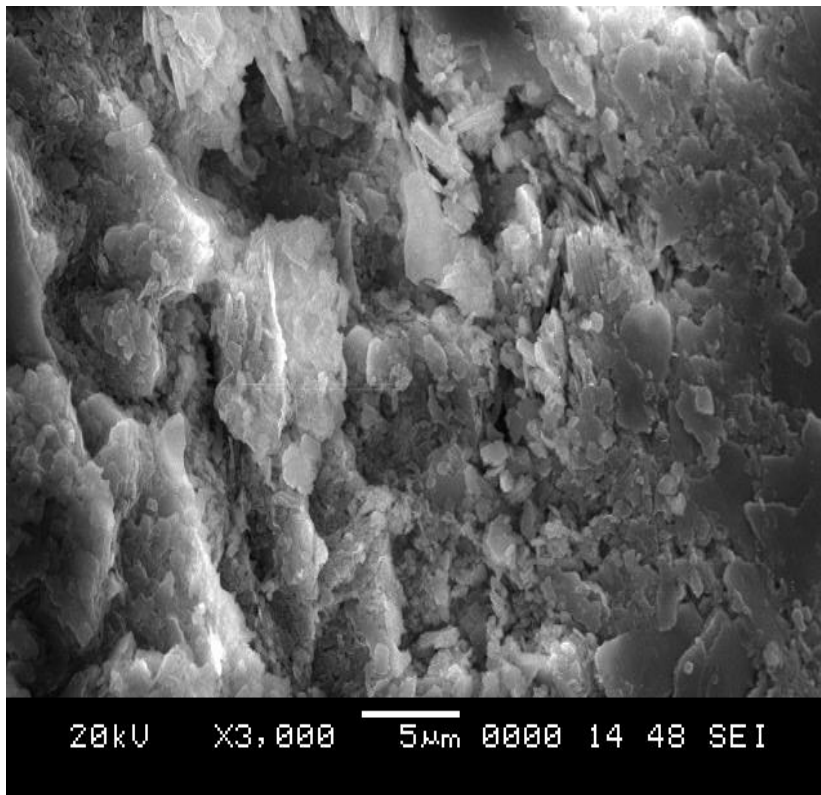


Figure 5.47 SEM image of soil cement after 5 days curing

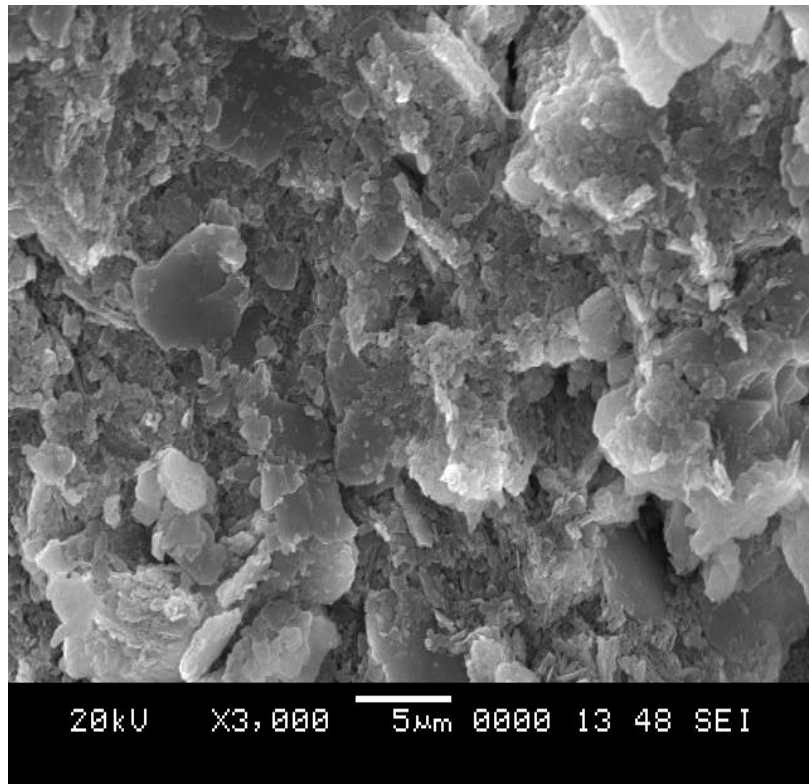


Figure 5.48 SEM image of soil cement after 6 days curing

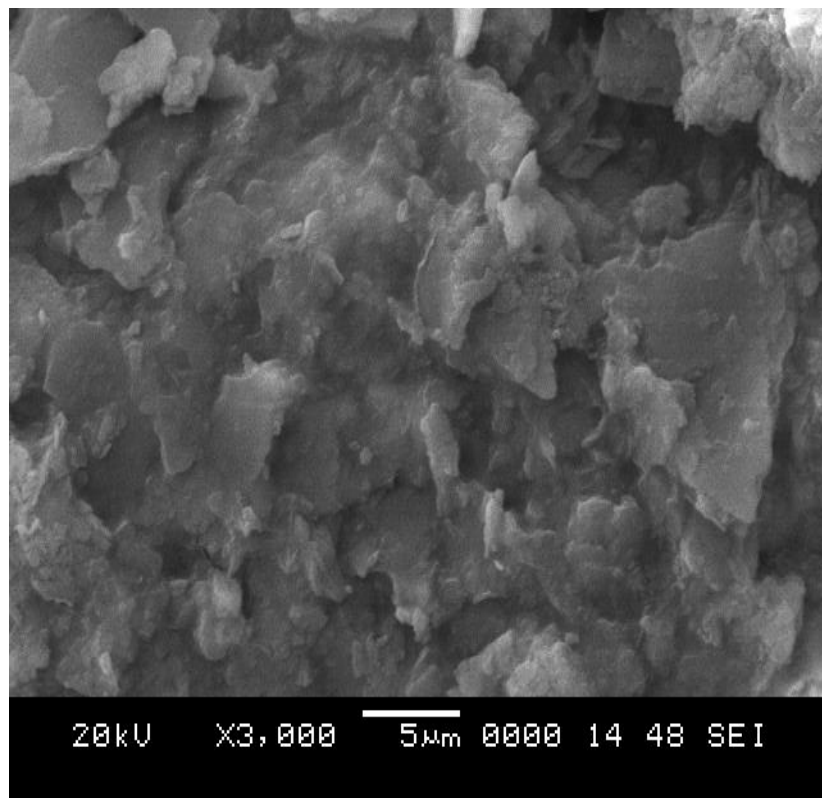


Figure 5.49 SEM image of soil cement after 7 days curing

From SEM photos for sample A2 at different curing periods, (as shown in Figs. 5.42 to 5.49), it is observed that the pore spaces or the conductive path rapidly decreases with curing time. The structure becomes more clustered with lesser voids with increase of curing time. This is because of the formation of hydration products which fills in the pore spaces and develops the bond strength and increases the resistivity with curing time. Similarly for all the other samples A4, A6, B2, B4, B6, C2, C4, C6, D2, D4 and D6 also, the micro structure becomes more dense and clustered with increase in curing time.

### 5.6.6 Resistivity with Unconfined Compressive Strength (UCS)

Figures 5.50 to 5.52 show resistivity variation at different times such as in the freshly prepared state, after one hour of curing and after seven days of curing with 7<sup>th</sup> day UCS. With the increase in percentage of cement and river sand added, UCS is found to increase as particles become more clustered and gets bonded by the cementing action and the sand particles which replace the finer particles of soil takes up more load. The difference in controlling parameters of the electrical resistivity and the compressive strength such as ion concentration in pore fluid, surface charges of the soil particles, which are factors affecting ER but not UCS was suggested as the reason behind the nonlinear relationship between electrical resistivity and unconfined compressive strength of soil-cement by Zhang et al. (2012).

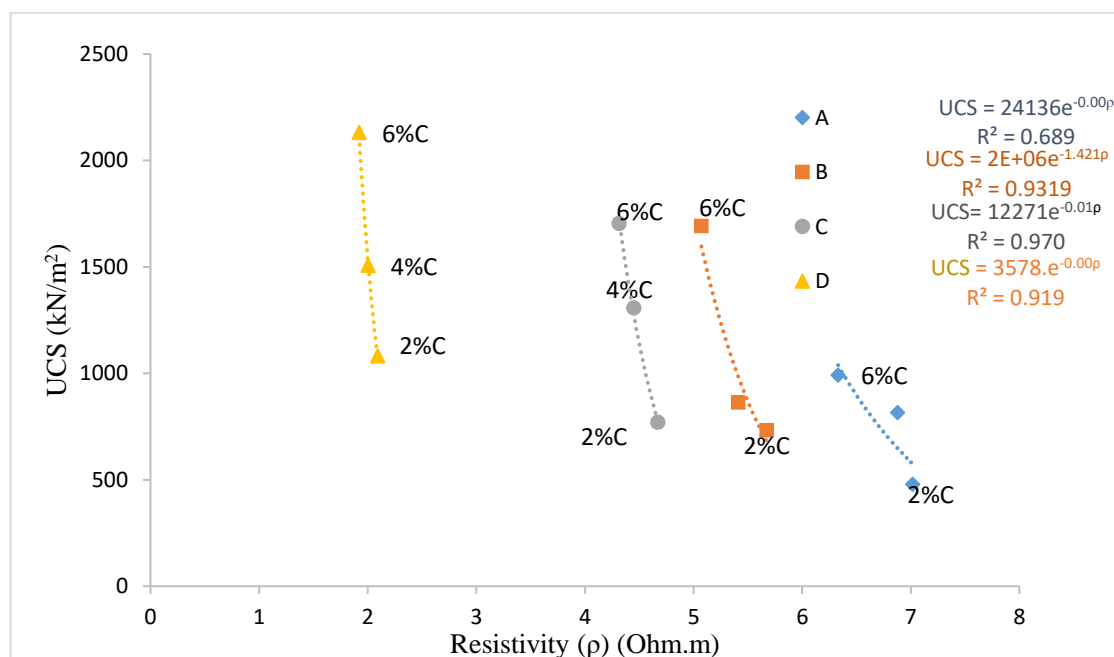


Figure 5.50 7 day UCS vs Resistivity (at freshly prepared state)

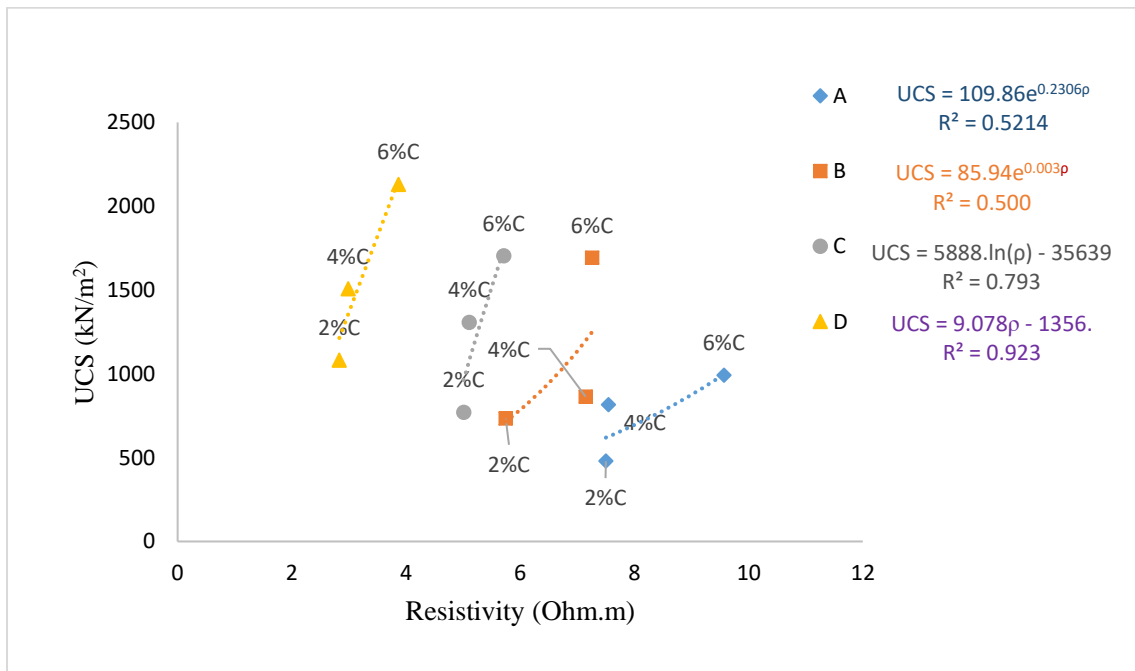


Figure 5.51 7 day UCS vs Resistivity (after 1 hour curing)

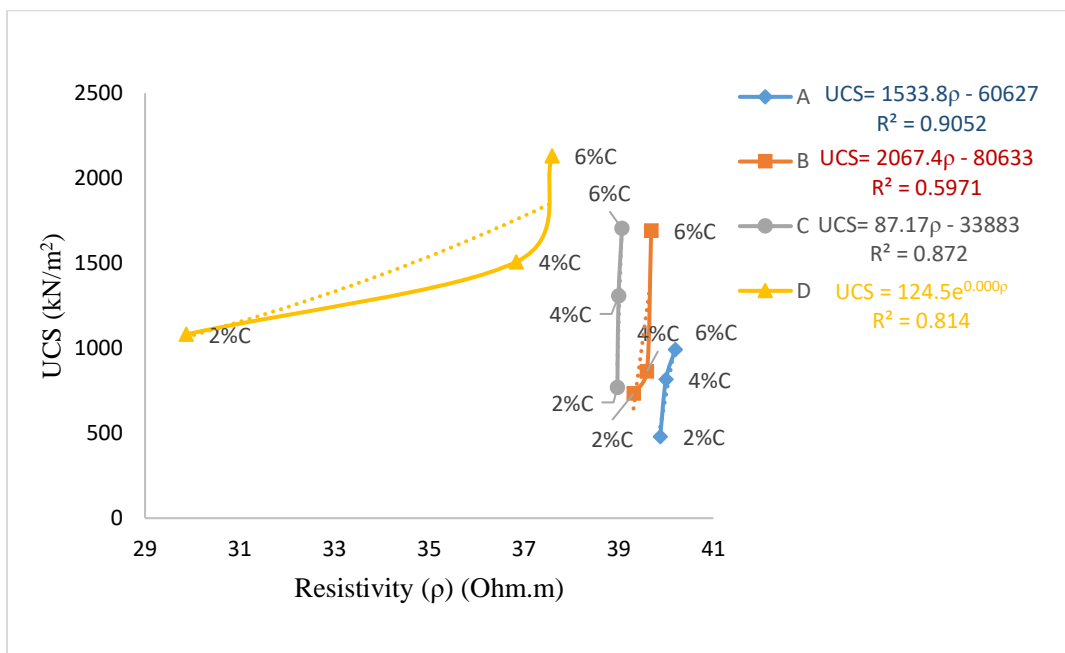


Figure 5.52 7 day UCS vs Resistivity (after 7 days curing)

From Fig. 5.50, an inverse relation is observed, between UCS (after 7 days curing) and resistivity (of freshly prepared samples) when the cement content is varied. At freshly prepared state, as the cement content increases electrical resistivity decreases due to low electrical conduction exhibited by the ions released due to chemical reactions by cement

and water, which gradually slows down with time. At the same time, electrical resistivity after 1 hour curing and 7 days curing show a direct relation with the unconfined compressive strength of soil-cement with increase in cement content (Figs. 5.51 and 5.50).

Resistivity also follows the same trend as UCS with time of curing and increase in cement content, the samples with higher cement showed higher resistivity, since more hydration products formed fill the pore spaces and create a highly tortuous structure, bringing down the electrical conduction.

Multiple regression analysis carried out derived generalised equations which predicts the 7 day UCS of cement stabilized soil, by using the cement content (%) and the resistivity (Ohm.m) measured at freshly prepared state and also after 1 hour curing period. The regression coefficients are 0.9 and 0.95 for Equations 5.1 and 5.2 respectively. The equations are as follows.

$$UCS \left( \frac{kN}{m^2} \right) = 197.3 \times C(\%) - 164.3 \times \rho_0(ohm\ m) + 1147.7..... (5.1)$$

Where, C is the cement content,  $\rho_0$  is the electrical resistivity at freshly prepared state.

$$UCS \left( \frac{kN}{m^2} \right) = 269.3 \times C(\%) - 160.6 \times \rho_1(ohm\ m) + 1035894..... (5.2)$$

Where, C is the cement content,  $\rho_1$  is the electrical resistivity measured after 1 hour curing.

### 5.6.7 Resistivity with cohesion

Undrained unconsolidated triaxial compression test was conducted on blended specimens after 7 days curing in dessicator to find out the cohesion and angle of internal friction. The test was carried out as described in IS: 2720 (Part 11) – 1971.

Figures 5.51 to 5.53 show the variation of cohesion with electrical resistivity measurements in the freshly prepared state and after curing periods of one hour and seven days at different percentages of cement content for the soil samples. Cohesion after seven days curing was found by triaxial testing. With increase of cement content, more hydration products are formed and more binding results in increase in the value of cohesion. But in the freshly prepared state, more ion concentrations results in lesser values for resistivity as the cement content increases and hence shows an inverse relation with cohesion in this state. But a direct relation is seen after curing since pore water gets used up for hydration resulting in more air in the voids which increases resistance.

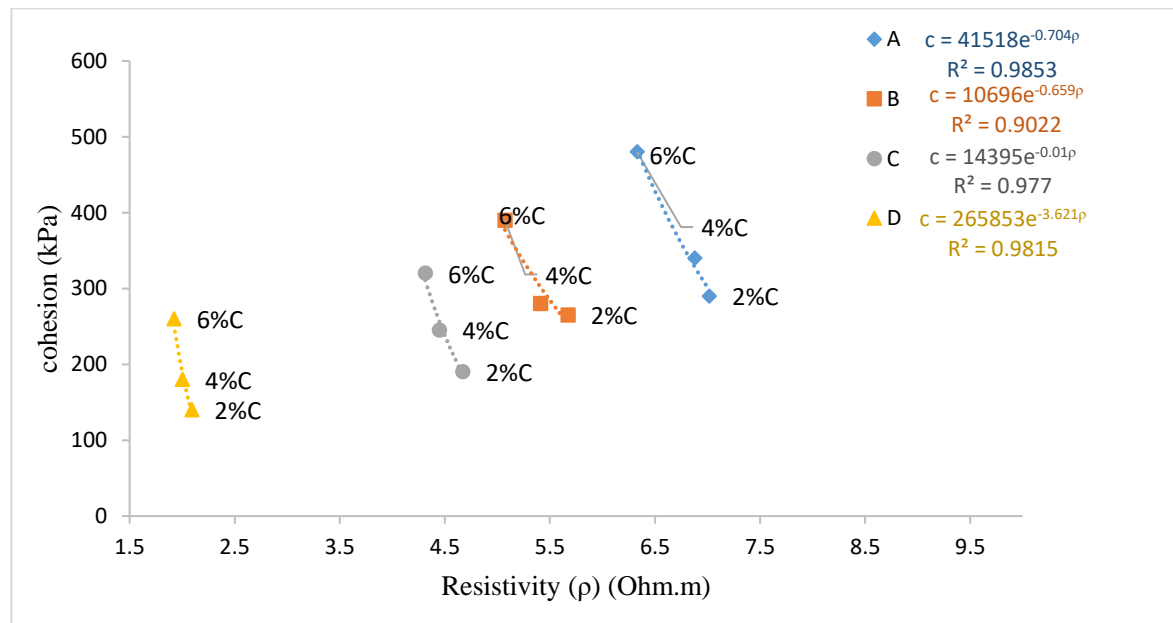


Figure 5.53 7 day cohesion with resistivity (freshly prepared)



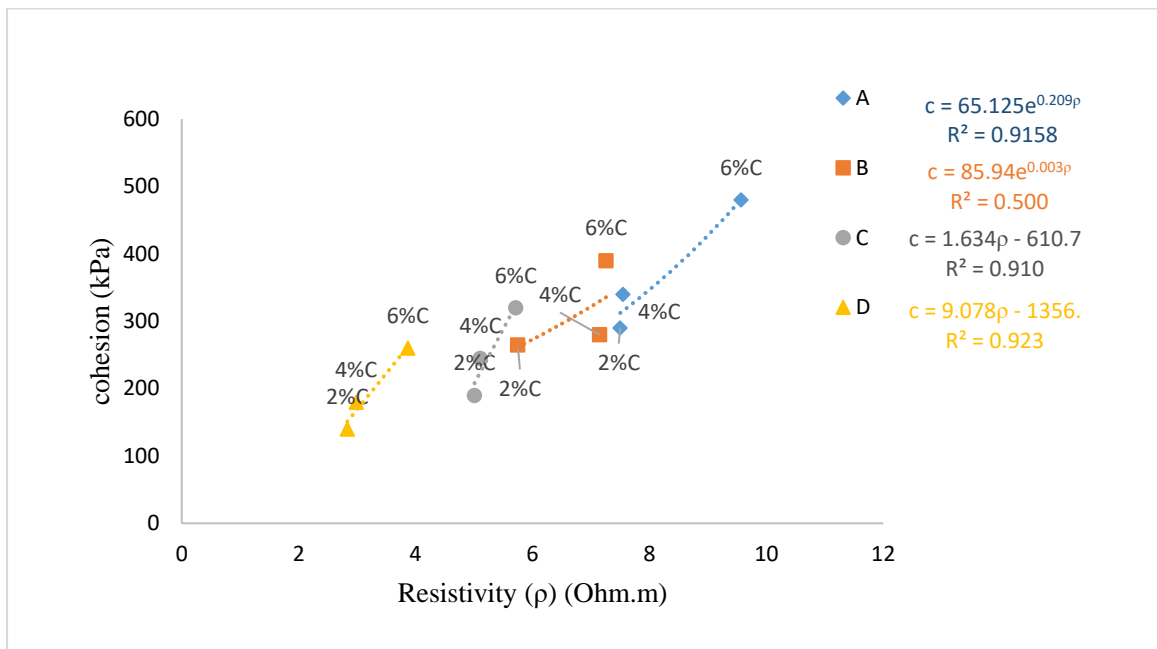


Figure 5.54 7 day cohesion with resistivity (after 1 hour curing)

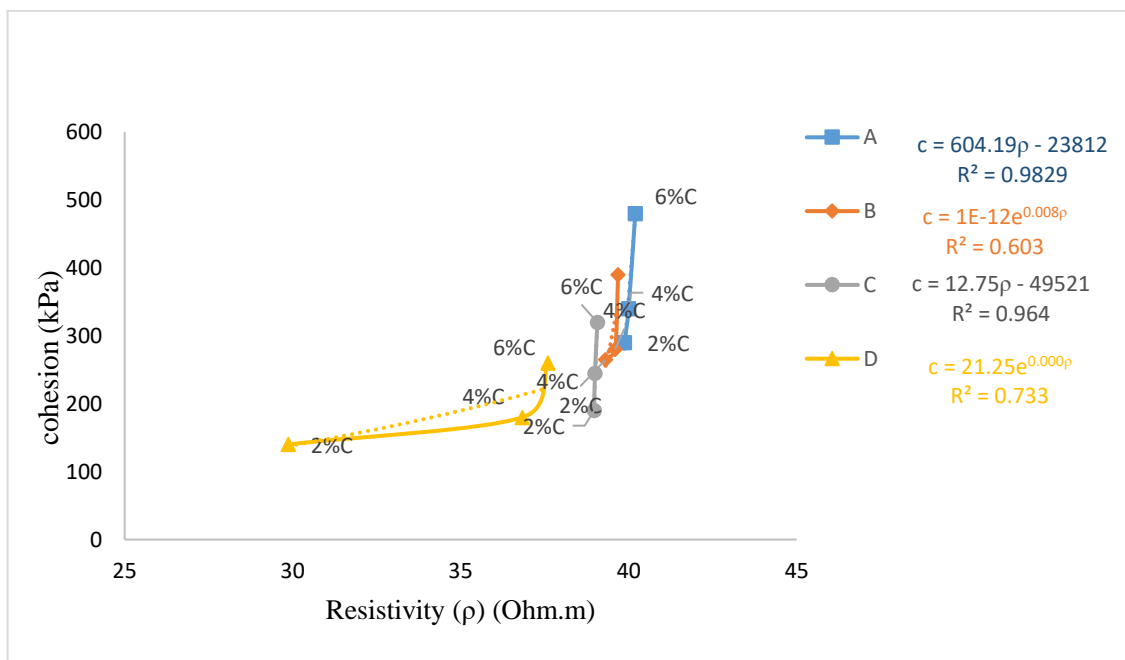


Figure 5.55 7 day cohesion with resistivity (after 7 days curing)

### 5.6.8 Resistivity with angle of internal friction

The shear strength parameter, angle of internal friction was found by triaxial testing on samples after a curing period of seven days. Figures 5.56 to 5.58 show the variation of electrical resistivity with angle of internal friction. As cement content increases, angle of friction is found to increase which results in an inverse relation with resistivity in the freshly

prepared state and direct relation in all other curing periods when plotted for all the soil-cement samples.

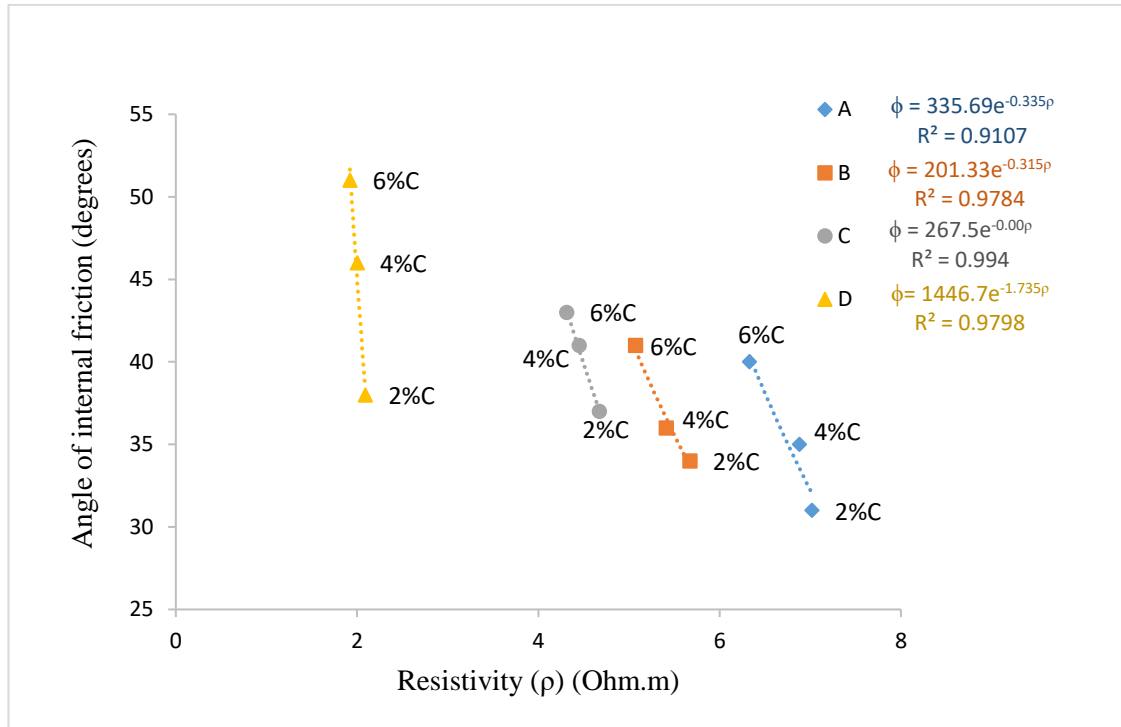


Figure 5.56 7 day angle of internal friction with resistivity (freshly prepared)

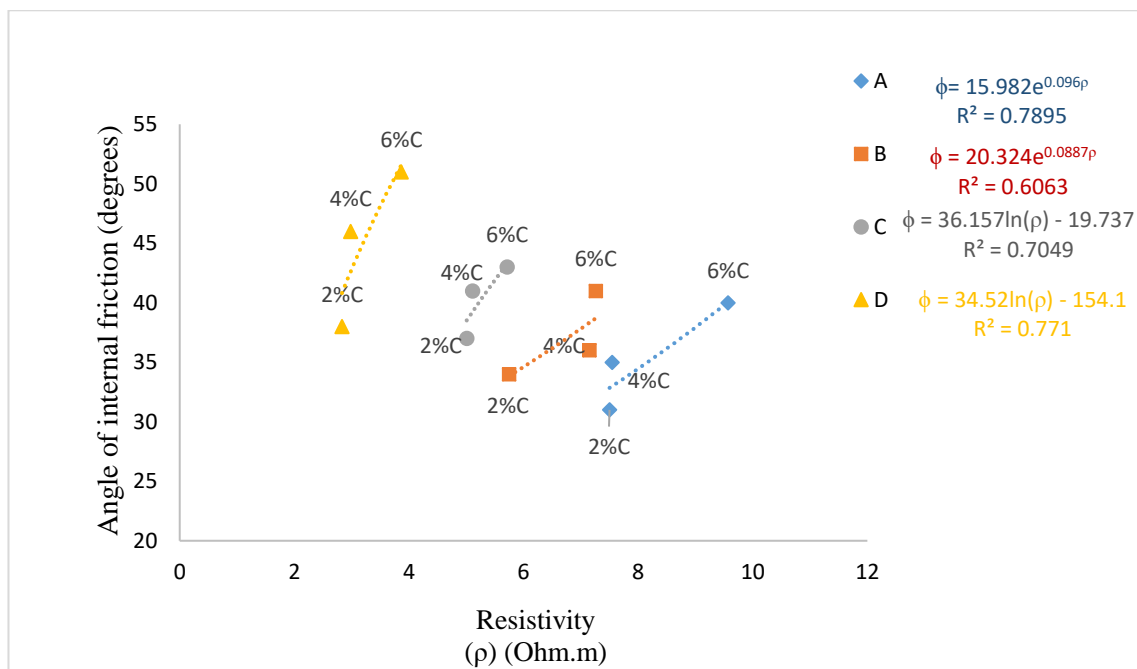


Figure 5.57 7 day angle of internal friction with resistivity (after 1 hour curing)

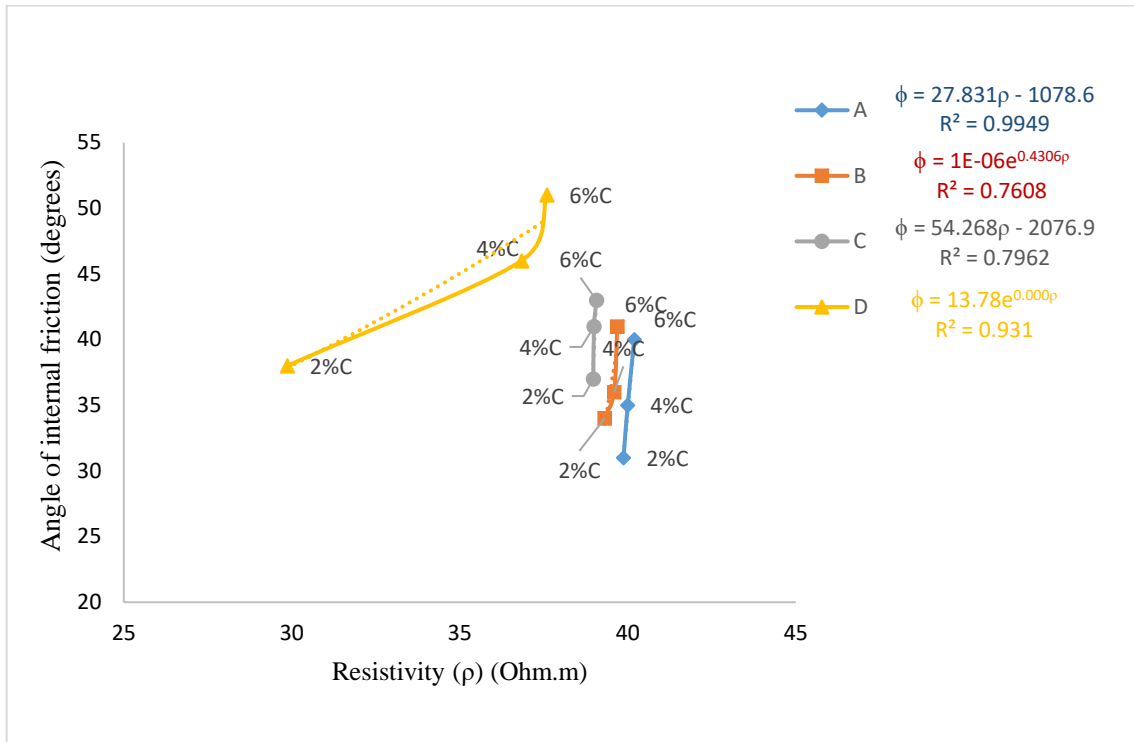


Figure 5.58 7 day angle of internal friction with resistivity (after 7 days curing)

### 5.6.9 Resistivity with split tensile strength

Cylindrical samples of 10 cm height and 6.7 cm diameter were prepared for all the combinations at MDD and OMC obtained from Standard Proctor test. The samples were placed with their axes parallel to the testing plane and tested to find the tensile strength.

$$\text{Tensile strength in kPa, } S_t = \frac{2P}{\pi dt} \quad (5.1)$$

$$\text{where } P = 0.0603 \times \text{Reading} + 0.0109 \text{ (kN)}$$

$$d = \text{diameter in m}$$

$$t = \text{thickness in m}$$

Split tensile strength after seven days curing time and resistivity in the freshly prepared state and after curing periods of one hour and seven days is correlated in Figs.5.59 to 5.61. When cement content increases, the binding increases and hence the samples with higher cement content can take up more load when tested resulting in increase of split tensile strength value. For all the soil samples, when the cement content is varied, resistivity shows inverse relation with split tensile strength for fresh samples and direct relation for cured samples. Tensile strength could be a measure of pore tortuosity. The concept of tortuosity is generally shown as a kind of factor influencing the macroscopic transport

movements to reflect the complex transport paths in porous media and characterize the structure of these environments.

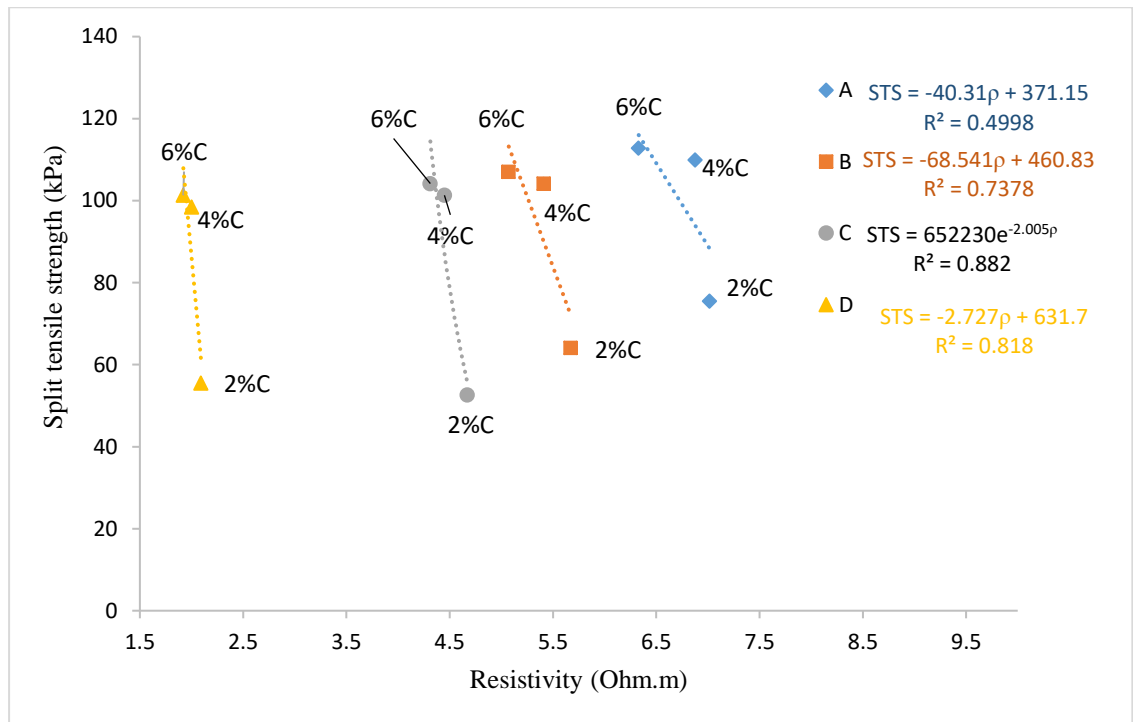


Figure 5.59 7 day split tensile strength with resistivity (freshly prepared)

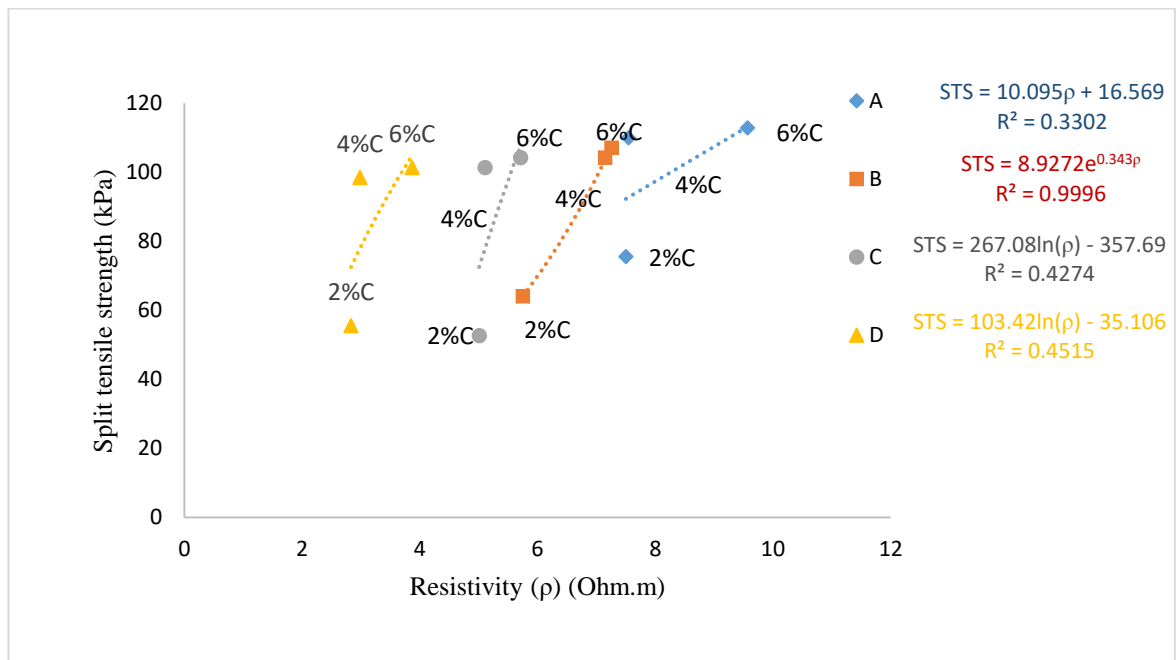


Figure 5.60 7 day split tensile strength with resistivity (after 1 hour curing)

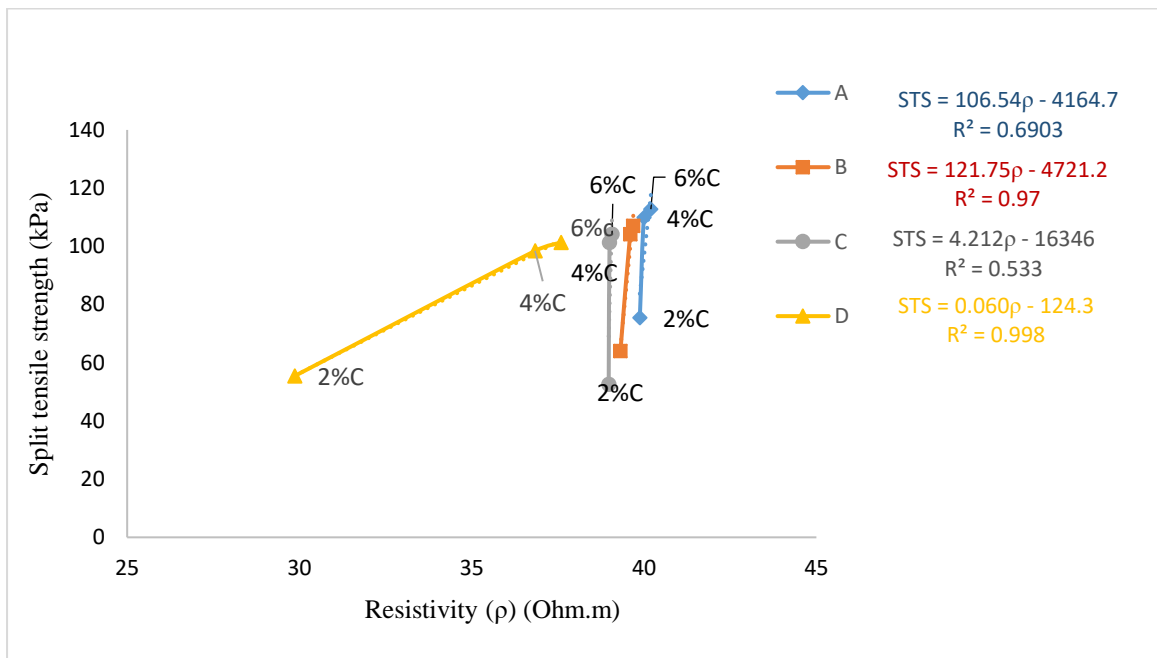


Figure 5.61 7 day split tensile strength with resistivity (after 7 days curing)

### 5.7 Summary

In this study, electrical resistivity measurement of freshly prepared uncured and cured soil cement materials are done and the correlation between the factors controlling the performance of soil-cement and electrical resistivity are studied. By the time an unconfined compressive strength test can be performed, to check the quality of the soil-cement, the material will be hardened in the field and if it does not meet the strength, performance criteria, the material will have to be removed, collapsed and remixed with additional cement which is a very time and cost consuming task. At this phase, electrical measurements of soil-cement material saves a great deal of cost and time by predicting the strength properties without hardening of the material. Equations developed in this study, by multiple regression analysis, predict the Unconfined Compressive Strength of the soil-cement samples, at the freshly prepared state or after 1 hour curing. If the strength requirement is not met, it could be remixed with additional cement at the fresh state itself and reused.

## CHAPTER 6

### LABORATORY ELECTRICAL RESISTIVITY STUDIES ON LIME STABILIZED SOIL

#### 6.1 Introduction

Numerous kinds of stabilizers were used as soil additives to improve its engineering properties such as lime, cement and fly ash, depending on their chemical reactions with the soil elements in the presence of water. Lime is the oldest traditional chemical stabilizer used for soil stabilization. It is an excellent choice for short-term modification of soil properties. It can modify almost all fine-grained soils, but the most effective improvement is observed in clay soils with moderate to high plasticity. Modification occurs because calcium cations supplied by the hydrated lime replace the cations normally present on the surface of the clay mineral, promoted by the high pH environment of the lime-water system. Thus, the clay surface mineralogy is altered, producing plasticity reduction, reduction in moisture-holding capacity, swell reduction, improved shear strength.

Stabilised soil has been commonly used for pavement construction, slope protection, seepage control and foundation stabilization. It is required to evaluate the performance of the “improved” soil by using cost effective testing techniques. Resistivity imaging can be utilised as an effective tool for the performance analysis of stabilised soil. In this study, attempts were made to correlate resistivity of uncured and cured soil-lime mixes with its geotechnical parameters. Electrical resistivity is a physical property every material possesses, which indicates the degree of difficulty of an electric current to pass through it. The electrical measurement method is one of the non-destructive geophysical methods which can be applied both in the laboratory and in the field. Investigators and engineers working in various fields such as mining, geotechnical, and civil, underground engineering commonly use the electrical measurement technique.

## 6.2 Materials used

### 6.2.1 Shedi soil and River sand

The soil used in the present study are lithomargic clay (locally known as Shedi soils), which constitutes an important group of residual soils existing under lateritic soils. In order to vary the percentage of fines, in the different test samples, controlled soil samples were prepared by blending the shedi soil with river sand. The percentages of river sand used were 0, 10, 20 and 30% by weight of dry soil. The samples are designated as L, M, N and O respectively. For the experimental investigations, river sand passing IS 4.75mm sieve and retained on IS 75 micron sieve was considered. Grain size analysis curves of the samples are shown in Fig. 6.1.

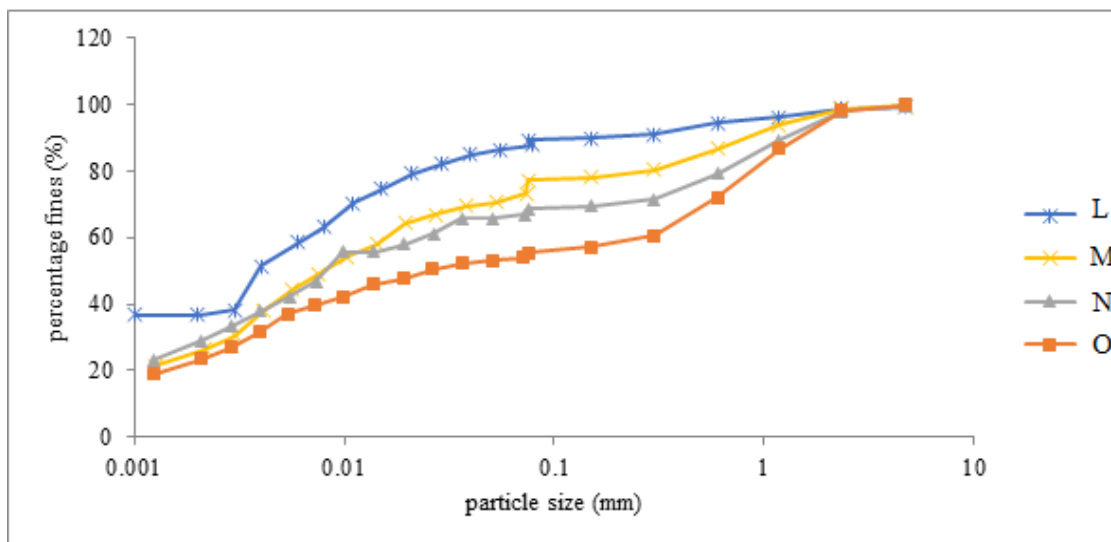


Figure 6.1 Grain size analysis curves

### 6.2.2 Lime

Hydrated lime was used in proportion of 2, 4 and 6% by dry weight of soil in each of the four soil samples, L, M, N and O. These samples are designated as L2, L4, L6, M2, M4, M6, N2, N4, N6, O2, O4 and O6.

## 6.3 Compaction

In order to obtain the maximum dry density (MDD) and optimum moisture content (OMC) standard Proctor tests were conducted as per IS 2720-1980 Part 7.

Samples were prepared at 5 compaction conditions a, b, c, d, e, as shown in Figs. 6.2 to 6.25 for the electrical resistivity test. Table 6.1 show values of MDD and OMC for all the 12 soil mixes for standard and modified Proctor test respectively. For standard Proctor test, it is observed that as the coarser fraction increases there is a reduction in optimum moisture content (OMC) and increase in maximum dry density (MDD) and it is also observed that as lime content increases MDD decreased and OMC value increased (Bell,1996).

#### **6.4 Test method**

Electrical resistivity of all the controlled samples were measured by making cylindrical samples of size 7.6 cm height and 3.8 cm diameter. For each combination, just like as done for soil cement, in addition to the point of maximum dry density and optimum moisture content obtained from Standard Proctor and Modified Proctor tests, two points each were selected on the dry side and wet side of the compaction curve to study resistivity variation for different compaction conditions (Figs. 6.2 to 6.25). The resistivity measurements were taken for all the seven curing days. Electrical resistivity was measured by using a circuit consisting of a 30 V DC power supply, two high precision multimeters serving as ammeter and voltmeter and electrodes connecting to the sample as explained in the previous Chapter.

Resistivity was measured in the freshly prepared state, after one hour curing and after one to seven days of curing. The basic geotechnical properties of the soil stabilized with different percentages of lime are given in Table 6.1

#### **6.5 Results and Discussions**

Compaction and strength characteristics of the soil lime samples are shown in Table 6.1



Table 6.1 Compaction and strength characteristics of soil lime samples

Parameter	Soil-lime samples															
	L0	L2	L4	L6	M0	M2	M4	M6	N0	N2	N4	N6	O0	O2	O4	O6
$\gamma_{dmax}$ , kN/m <sup>3</sup> (LC)	14.5	1.495	14.85	14.85	15.6	15.2	15.1	14.9	15.9	16.2	15.9	15.75	16.4	16.95	16.85	16.75
<b>OMC (%)</b> (LC)	28.0	26.5	27.8	28.0	25.0	26	26.5	27.5	23.2	23.4	23.8	24.1	21.0	20.1	21.0	21.8
$\gamma_{dmax}$ , (kN/m <sup>3</sup> ) (HC)	14.9	21.7	22.8	22.2	15.9	20.5	18.1	17.7	16.4	16.0	16.5	17.9	17.5	14.5	15.7	16.2
<b>OMC (%)</b> (HC)	27.0	21.7	22.8	22.2	22.0	20.5	18.1	17.7	21.0	16.0	16.5	17.9	18.0	14.5	15.7	16.2
<b>7 day UCS</b> (kPa) (LC)	130.8	468.7	673.2	757.2	155.6	504.3	692.4	833.3	162.2	713.2	862.5	976.8	289.2	853.9	1105.8	1289.9
<b>C</b> (kPa) (LC)	23.5	215	220	235	21.0	175	190	210	19.0	140	165	180	18.5	105	130	155
<b>Φ</b> (degrees) (LC)	20.0	22.0	24.0	25.0	25.0	26.0	28.0	29.0	31.0	28.0	30.0	32.0	31.0	35.0	36.0	38.0
<b>STS</b> (kPa) (LC)	-	58.36	69.83	75.56	-	52.63	58.36	64.09	-	46.90	52.63	58.36	-	41.16	46.90	52.63

NOTE:  $\gamma_{dmax}$ - max dry density, OMC- Optimum Moisture Content, LC- Light Compaction, HC- Heavy Compaction, UCS- Unconfined

Compressive Strength, C- Cohesion, Φ- Angle of internal friction, STS- Split Tensile Strength.

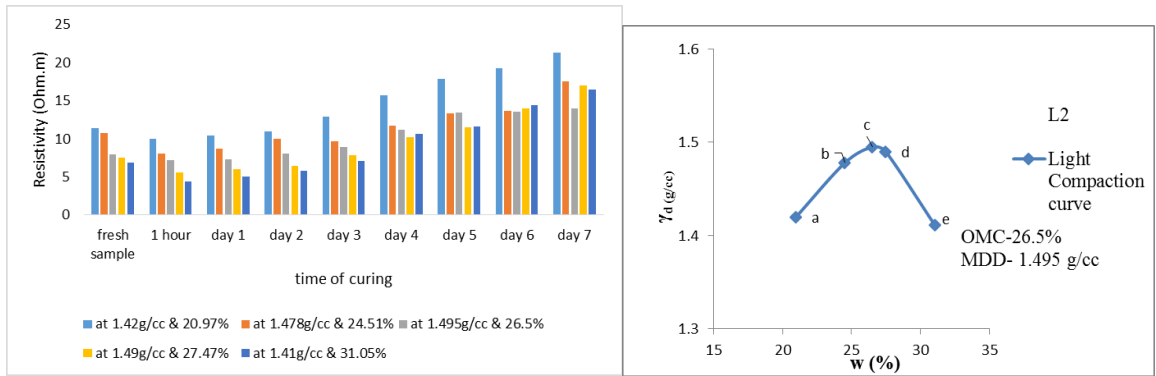


Figure 6.2 Variation of Electrical Resistivity with time for different compaction conditions (Light) for sample L2

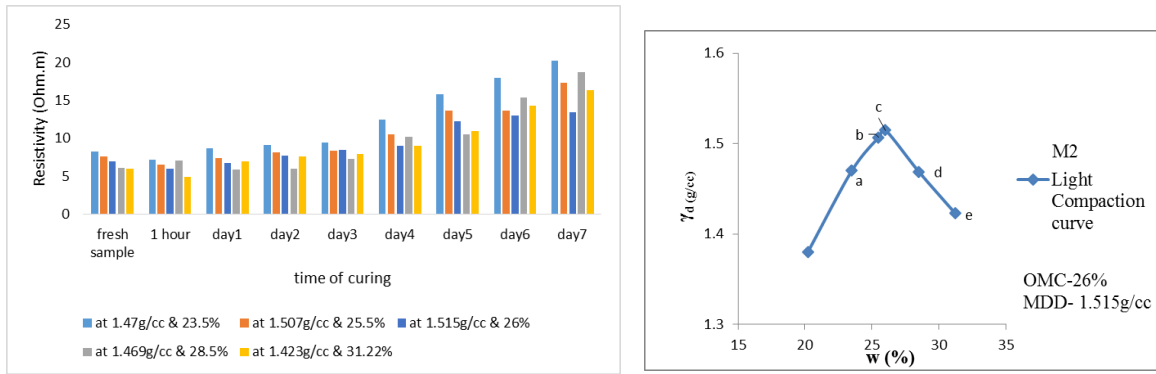


Figure 6.3 Variation of Electrical Resistivity with time for different compaction conditions (Light) for sample M2

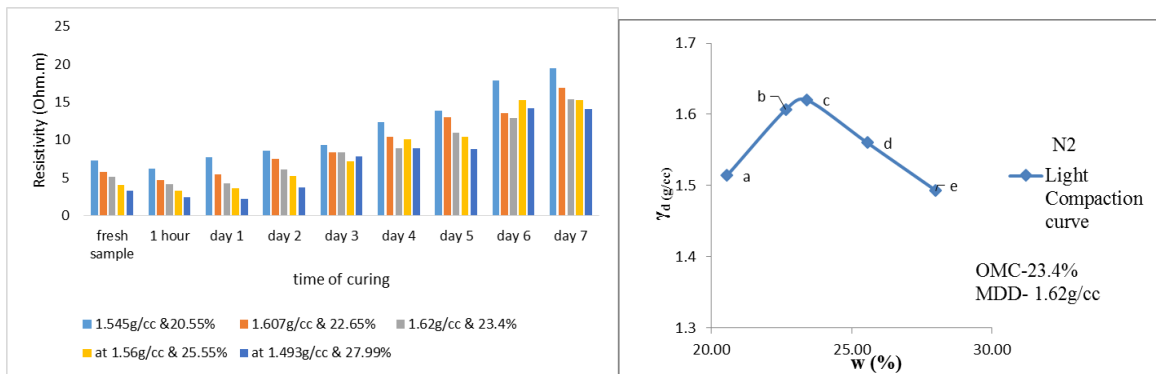


Figure 6.4 Variation of Electrical Resistivity with time for different compaction conditions (Light) for sample N2

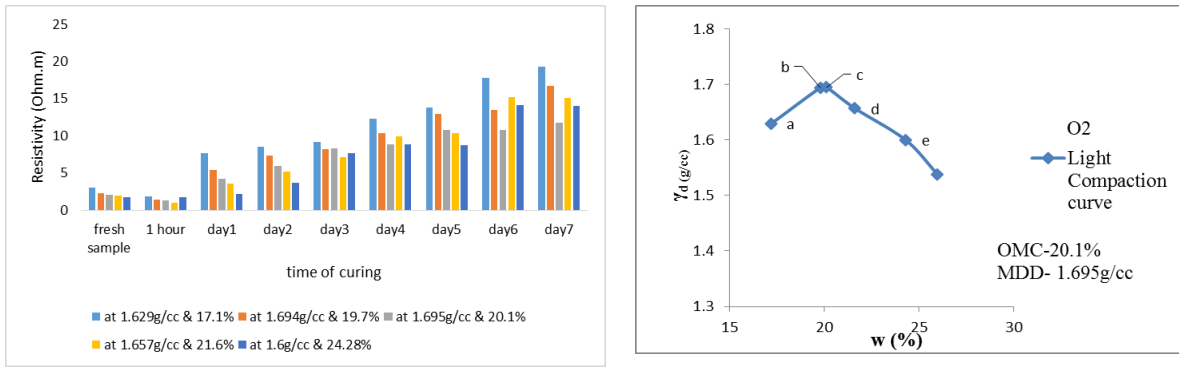


Figure 6.5 Variation of Electrical Resistivity with time for different compaction conditions (Light) for sample O2

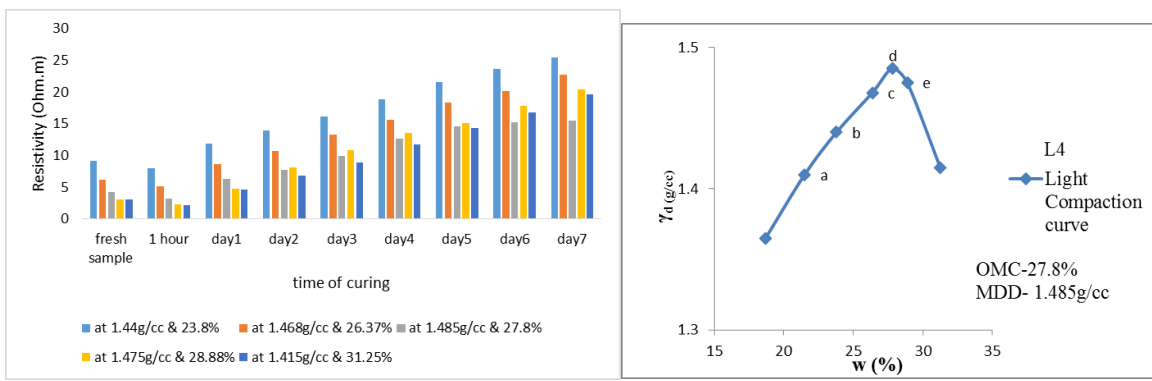


Figure 6.6. Variation of Electrical Resistivity with time for different compaction conditions (Light) for sample L4

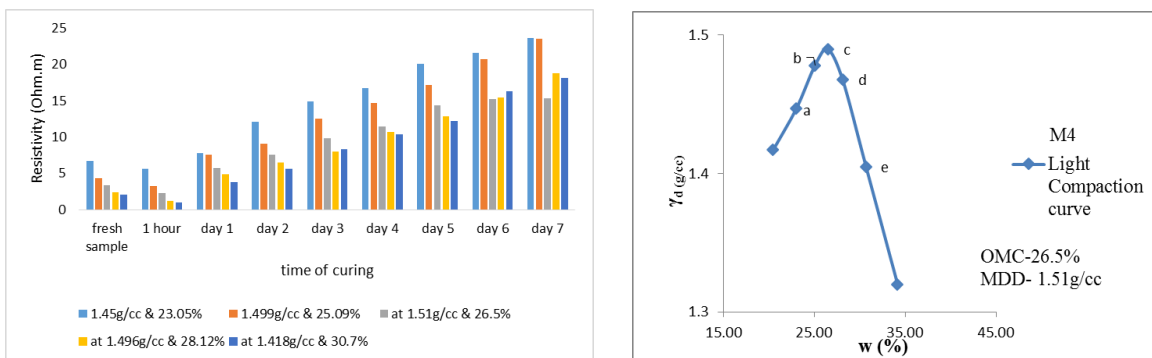


Figure 6.7 Variation of Electrical Resistivity with time for different compaction conditions (Light) for sample M4

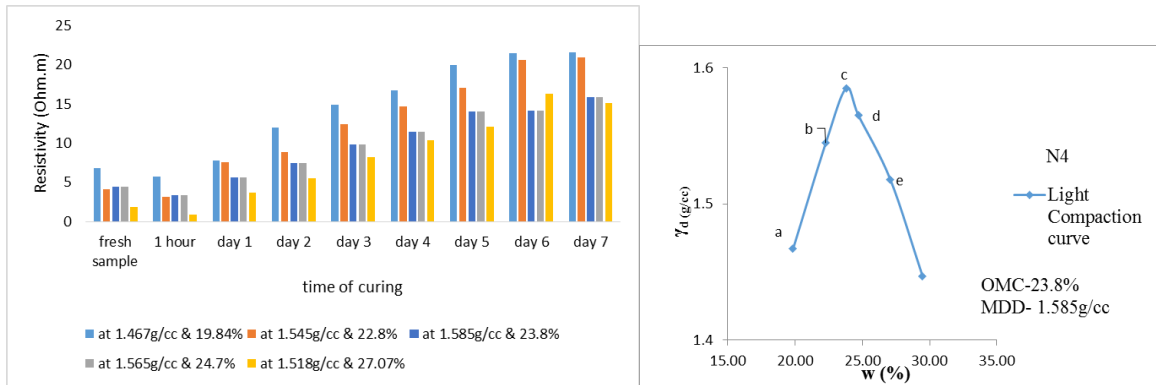


Figure 6.8 Variation of Electrical Resistivity with time for different compaction conditions (Light) for sample N4

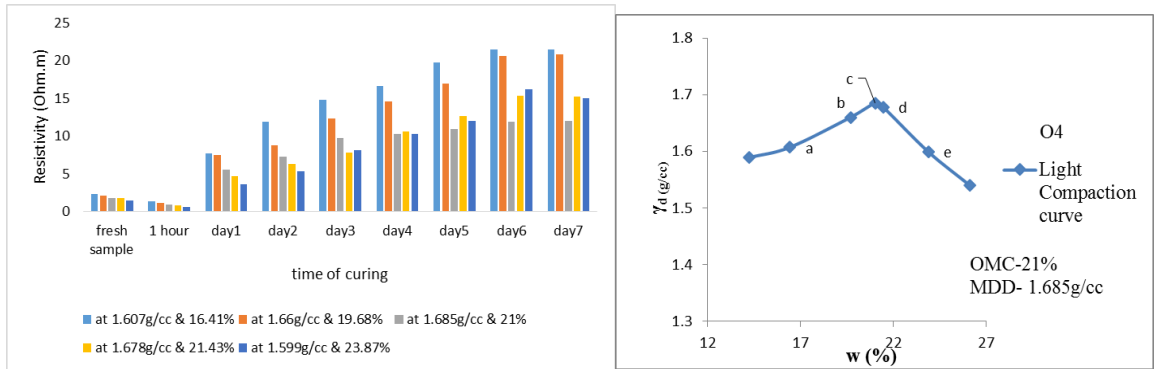


Figure 6.9 Variation of Electrical Resistivity with time for different compaction conditions (Light) for sample O4

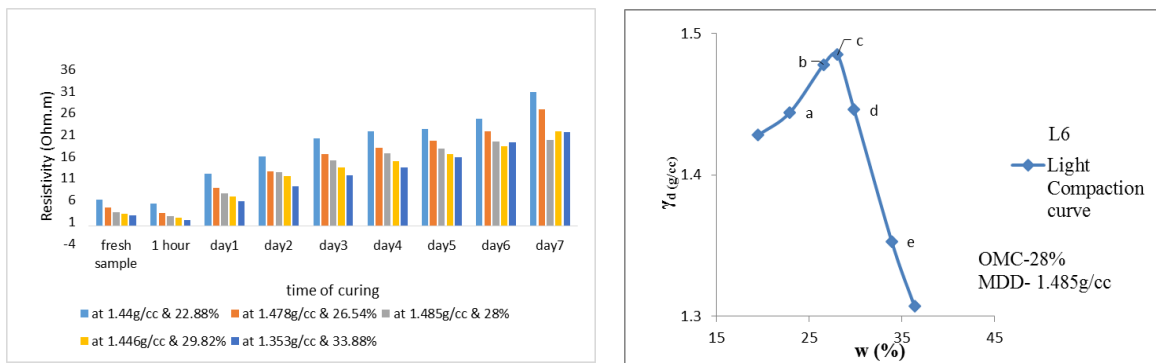


Figure 6.10 Variation of Electrical Resistivity with time for different compaction conditions (Light) for sample L6

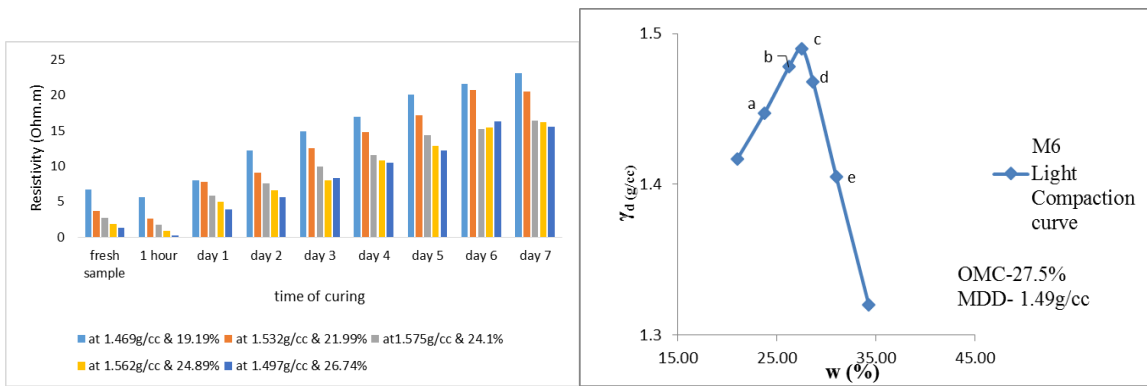


Figure 6.11 Variation of Electrical Resistivity with time for different compaction conditions (Light) for sample M6

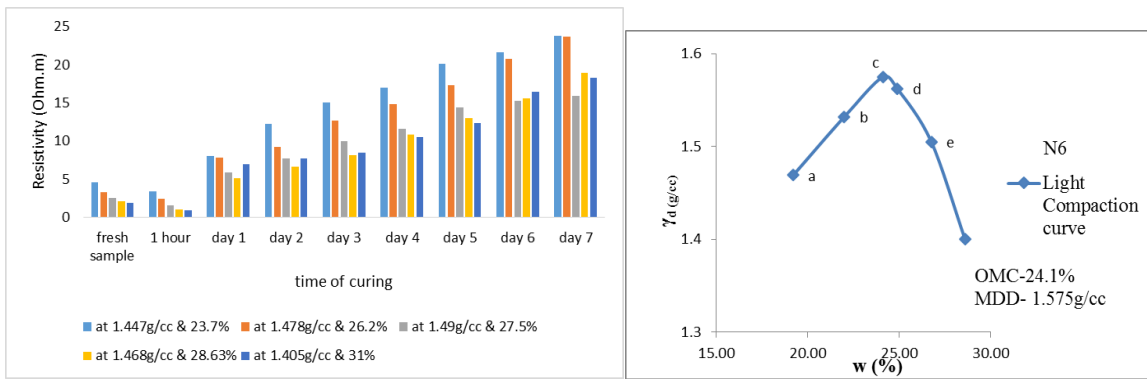


Figure 6.12 Variation of Electrical Resistivity with time for different compaction conditions (Light) for sample N6

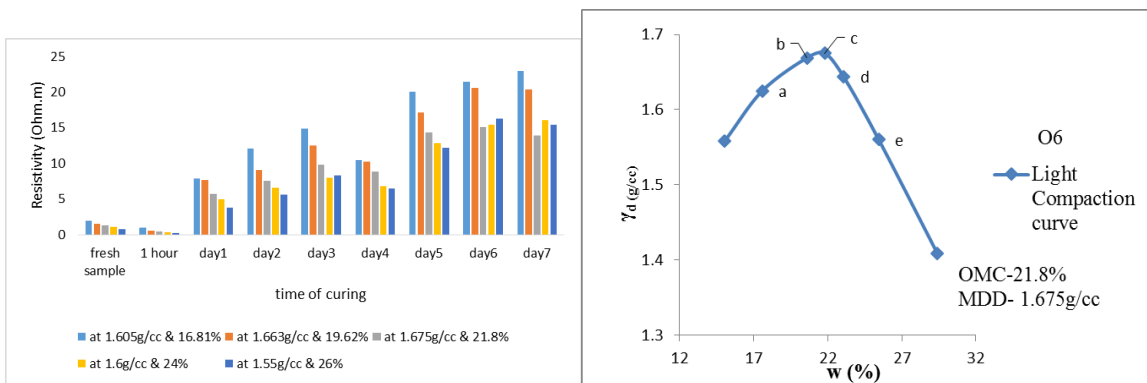


Figure 6.13 Variation of Electrical Resistivity with time for different compaction conditions (Light) for sample O6

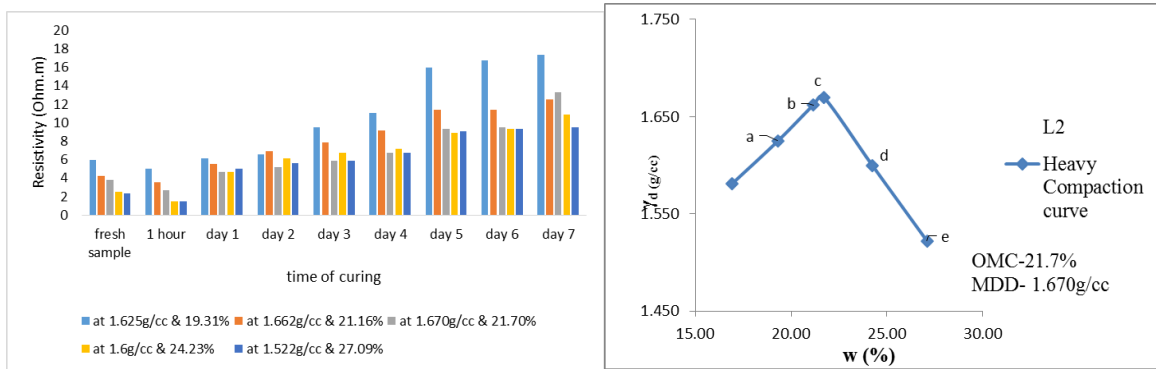


Figure 6.14 Variation of Electrical Resistivity with time for different compaction conditions (Heavy) for sample L2

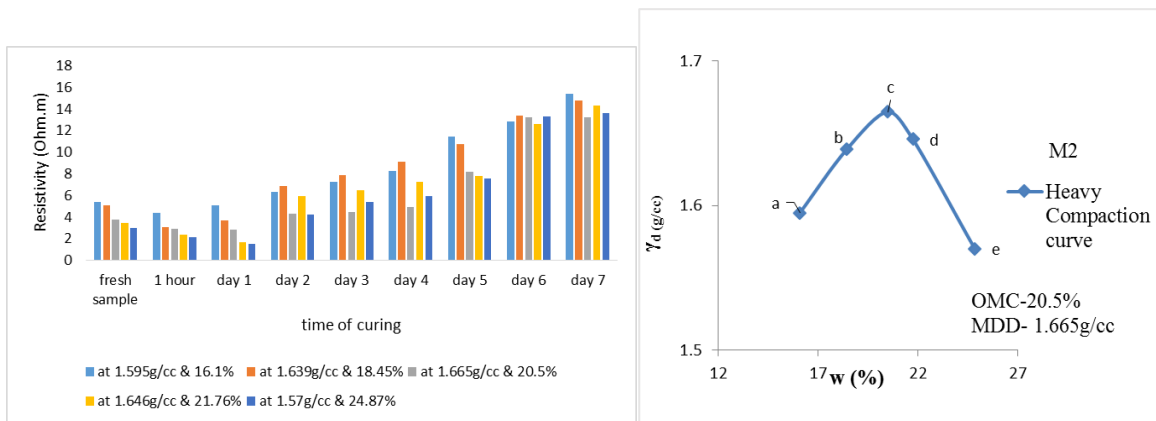


Figure 6.15 Variation of Electrical Resistivity with time for different compaction conditions (Heavy) for sample M2

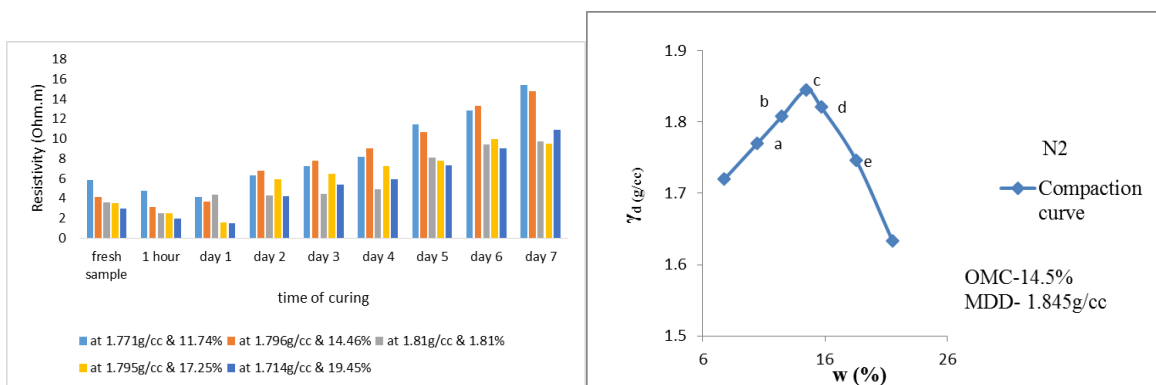


Figure 6.16 Variation of Electrical Resistivity with time for different compaction conditions (Heavy) for sample N2

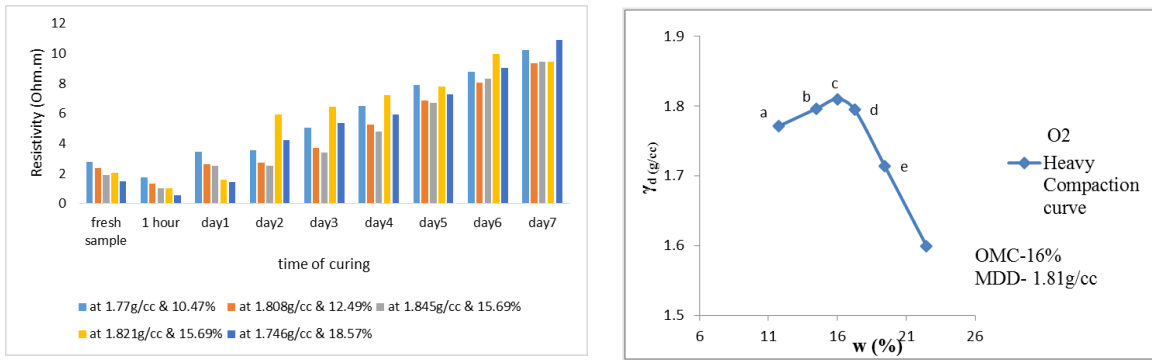


Figure 6.17 Variation of Electrical Resistivity with time for different compaction conditions (Heavy) for sample O2

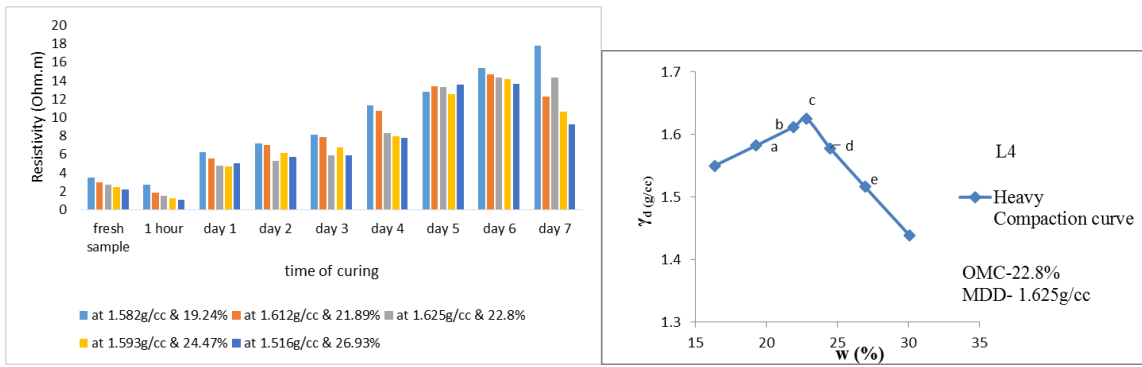


Figure 6.18 Variation of Electrical Resistivity with time for different compaction conditions (Heavy) for sample L4

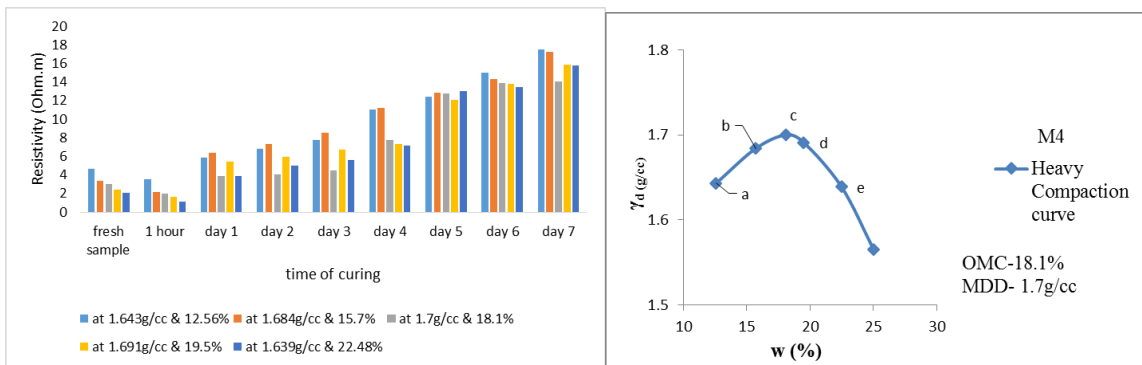


Figure 6.19 Variation of Electrical Resistivity with time for different compaction conditions (Heavy) for sample M4

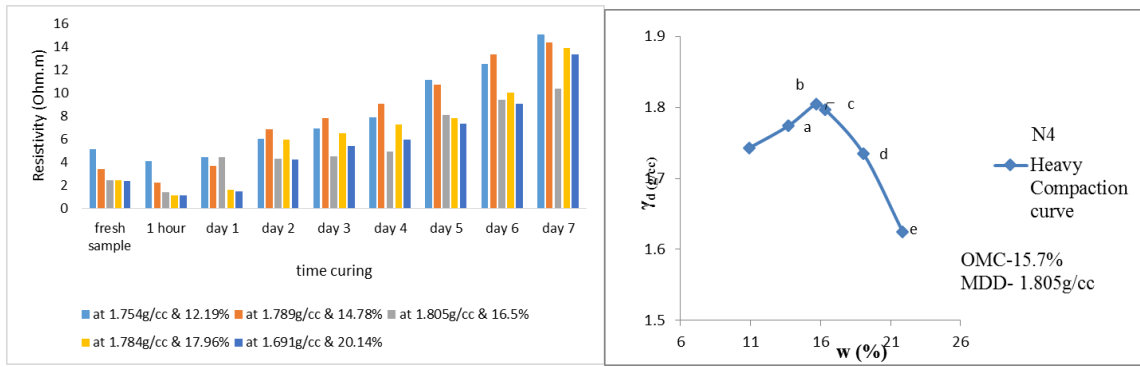


Figure 6.20 Variation of Electrical Resistivity with time for different compaction conditions (Heavy) for sample N4

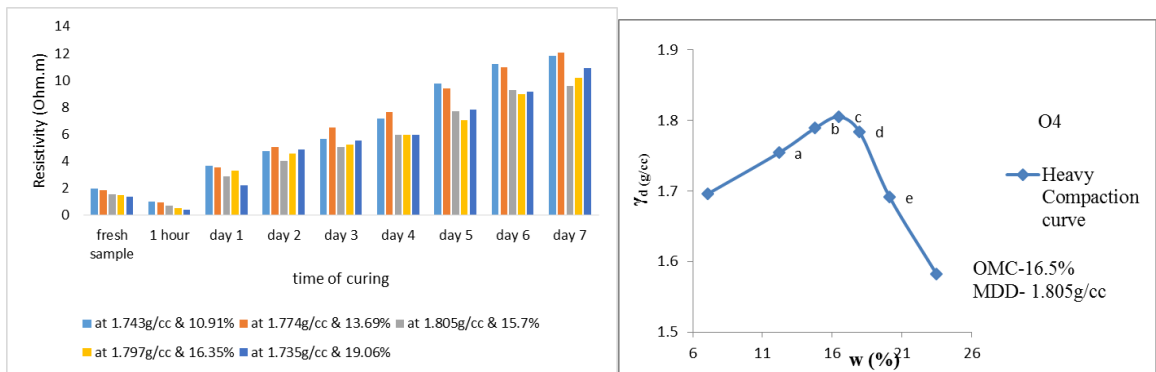


Figure 6.21 Variation of Electrical Resistivity with time for different compaction conditions (Heavy) for sample O4

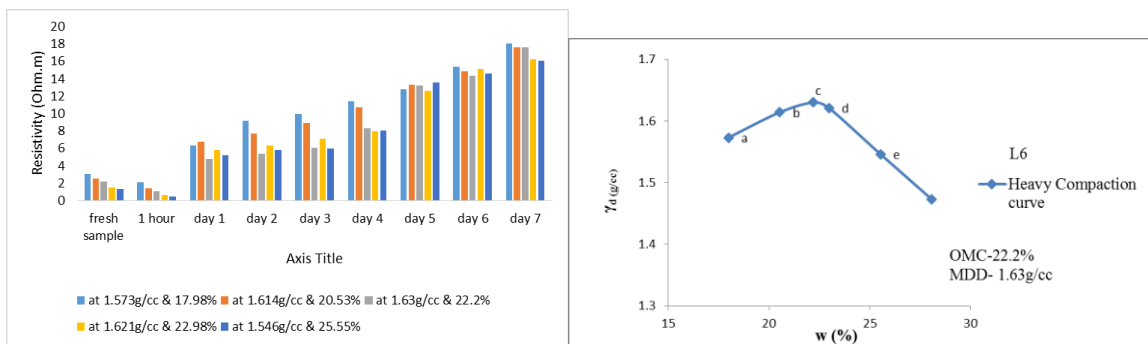


Figure 6.22 Variation of Electrical Resistivity with time for different compaction conditions (Heavy) for sample L6



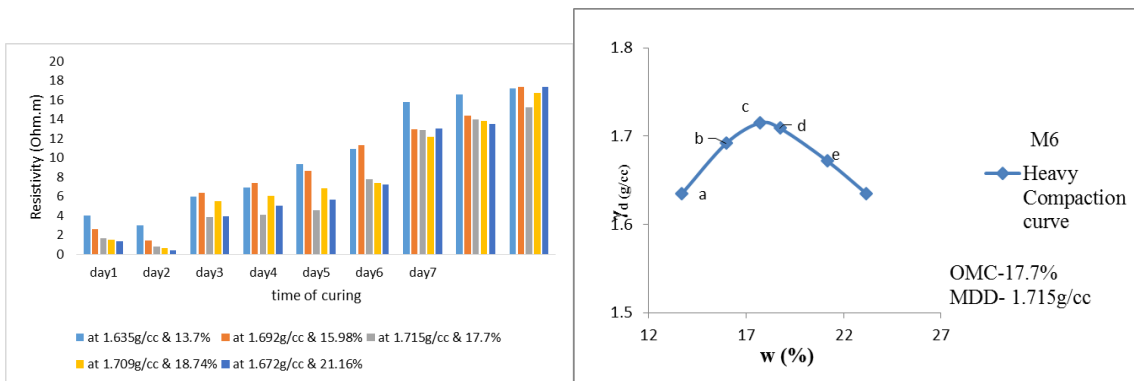


Figure 6.23 Variation of Electrical Resistivity with time for different compaction conditions (Heavy) for sample M6

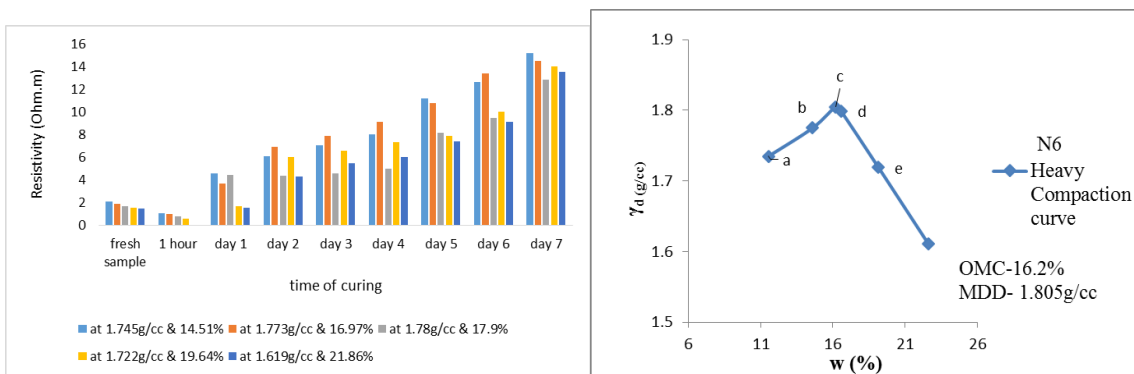


Figure 6.24 Variation of Electrical Resistivity with time for different compaction conditions (Heavy) for sample N6

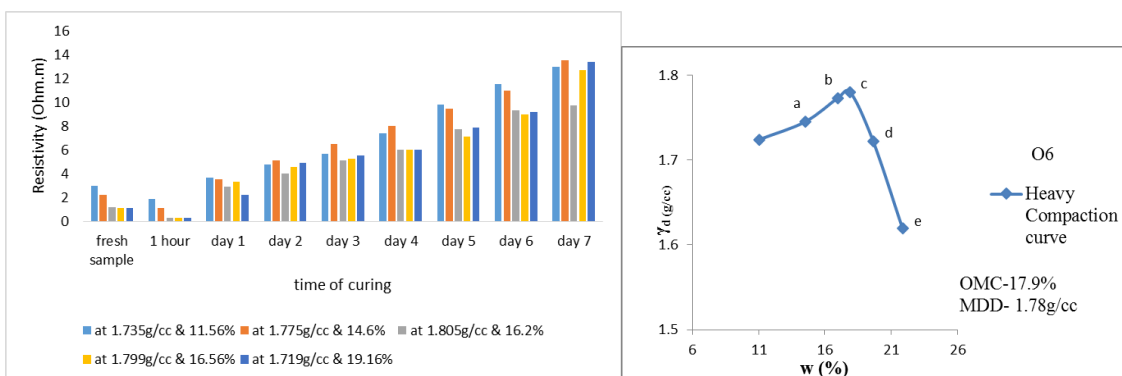


Figure 6.25 Variation of Electrical Resistivity with time for different compaction conditions (Heavy) for sample O6

### 6.5.1 Variation of resistivity of soil-lime with time of curing

Figures 6.2 to 6.25 shows that resistivity increases as the time of curing increases. Initially electrical resistivity decreases due to the ionic conduction carried out by the ions  $\text{Ca}^{2+}$  and  $\text{OH}^-$  ions released, when lime reacts with water. It is seen that after 1 hour of curing this electrical resistivity is even more decreased, due to more and more ions released. But after the initial setting time of lime the electrical resistivity is found to be increasing due to the formation of complex hydration products in the voids. As a result of that electrical resistivity increases more significantly. It is observed that resistivity variation is independent of compaction condition as the time of curing is increased. Hence, with the increase of time, more complexes will be produced and hence more electrical resistivity.

### 6.5.2 Variation of resistivity with lime content

Figures 6.26 to 6.29 show variation of ER with lime content for freshly prepared state at maximum dry density and optimum moisture content. It is observed that for freshly prepared samples electrical resistivity decreases as lime content increases. For freshly prepared samples, more ions will be present to conduct electricity as lime content increases. These ions are produced due to the pozzolanic reactions taking place after lime addition. More the lime content more will be the ions present in the soil-lime mix.

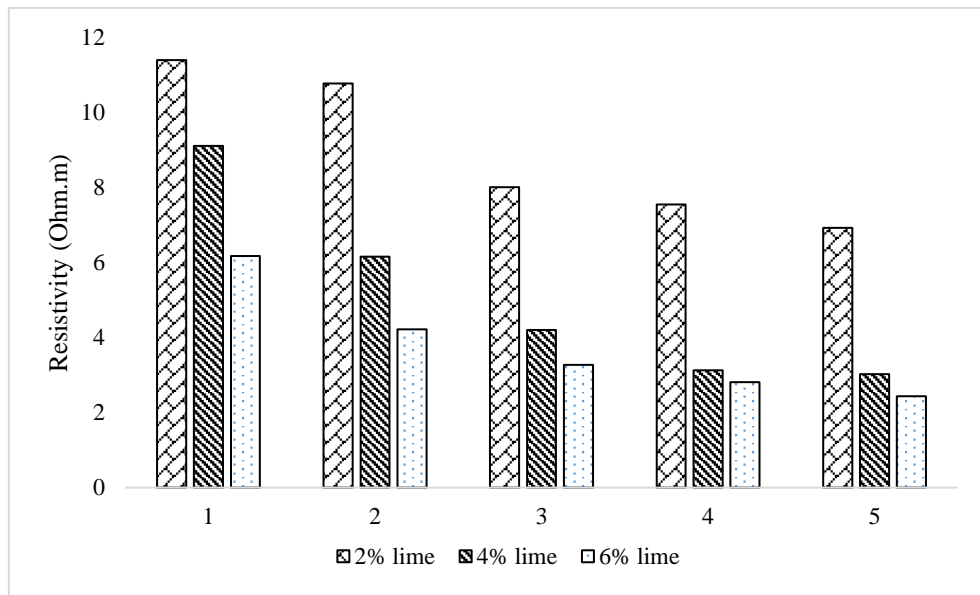


Figure 6.26 Variation of Resistivity with lime content at dry side and wet side points on the standard proctor compaction curve at freshly prepared state for sample L

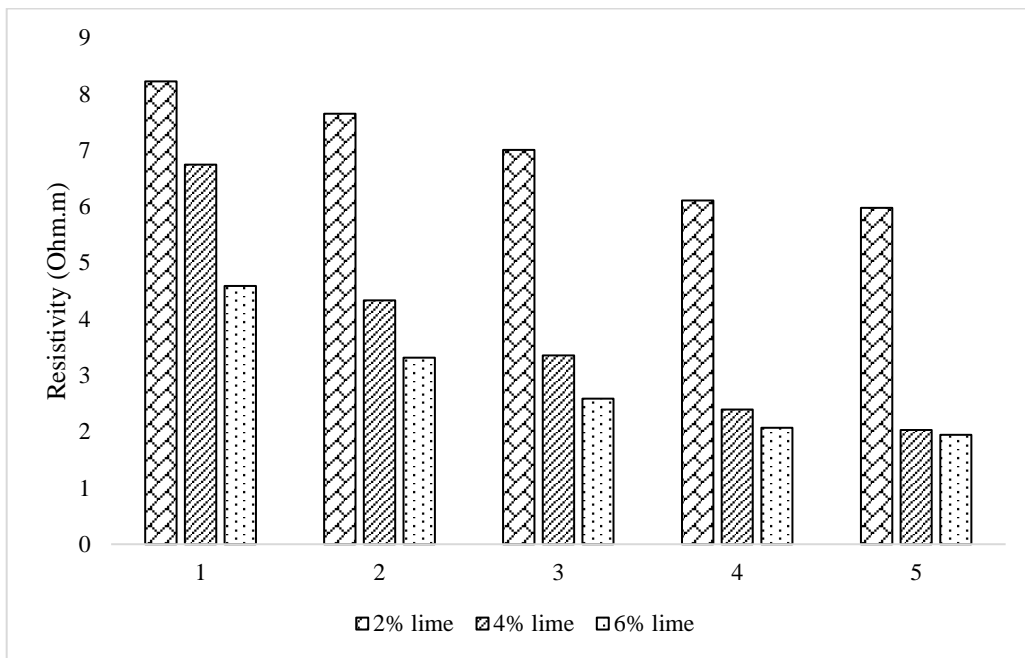


Figure 6.27 Variation of Resistivity with lime content at dry side and wet side points on the standard proctor compaction curve at freshly prepared state for sample M

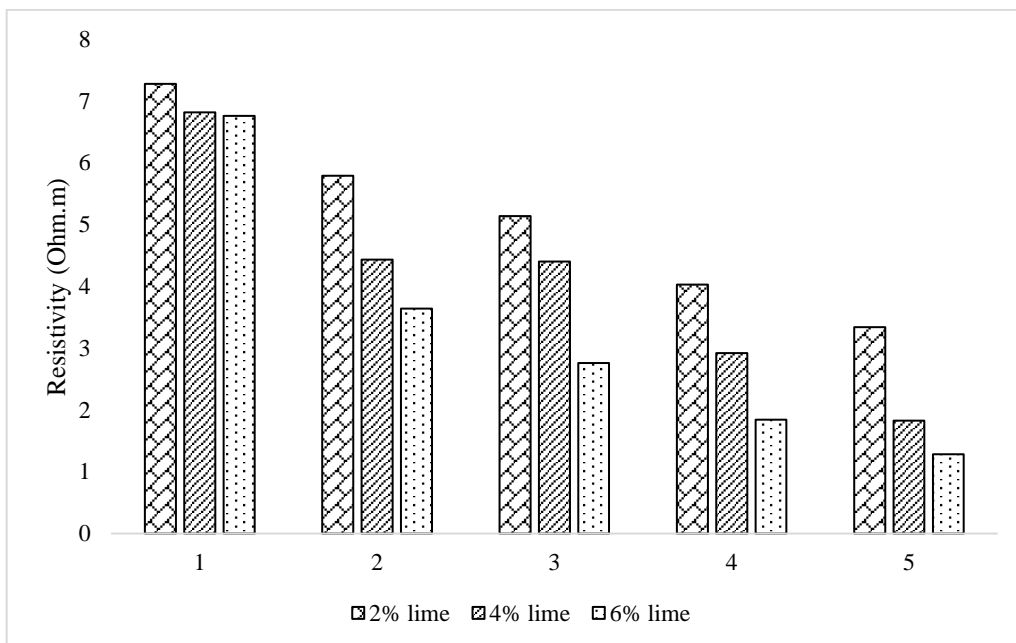


Figure 6.28 Variation of Resistivity with lime content at dry side and wet side points on the standard proctor compaction curve at freshly prepared state for sample N

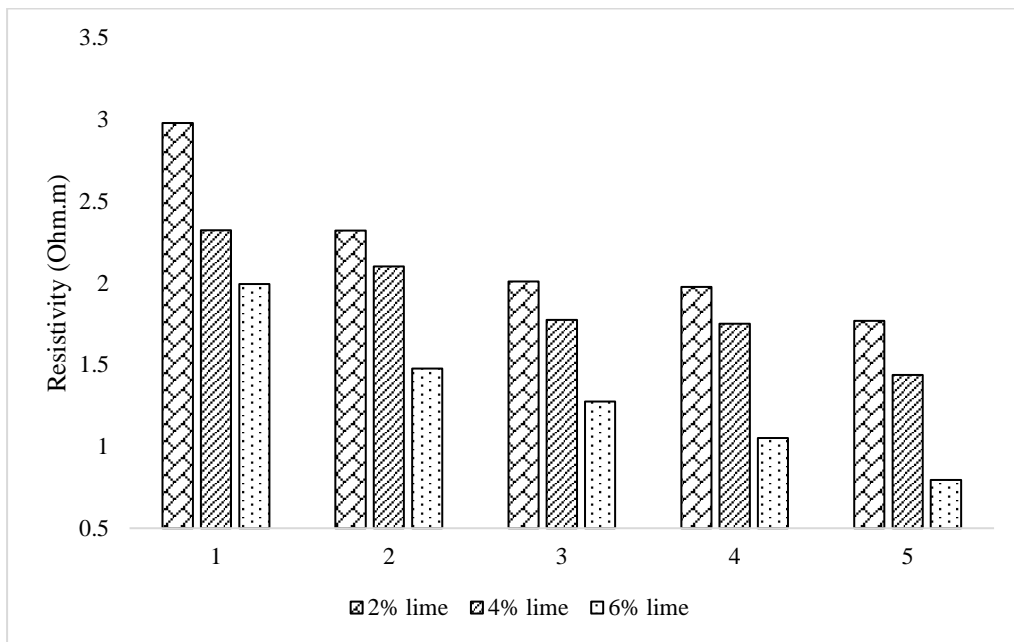


Figure 6.29 Variation of Resistivity with lime content at dry side and wet side points on the standard proctor compaction curve at freshly prepared state for sample O

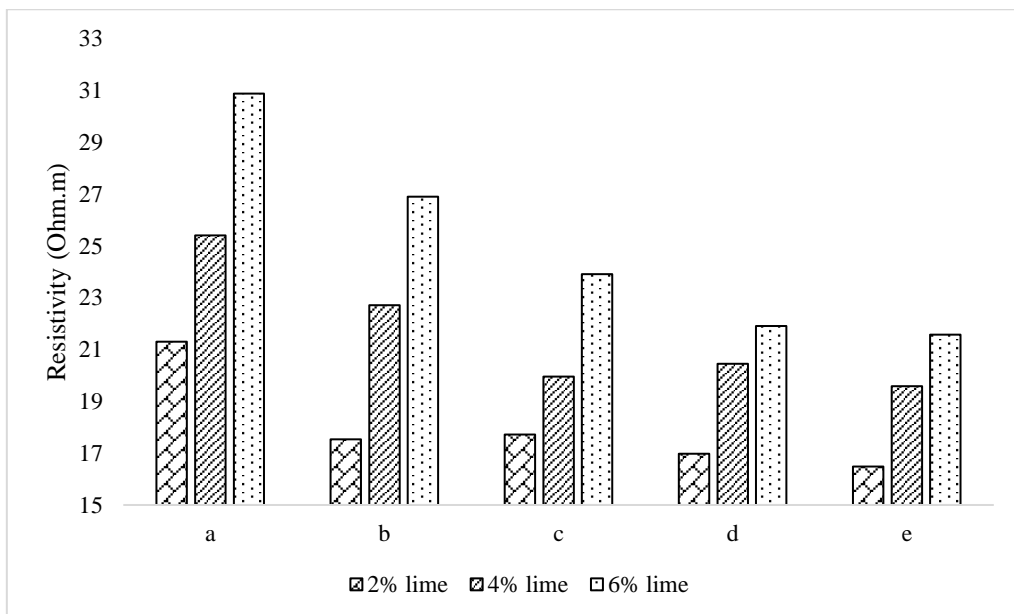


Figure 6.30 Variation of Resistivity with lime content at dry side and wet side points on the standard proctor compaction curve after 7 days curing for sample L

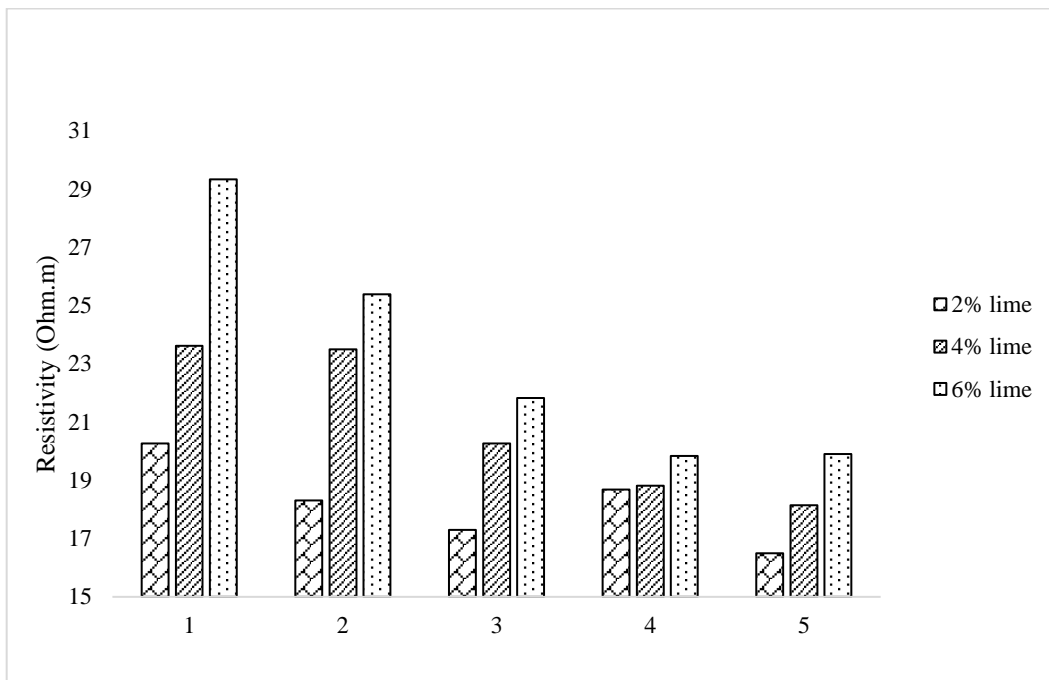


Figure 6.31 Variation of Resistivity with lime content at dry side and wet side points on the standard proctor compaction curve after 7 days curing for sample M

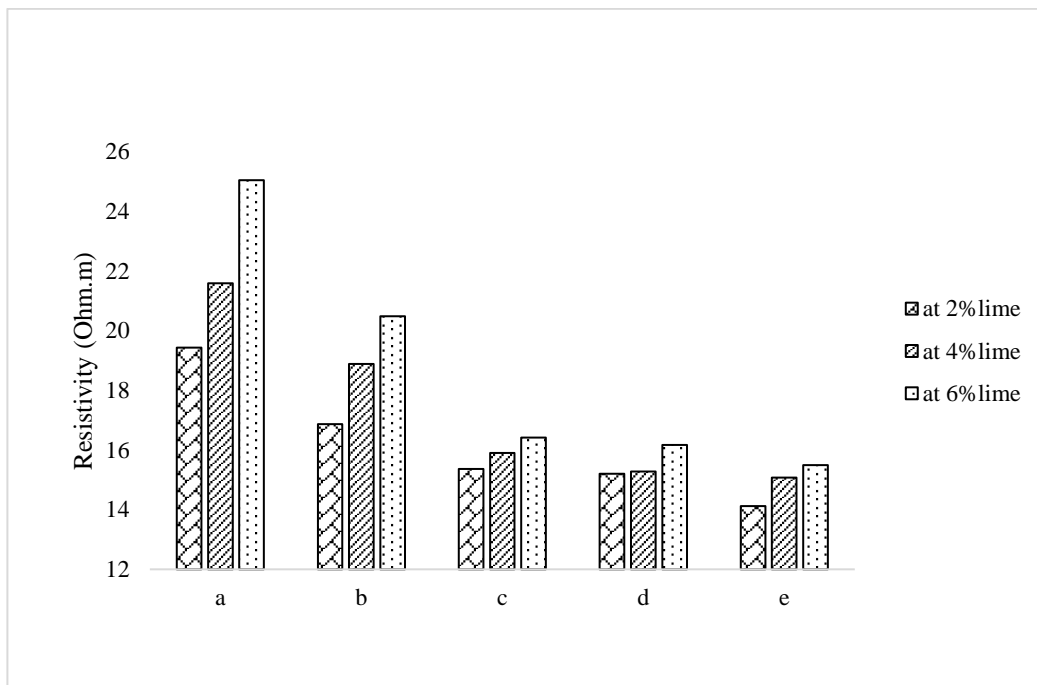


Figure 6.32 Variation of Resistivity with lime content at dry side and wet side points on the standard proctor compaction curve after 7 days curing for sample N

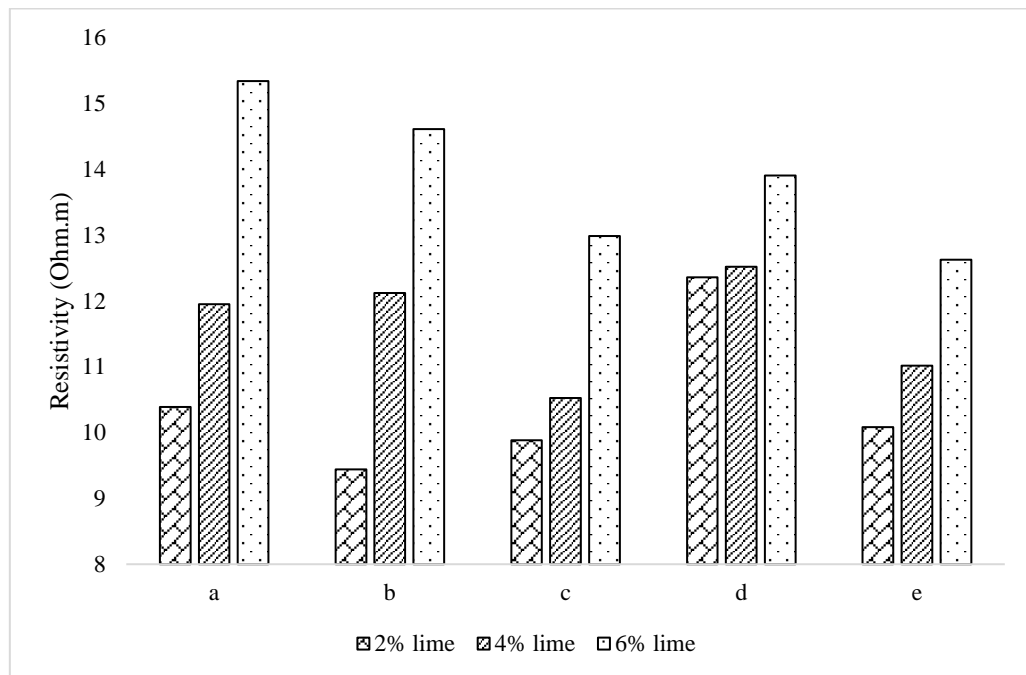


Figure 6.33 Variation of Resistivity with lime content at dry side and wet side points on the standard proctor compaction curve after 7 days curing for sample O

Figures 6.30 and 6.33 show variation of ER with lime content for 7 day cured samples at maximum dry density and optimum moisture content. For 7 day cured samples ER value increases with lime content. After 7 days of curing higher lime content yields greater amount of hydration compounds such as calcium silicate hydrate and calcium aluminate hydrates gels as a result of hydration processes. The hydration compounds fill in pore spaces and intersect each other to form solid networking resulting in a denser structure. Meanwhile, the free water space and porosity decrease, and resistance to the current flow increases.

### 6.5.3 Variation of resistivity with compaction effort

Light and Heavy mechanical compaction was performed on the soil samples. The variation of resistivity at different compaction points in wet side and dry side is studied. Similarly as observed in soil-cement, electrical resistivity is higher on the dry side and the reduction of resistivity is dependent only on the water content in the wet side (Fig. 6.34 and 6.35). Figure 6.36 shows there is a noticeable decrease of soil resistivity with the increase of the degree of compaction. At heavy compaction conditions, soil attain a more dense state with higher degree of saturation and lesser air voids, which results in a lower apparent resistivity of the soils (Seladji, 2010).

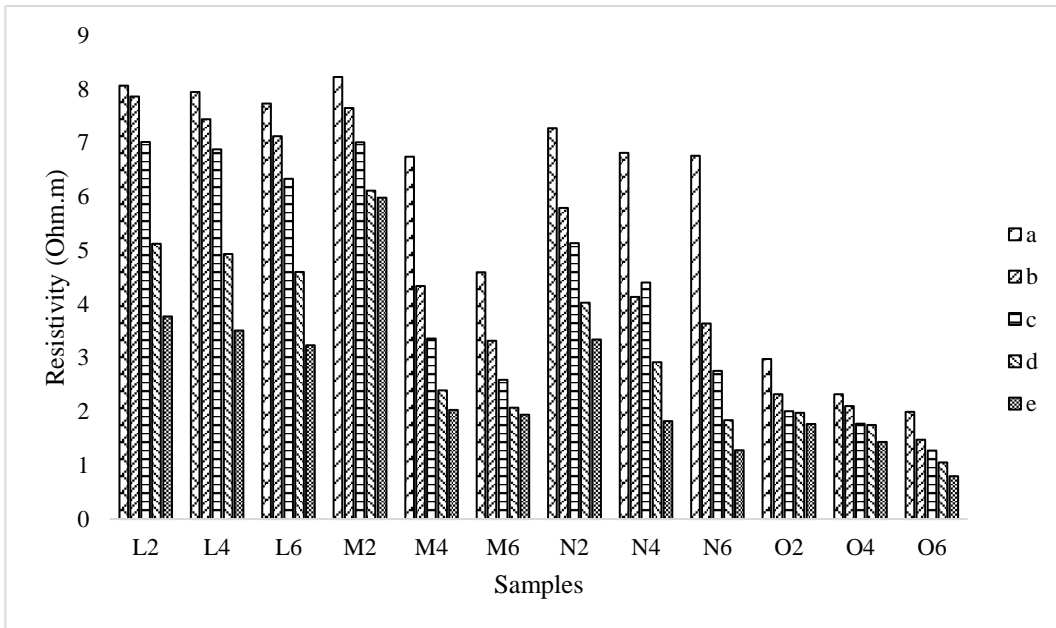


Figure 6.34 Variation of Resistivity at dry side and wet side points on the standard Proctor compaction curve at day zero

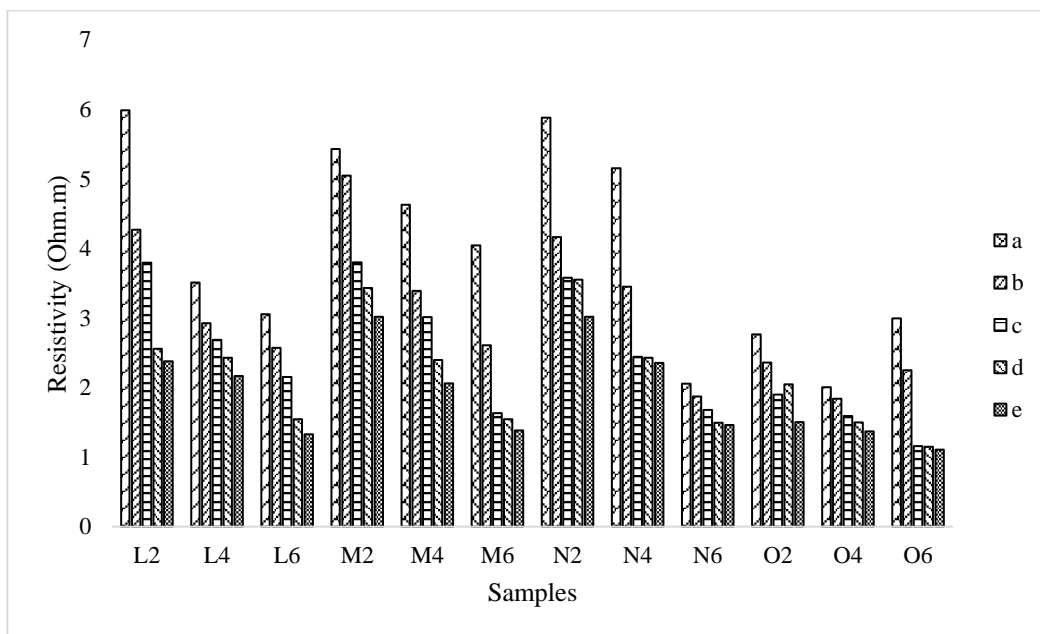


Figure 6.35 Variation of Resistivity at dry side and wet side points on the modified Proctor compaction curve at day zero

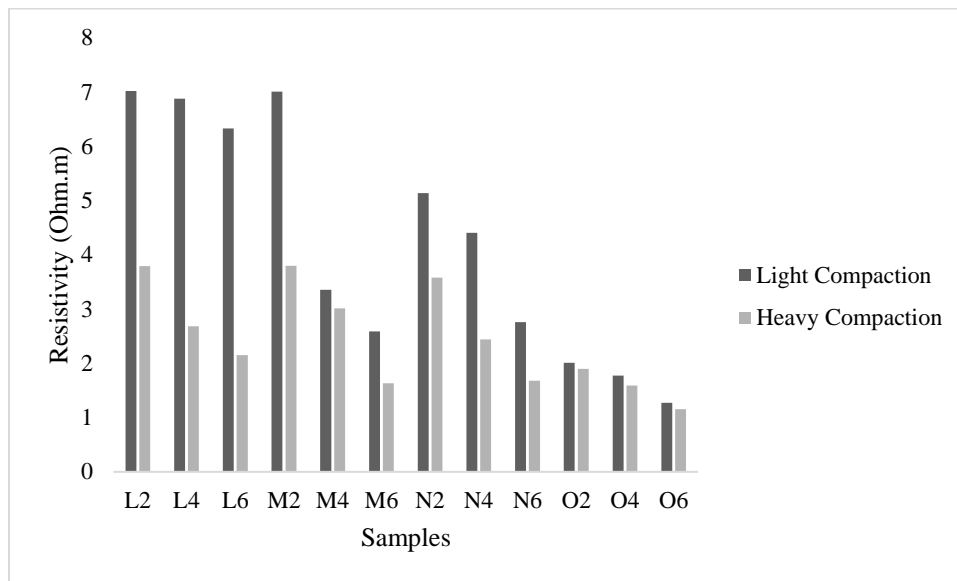


Figure 6.36 Variation of Electrical Resistivity at light (LC) and heavy (HC) day zero compaction conditions at OMC and maximum dry density conditions

#### 6.5.4 Variation of Resistivity with Porosity

Porosity of all 12 samples were found for a curing period of 1 day, 2 day till 7<sup>th</sup> day (Figs. 6.37 to 6.47). It is observed that as curing period increases porosity reduces due to the production of cementitious compounds filling up in pore spaces. It is also observed that as river sand content increases porosity reduces due to increase in coarser fraction.

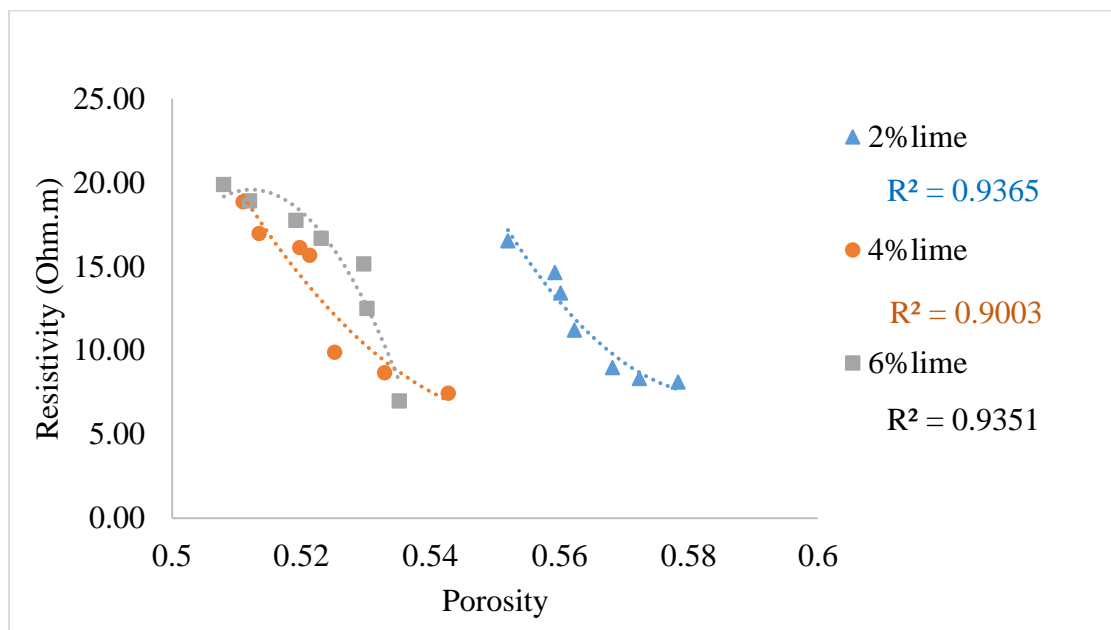


Figure 6.37 Variation of resistivity with porosity for sample L



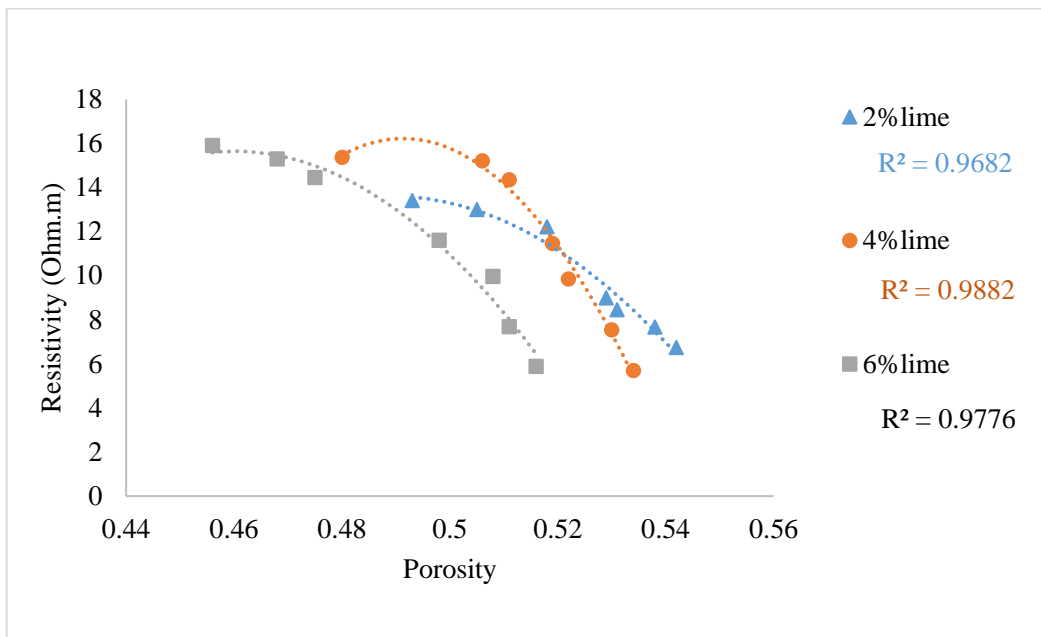


Figure 6.38 Variation of resistivity with porosity for sample M

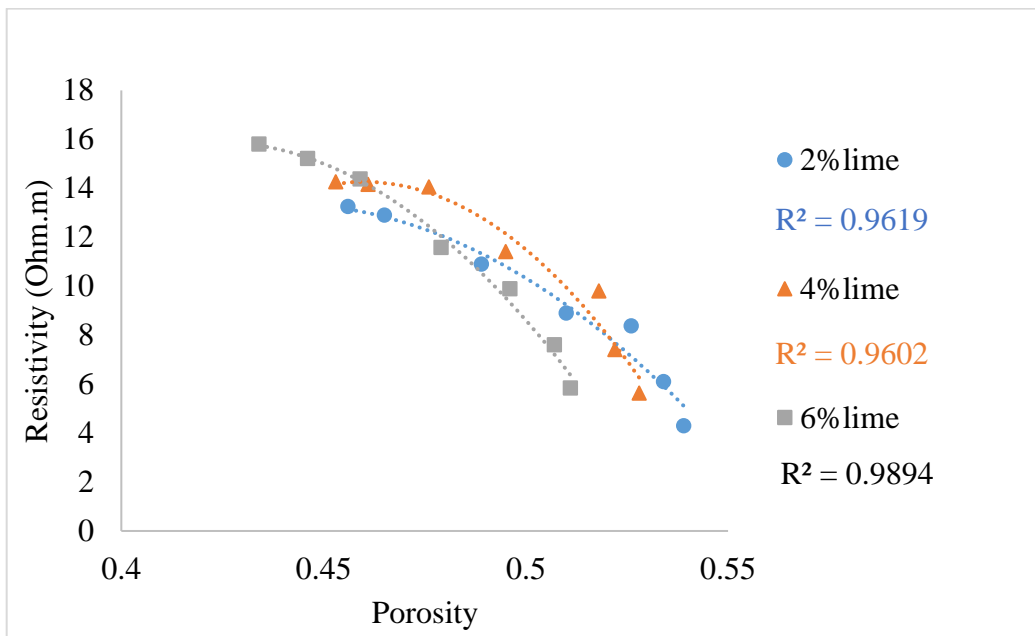


Figure 6.39 Variation of resistivity with porosity for sample N

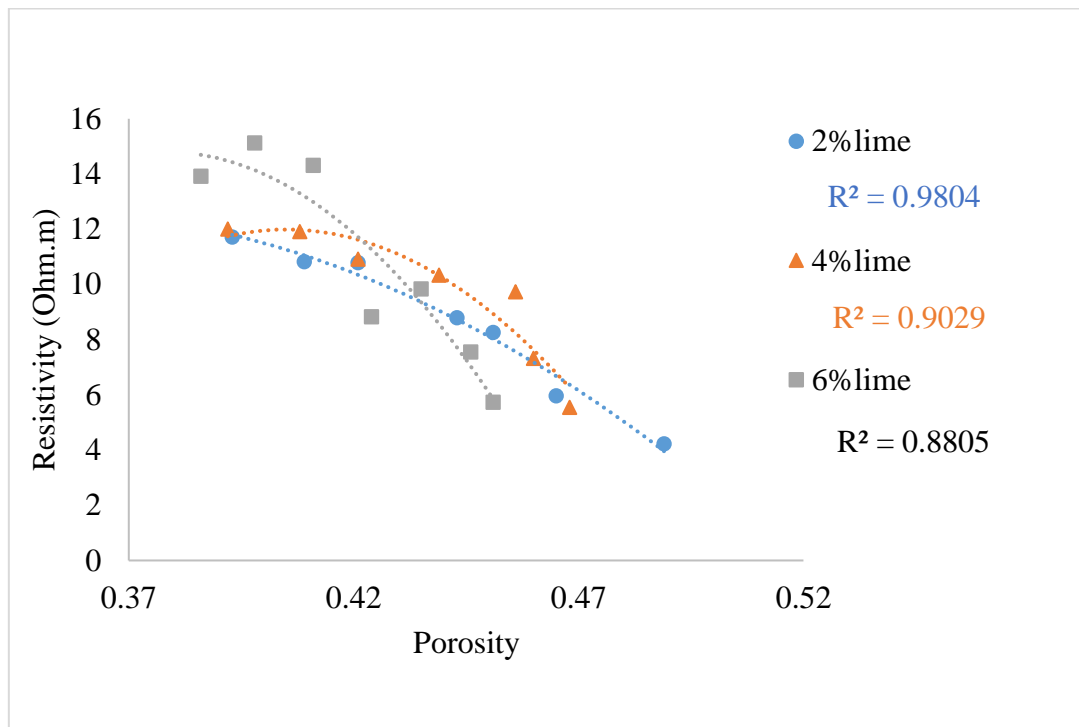


Figure 6.40 Variation of resistivity with porosity for sample O

### 6.5.5 Scanning Electron Microscope Images (SEM)

Scanning Electron Microscope technique was used to study the change in micro level structure of the soil-lime sample L2 (shedi soil with 2% lime) at different curing periods (as shown in Figs. 6.41 to 6.48). It is observed that as curing period increases microstructure attains more confined structure with lesser voids due to the hydration products formed as explained in the case of soil cement (Fig. 6.48). Hence the conductive path available rapidly decreases with curing time. The structure becomes more clustered with lesser voids with increase of curing time. Similarly for all the other samples L4, L6, M2, M4, M6, N2, N4, N6, O2, O4 and O6 also, the micro structure becomes more dense and clustered with increase in curing time.

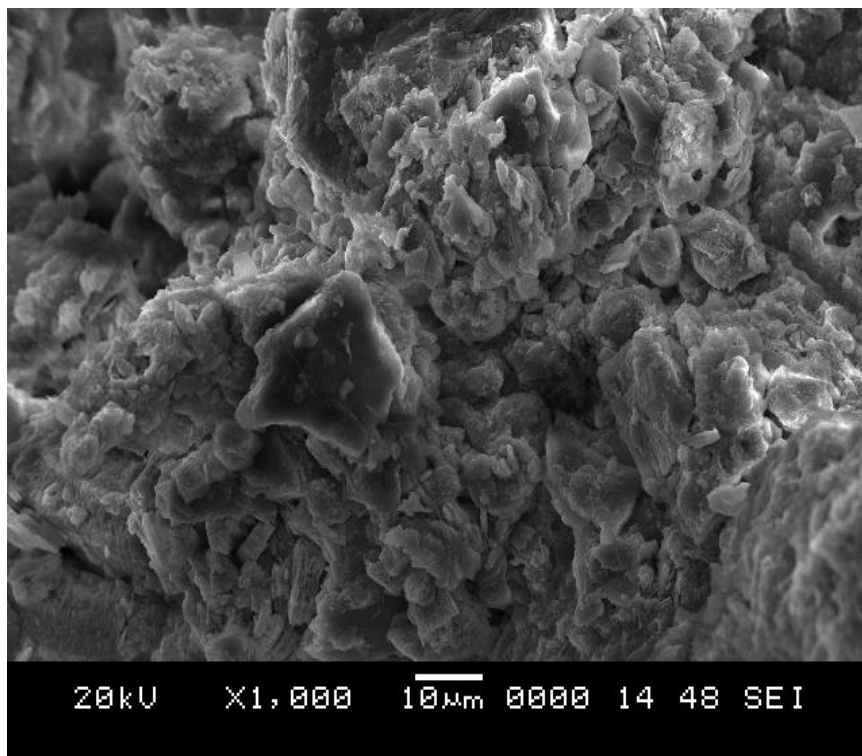


Figure 6.41 SEM image of soil lime at freshly prepared state

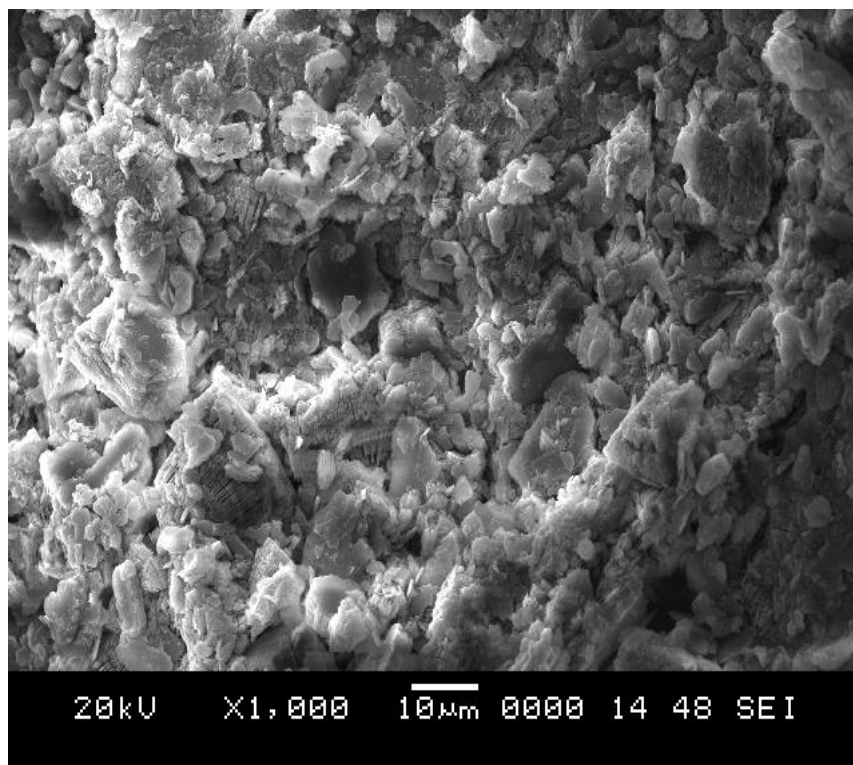


Figure 6.42 SEM image of soil lime after 1 day curing

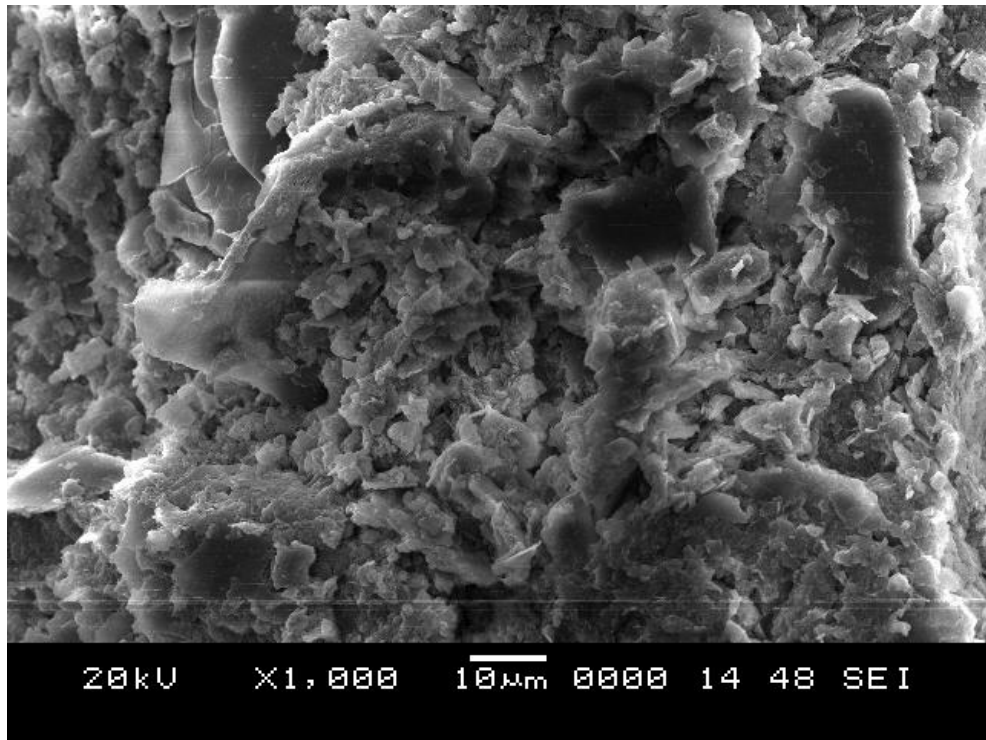


Figure 6.43 SEM image of soil lime after 2 days curing

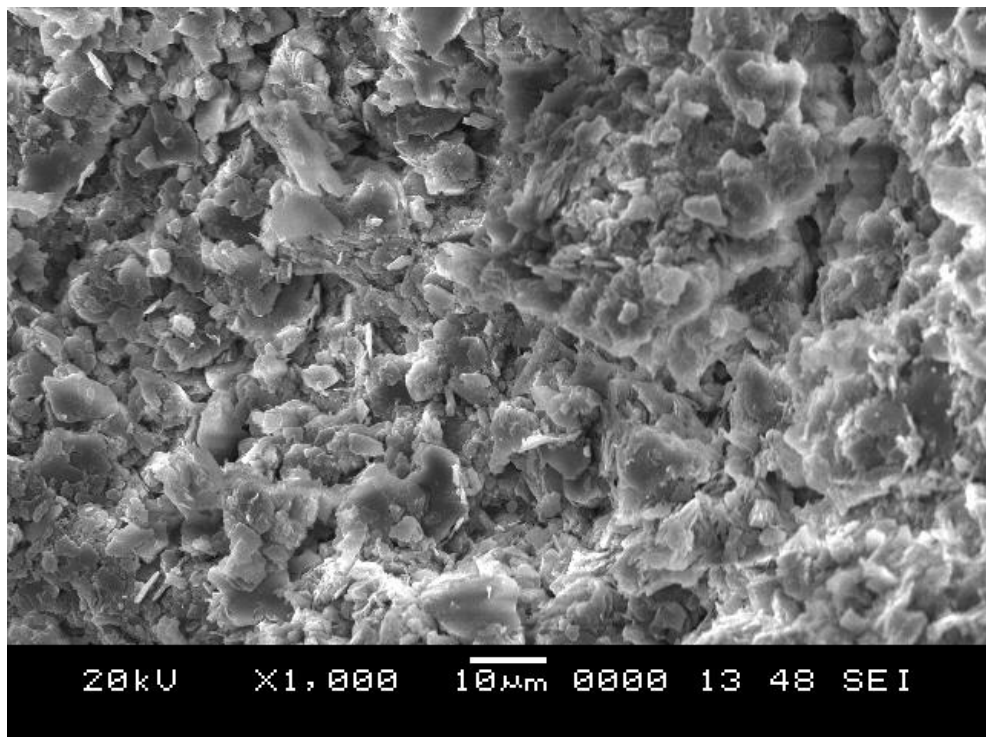


Figure 6.44 SEM image of soil lime after 3 days curing

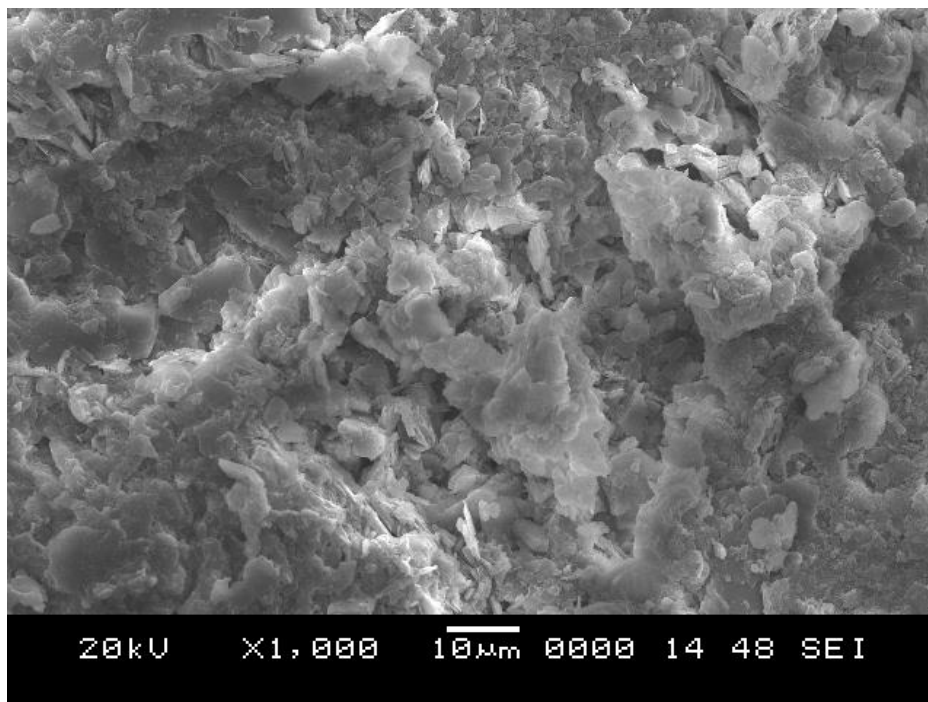


Figure 6.45 SEM image of soil lime after 4 days curing

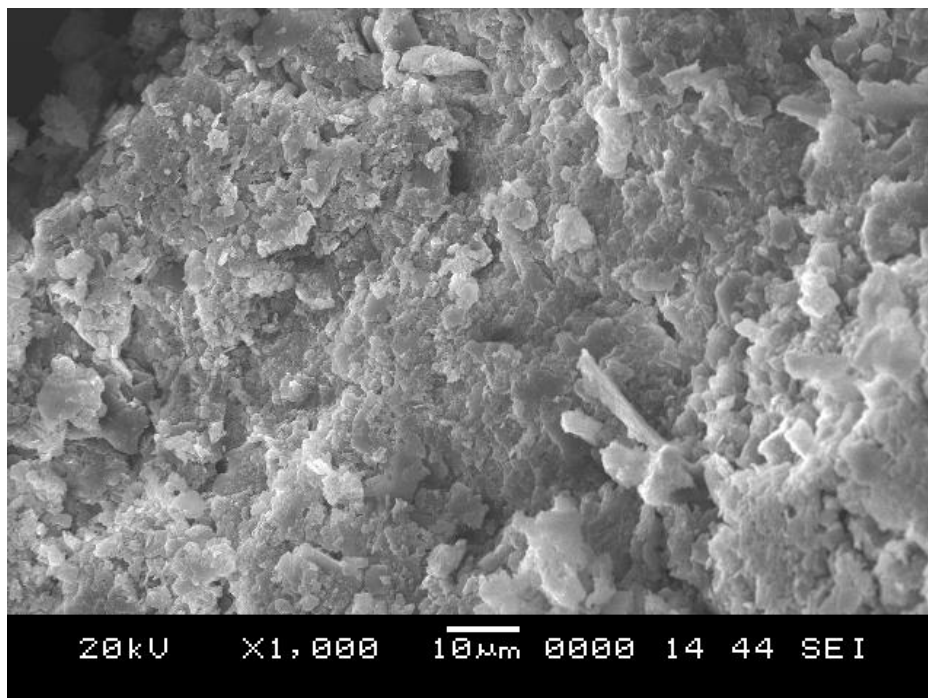


Figure 6.46 SEM image of soil lime after 5 days curing

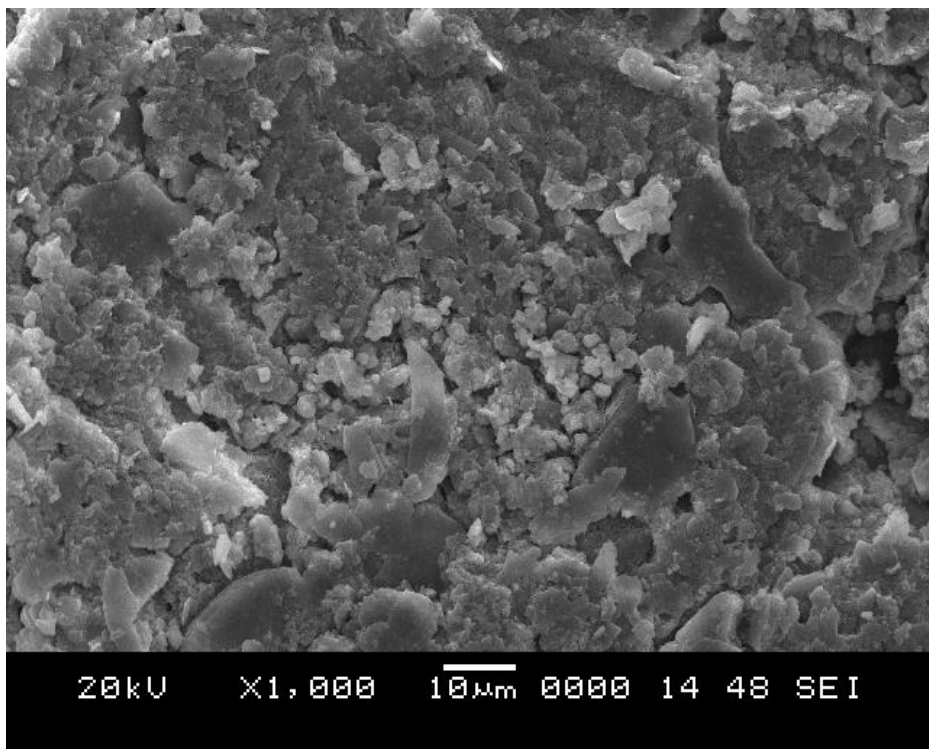


Figure 6.47 SEM image of soil lime after 6 days curing

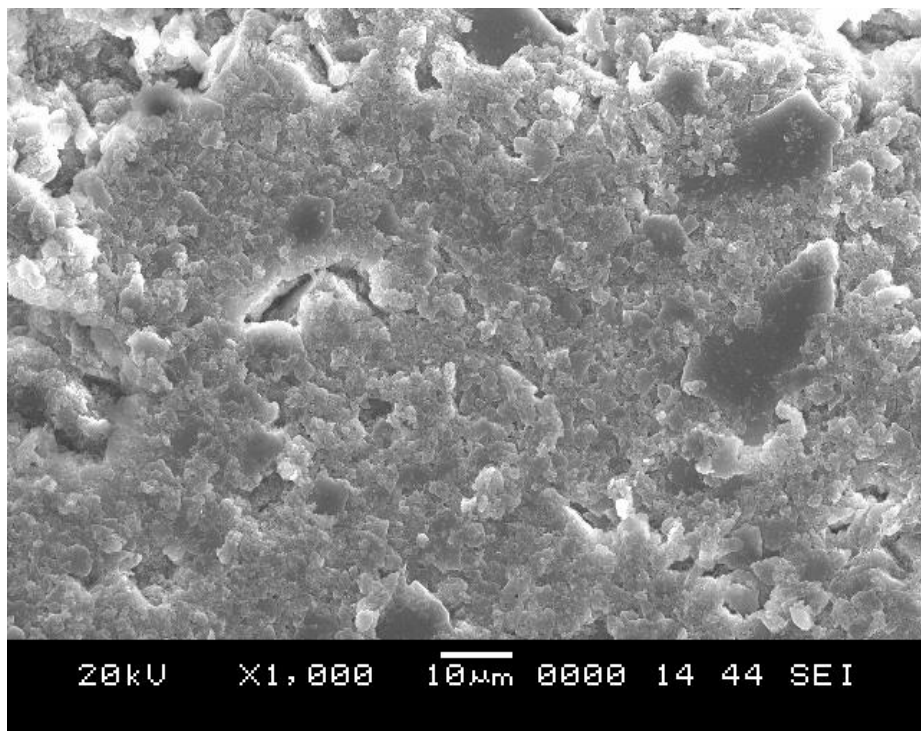


Figure 6.48 SEM image of soil lime after 7 days curing

### 6.5.6 Correlation of Resistivity with UCS value

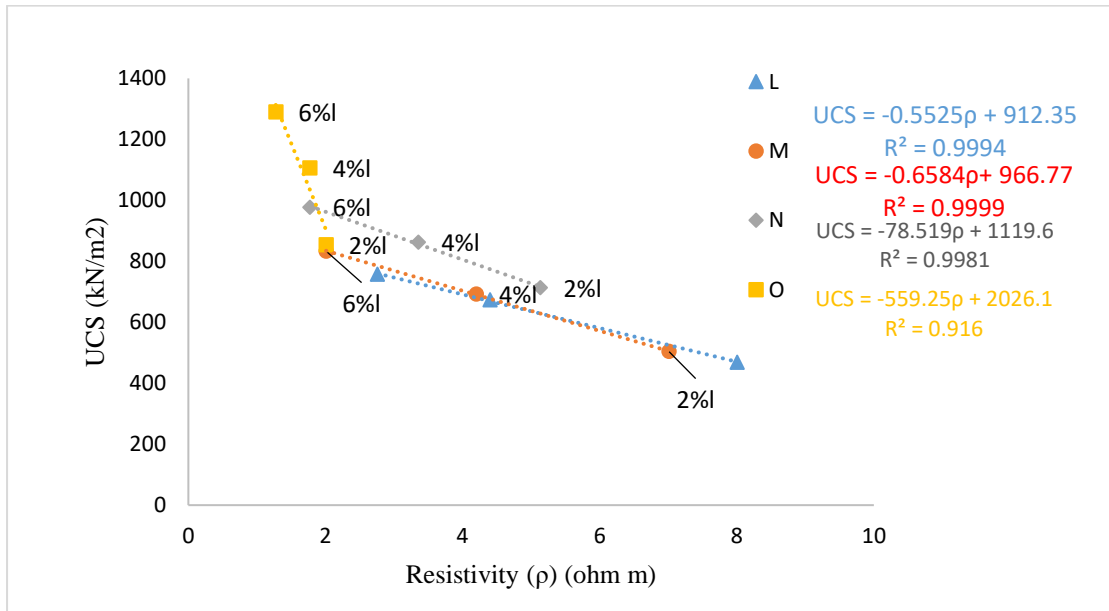


Figure 6.49 7 day UCS vs Resistivity (at freshly prepared state)

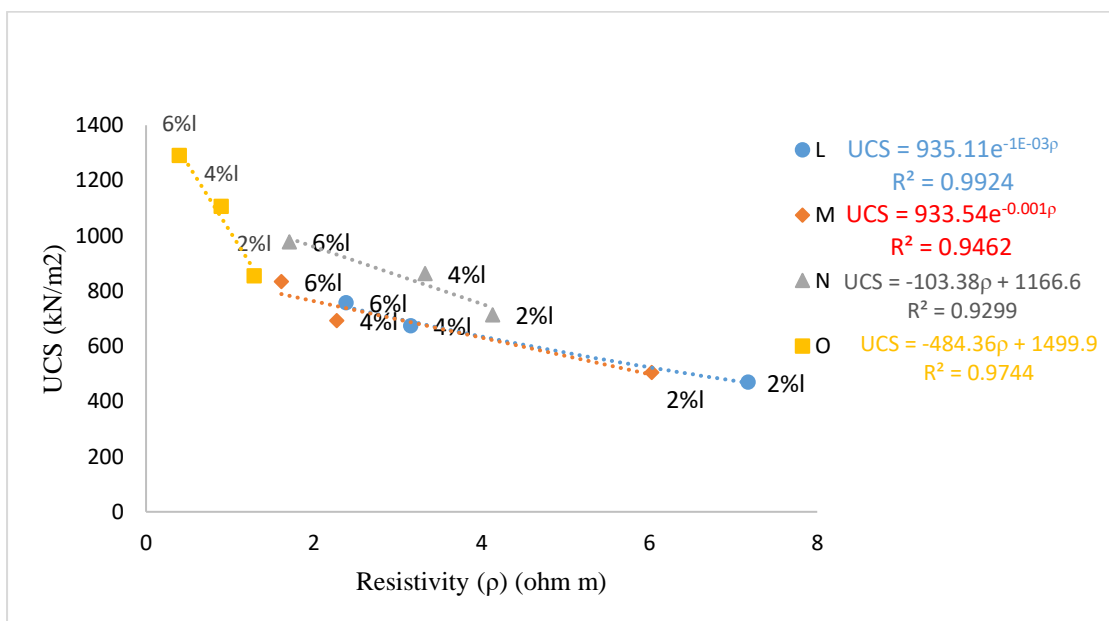


Figure 6.50. 7 day UCS vs Resistivity (after 1 hour curing)

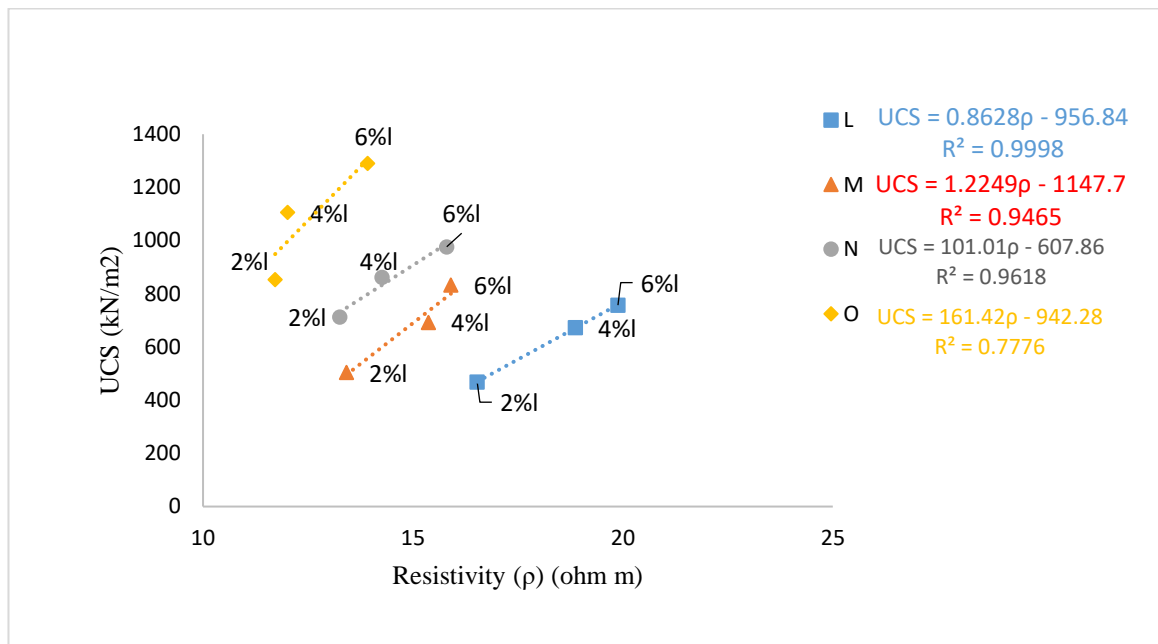


Figure 6.51 7 day UCS vs Resistivity (after 7 days curing)

Figure 6.49 show variation of UCS with ER of freshly prepared samples at different % of lime content. It is observed that UCS value increases with lime content and river sand addition due confinement produced by the hydration products. As explained in the previous Chapter, UCS is found to increase as particles become more clustered and gets bonded by the cementing action. 7 day UCS and electrical resistivity of freshly prepared and 1 hour cured soil sample shows an inverse relation (Fig. 6.50). Because at these stages as lime content increases ER value reduces, but 7 day UCS increases with lime content. Unlike in soil-cement, in soil lime, since the initial setting time for lime is more than that for cement, more ions were still available for electrical conduction after 1 hour curing. Since, as curing increases there is an increase in strength as well as electrical resistivity of soil-lime as a result of formation of hydration products in the void spaces, after 7 days curing, UCS and ER shows direct relation (Fig. 6.51).

Multiple regression analysis carried out derived generalised equations which predicts the 7 day UCS of lime stabilized soil, by using the lime content (%) and the resistivity (Ohm.m) measured at freshly prepared state and also after 1 hour curing period. The regression coefficients are 0.82 and 0.95 for equations 6.1 and 6.2 respectively. The equations are as follows.

$$UCS \left( \frac{kN}{m^2} \right) = 48.22 \times l(\%) - 89.25 \times \rho_o(Ohm.m) + 921.68 \quad (6.1)$$



Where,  $l$  is the lime content,  $\rho_0$  is the electrical resistivity at freshly prepared state.

$$UCS \left( \frac{kN}{m^2} \right) = -97.14x l(\%) - 4.78 x \rho_1(Ohm.m) + 1193.03 \quad (6.2)$$

Where,  $l$  is the lime content,  $\rho_1$  is the electrical resistivity measured after 1 hour curing

### 6.5.7 Correlation of resistivity with angle of friction

Figure 6.52 and Figure 6.52 shows variation of 7 day  $\Phi$  with ER of freshly prepared and 1 hour cured samples. From the results, it is observed that as lime content and river sand content increases  $\Phi$  increases. 7 day  $\Phi$  and electrical resistivity of freshly prepared and 1 hour cured soil sample shows an inverse relation. Because at these stages, as lime content increases ER value reduces but 7 day  $\Phi$  increases with lime content. Figure 6.53 show variation of 7 day  $\Phi$  with ER of 7 day cured samples. For 7 day cured samples, ER value and  $\Phi$  shows same trend, i.e. increases with lime content. Therefore for this case, it shows direct relation.

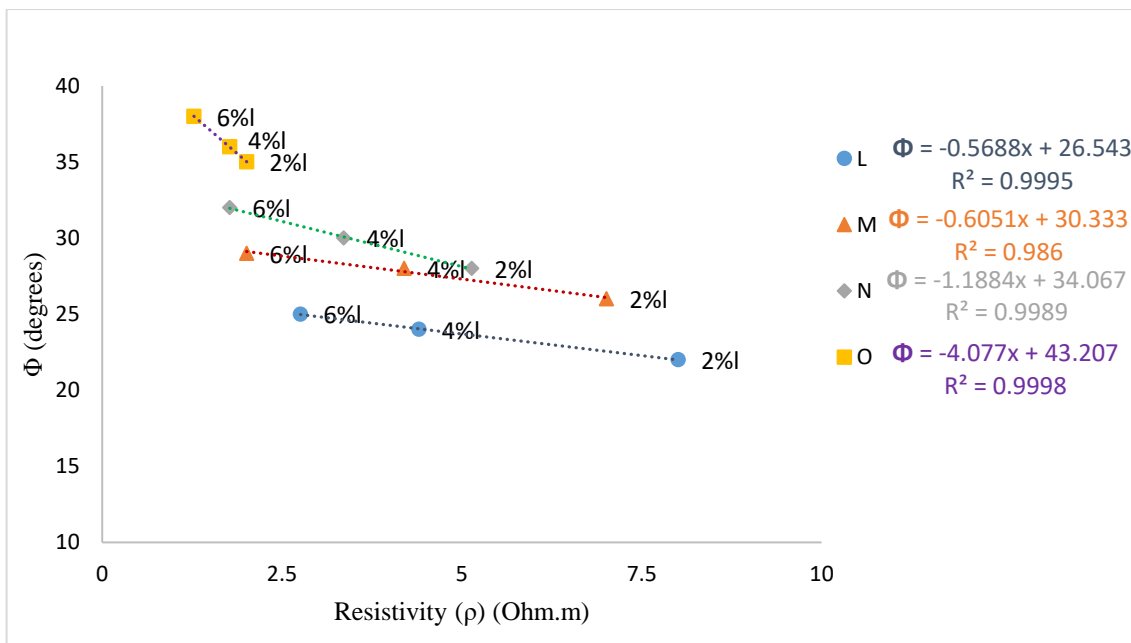


Figure 6.52 7 day angle of friction vs Resistivity (at freshly prepared state)

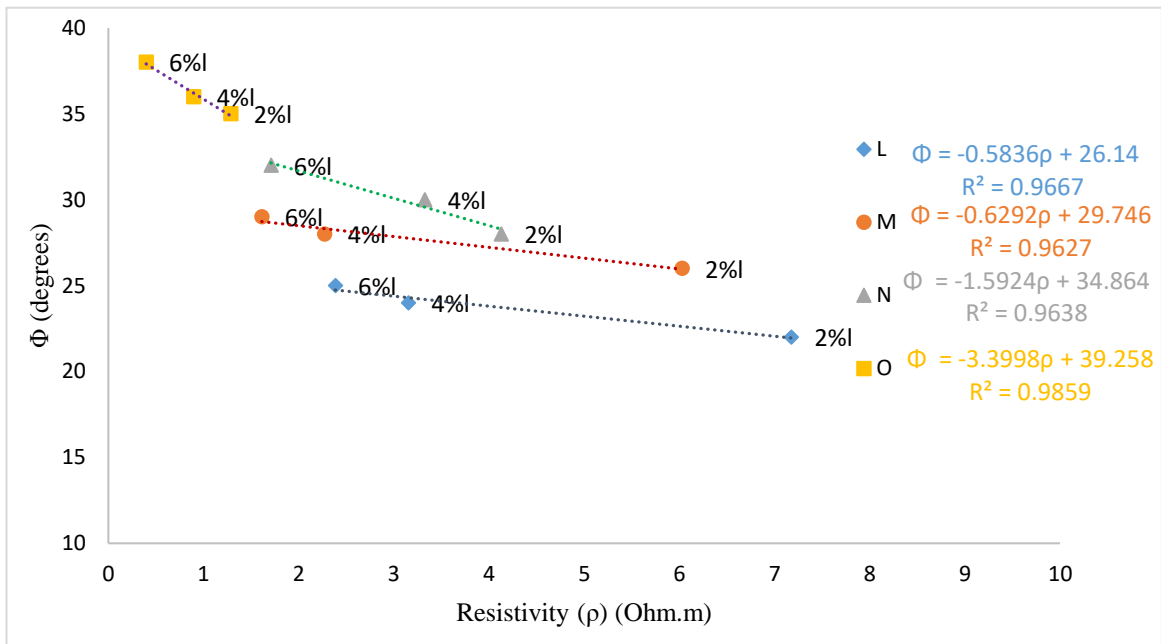


Figure 6.53 7 day angle of friction vs Resistivity (after 1 hour curing)

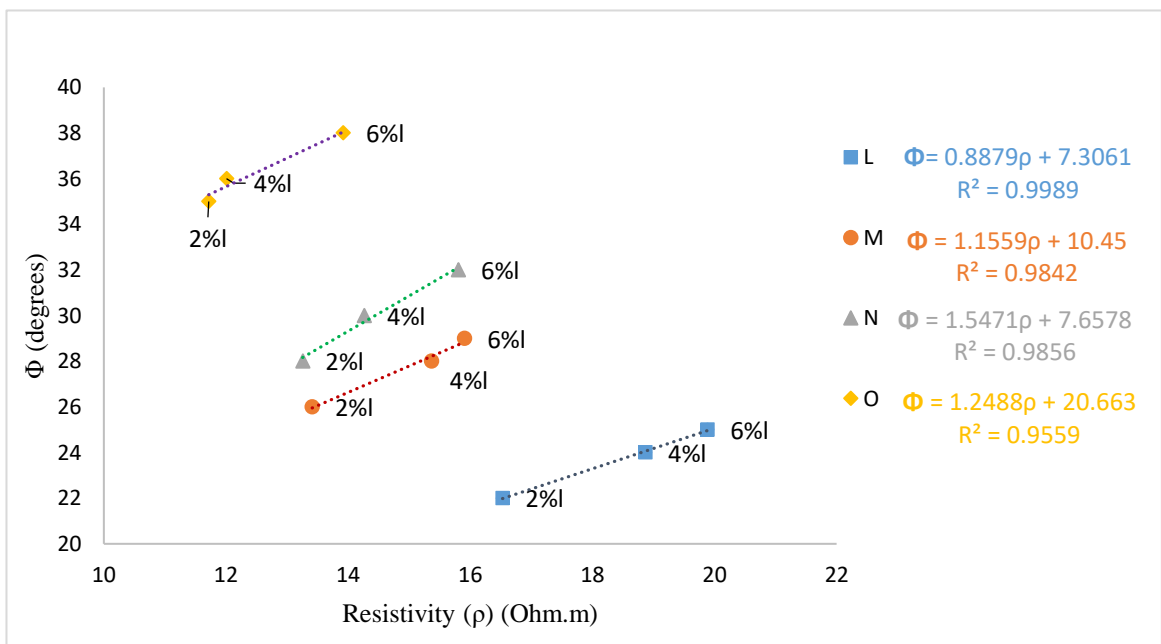


Figure 6.54 7 day angle of friction vs Resistivity (after 7 days curing)

### 6.5.8 Correlation of resistivity with cohesion

UU tests were conducted on the soil-lime samples. The test details are as explained chapter 5. Figure 6.55 and Figure 6.56 shows variation of 7 day cohesion with

ER of freshly prepared and 1 hour cured samples at different lime content. From the results it is observed that as lime content increases cohesion increases. 7 day and electrical resistivity of freshly prepared and 1 hour cured soil-lime sample shows an inverse relation. Because at these stages as lime content increases ER value reduces, but 7 day c increases with lime content. There exists good correlation between ER and cohesion. Figure 6.57 show variation of 7 day cohesion with ER of 7 day cured samples at different lime content. For 7 day cured sample, ER value and cohesion shows same trend, i.e. increases with lime content. Therefore for this case it shows direct relation. With increase of lime content, more hydration products are formed and more binding results in increase in the value of cohesion. But in the freshly prepared state, and after one hour curing period, more ion concentrations results in lesser values for resistivity as the lime content increases and hence shows an inverse relation with cohesion in this state. But a direct relation is seen after 7 days curing, since pore water gets used up for hydration resulting in more air in the voids which increases resistance as seen in the case of soil-cement.

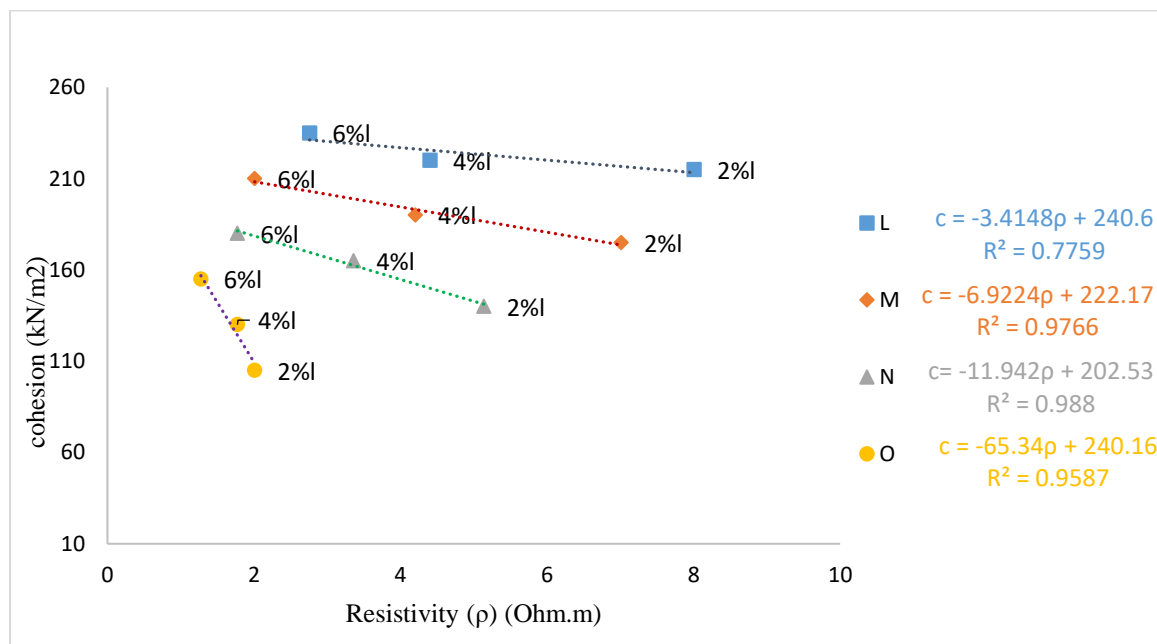


Figure 6.55 7 day cohesion vs Resistivity (at freshly prepared state)

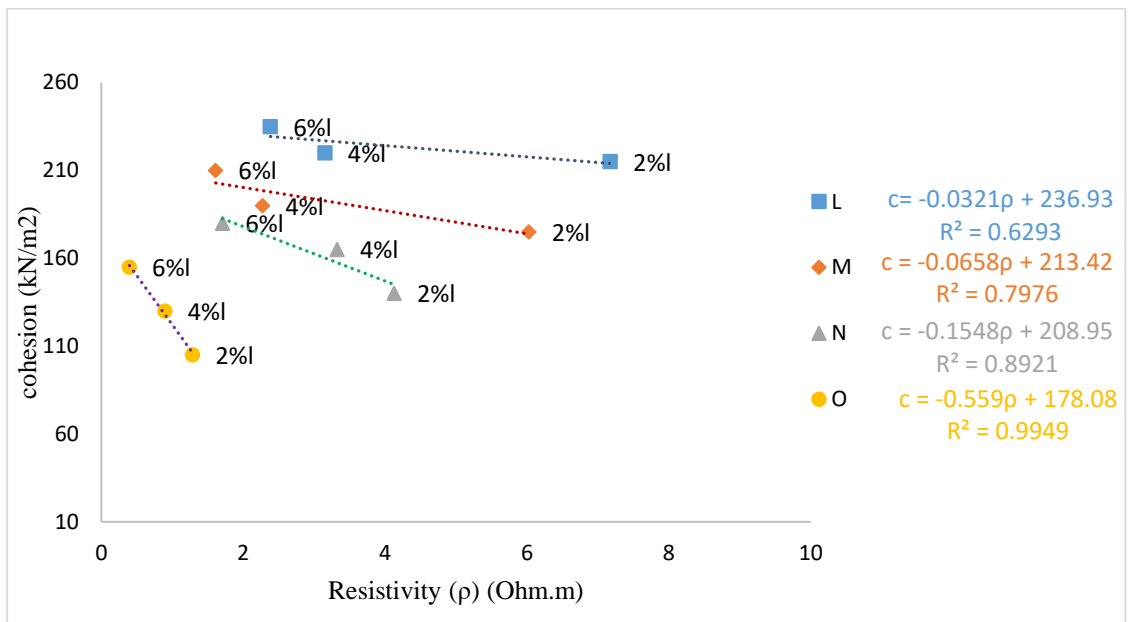


Figure 6.56 7 day angle of friction vs Resistivity (after 1 hour curing)

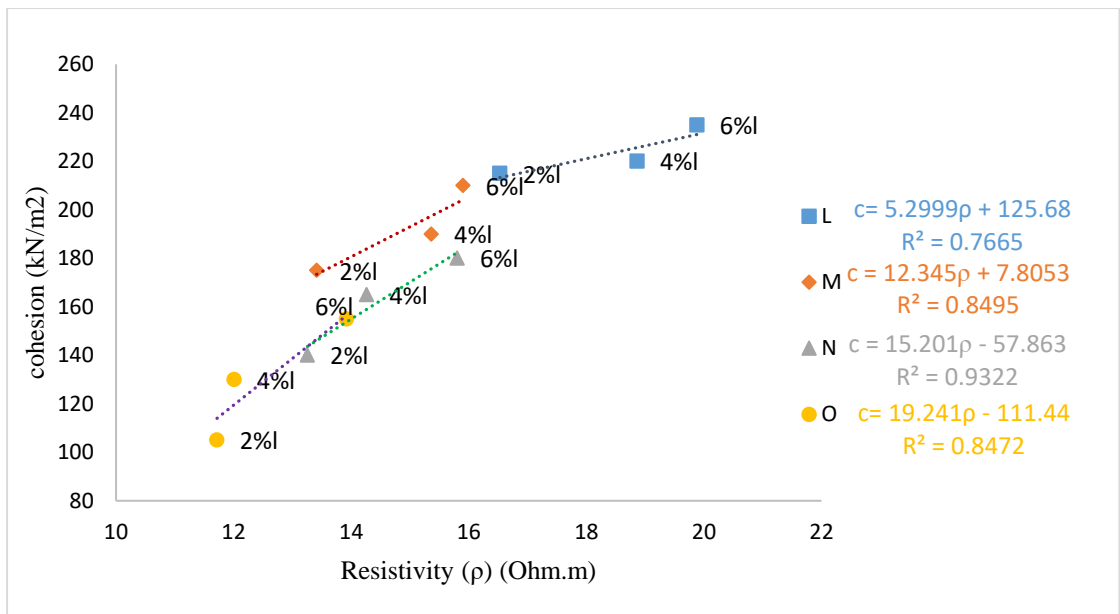


Figure 6.57 7 day angle of friction vs Resistivity (after 7 days curing)

### 6.5.9 Correlation of Resistivity with Split Tensile Strength

Split tensile strength of soil-lime samples were measured as explained in chapter 5. Split tensile strength after seven days curing time and resistivity in the freshly prepared state and after curing periods of one hour and seven days is correlated in Figs. 6.58 to 6.60. When lime content increases, the binding increases and hence the samples with higher lime content can take up more load when tested resulting in increase of split tensile strength

value. For all the soil samples, when the lime content is varied, resistivity shows inverse relation with split tensile strength for fresh samples and 1 hour cured samples and direct relation for 7 days cured samples.

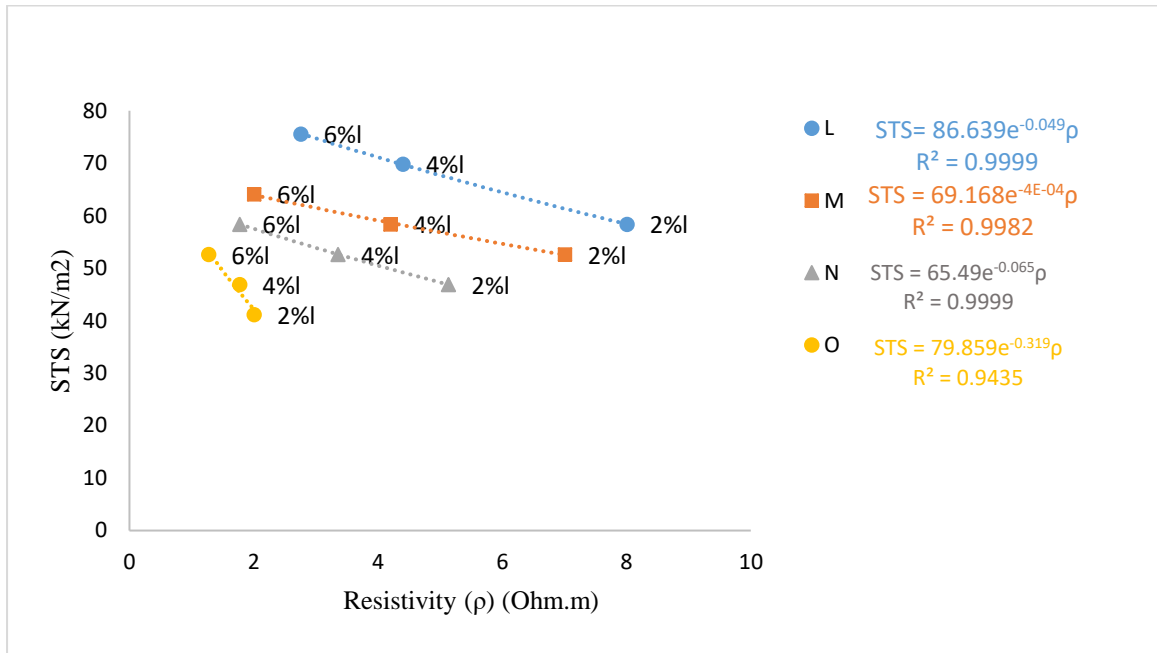


Figure 6.58 7 day Split Tensile Strength vs Resistivity (at freshly prepared state)

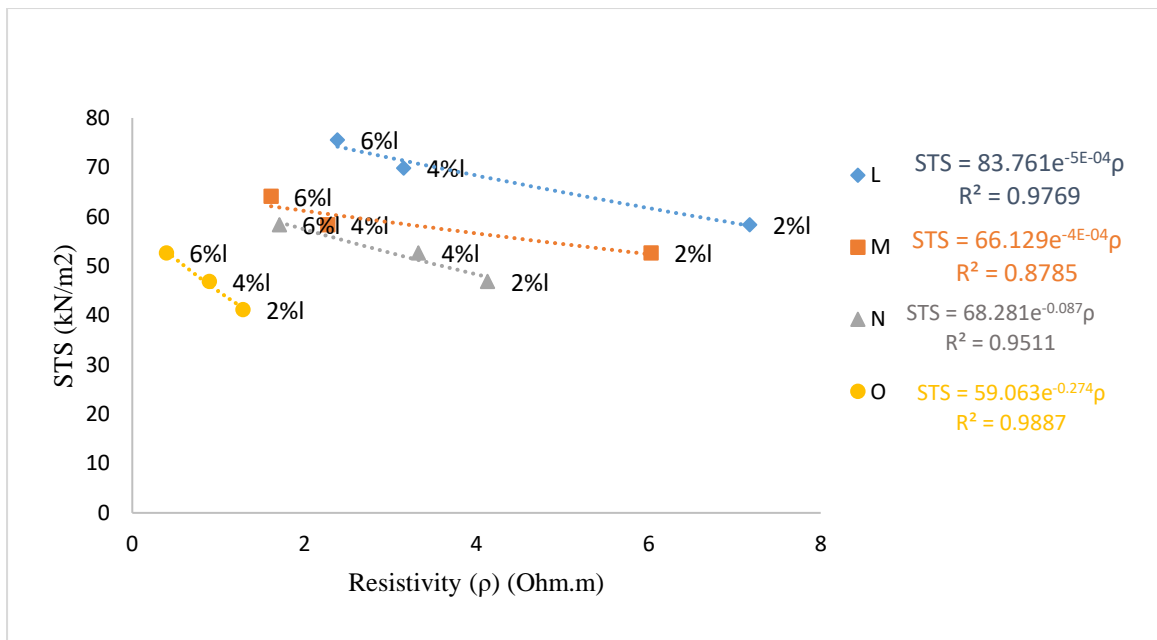


Figure 6.59 7 day Split Tensile Strength vs Resistivity (after 1 hour curing)

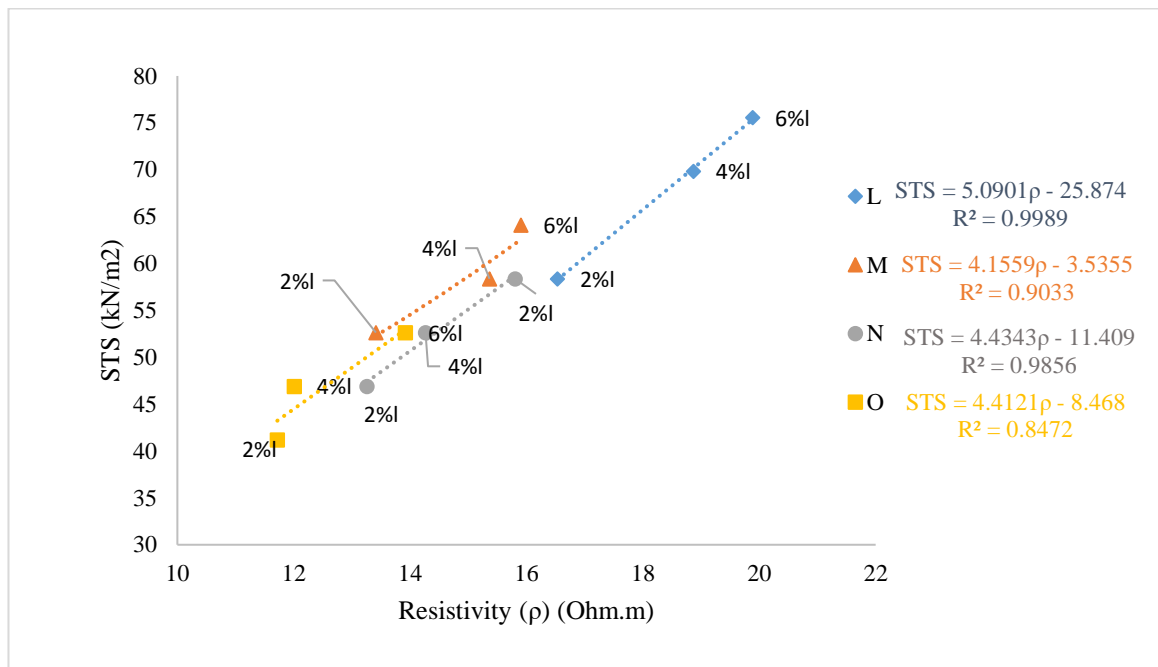


Figure 6.60 7 day Split Tensile Strength vs Resistivity (after 7 days curing)

## 6.6 Summary

Electrical resistivity measurement of freshly prepared uncured and cured soil lime materials are done and the correlation between the factors controlling the performance of soil-lime and electrical resistivity are studied in this Chapter. As explained in the previous Chapter, similarly as in soil-cement, by the time an unconfined compressive strength test can be performed, to check the quality of the soil-lime, the material will be hardened in the field and if it doesn't meet strength, performance criteria, the material will have to be taken out, broken down and remixed with additional lime. This is expensive and time consuming. At this stage, electrical measurements of soil-lime material saves a great deal of cost and time by predicting the strength properties without hardening of the material. Equations developed in this study, by multiple regression analysis, predict the Unconfined Compressive Strength of the soil-lime samples, at the freshly prepared state or after 1 hour curing. If the strength requirement is not met, it could be remixed with additional lime at the fresh state itself and reused.



## CHAPTER 7

### STUDIES ON RESISTIVITY-MOISTURE CONTENT RELATIONSHIP

#### 7.1 Introduction

Soil derives its spontaneous electrical resistivity properties because of its soil solid and liquid phase structure. Soil air can be considered as dielectric. This Chapter discusses in detail, the resistivity-moisture content relationship, which was briefly discussed in Chapter 4. A graphical method which locates the point of “just saturation”, which correlates with the Shrinkage Limit of the soil, is proposed. The method is verified with phosphoric acid contaminated lithomargic clay and bentonite blended lithomargic clay, wherein the Atterberg limits got altered. The reasons for the alteration in Atterberg Limit is also examined in this Chapter.

##### 7.1.1 States and Limits of Consistency

Atterberg limits namely Liquid Limit, Plastic Limit, Shrinkage Limit are water contents where in the soil transforms from one state to another and it also undergoes change in behaviour. There is ofcourse a lot of ambiguity in correctly identifying each of these states. As per our present general understanding, the soil at all the three limits is fully saturated. At liquid state, as the water content in soil is being reduced, the soil begins to show some measurable shearing resistance. Plastic Limit is defined as that water content at which a pat of soil can be rolled into threads of 3mm diameter without crack on the surface. It should break up into segments about 3mm to 10mm (Holtz et al. 2015). At Shrinkage Limit, the soil is just fully saturated. Any further reduction in water content will not cause a reduction in volume of soil mass and will make the soil partially saturated. Soils may also swell as water content exceeds the shrinkage limit. When the saturation is lower, a small amount of water wraps the particle surface in the form of bound water, which cannot form a continuous water body and pass water pressure, and a large amount of air is interconnected and can pass water pressure, and this is named as closed-water unsaturated soil. On the contrary, when the saturation is higher, the air in the pore space forms isolated bubbles which are entirely enclosed by surrounding pore water, and this is named closed-air unsaturated soil (Hong-Jing 2014).



### **7.1.2 Atterberg limits – Importance in soil behaviour**

The Atterberg limits are important for classification of cohesive soil materials and are useful for interpreting shear strength, bearing capacity, compressibility, and swelling potential of the soil. As the moisture content of a clayey soil decreases, it goes through four distinct states of consistency: liquid, plastic, semi-solid, and solid. Each stage is defined by significant changes in strength, consistency, and behaviour. Knowledge of these values helps in foundation design of structures and to predict behavior of soils in fills and embankments. The values can contribute to estimates of shear strength and permeability, prediction of settlement, and identification of potentially expansive soils.

Depending on the type of fine-grained soil the Atterberg limits have different values. For example, shrinkage limit of illite is in range of 15% to 17% depending on particle sizes, its plastic limit varies from 24% to 52%, while its liquid limit is from 30% to 110%; SL of kaolinite is from 25% to 29%, its PL is in range of 30% to 40%, while LL is from 35% to 72%, etc. Determination of Atterberg limits of soils is very important prior to construction.

### **7.1.3 Resistivity-water content relationship**

Though already many researchers have utilized resistivity measurements to predict the geotechnical parameters, including ER-moisture content relationships, nobody has attempted to estimate shrinkage limit of soils from ER-moisture content relationship. This paper looks into the relationship between ER (determined from laboratory experiments) and moisture content, especially between ER and Atterberg limits, and between ER and Shrinkage Limit in particular. A very good agreement is obtained between Shrinkage limit determined from standard (conventional) Shrinkage Limit test and resistivity-water content profile. The veracity of electrical resistivity measurements in estimating the shrinkage limit of soils was further confirmed by experiments on phosphoric acid contaminated lithomargic soils and bentonite blended lithomargic soils.

## 7.2 Resistivity-moisture content studies on Lateritic Soils

### 7.2.1 Test materials

In order to vary the percentage of fines, in the different test samples, controlled soil samples were prepared. River sand was used for blending the shedi soil. All these soil samples were used to study the geotechnical and electrical properties. Different percentages of river sand added were 0, 10, 20, 30, 40 and 50% by weight of dry soil. The soil samples are denoted as S0, S1, S2, S3, S4, and S5 respectively.

Laboratory testing on the prepared samples were conducted to determine grain size distribution, compaction characteristics, specific gravity, and Atterberg limits and the results are presented in Table 7.1. Electrical resistivity measurements were also carried out on these samples in the laboratory to bring out the correlation between physical properties and electrical resistivity of the soil samples.

Table 7.1 Basic Geotechnical parameters of the soil samples

Parameter	Soil sample					
	S0	S1	S2	S3	S4	S5
G	2.58	2.58	2.60	2.61	2.61	2.62
PL (%)	33.90	31.42	30.50	29.90	27.10	25.30
LL (%)	47.0	44.5	40.6	39.4	37.7	34.4
SL (%)	26.10	24.13	23.70	21.50	20.15	19.09
OMC (%)	28.0	25.0	23.0	21.0	18.0	17.0
$\gamma_{dmax}$	1.45	1.56	1.59	1.64	1.74	1.77
e	0.743	0.654	0.605	0.517	0.450	0.400
S <sub>SL</sub> (%)	90	95.2	100	100	100	100
Clay (%)	36.6	26.9	28.9	23.4	19.4	15.2
Silt (%)	52.6	50.8	39.6	32.1	28.3	24

Sand (%)	10.8	22.3	31.5	44.5	52.3	60.8
----------	------	------	------	------	------	------

G- Specific Gravity, PL- Plastic Limit, LL- Liquid Limit, OMC- Optimum Moisture Content,  $\gamma_{dmax}$ - maximum dry density, SL- Shrinkage Limit, e- void ratio,  $S_{SL}$ - degree of saturation at shrinkage limit

### 7.2.2 Test method

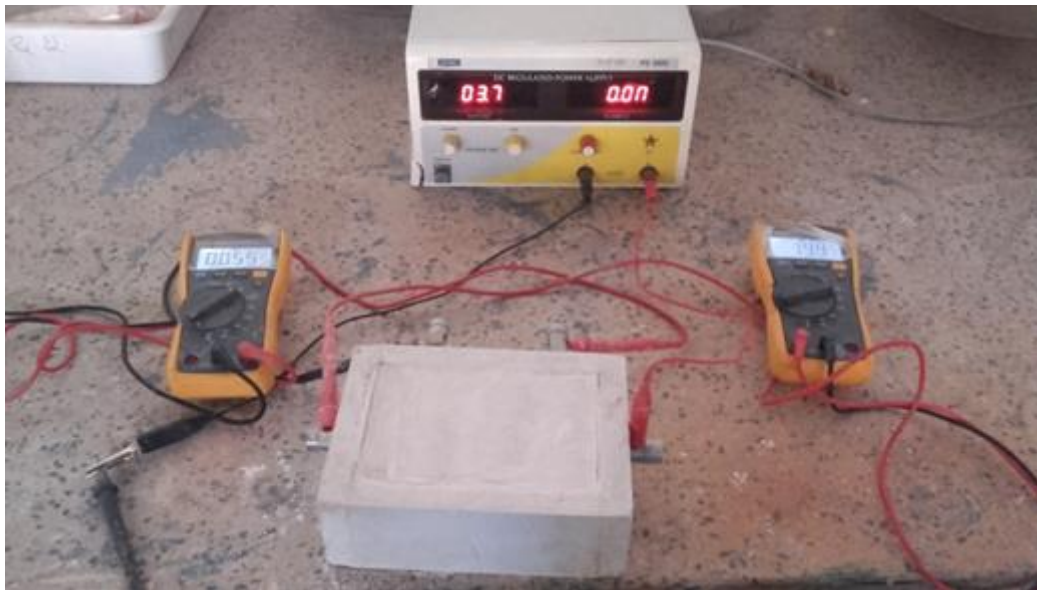


Figure 7.1 Resistivity measurement

Standard solutions of NaCl and KCl, with different moralities (0.2 to 1 M) were used for standardizing the test setup. First as a trial, soil was filled in the resistivity box by compacting to the maximum possible extent (without over exerting) with a tamping rod to determine what is the maximum achievable compaction. For all the samples this maximum compaction was found to be around 95% of Standard Proctor maximum dry density. Therefore during the ER studies, soil was mixed with the predetermined moisture content and was filled in the resistivity box by compacting at constant dry density, which was taken as 95% of the Standard Proctor maximum dry density. Resistivity measurements were made (Fig. 7.1) for soil samples prepared at constant dry density and moisture contents ranging from 10% to 50%, each trial being conducted at intervals of 5% variation in moisture content.

### 7.2.3 Results and Discussions

An increase in the soil water content results in a decrease in the electrical resistivity of soil (Cosenza *et al.* 2006). This correlation indicates that resistivity is a good indirect predictor of water content. However, generally soils with higher fines content (clays) also have a higher specific surface, which improves surface conductance. Moreover, electrical resistivity shows a definitive relationship with wet unit weight, saturation, air void ratio (ratio of the volume of air-void to the total volume of air, water, and solids), and compressive strength (Fallah-Safari *et al.* 2013). When the chemical content of water filling the pore spaces is same, then resistivity of clays are mostly influenced by water content, void ratio, and dry unit weight (Fallah-Safari *et al.* 2010). Hence it is clear that resistivity is a good indirect predictor of geotechnical data in clays.

When water comes into the clay soil, cations and anions float around the structure. The mobility of electrical charge in soil is highly affected by water. If moisture content present in soil increases from dry to full saturation level, adsorbed ions in the solid particles get released, thus the mobility of electrical charges increases and hence conduction increases. (Kibria *et al.* 2011). Coming to the microstructure level of soil, Voronin (1986) described the changes that occur in the pore spaces as follows (Fig. 7.2). The rapid decrease in ER is observed in the adsorption water zone. Initially, immobile water molecules are present in this zone. However, dipolar water ions create a conductive path and hence electrical resistivity decreases sharply. In film water zone, van der Waal's force increases and hence decrease in resistivity is less sharpening. When water reaches fissures, the relative portion of film water decreases and capillary water increases. In film capillary and capillary water zone, molecular attraction is higher than the capillary force. Hence ER decreases less dramatically. In the gravitational water zone, there is not much relation between the mobility of electric charges and movement of water molecules. Hence, in this region, ER is almost independent of water content. A small decrease in the electrical resistivity can still occur in the gravitational water range due to the continuous dissolution of the adsorbed and precipitated ions from the soil solid phase (Fallah-Safari, 2010).

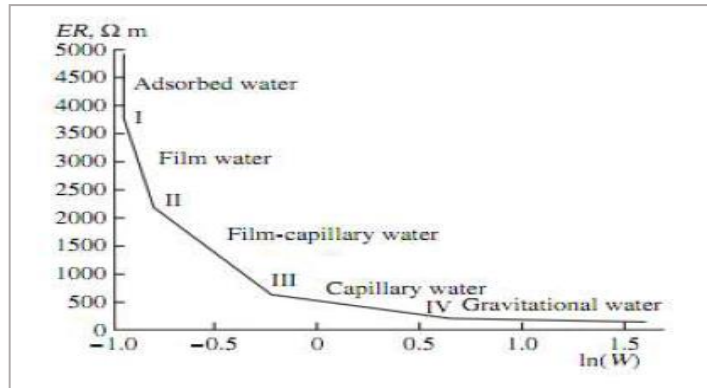


Figure 7.2 Relationship between soil moisture and ER (Voronin, 1986)

Graphs were plotted with resistivity and water content for all the six soil samples tested (Fig. 7.3 to Fig. 7.8). An asymptotic profile was obtained in all cases. When the water content is increased at unsaturated state of the soil, the sectional area of conductive path increases and facilitates smoother ionic conduction, so the electrical resistivity is decreased. However after saturation, the water film is in continuous state and has little effect on the electrical resistivity, with any further addition of water, so the change of the electrical resistivity tends to be stable, and reaches to a constant. The variations of resistivity with moisture content for different soil samples are presented in Figs. 7.3 to 7.8. The  $R^2$  values vary from 0.90 to 0.99. It is observed that as the soil moisture content increases, the soil resistivity decreases and becomes asymptotic.

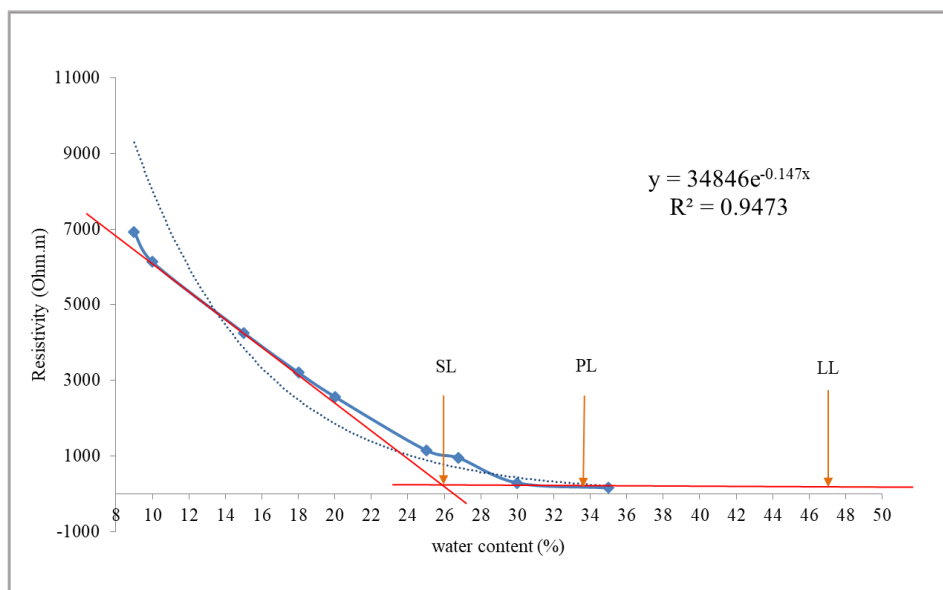


Figure 7.3 Resistivity-moisture content profile for soil sample S0

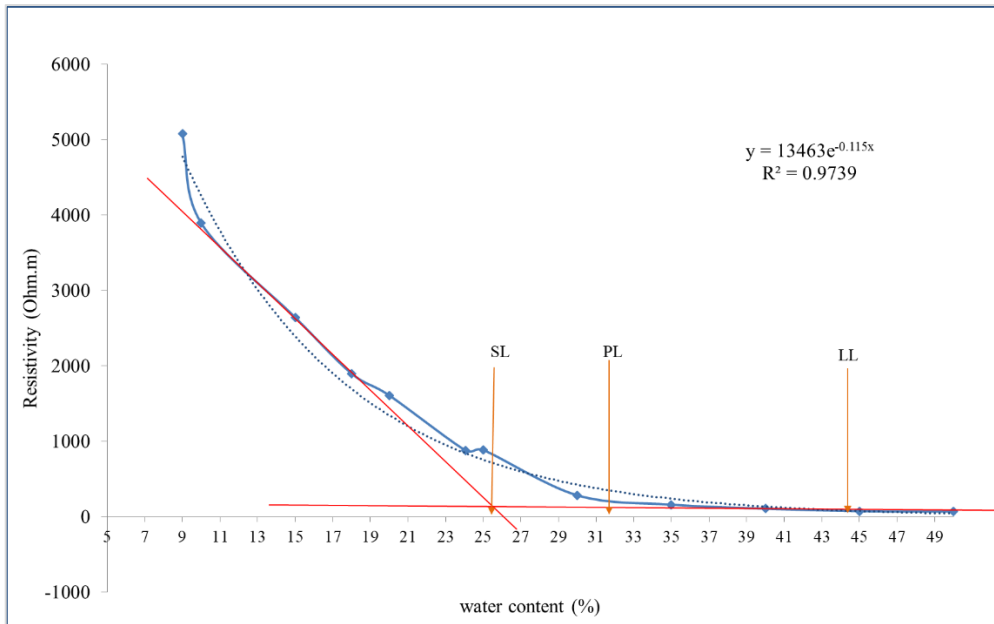


Figure 7.4 Resistivity-moisture content profile for soil sample S1

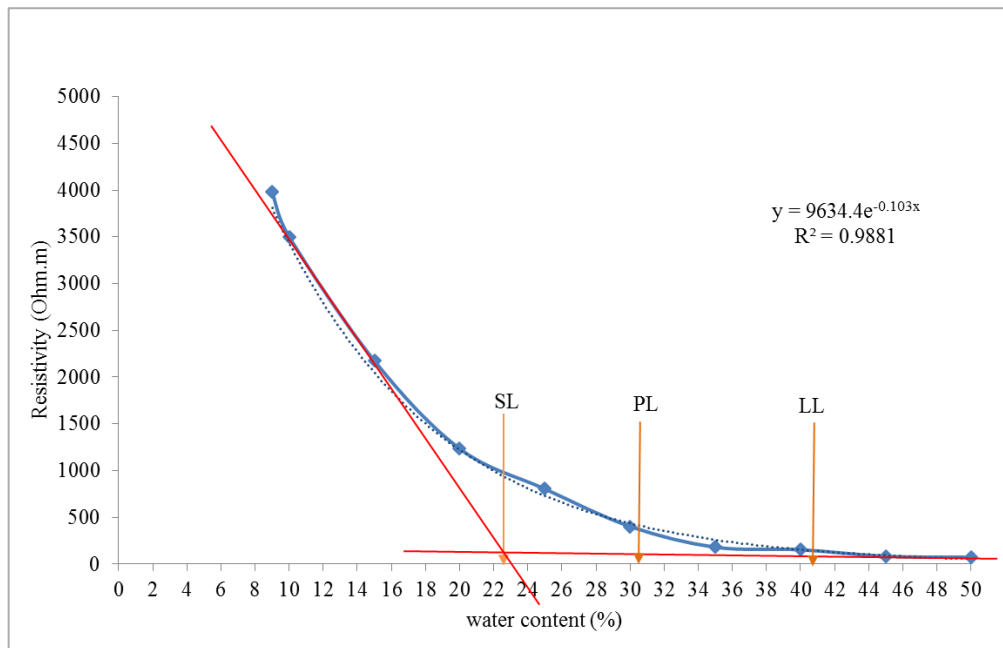


Figure 7.5 Resistivity-moisture content profile for soil sample S2

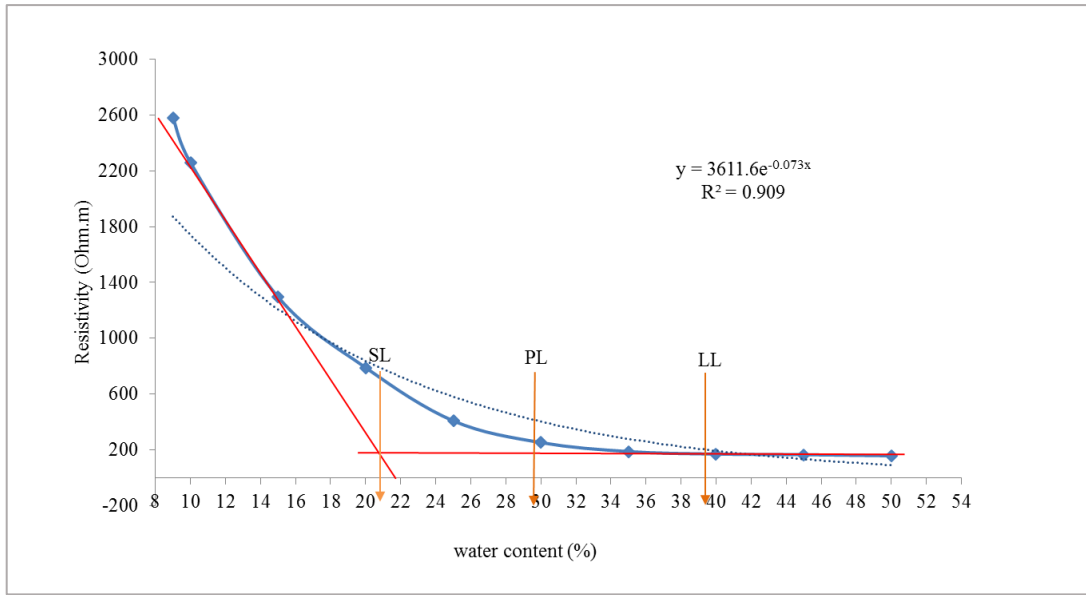


Figure 7.6 Resistivity-moisture content profile for soil sample S3

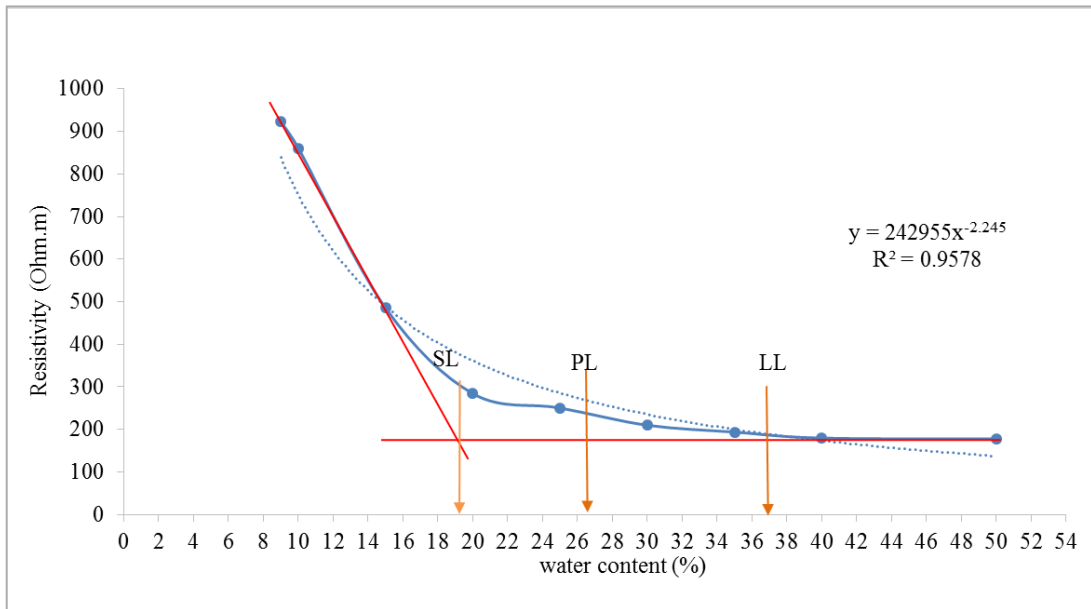


Figure 7.7 Resistivity-moisture content profile for soil sample S4

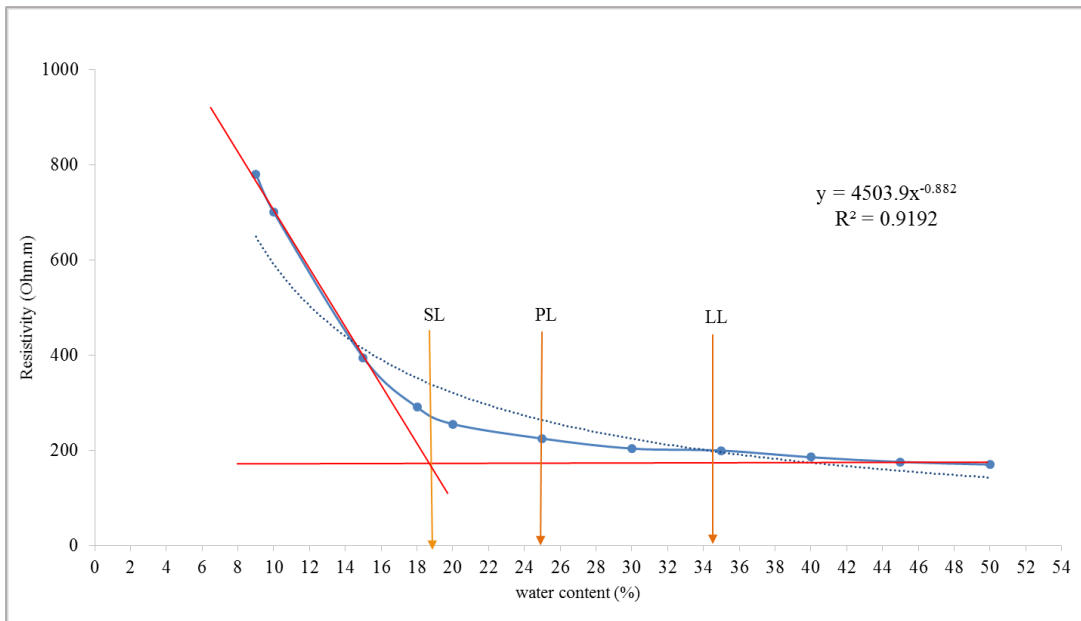


Figure 7.8 Resistivity-moisture content profile for soil sample S5

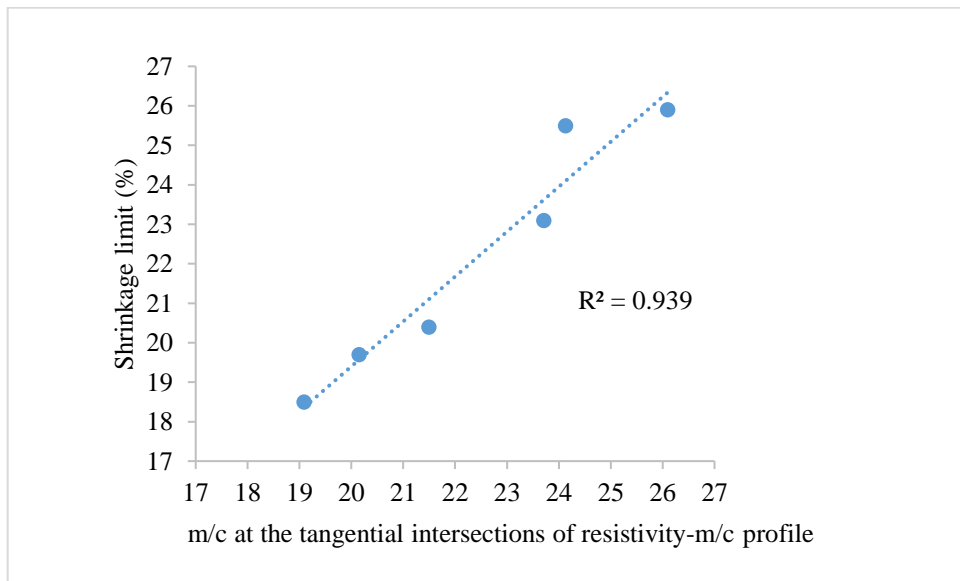


Figure 7.9 Comparison of Shrinkage limits of soil samples obtained from traditional shrinkage limit test and moisture content value at the tangential intersection on resistivity-water content profiles

From the Figs. 7.3 to 7.8, it is observed that when the soil change from the unsaturated state to saturated state, the phase where the soil is just saturated, can be demarcated by tangential intersection i. e. by projecting the straight line portion of the unsaturated phase downwards and projecting the straight line portion of the saturated



phase backwards. The water content (%) corresponding to the point of intersection of these lines is compared with “Shrinkage limit” of the soil and there is a very good comparison (Fig. 7.9). Thus the tangential intersection value of the moisture content of a **well compacted soil** in the electrical resistivity box, can be considered as a good estimate of the shrinkage limit of the soil. Well compacted soil here represents the state wherein the soil particles are optimally packed and there is no possibility of further reduction in the volume of voids, and thereby in the volume of the soil mass. In conclusion, ER measurements on soil samples can be used for a quick assessment of the shrinkage limit of soils.

### **7.3 Electrical resistivity- moisture content studies on Phosphoric acid contaminated Shedi soil and Bentonite blended Shedi soil**

In this section, electrical resistivity studies conducted on acid contaminated shedi soil, bentonite blended shedi soil are discussed. The determination of Shrinkage Limit (the point where soil is just saturated) from the graphical method proposed is validated with this study.

Both laboratory as well as resistivity studies, are conducted on all the samples. Orthophosphoric acid is mixed with shedi soil in four different normalities (2.5 N, 5 N, 7.5 N, and 10 N). It is observed that at some point shrinkage limit is even higher than the plastic limit. Electrical resistivity studies on the samples also give the same results. Bentonite mixed with shedi soil in varying proportions (20%, 40%, 60%, and 80%) and pure bentonite are tested for index properties. With the addition of bentonite, Atterberg limits of bentonite mixed shedi soil samples show a gradual variation. Shrinkage limit found out using electrical resistivity studies are in good agreement with that of laboratory values. Due to high shrinking property of bentonite, it is very difficult to find out the volume after shrinkage and hence laboratory determination shrinkage limit is very difficult. For such cases, we can suggest electrical resistivity method as a fast and accurate method for shrinkage limit determination.

#### **7.3.1 Is Shrinkage limit the lowest limit?**

There is no doubt that liquid limit is always the largest of the Atterberg limits. However many questions are being raised, for quite sometime now, about the plastic

limit vis-a-vis the shrinkage limit. Nitterberg (1982) based on his work observed that the shrinkage limit of calcretes to be often higher than the plastic limit, as high as 9%. Nagaraj and Srinivasamurthy (1987) concluded from their research work that for some soils, the shrinkage limit is more than the plastic limit and this (anomalous) behaviour has been attributed to soil fabric (Gayathri 2006). Sridharan and Prakash (1998) have proved that the plastic limit of some soils and that of some other soils contaminated with certain chemicals/ pollutants/ effluents can be lower than shrinkage limit. Findings of all such studies means that soil at plastic limit need not always be fully saturated.

In this study, this anomalous behaviour of Atterberg limit in certain soils, such as phosphoric acid contaminated lithomargic clay (shedi soil) and bentonite blended lithomargic clay is examined. The method of shrinkage limit determination from resistivity-moisture content profile is verified and confirmed with the resistivity-moisture content studies on acid contaminated and bentonite blended shedi soil.

### **7.3.2 Materials used**

#### **7.3.2.1 Shedi Soil**

Shedi soil is the local name given to the lithomargic soil which is locally available. The top layers of laterite formations are highly porous but strong and hard. Shedi soil actually lies in between top hardened layers and bottom residual layers. The soil gets dissolved and flows when comes into contact with water, hence cause subsequent settlement. Low permeability and poor drainage are the major causes of the problems encountered during constructions in lithomargic clay. Water may lead to wash off fine lithomargic clay, creates cavities and may even cause subsidence and sliding. Pockets of white kaolinitic clays are also visible. This soil is very soft with some occasional pieces of iron-rich hematite material and found in varieties of colours such as red, purple, yellow, cream etc. This soil is essentially composed of fine-grained microcrystalline aggregates of clay minerals along with the varying proportion of goethite and limonite. Usually, shedi soil possesses moderately good strength under dry condition but when comes into contact with water, its strength reduces drastically and starts flowing like water.

The collected soil was kept for air drying for 24 hrs. After air drying, these soil samples were sieved through 425  $\mu\text{m}$  and kept in the oven for 24 hrs. This oven dried soil was used for various tests as per the procedures mentioned in IS codes.

### **7.3.2.2 Bentonite**

Due to lack of availability of good and low permeability clays locally, the locally available silty soil (lithomargic clays) are blended with bentonite to satisfy the requirements or specifications of clay liners in landfill sites. Bentonite is a highly colloidal and plastic clay composed mainly of montmorillonite and is also mixed with other related minerals like nontronite, and beidellite. It was named after Fort Benton, the locality where it was found. It is actually a clay based industrial material. It is a mixture of minerals. Coming to the structure, bentonite is generally composed of 3 layered aluminosilicates with molecular water in between these layers. For natural Sodium bentonite, exchangeable sodium cations are predominant rather than any other cations. For Calcium bentonite, calcium ions are predominant. Out of all, sodium bentonite has high swelling and gelling properties along with good viscosity and liquid limit.

Bentonites were formed by mechanical and chemical weathering of parent rock such as volcanic tuffs and tuffities, rhyolites, basalts, etc. in the alkaline environment. Most of the bentonite deposits in India are of natural sodium bentonite with higher iron content, which gives them the darker colour. Due to very fine particle size, this bentonite shows extraordinary swelling nature and bonding powers.

Bentonite is widely used for applications like drilling, effluent treatment, electrical engineering, fertilizer, foundry, pesticides, pharmaceutical, iron ore pelletization etc.

### **7.3.2.3 Phosphoric Acid**

Soils in industrial area are likely to be contaminated by effluents such as phosphoric acid. The chemical formula of phosphoric acid is  $\text{H}_3\text{PO}_4$ . Orthophosphoric acid is used in the present study. Its specific gravity is 1.83 at 18°C, which is having solubility in alcohol and water. Orthophosphoric acid is widely used in the fertilizer

industry, dentistry, sugar and textile industry, food processing industry etc. It is used in detergents and in cleaning and rust proofing agents.

### **7.3.3 Sample Preparation**

In this study, phosphoric acid has been mixed at various normalities such as 2.5N, 5N, 7.5N, and 10N with shedi soil into a soft and easily mouldable state. The samples are designated as C1, C2, C3 and C4. Acid is added along with water at particular OMC to soil. Because of the soapy nature of acid, it formed the balls of varying size. These balls are pulverized and kept in plastic containers to cure for ten days before testing. For the second set of experiments, samples were prepared by blending shedi soil with 0%, 20%, 40%, 60%, 80% and 100% bentonite.

### **7.3.4 Tests conducted**

Shedi soil was sieved through 425 $\mu$ m sieve and the following tests were conducted:

- Specific gravity as per IS:2720 (Part 3)-1980
- The liquid limit test was according to the Casagrande method as per IS: 2720 (Part 5)-1985. In one case where this method could not be conducted, the cone penetration method was adopted (British Standard Methods of Test for Soil for Engineering Purposes. Part 2: Classification Tests: BS: 1377--Part 2, 1990).
- Plastic limit test according to conventional 3 mm thread method as per IS:2720 (Part 5)-1985
- Shrinkage limit test as per IS 2720 (Part 6)- 1972
- Grain size distribution by sieve analysis and hydrometer analysis as per IS:2720 (Part 4)-1985
- pH as per IS : 2720 (Part 26) - 1987
- Compaction test as per IS: 2720 (Part 7) – 1980
- Scanning Electron Microscope (SEM)
- XRD

- Electrical resistivity measurement

#### 7.3.4.1 Specific gravity test

The specific gravity of solid particles is the ratio of the mass density of solids to that of water. Specific gravity value of a soil helps for determination of void ratio and particle size. The test follows as per IS: 2720(part 3/section1)-1974. During the experiment, extra care must be taken for expelling entrapped air.

#### 7.3.4.2 Atterberg Limits

Liquid limit of a soil is the water content at which it behaves practically like a liquid but has small shear strength. Liquid limits of soil samples were determined using Casagrande's apparatus (Fig. 10(a)) as per IS: 2720 (part 5) – 1985. But for bentonite clay mixes the cone penetration method (Fig. 10(b)) was adopted (British Standard Methods of Test for Soil for Engineering Purposes. Part 2: Classification Tests: BS: 1377--Part 2, 1990).



Figure 7.10(a) Cone penetration method and (b) Casagrande's apparatus

Plastic limit is the water content below which it ceases to be plastic (begins to crumble when rolled into threads of 3 mm diameter. Testing was carried out as per IS: 2720 (Part 5)-1970.

Shrinkage limit is the water content at which all the pores are just fully filled with water and the soil is just fully saturated. There is no volume reduction below shrinkage

limit. Tests were carried out as per IS 2720 (Part 6) - 1972. While doing the experiments care has been taken to avoid entrapped air by thoroughly compacting the specimen. Crack formation was prevented by allowing the soil to dry in air followed by oven drying to a constant mass. For bentonite mixed samples 15 – 20 days of air drying is required to avoid the breaking of pats.

#### **7.3.4.3 pH**

pH of the soil mixes has been found out by pH meter 20g of air dried sample was taken and mixed with 50 ml of distilled water; stirred well and kept for an hour. Just before testing the mix shall be again stirred well and take the reading by inserting pH meter. Experimental procedure follows as per IS: 2720 (part 26) – 1987.

#### **7.3.4.4 Compaction**

Standard Proctor's mould with internal diameter 10 cm and height 11.7 cm was used for compacting the soil. The procedure follows as per IS 2720 (part 7) – 1980. Samples were oven dried before starting the compaction. Results of dry densities versus moisture content were plotted to find the maximum dry densities and optimum moisture contents for each sample.

#### **7.3.4.5 Grain size distribution**

The soil used in the present study is shedi soil passing through 425 $\mu$ m. Grading of the sample and its blends were examined by conducting dry sieve analysis, wet sieving and hydrometer analysis as per IS: 2720 (part 4) – 1985. Hydrometer analysis was carried out with sodium hexametaphosphate as a dispersing agent for uncontaminated soil samples. For contaminated soils dispersing agent is not used to avoid further chemical reactions. Contaminated soils found to settle early compared to the pure soil sample, which indicates the particle growth. It was found that the contaminated soil samples settled early even when the dispersing agent is added to it. Settling of soil solids in hydrometer just after mixing and one hour later are shown in Fig. 7.11.



Figure 7.11 Hydrometer test for contaminated soil (a) just after mixing (b) one hour later

#### **7.3.4.6 Scanning Electron Microscope (SEM)**

It is a valuable tool for the study of soils, using which distances less than  $100 \text{ \AA}$  can be resolved. Thus small clay particles can be analysed. The electron beam is used for the examination. Secondary electrons emitted from a sample surface form what appear to be three-dimensional images. SEM has a magnification range of  $\times 20$  to  $\times 150,000$  and a depth of field some 300 times greater than that of a light microscope. These features led to extensive use of SEM for analysis of clays. Sample preparation included mounting samples on carbon double-stick tape on aluminium stubs. The samples were then coated with gold sputter coater. First, the entire surface is scanned under low magnification and then, the chosen areas are magnified to get the clear picture of the micro fabric arrangement.

For the present study a scanning electron microscope JSM – 840A JEOL, JAPAN was used (Fig. 7.12). A small amount of oven dried finely powdered sample is mounted on to the tape glued to the SEM stub and sputter coated with gold prior to scanning.



Figure 7.12 SEM equipment

#### **7.3.4.7 X-Ray Diffraction Analysis**

X-ray diffraction is now a common technique for the study of crystal structures and atomic spacing. X-ray diffraction is based on constructive interference of monochromatic X-rays and a crystalline sample. These X-rays are generated by a cathode ray tube, filtered to produce monochromatic radiation, collimated to concentrate, and directed toward the sample. The interaction of the incident rays with the sample produces constructive interference (and a diffracted ray) when conditions satisfy Bragg's Law ( $n\lambda=2d \sin \theta$ ). This law relates the wavelength of electromagnetic radiation to the diffraction angle and the lattice spacing in a crystalline sample. These diffracted X-rays are then detected, processed and counted. By scanning the sample through a range of  $2\theta$  angles, all possible diffraction directions of the lattice should be attained due to the random orientation of the powdered material. Conversion of the diffraction peaks to d-spacings allows identification of the mineral because each mineral has a set of unique d-spacings. Typically, this is achieved by comparison of d-spacings with standard reference patterns.

### **7.3.5 Results and Discussions on studies on Phosphoric acid contaminated shedi soil**

#### **7.3.5.1 Results of X-Ray Diffraction Analysis**

X – ray diffraction studies of shedi soil (Fig. 7.13) were carried out using the Cu  $K\alpha$  radiation source (background) and peaks were obtained corresponding to kaolinite



(Aluminium Silicate Hydroxide) with JCPDS reference code 01-089-6538 and smectite group mineral saponite (Magnesium Aluminium Silicate Hydroxide Hydrate) with JCPDS reference code 00-013-0086. Kaolinite mineral shows its characteristic peaks at  $7.16 \text{ \AA}$ ,  $3.57 \text{ \AA}$ ,  $2.5 \text{ \AA}$ , indicating 1:1 (1 silica sheet and 1 alumina sheet), whereas Saponite at  $14.2 \text{ \AA}$ ,  $1.54 \text{ \AA}$ .

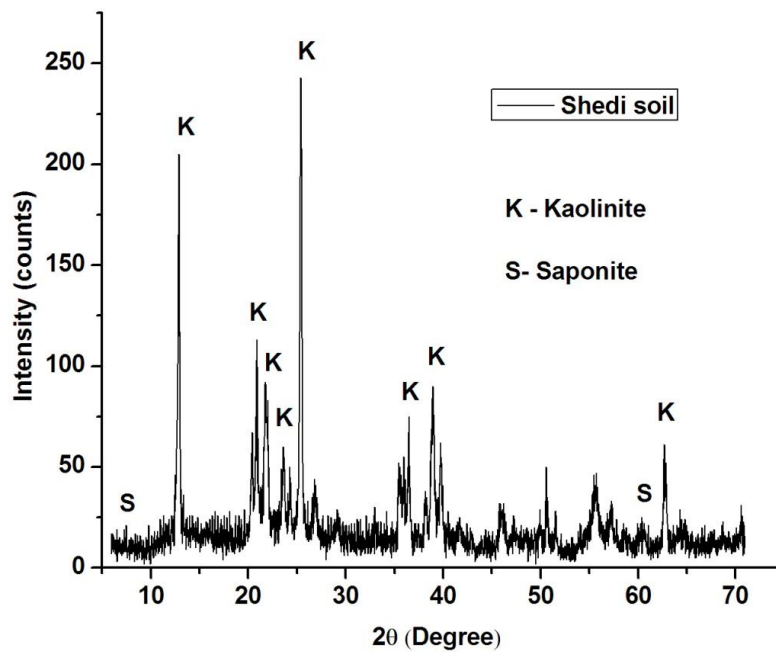


Figure 7.13 X – ray diffraction pattern for shedi soil with minerals Kaolinite -  $\text{Al}_2(\text{Si}_2\text{O}_5)(\text{OH})_4$  and Saponite -  $\text{Mg}_3(\text{Si Al})_4\text{O}_{10}(\text{OH})_2 \cdot 4\text{H}_2\text{O}$

### 7.3.5.2 Effect of phosphoric acid contamination on basic geotechnical properties

Table 7.2 Index properties of shedi soil contaminated with phosphoric acid

Acid Normality		0	2.5	5	7.5	10
Liquid limit (%)		55.0	41.6	35.5	27.8	20.4
Plastic limit (%)		32.1	26.8	19.7	16.5	12.2
Shrinkage	Lab result	29.2	22.6	17.1	16.5	15.0

Limit (%)	From resistivity measurement	29.0	22.1	17.9	16.9	15.0
Plasticity index		22.9	9.5	7.8	7.5	7.4
pH		4.30	2.30	2.23	2.20	2.17
Specific gravity (G)		2.51	2.49	2.43	2.42	2.34
Void ratio (e)		0.73	0.62	0.55	0.53	0.44
Optimum moisture content (%)		26.0	24.4	20.5	21.0	18.5
Maximum dry density (g/cc)		1.46	1.54	1.57	1.59	1.59

When phosphoric acid is added to shedi soil, kaolinite and smectite minerals present in the shedi soil undergo several chemical changes, which alter the geotechnical properties of the soil, which is shown in Table 7.2. Addition of phosphoric acid leads to breaking of the hydrogen bonding present in kaolinite mineral and causes an increase in water holding capacity. Hydroxyl ions get replaced by phosphate. But it acts in a different manner for smectite mineral. By the addition of phosphoric acid, unit layers of smectite get linked together and effective surface area reduces. Thus water holding capacity decreases. (Sivapullaiah, 2015).

It is seen that the liquid limit and plasticity index decrease with increase in the amount of phosphoric acid (Fig. 7.14). The plasticity index decreases with the increase in the percentage of acid content indicating the growth of particle size from clay size to silt. The soil changes from highly plastic (natural sample) to medium plastic. Water can be held tighter in small pores than in large ones, so fine soils can hold more water than coarse soils. Liquid limit goes on decreasing because of decrease in water holding capacity by the linking of unit layers of smectite mineral by phosphate adsorption.

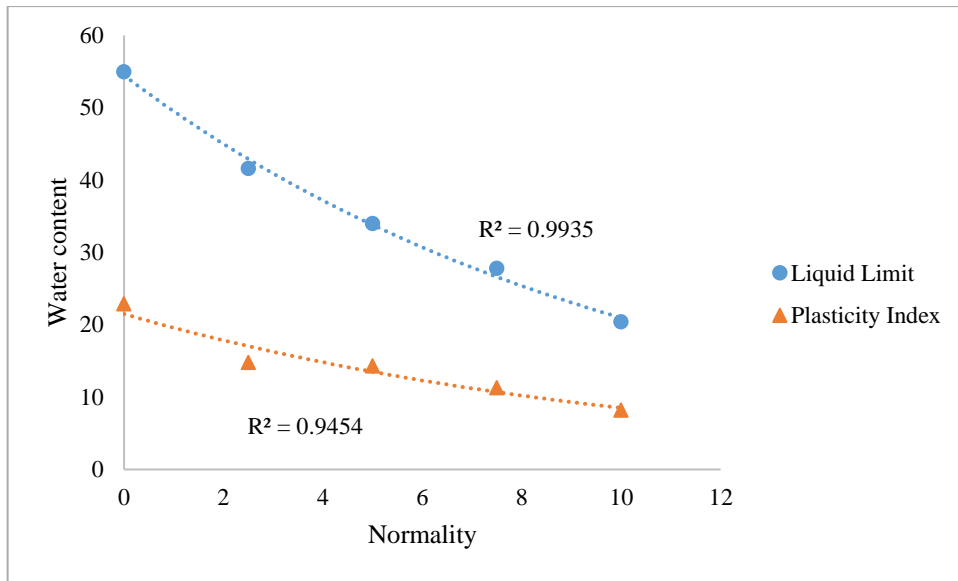


Figure 7.14 Variation of liquid limit and plasticity index with acid normality

It can be seen from Fig. 7.15 that specific gravity reduces with increase in acid concentration. This may be due to lower specific gravity of acid (1.834). Also we can say that due to particle growth, void ratio decreases and hence volume of soil solids will be more. This will lead to decrease in density of soil solids and hence specific gravity decreases.

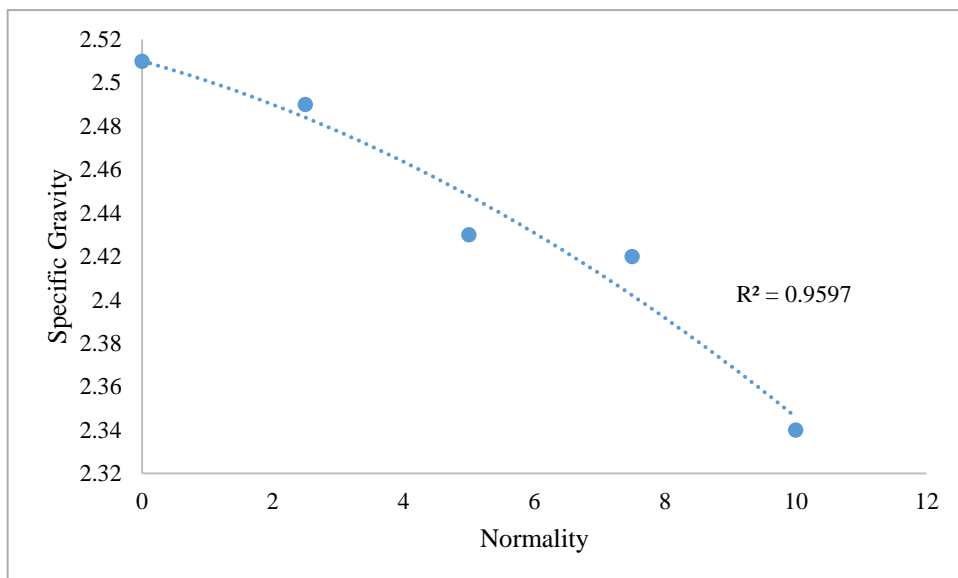


Figure 7.15 Variation of specific gravity with acid normality

From Table 7.2, it can be seen that pH of the soil is relatively low. On addition of phosphoric acid, this gets reduced further as seen from Fig. 7.16. It can be seen that this decrease is negligible after 1N.

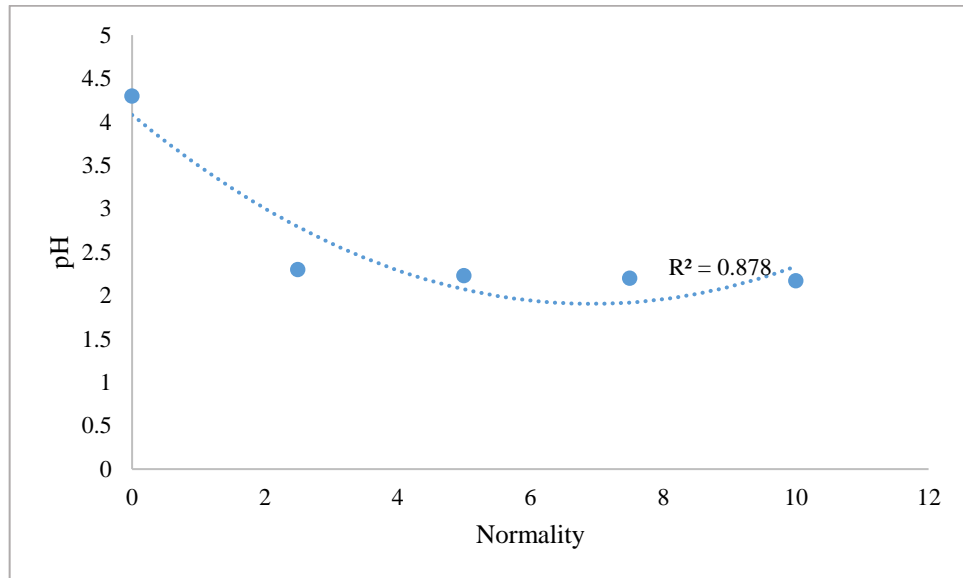


Figure 7.16 Variation of pH with acid normality

Gradation curve of contaminated soils (Fig. 7.17) shows that soil changes from well graded to poorly graded. Particle size increases in the presence of phosphate. Clay content almost disappears and particle growth occurs as a result of the phosphoric acid reaction. As the acid normality increases the curve shifts more towards right indicating an increase in the size of particles.

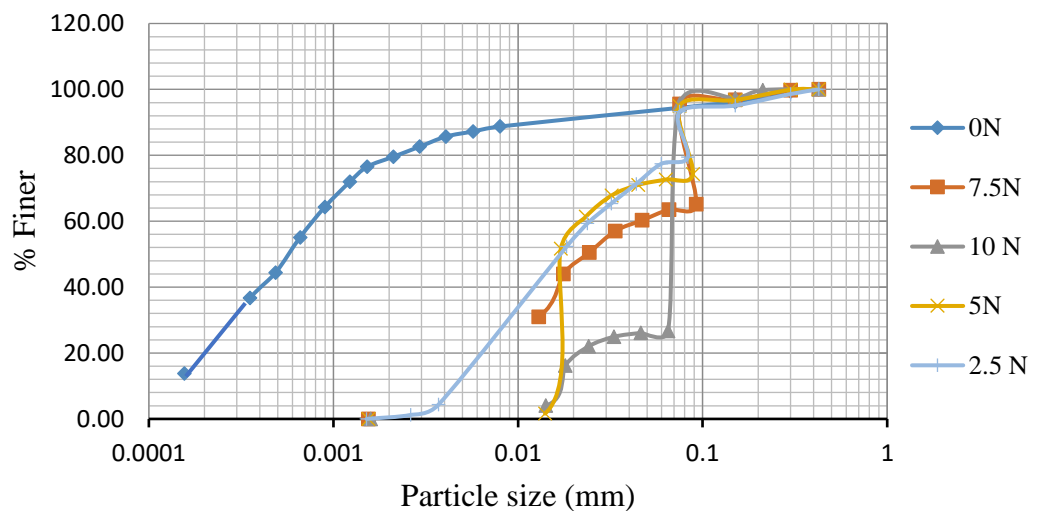


Figure 7.17 Combined grain size distribution curve for contaminated soils

From Table 7.3 it can be seen that pure shedi soil with  $PI > 17$  is primarily clayey in nature. But with the addition of acid, PI gets reduced and soil becomes medium plastic in nature with clayey silt gradation. From this, we can understand that particle growth occurs and the plasticity gets reduced.

Table 7.3 Plasticity index and soil properties

<b>Ip</b>	<b>Plasticity</b>	<b>Soil Properties</b>
0	Non plastic	Sand
<7	Low plasticity	Silt
7 – 17	Medium plasticity	Silty clay
>17	High plasticity	Clay

Shrinkage and plastic limits get decreased as the acid content increases (Fig. 7.18). this may be due to reduction of water content present in voids due to decrease in pore volume.

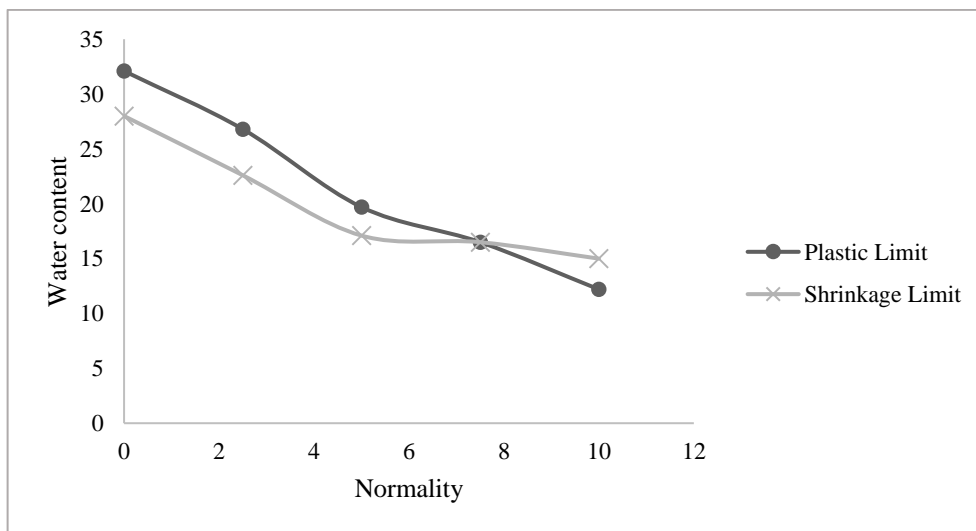


Figure 7.18 Shrinkage limit and Plastic Limit v/s acid normality curve

It is interesting to see that the shrinkage limit of the contaminated soil is even higher than the plastic limit for soil with 10N phosphoric acid. An optimal packing of soil particles gives the lowest shrinkage limit. In other words, the shrinkage limit is basically a result of the packing phenomenon and a function of relative grain-size

distribution. (Sridharan and Prakash 1998). Since the amount of fines gets reduced by the addition of acid, the soil becomes poorly graded (Fig. 7.17) which will in turn reduce the effective packing and the shrinkage limit attains a higher value than the plastic limit.

Light compaction test was conducted on contaminated soil samples. Compaction characteristics such as maximum dry density ( $\gamma_{d\ max}$ ) and optimum moisture content (OMC) were determined.

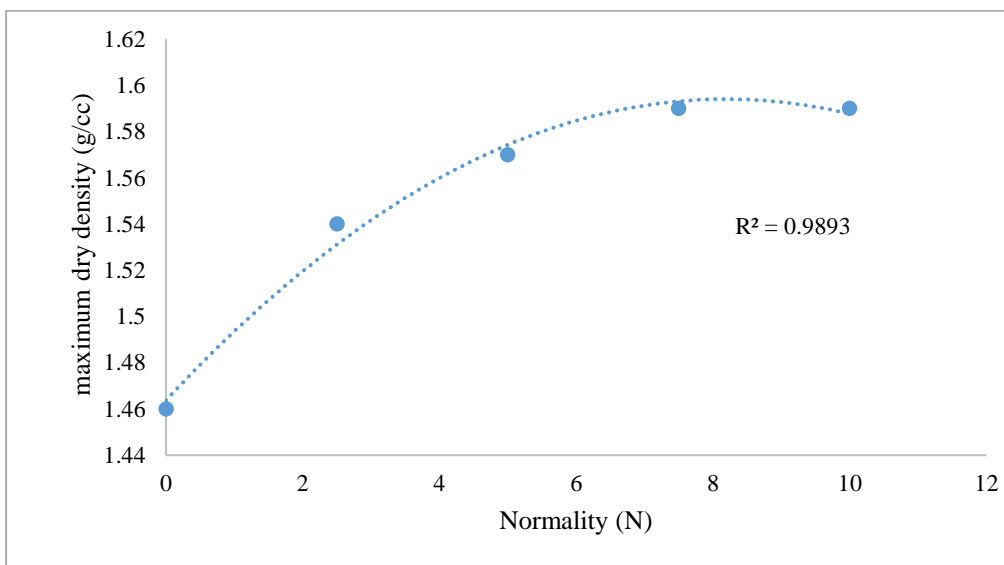


Figure 7.19 Acid normality Vs dry density

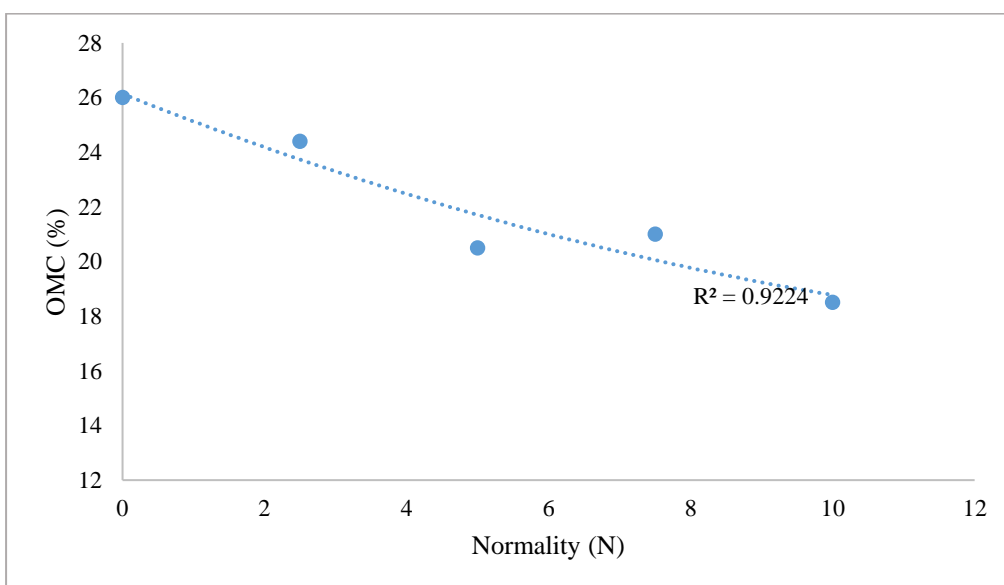


Figure 7.20 Acid normality v/s OMC

Maximum dry density and optimum moisture content varies from 1.46 g/cc and 26 % for pure shedi soil to 1.59 g/cc and 18.5 % for soil contaminated with 10 N acid. The results are plotted with varying acid normality as shown in Fig. 7.19 and Fig 7.20.

With the increase in addition of phosphoric acid, maximum dry density increases (Fig.7.19) and OMC decreases (Fig. 7.20). This may be due to the reduction in water holding capacity as a result of the dominating effect of phosphate linking of smectite particles over the effect of phosphate adsorption on kaolinite. Due to increase in particle growth, weight of solids per unit volume (dry density) increases.

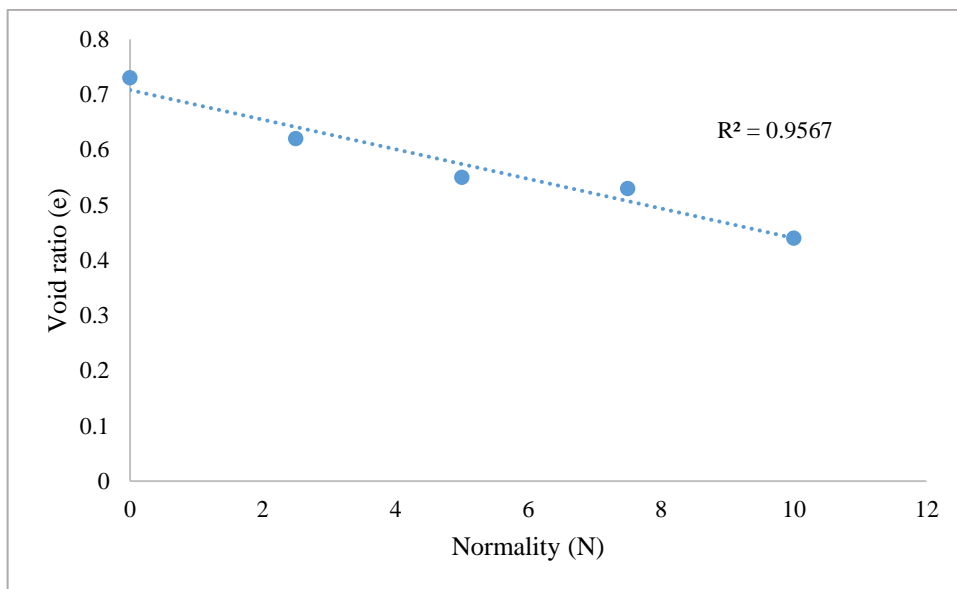


Figure 7.21 Acid normality v/s Void ratio

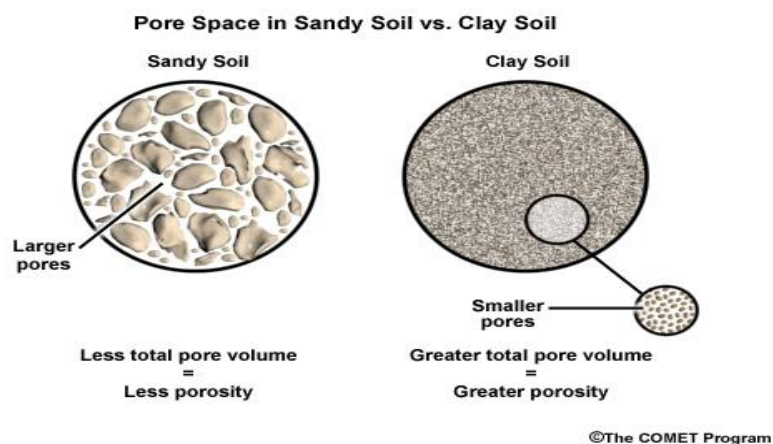


Figure 7.22 Pore space in sandy soil v/s clay soil

Even though the individual void spaces are larger in coarse-grained soil, the void ratio of the fine-grained soil is generally higher than those of coarse-grained soil. The reason is that the fine-grained soil has finely divided particles with repulsive nature in between. These chemical repulsions will not allow the particles to come closer which causes the void ratio of the fine-grained soils to be higher than that of coarse-grained soils. Here as acid normality increases, particle stacked together, and hence void ratio decreases (Fig. 7.21).

Soil Porosity is inversely related to the bulk density. Porosity varies depending on particle size and is greater in clayey soils than in coarse-grained soils. (Fig 7.22). As the electrolytic conduction is partly carried out through interconnected pores of soil, the electrical resistivity of soil also depends on the porosity. At a given water content, as the soil porosity decreases, the resistivity also decreases. Hence as acid normality increases, particle growth occurs, porosity decreases, conduction through interconnected pores occurs. This is one of the reasons for reduced resistivity value with increase in acid content.

### 7.3.5.3 SEM images of Pure and Contaminated Shedi Soil

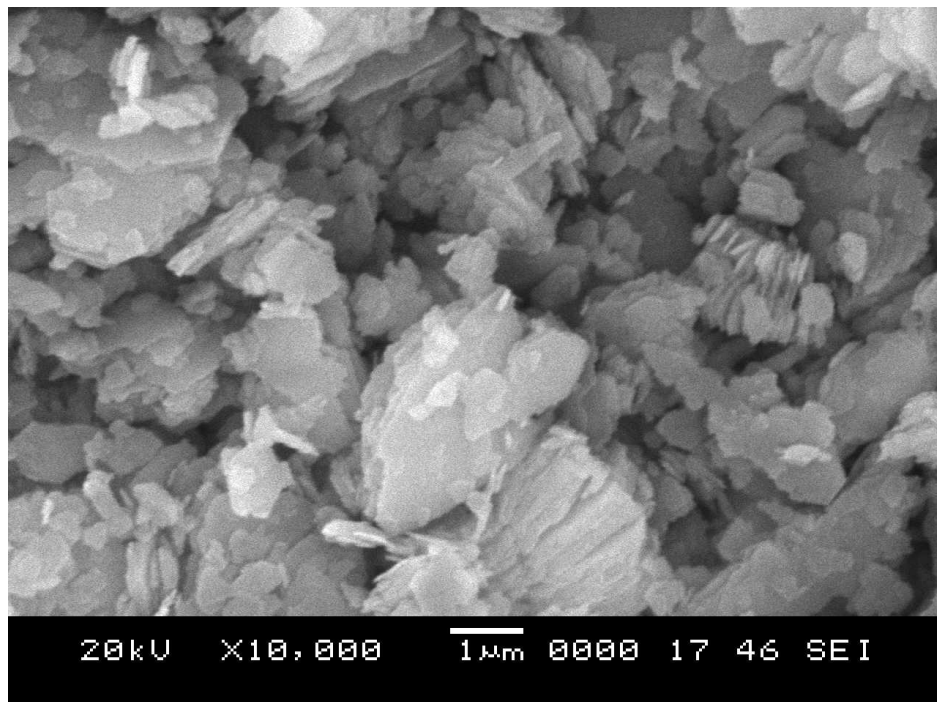


Figure 7.23 SEM image of Pure Shedi soil



Shedi soil is usually composed of kaolinite and the smectite group of minerals. The SEM image of well-crystallized particle of kaolinite looks like six sided plate (Fig. 7.23). Lateral dimensions of the plate are in the order of 0.1 to 0.4 micrometers and their thickness ranges from 0.05 to 2 micrometers (Mitchell and Soga 2005).

They are composed of one tetrahedral sheet linked to an octahedral sheet; therefore they are classified as 1:1 type layer silicates. The platelets of kaolinite are tightly bound together. Kaolinite is a non-expanding mineral; hence it is unable to absorb water into the interlayer position.

As we add acid to the shedi soil, unit layers of smectite minerals get stacked together (Fig. 7.27) and particle growth occurs by phosphate linkage, which reduces the gradation in the soil and consequently the packing.

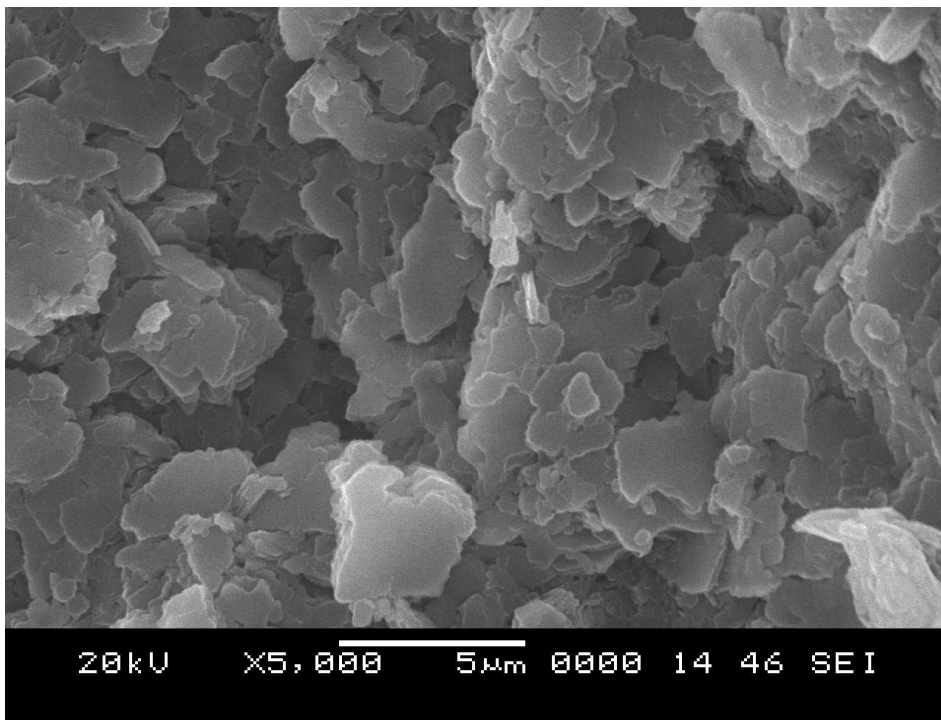


Figure 7.24 SEM image of 2.5 N acid mixed soil

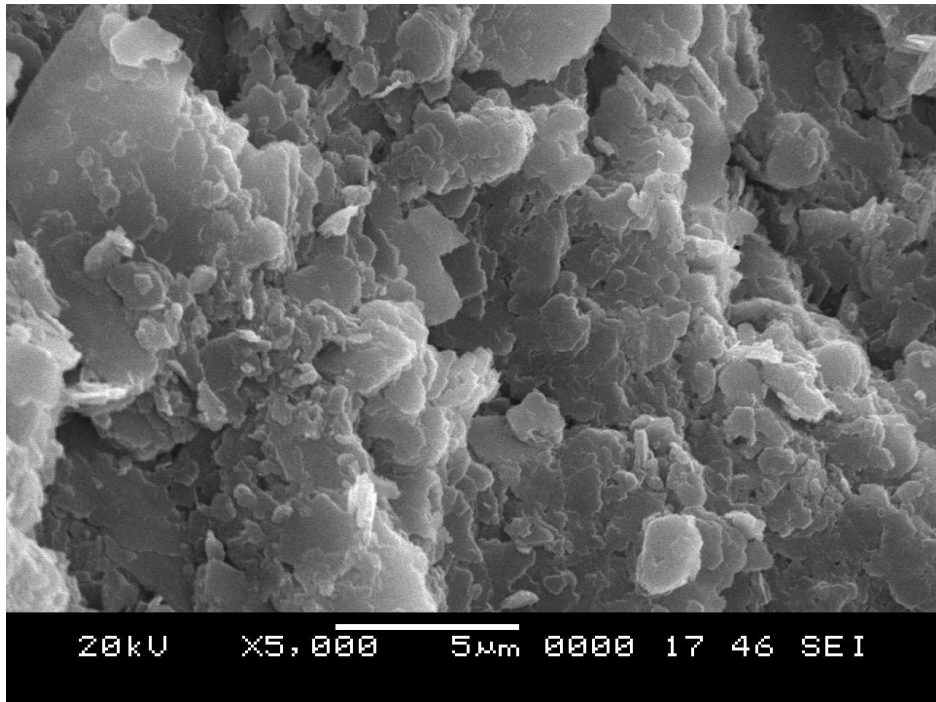


Figure 7.25 SEM image of 5 N acid mixed soil

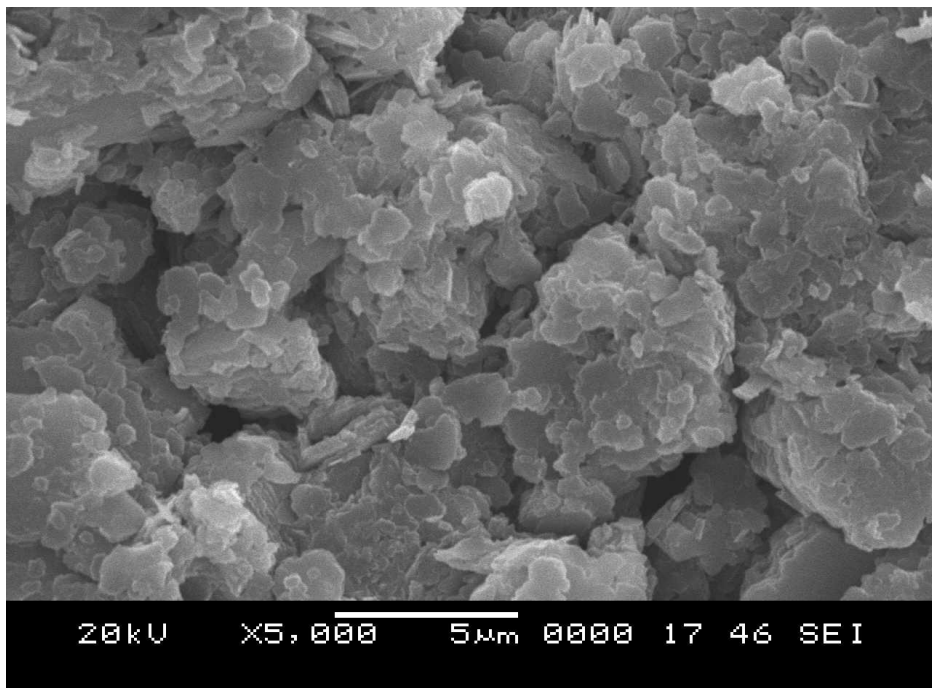


Figure 7.26 SEM image of 7.5 N acid mixed soil

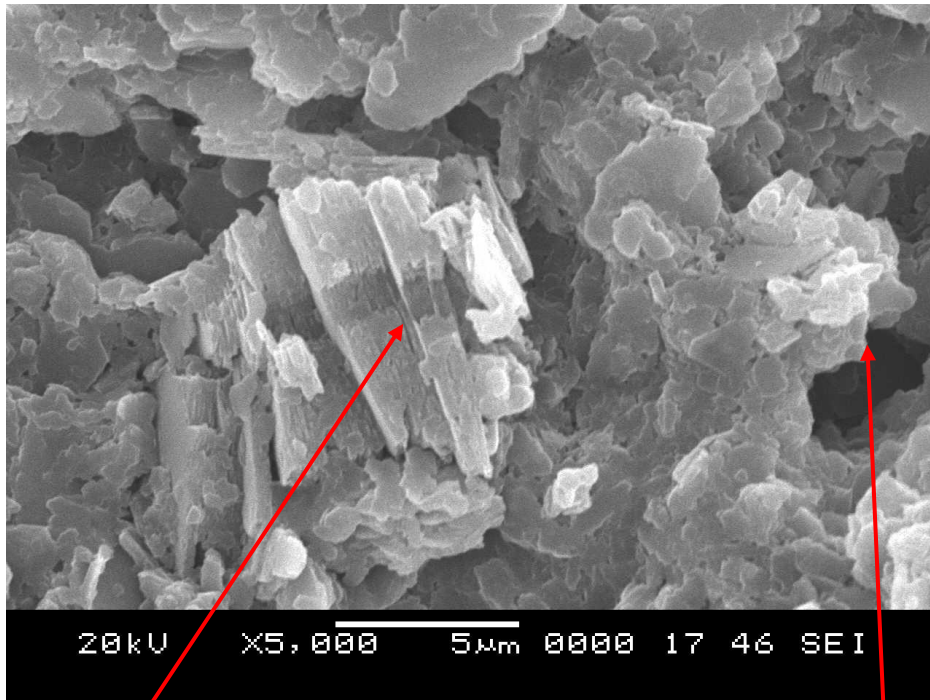


Figure 7.27 SEM image of 10 N acid mixed soil

**Stacking of unit layers**

**Void spaces**

SEM images (Figs. 7.23 to 7.27) gives an idea of the particle growth, which results in poor packing of soil grains, which leads to a higher shrinkage limit, lesser porosity. Figure 7.23 to 7.27 shows the gradual stacking of clay layers with the increase in acid normality. By the addition of 10 N, we can clearly see that individual clay particles stack together to bigger ones and individual void spaces become bigger.

#### **7.3.5.4 Soil Resistivity with Moisture Content**

ER measurements were carried out on contaminated shedi soil samples to find out the correlation between resistivity and geotechnical data.

As water content increases, there is a steep decrease in ER initially (Fig. 7.28). But later the decrease in resistivity is not prominent. Also resistivity values decrease drastically with addition of acid. This can be due to several reasons : (a) Increase in  $H^+$  ion concentration (b) Breaking of chemical bonding (H-bonding) which reduces electrical resistivity (Fukue *et al.* 1999).

The variation of resistivity with moisture content for different normalities of acid contamination are presented in Fig. 7.30 to Fig. 7.34. It is observed that soil resistivity

decreases sharply upto moisture content around 20 – 25%. Also, the resistivity values are found to be almost constant after 35 – 40% water content. This can be due to the continuity of pore water above this water content.

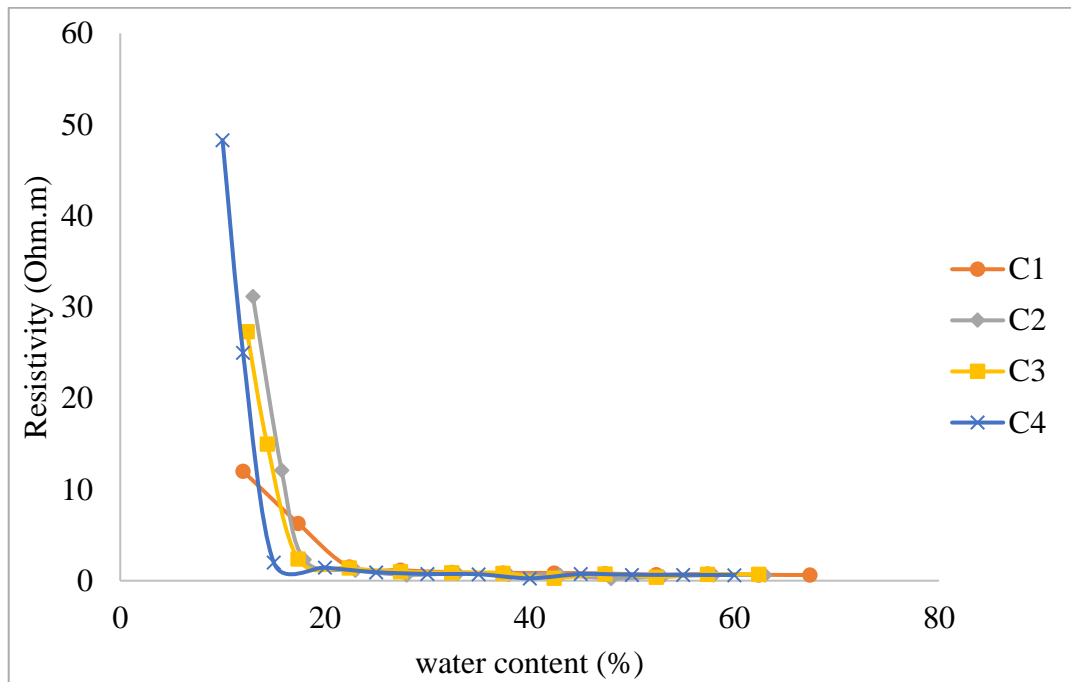


Figure 7.28 Variation of ER with moisture content for various acid normalities

### 7.3.5.5 Shrinkage limit assessment of contaminated soils by electrical resistivity measurements

Due to rapid industrialisation and urbanisation, soils are increasingly getting contaminated with a wide variety of contaminants. Literature reveals that the release of soluble contaminants into the subsurface alter the soil behaviour. It is noted from literature that Atterberg limits are fairly affected by phosphoric acid contamination. As explained before, in the present study, lithomargic clay was treated with, 2.5N, 5N, 7.5N, and 10N phosphoric acid. The treated soils were cured for 10 days and its Atterberg limits were measured. The contaminated soil samples are denoted as C1, C2, C3, C4 respectively. It is noted from the results that, the Atterberg limits of soil decrease continuously with increasing amount of phosphoric acid introduced into the soil. Also, conforming to results of Ramakrishnegowda, (2005), it is seen that for soil, with phosphoric acid of about 10N, the shrinkage limit is higher than the plastic limit. This

is attributed to the growth of smectite minerals in the soil by phosphate linkage, which reduces the amount of fines and hence the gradation in the soil and consequent packing.

This anomalous behaviour can be explained in terms of the grain size distribution. It can be understood from the gradation curve as explained earlier. By analyzing the SEM images we can clearly see the changes that occur in soil grains with the addition of acid.

In order to understand this behaviour of some soils (in which  $SL > PL$ ), let us take into consideration the definition of shrinkage limit. Shrinkage limit can be defined in three ways:

- Shrinkage limit is defined as the maximum water content at which any further reduction in water content will not cause a decrease in the volume of soil mass.
- It can be defined as the water content at which the soil changes from the semi-solid state to solid state.
- It is also be defined as the lowest water content at which the soil can still be completely saturated.

From the above definition, it is clear that the first and third definitions hold good even (make sense) for soils having  $SL > PL$  as the shrinkage limit itself is the limit of shrinking and no further volume reduction takes place and at shrinkage limit soil will be just fully saturated. Soils for which  $PL < SL$ ,  $PL$  lies beyond shrinkage limit (in the non-shrinkage or constant volume range) and such soils at plastic limit state may be partially saturated (Fig. 7.29). Possibly a layer of water covering the soil particles, surrounded by air, [closed water unsaturated soil as defined by Hong-Jing, 2014] is enough to give the soil, the property of malleability or ability to be moulded into thin threads (Holtz et al. 2015). Therefore, shrinkage limit need not necessarily represent the lowest Atterberg limit.

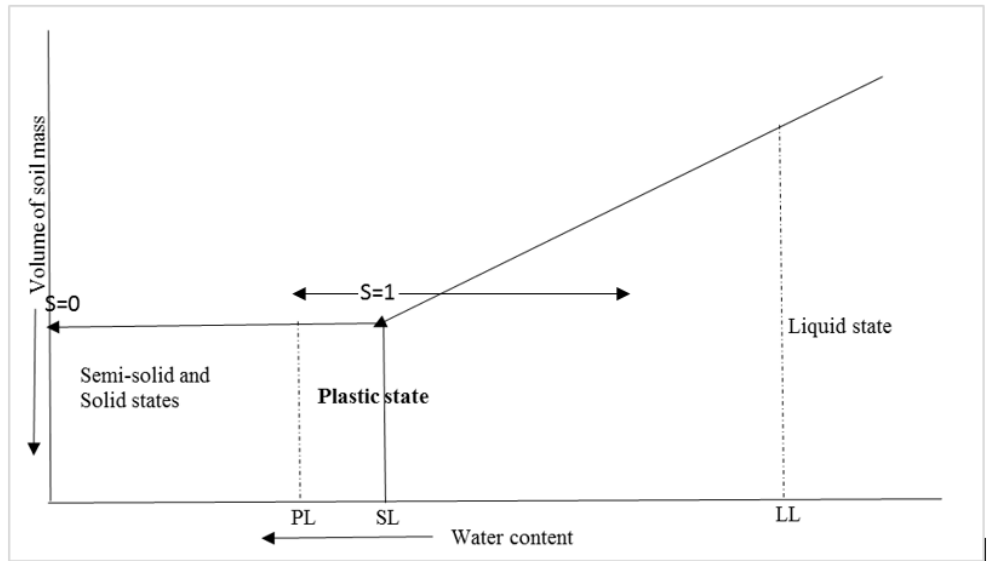


Figure 7.29 Soil could be in a plastic state at its water content equal to shrinkage limit value and soil could be partially saturated at its plastic limit

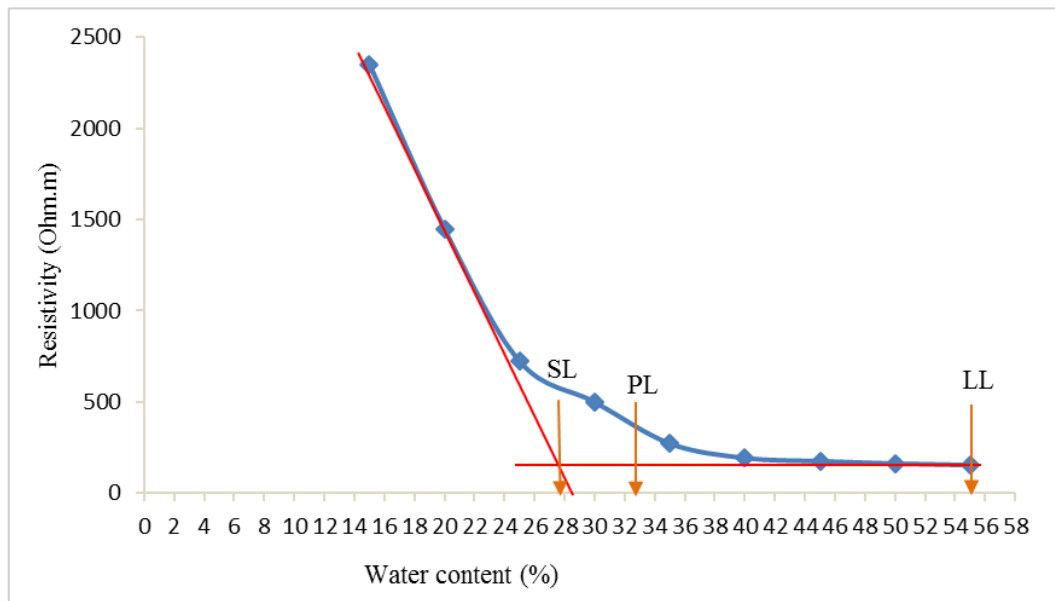


Figure 7.30 Resistivity-moisture content profile for contaminated soil sample C0

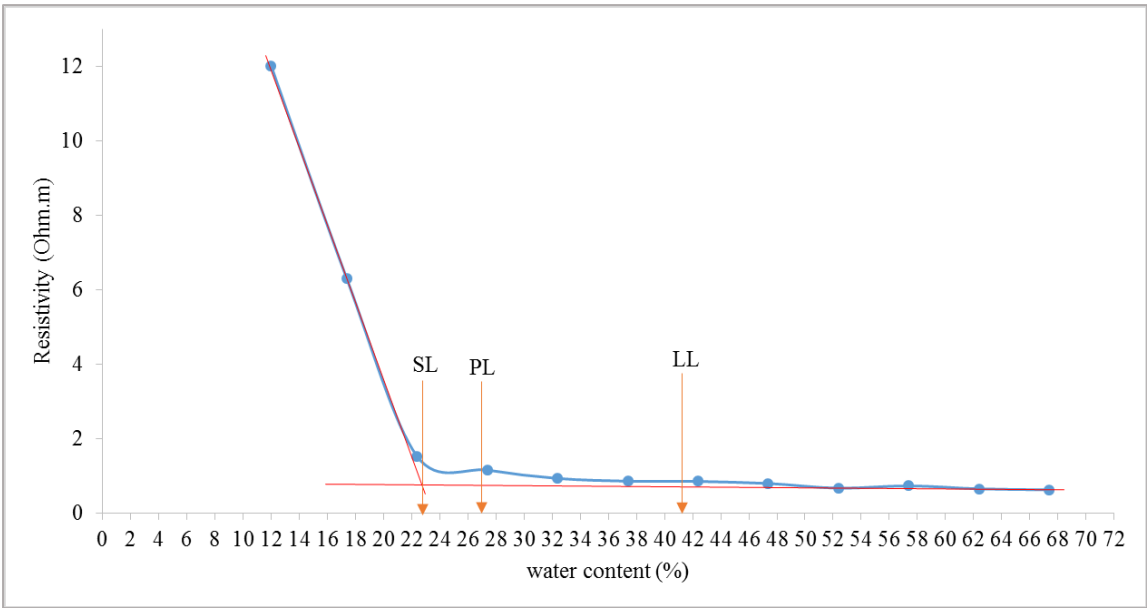


Figure 7.31 Resistivity-moisture content profile for contaminated soil sample C1

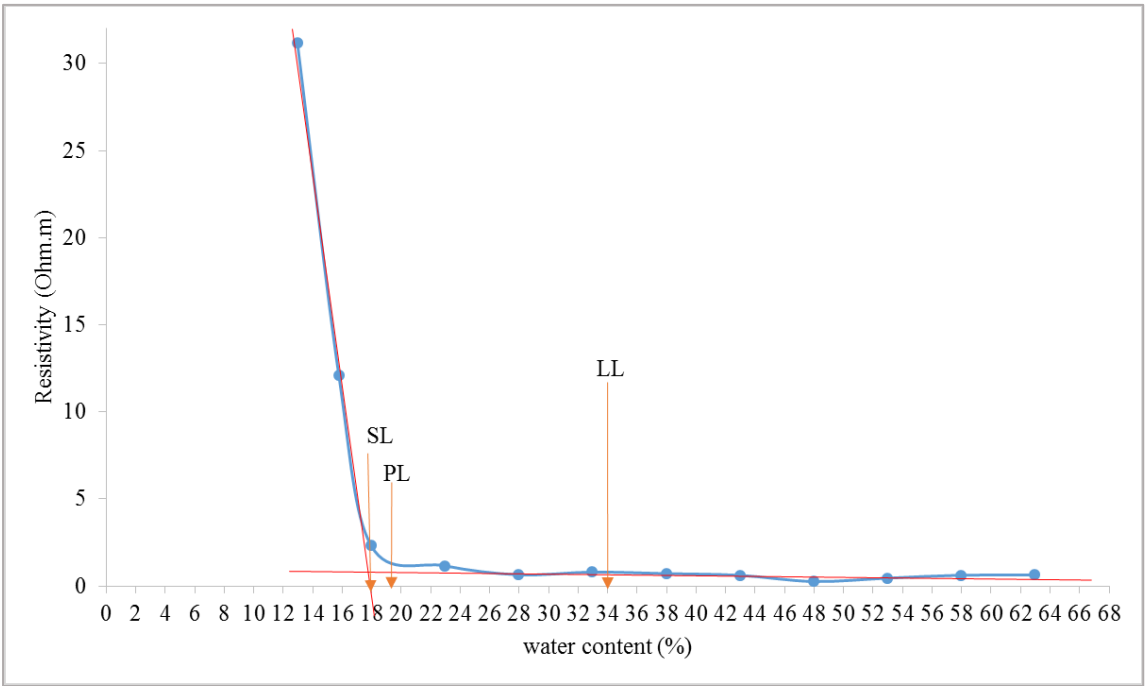


Figure 7.32 Resistivity-moisture content profile for contaminated soil sample C2

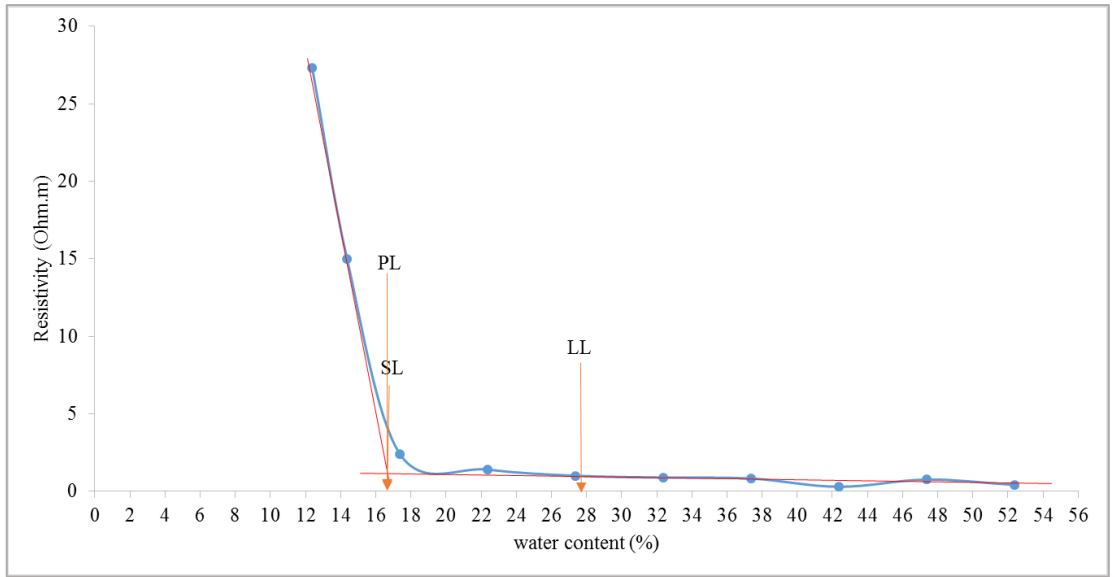


Figure 7.33 Resistivity-moisture content profile for contaminated soil sample C3

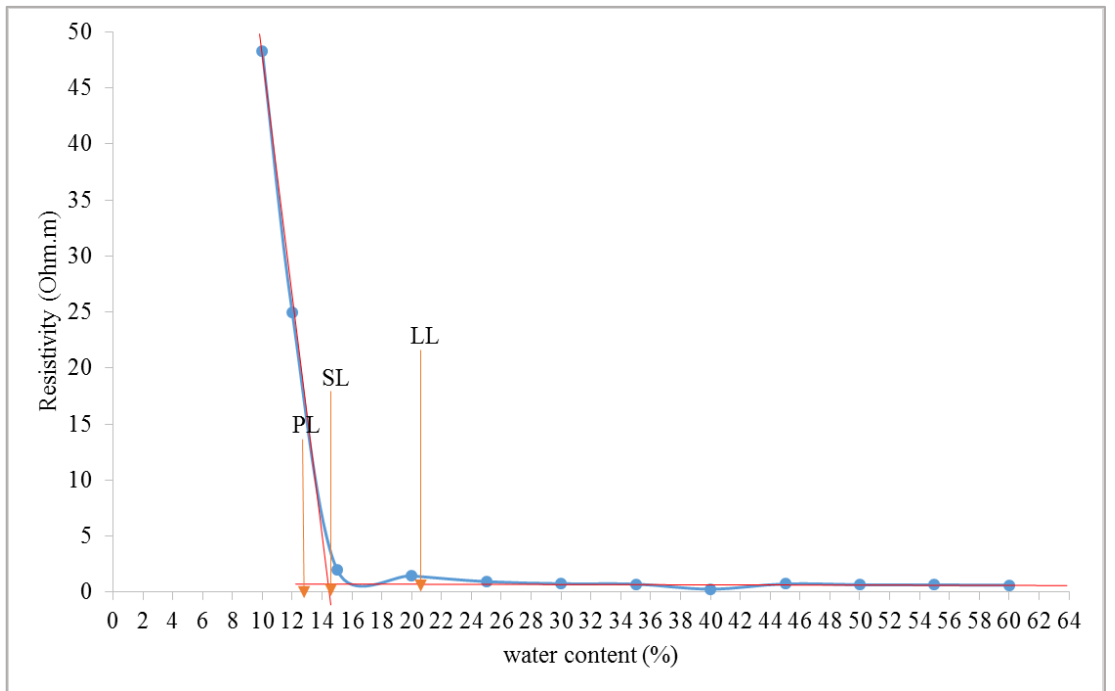


Figure 7.34 Resistivity-moisture content profile for contaminated soil sample C4

Electrical behaviour of the cured contaminated soil was studied. It was observed that even the change in the shrinkage limit of the contaminated soil was clearly captured by resistivity-water content profile. The shift in the shrinkage limits as the normality of



phosphoric acid is increased, has been evidently obtained from the plots (Figs. 7.30 to 7.34). The comparison of the shrinkage limits from the conventional shrinkage limit test (IS:2720(Part 6)-1972) and that from the resistivity-water content profile is given in the Fig. 7.35.

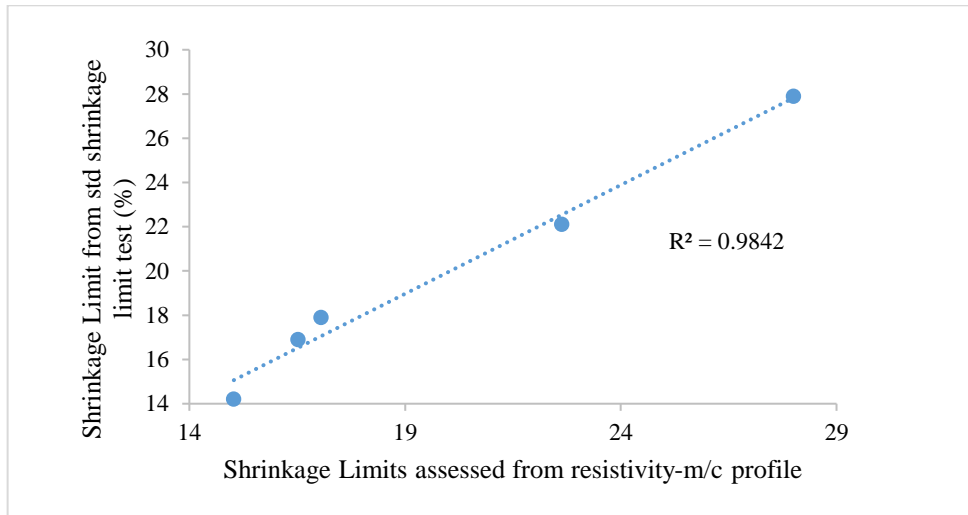


Figure 7.35 Comparison of Shrinkage limits determined from standard shrinkage limit test and assessed from resistivity-water content profiles

From Figure 7.35, it can be seen that lab shrinkage limit and ER shrinkage limit values shows good correlation. The curve between shrinkage limit values obtained from w/c v/s ER graphs shows the same response with the plastic limit as that observed for shrinkage limit (lab values) V/s plastic limit (Fig. 7.36).

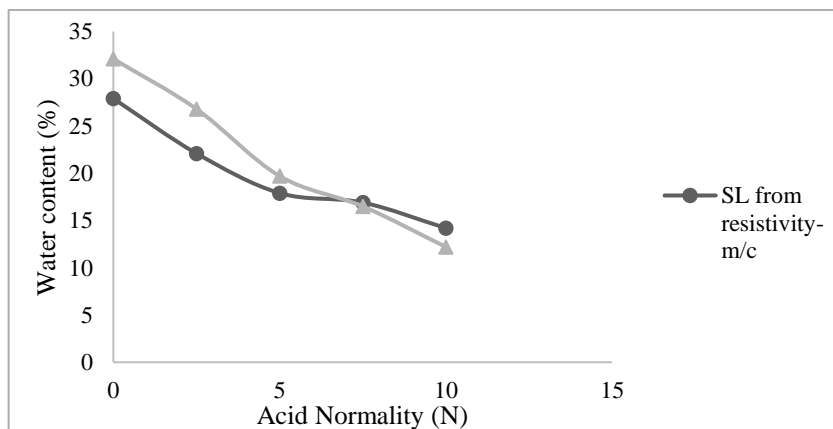


Figure 7.36 Variation of Plastic limit and Shrinkage limit obtained from ER test data

### 7.3.6 Results and Discussions on Bentonite blended shedi soil

#### 7.3.6.1 Basic Properties of Bentonite

Dry platelets of sodium bentonite are most commonly grouped together in a face-to-face arrangement, with exchangeable cations and small amounts of adsorbed wares in an interlayer region between each platelet. Thickness of the interlayer region is variable depending on the amount of water adsorbed between the platelets.

Montmorillonite looks like equidimensional flakes in scanning electron microscope. It appears like a thin film. Montmorillonite has a crystalline structure. It results in a "flake" particle shape that resembles a corn flake (Fig. 7.37). These flakes are extremely small, ranging in long dimension from 10 micrometers to 0.01 micrometers. Hundreds of such flakes aggregate to form a thin particle.

Bentonite is more plastic and has greater dry strength but higher shrinkage than kaolinite. The clay particles are much thinner than those of kaolinite, less than a tenth of the thickness, like thin flakes rather than plates. Calcium bentonite swells less than sodium bentonite, but it has the useful property of attracting organic molecules and is used as an adsorbent in cat litter.

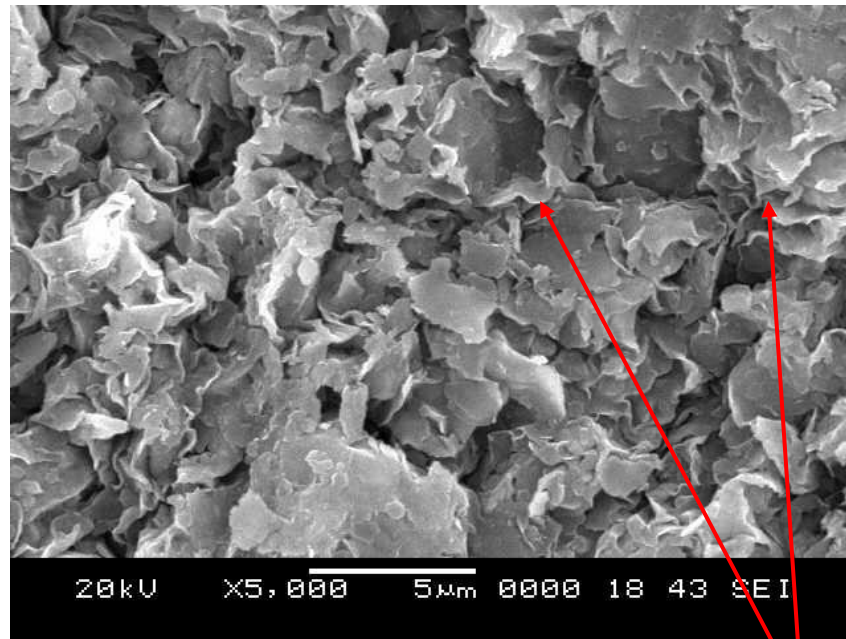


Figure 7.37 Bentonite Flakes (Sample B100)

**Flake shaped particles**

Basic properties of bentonite used in the present investigation are listed below (Table 7.4). The grain size distribution curve for this sample is given in Fig.7.38. It can be seen that bentonite consists of 84% clay particles and 16% silt. Activity of bentonite obtained is 3.11. From Table 7.4 we can understand that the clay belongs to very active category.

Table 7.4 Basic properties of bentonite used

	Consistency Limits	
1	Liquid Limit (%)	300
	Plastic Limit (%)	39
	Shrinkage Limit (%)	11.18
	Plasticity Index (%)	261
	Particle Size Distribution	
2	Sand (%)	0
	Silt (%)	16
	Clay (%)	84
3	Activity	3.11
4	Specific Gravity	2.65

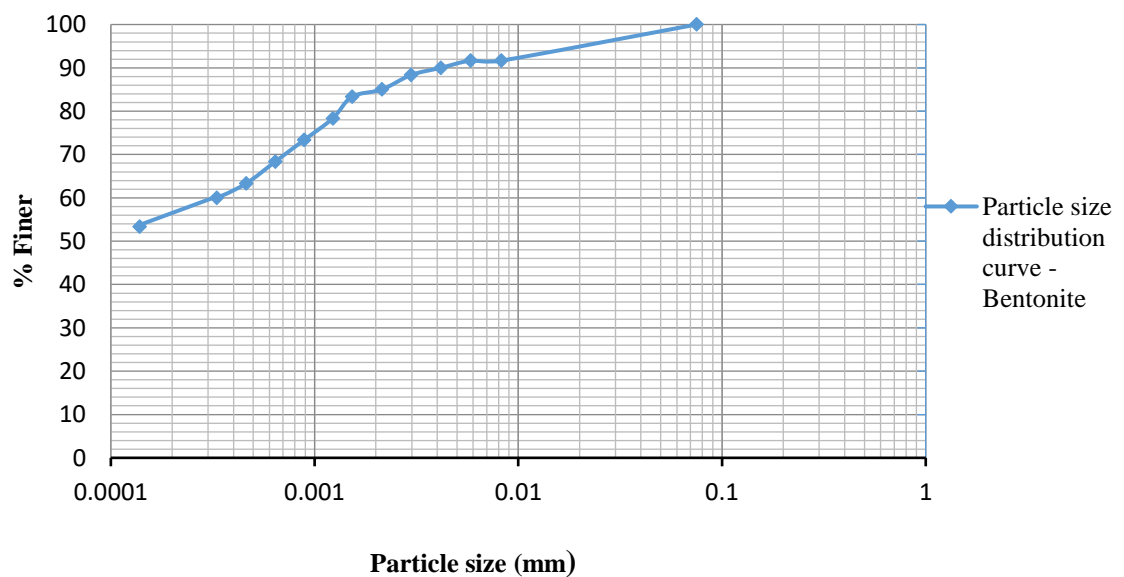


Figure 7.38 Grain size distribution curve for bentonite

### 7.3.6.2. Results of X Ray diffraction studies on bentonite

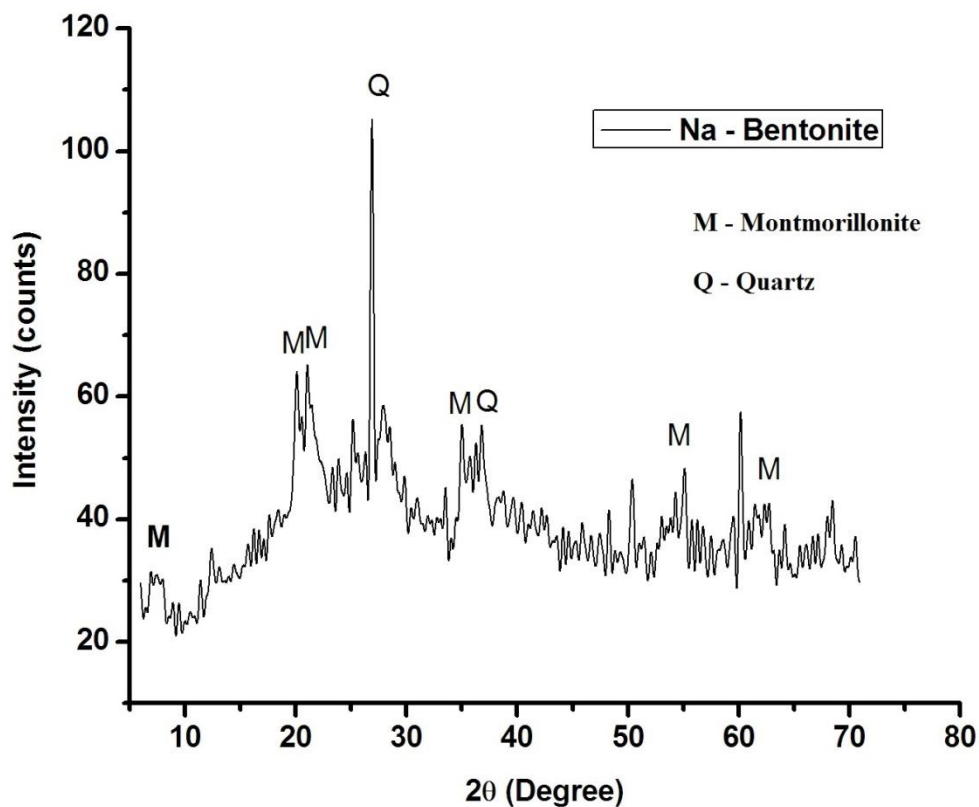


Figure 7.39 X-ray diffraction pattern for Na - Bentonite with minerals Montmorillonite -  $\text{Na}_{0.3}(\text{Al}, \text{Mg})_2 \text{Si}_4\text{O}_{10}(\text{OH})_2 \cdot 8\text{H}_2\text{O}$  and Quartz -  $\text{SiO}_2$

X - ray diffraction studies of shedi soil (Fig. 7.39) were carried out using the  $\text{Cu K}\alpha$  radiation source (background) and peaks were obtained corresponding to Montmorillonite - Sodium Magnesium Aluminum Silicate Hydroxide Hydrate (JCPDS reference code 00-029-1499) and Quartz (Silicon dioxide). XRD results reveal the presence of montmorillonite mineral with hexagonal crystal system.

### 7.3.6.3 Effect on basic geotechnical properties of shedi soil on blending with Bentonite

Table 7.5 Experimental results obtained from laboratory and ER tests on shedi soil blended with bentonite

Samples		B0	B20	B40	B60	B80	B100
Bentonite (%)		0	20	40	60	80	100
Liquid limit(%)		55.0	80.0	170.0	180.0	240.0	300.0
Plastic limit(%)		32.10	31.22	32.18	32.72	37.13	39.00
Shrinkage Limit (%)	Lab result	28.0	19.57	17.65	15.85	14.80	11.18
	From resistivity measurement	27.9	18.0	17.5	16.0	15.0	11.0
Plasticity index (%)		22.90	48.78	137.82	147.28	202.87	261.00
Shrinkage index (%)		25.84	57.43	152.35	164.15	240.00	288.82
Specific gravity (G)		2.51	2.60	2.66	2.61	2.65	2.65
Void ratio (e)		0.73	0.81	0.86	0.92	1.04	1.05
Porosity (n)		0.42	0.45	0.46	0.48	0.51	0.51
Optimum moisture content (%)		26.0	29.0	30.0	36.0	37.0	37.2
Maximum dry density (g/cc)		1.46	1.44	1.43	1.36	1.3	1.22

Bentonite mixed in different proportions (20%, 40%, 60%, and 80%) with shedi soil and pure bentonite were tested in the lab for basic geotechnical properties, SEM analysis, and electrical resistivity studies. Results are summarized in Table 7.5.

### 7.3.6.4 SEM images of bentonite mixed shedi soil samples

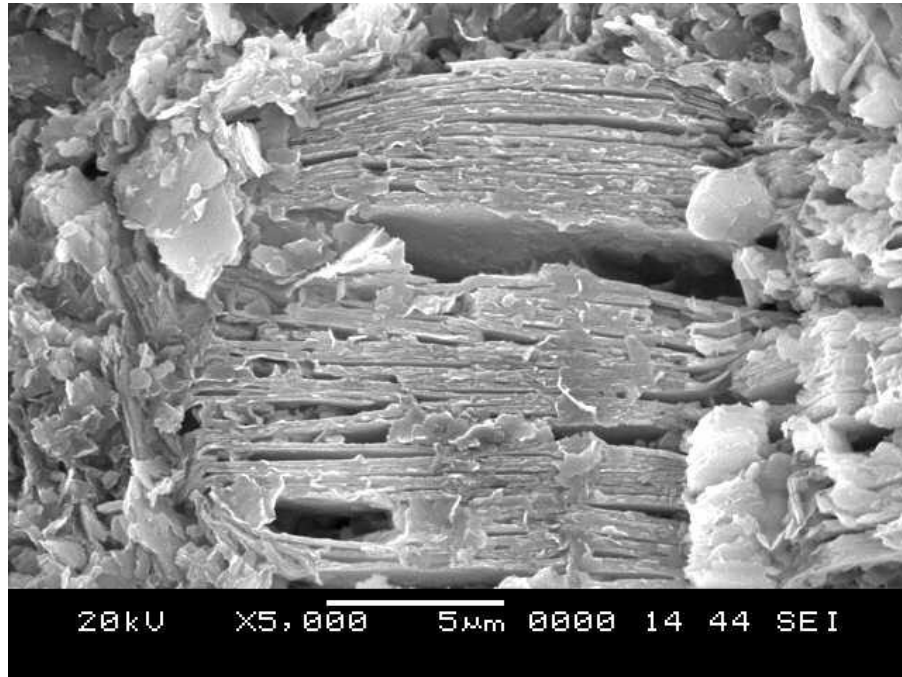


Figure 7.40 SEM- Sample B20

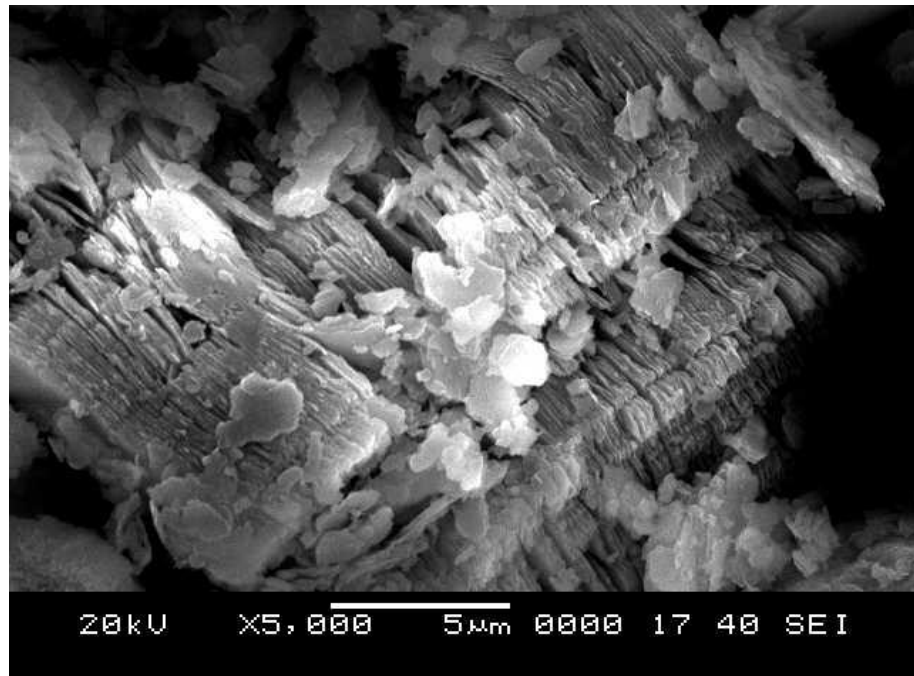


Figure 7.41 SEM- Sample B40

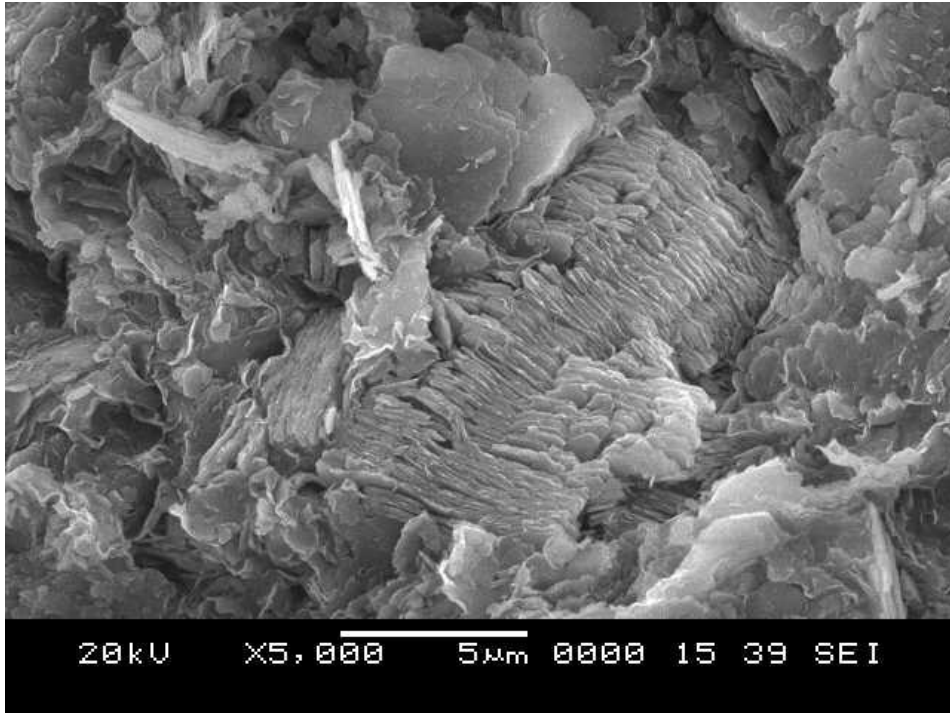


Figure 7.42 SEM- Sample B60

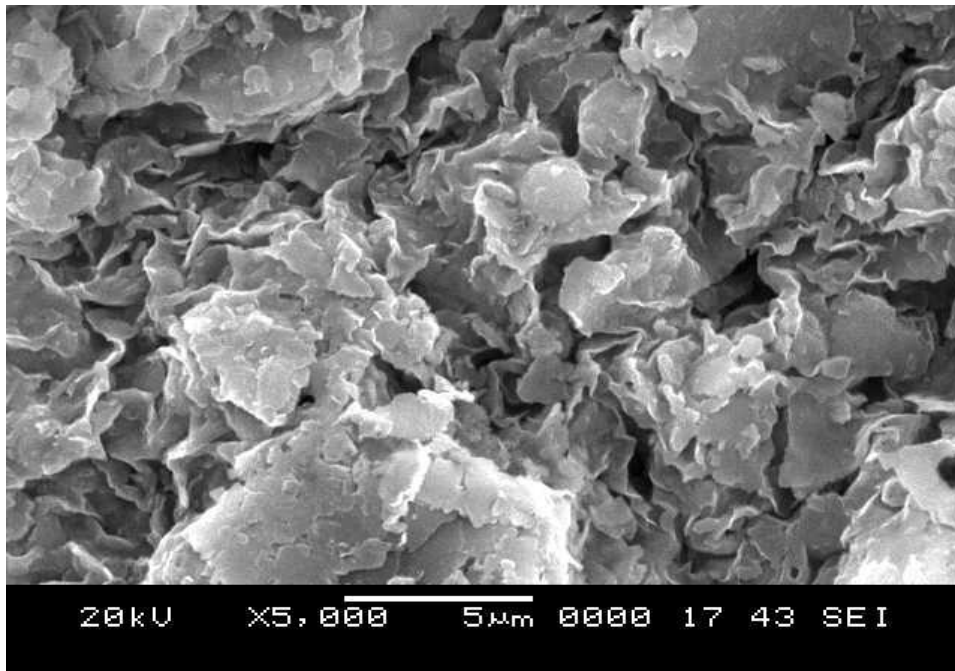


Figure 7.43 SEM- Sample B80

From SEM images (Fig. 7.40 to Fig. 7.43), we can see the distribution of various grain sizes within each sample. For 80%shedi soil+20% Bentonite mix, well-crystallized particle of kaolinite dominates (Fig. 7.40). Coming to 60% Shedi soil + 40% Bentonite mix, plate like

kaolinite dominates; but flakes of bentonite is also present more than the previous SEM image (Fig. 7.41). Coming to 40% Shedi soil + 60% Bentonite mix, bentonite flakes are more visible and they start occupying the spaces in between kaolinite plates (Fig. 7.42). Coming to 20% Shedi soil + 80% Bentonite mix, it's almost similar to the flaky appearance of bentonite, kaolinite plates are rarely seen (Fig. 7.43). This gradual change in texture reflects in its properties also.

### 7.3.6.5 Variation of Void ratio with increase in Bentonite %

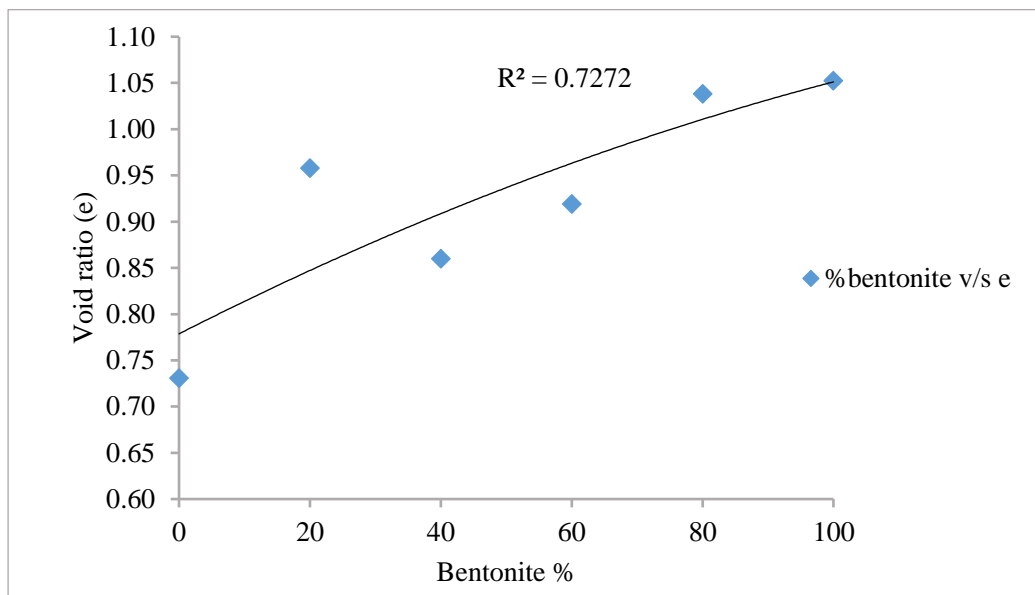


Figure 7.44 Variation of void ratio with bentonite % in shedi soil

As bentonite percentage increases in shedi soil, amount of fines increase, and subsequently, the volume of voids got increased. Hence void ratio shows an increasing trend with bentonite addition (Fig. 7.44).

### 7.3.6.6 Variation of Compaction Characteristics with increase in Bentonite %

As the percentage of bentonite increases dry density decreases, because of increase in the number of fines in the mix. As the percentage of fines increases to a value more than that required to fill the voids in coarse grains, maximum dry density decreases (Fig. 7.45). Also, as the bentonite percentage increases, the mix requires more water and therefore the optimum water content is high (Fig. 7.46). Hence bentonite rich mix shows of very high plasticity have very low dry density and very high optimum water content.



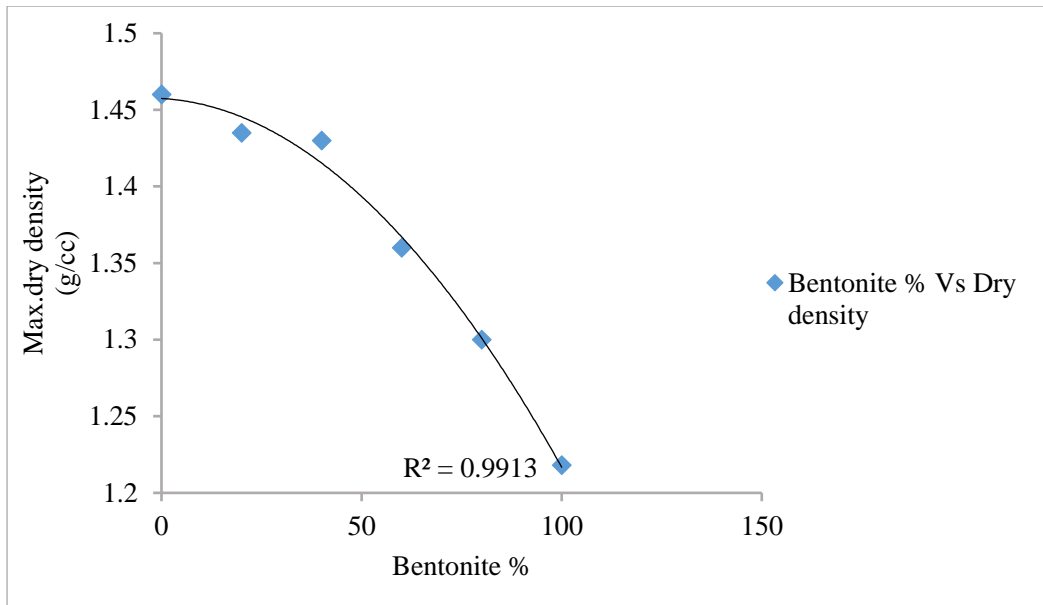


Figure 7.45 Variation of dry density with bentonite % in blended samples

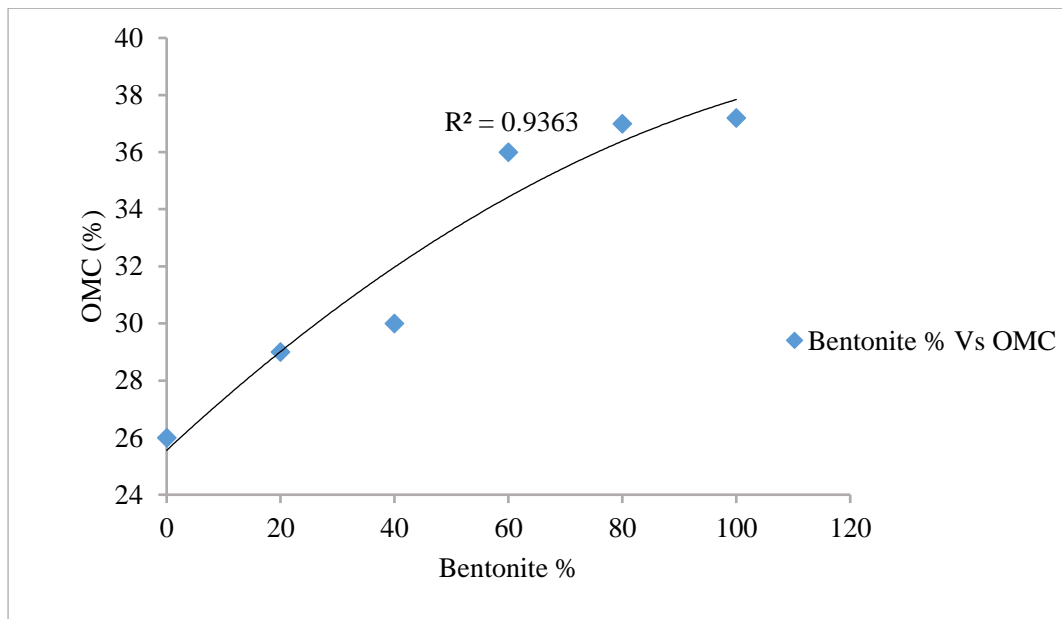


Figure 7.46 Variation of optimum moisture content (%) with bentonite % in blended samples

### 7.3.6.7 Variation of Atterberg Limits with increase in Bentonite %

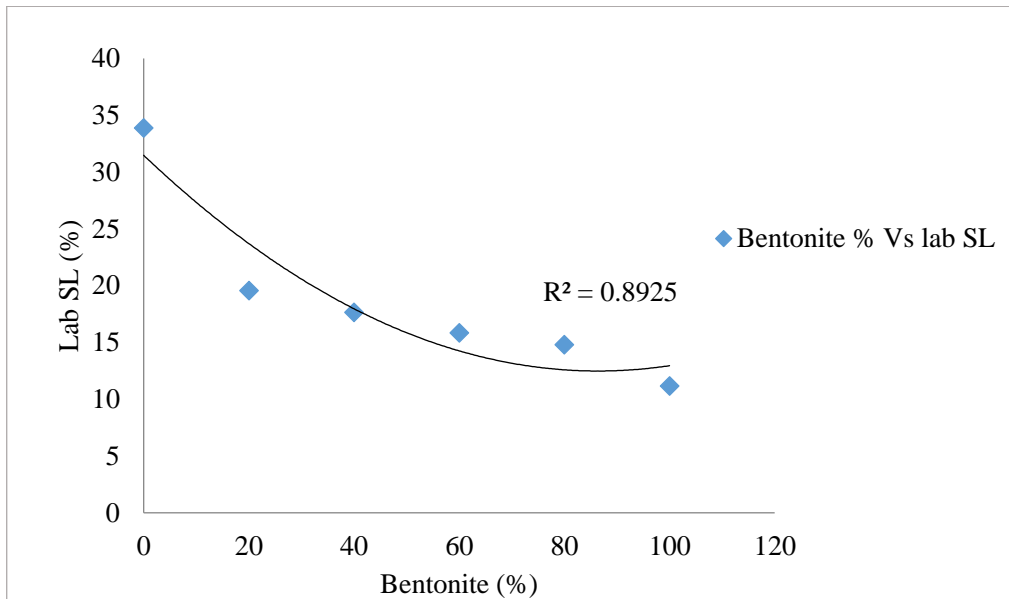


Figure 7.47 Bentonite% in blended sample v/s lab shrinkage limit

Bentonite soil shows large liquid limit (300 %) and low shrinkage limit (11.8 %). As bentonite percentage increases the soil mix shows a decreasing trend for shrinkage limit (Fig. 7.47).

Whereas liquid limit (LL), plasticity index (PI), and plastic limit (PL) shows an increasing trend with increase in % of bentonite (Fig. 7.48).

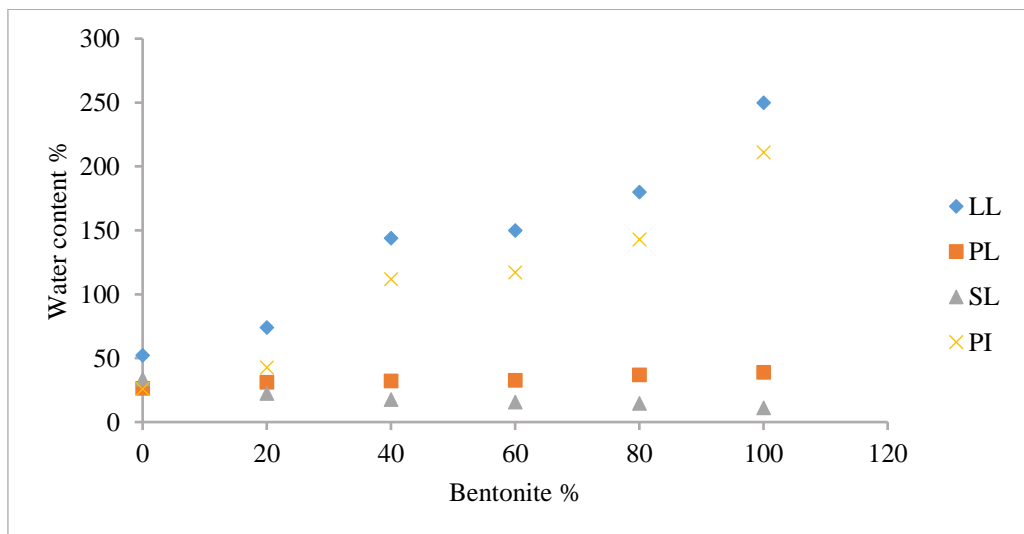


Figure 7.48 Variation of Atterberg limits with percentage of bentonite in blended sample

Shrinkage pats prepared by pure bentonite were highly shrunk both vertically and laterally. Highly shrinking behaviour of bentonite clay can be explained based on its fabric. Bentonite pats get cracked easily into small pieces and it was very difficult to find the volume after shrinkage (Fig. 7.49).



Figure 7.49 Pure bentonite shrinkage pats (a) wet state and (b) After air and oven drying



Figure 7.50 Shrinkage pats prepared with varying % of bentonite in shedi soil  
(20%, 40%, 60%, 80%, and 100%)

From figure 7.50, it can be observed that as the bentonite percentage increases, there is a gradual increase in shrinkage of dried pats and an increase in air drying period. Before keeping the pats in the oven in order to prevent cracking, 20-30 days of air dry period was taken by pure bentonite soil pat to get a pat without cracks. Determination of shrinkage limit using conventional laboratory method was very difficult for pure

bentonite and bentonite rich soil pats (80%), because the conventional glass plate with prongs can't immerse the pat completely under mercury.

### 7.3.6.8 Electrical resistivity-moisture content studies on bentonite – shedi soil mix

Electrical resistivity studies were conducted on the bentonite and its blends with shedi soil. Water content v/s Electrical resistivity graphs were plotted and are shown in Fig. 7.51 to Fig. 7.55. Water content corresponding to the sharp change in resistivity was noted down. It is interesting to see that these values are almost equal to shrinkage limits obtained from lab tests.

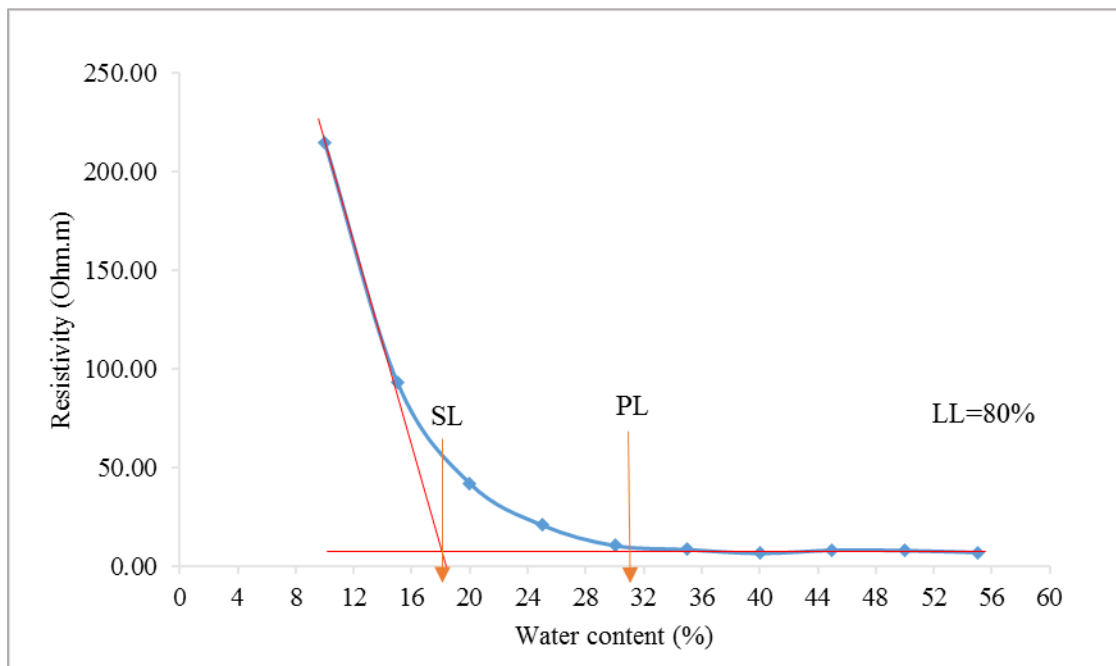


Figure 7.51 Water content-ER graphs for B20

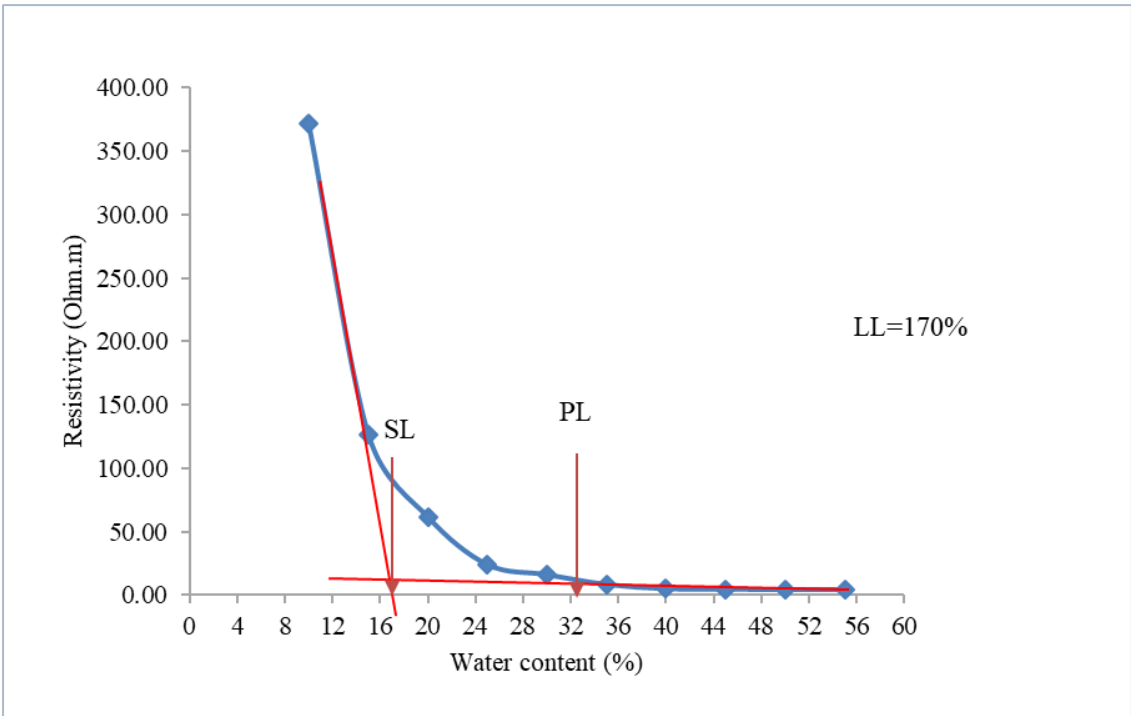


Figure 7.52 Water content-ER graphs for B40

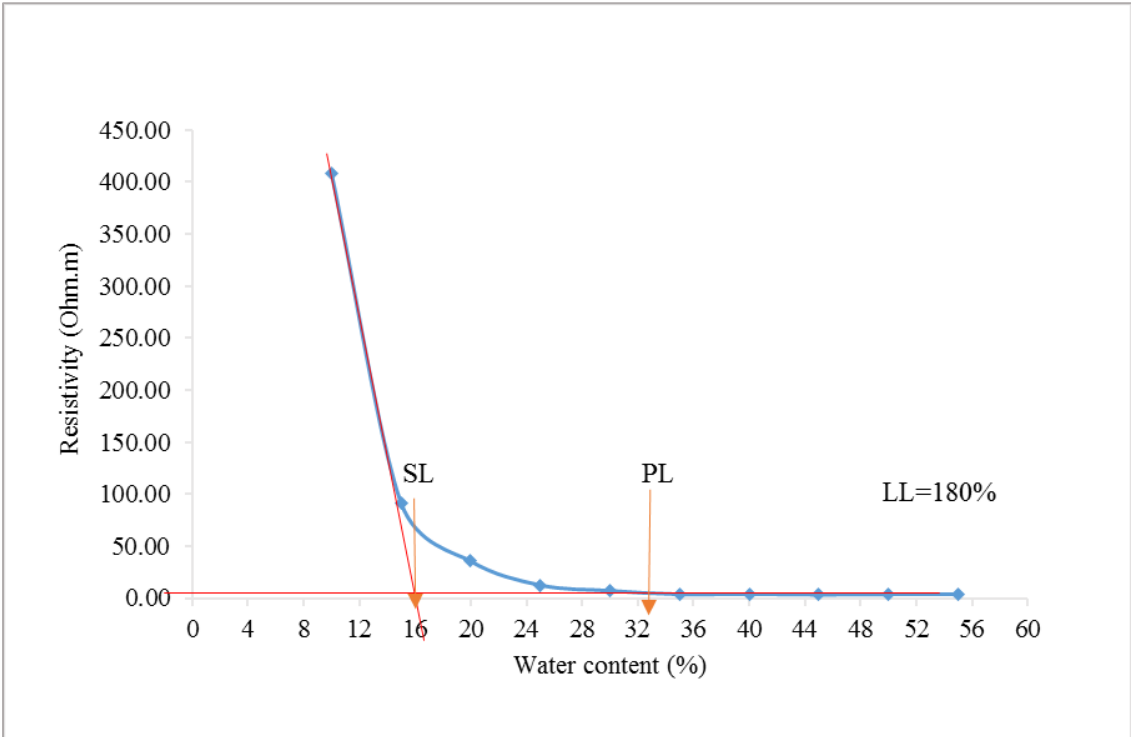


Figure 7.53 Water content-ER graphs for B60

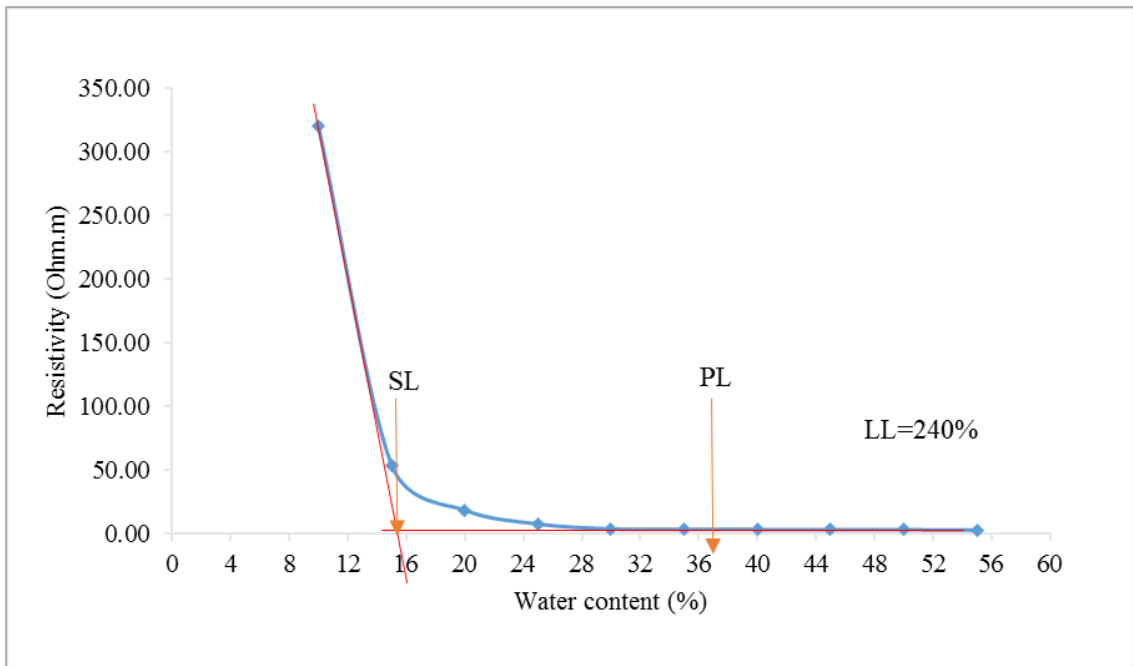


Figure 7.54 Water content-ER graphs for B80

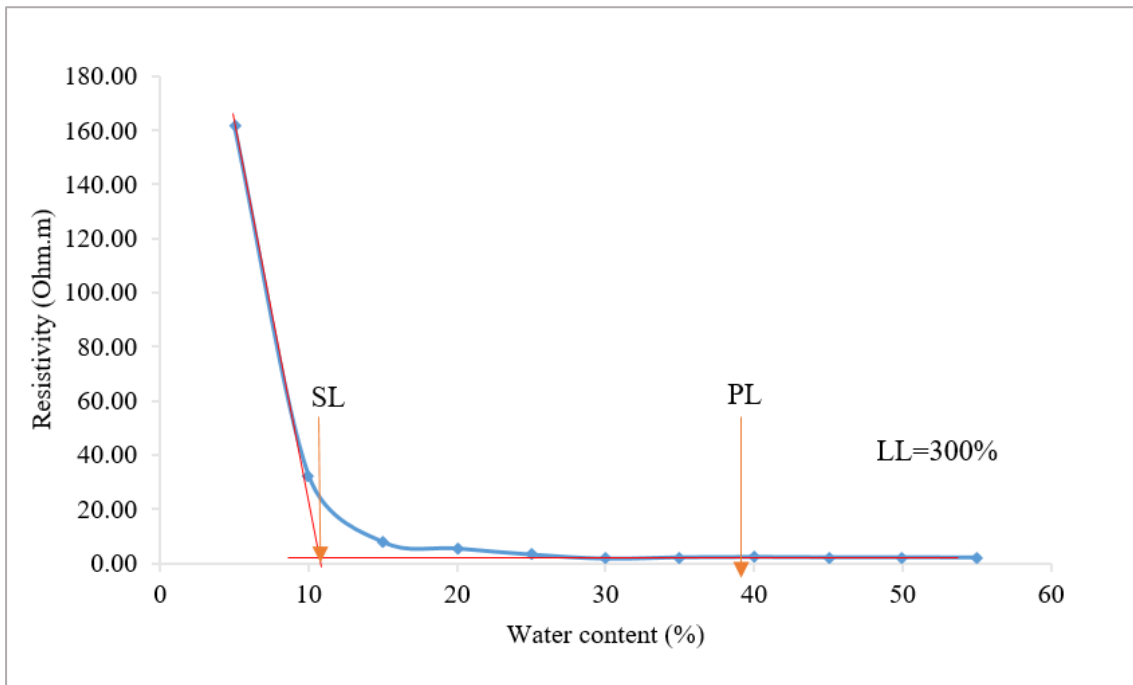


Figure 7.55 Water content-ER graphs for B100

From Fig. 7.52 to Fig. 7.55 we get shrinkage limit values as 20%, 17.5%, 16%, 15%, 11% respectively for 20%,40%.60%,80 and 100% bentonite blended shedi soil samples. From laboratory shrinkage limit tests, we got 22.57%, 17.65%, 15.85%, 14.8% and 11.18% respectively. These values are plotted in Figure 7.56, and it shows regression coefficient of 0.99.

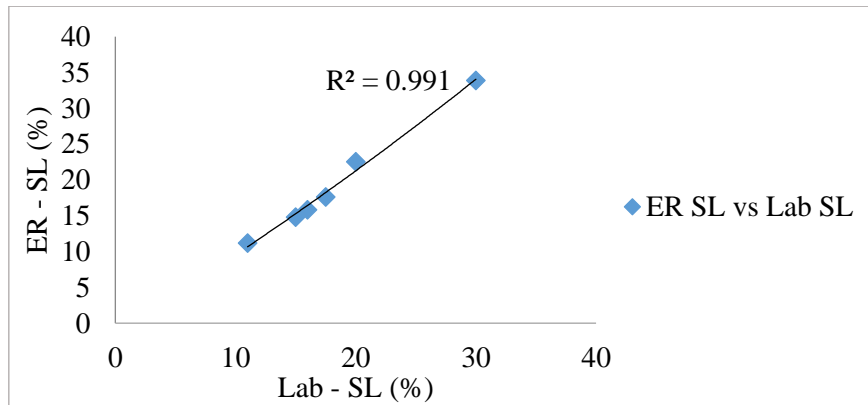


Figure 7.56 Correlation of Shrinkage Limit assessed from ER-m/c relationship with Shrinkage limit obtained from standard laboratory test

Since the determination of shrinkage limit from conventional laboratory testing is difficult in the case of highly expansive bentonite clay, assessment of Shrinkage Limit from ER-water content profile can be suggested as a good alternative for the preliminary determination of shrinkage limit. It will give an idea about the shrinkage limit water content. It is more rapid and easier method than conventional mercury displacement method.

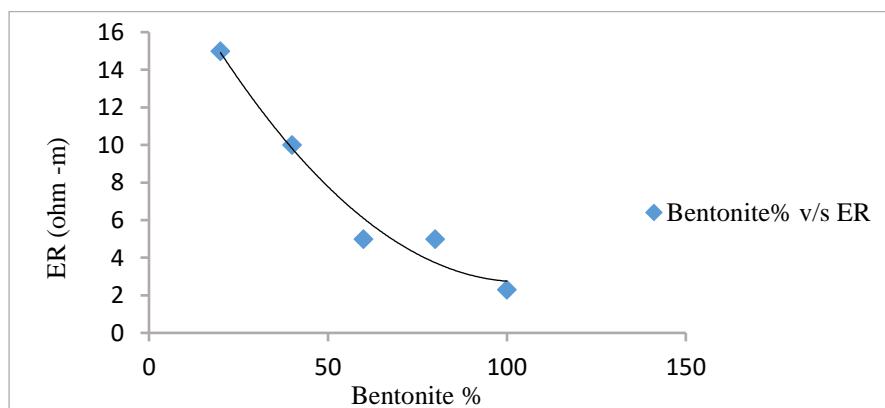


Figure 7.57 Variation of electrical resistivity (at OMC and max dry density) with bentonite percentage

The electrical conductivity of a soil or soil - water slurry increases as the clay content or electrochemical activity of the clay is increased (Fig. 7.58). Active clays show higher conductivity. As bentonite have higher surface conductance, increase in bentonite content can have a significant effect on its electrical conductivity (Abu-Hassanein, 1995). Again as bentonite % increases, due to increase in fines, void ratio increases. Since fines increases, numbers of distinct pores increases and dry density decreases. So we can see a direct relation between dry density and electrical resistivity (Fig. 7.59).

### 7.3.6.9 Variation of dry density and OMC with Resistivity for Bentonite blended Shedi soil samples

Since with addition of bentonite, the mix requires more water and therefore the optimum water content is high. Also the ER decreases with bentonite addition; hence as optimum moisture content increases, ER decreases (Fig. 7.60).

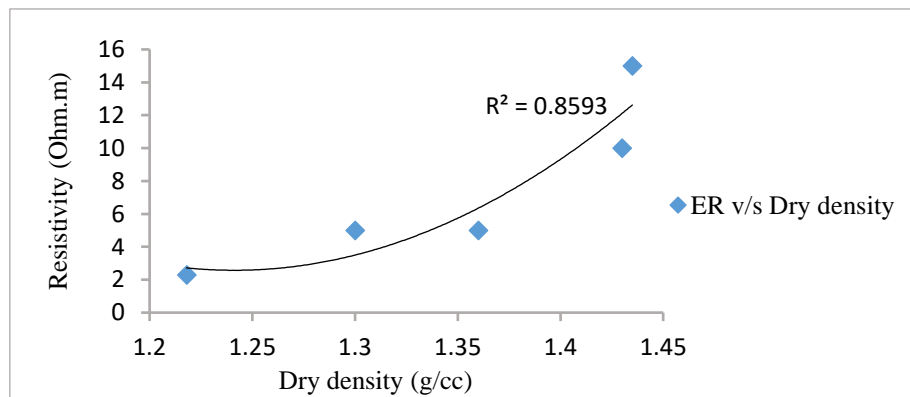


Figure 7.58 ER v/s Dry density for bentonite mixed soil

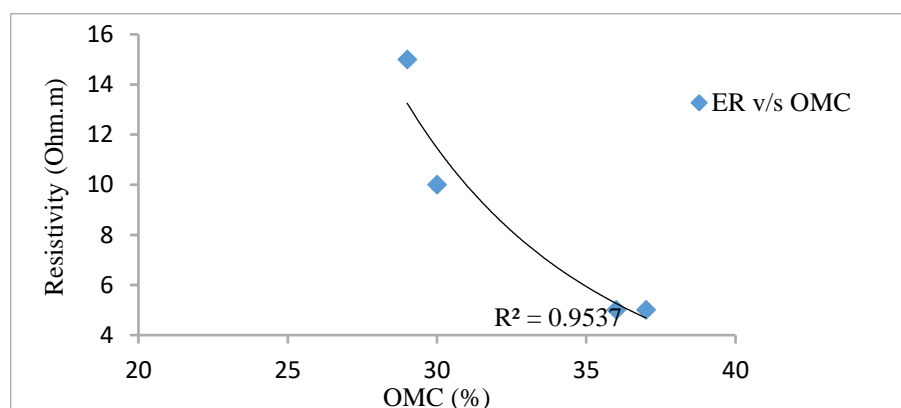


Figure 7.59 ER v/s optimum moisture content for bentonite mixed soil



### 7.3.6.10 Variation of Porosity with Resistivity for Bentonite blended Shedi soil

Increase in bentonite increase the void ratio and increases the conductance. Hence we can observe an inverse relation between porosity with electrical resistivity (Fig. 7.61).

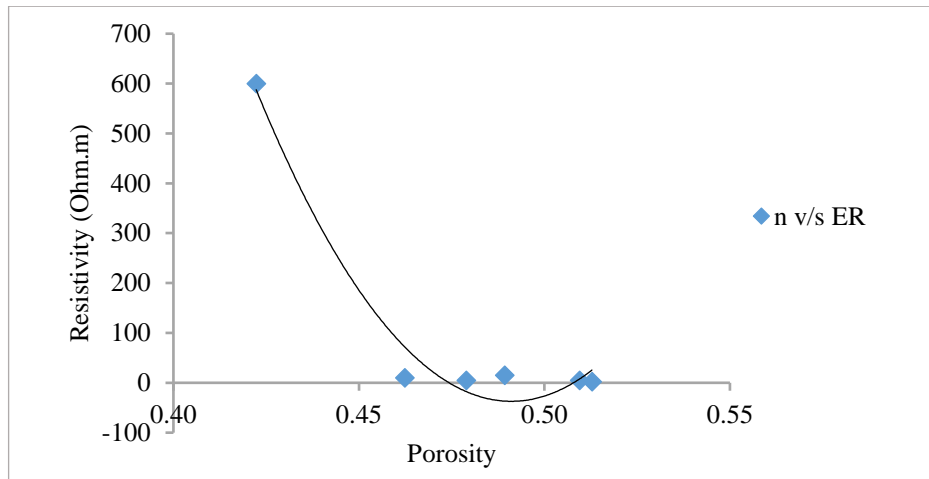


Figure 7.60 Porosity v/s electrical resistivity of bentonite mixed soil

## 7.4 Summary

All investigations till date have thrown light towards the use of electrical resistivity as an indirect or auxiliary method for computing geotechnical parameters. This study shows that electrical resistivity measurements (ER-moisture content profile) of a well compacted soil can be a useful tool for assessing shrinkage limit of soils. The following are the conclusions arrived at.

- The electrical resistivity of the soil sample is sensitive to the moulding water content and degree of saturation initially and becomes stable once the soil is fully saturated. The point where a well compacted soil is “just saturated” is clearly captured by the resistivity-water content profile, which is a good estimate of the “shrinkage limit” of the soil. The assessment is proven to be valid for contaminated soils too, where in the Atterberg limits got altered. Hence, resistivity measurements prove to be a quick method for assessing the shrinkage limit of soils.

- It is seen that the liquid limit, plasticity index, specific gravity, plastic limit, shrinkage limit and pH decreases with increase in the amount of phosphoric acid. The plasticity index decreases with the increase in the percentage of acid content indicates the growth of particle size from clay size to silt size. The soil changes from highly plastic (natural sample) to medium plastic and becomes poorly graded. This happens because of stacking of unit layers of smectite mineral by the acid reaction.
- Shrinkage limit need not be always less than plastic limit. For acid content of 10N shrinkage limit even exceeds plastic limit, i.e. plastic limit exists at partially saturated condition (Ramakrishnegowde, 2005).
- Individual mineral constituents were identified using X-Ray diffraction technique.
- SEM images clearly shows that by the addition of phosphoric acid, individual soil particles get stacked together and voids become bigger.
- Blending of shedi soil with bentonite increases the percentage of fines. This will lead to increase in void ratio, number of distinct pores, decrease in dry density, and increase in surface conductance, and hence, decrease in electrical resistivity. Bentonite clays are active in nature (activity > 1.25) because of presence of montmorillonite mineral. Whereas shedi soil is inactive (activity < 0.75) due to the presence of kaolinite mineral. Active clays show higher conductivity. Hence presence of bentonite imparts conductivity to soil blends. SEM images of bentonite mixed shedi soil show the flaky nature of montmorillonite as well as the sheet like structure of kaolinite.
- ER shows very good correlation with water content. There is a sharp decrease in resistivity when water is in adsorbed state. This decrease in resistivity is less sharpened in capillary-film state and in reaching gravitational state, there is not much further change in electrical resistivity. Hence the tangential intersection value of the moisture content of a well compacted soil in the electrical resistivity box can be considered as a good estimate of the shrinkage limit of the soil. This method can be suggested as a good alternative for shrinkage limit determination,

especially for highly expansive soils for which the exact volume determination of the dried pat is very difficult. This method holds true for both contaminated as well as bentonite mixed shedi soil samples.

## CHAPTER 8

### SUMMARY AND CONCLUSIONS

#### 8.1 Summary and Conclusions

This study looks into the relationships between the physical factors influencing the engineering properties of soils and their measurable electrical parameters, a proper understanding of which provides a methodology by which the engineering behaviour of soils can be predicted non-intrusively. High precision digital multimeters, a resistivity box and a dc power source are utilised to measure the electrical resistivity of the soil samples. Signal Stacking Resistivity meter is used to measure the electrical resistivity in the field. The conclusions of the present study are briefly given below.

- Quantitative correlations are obtained between geotechnical and geo-electrical properties of laterites and lateritic soils, in regulated laboratory conditions and in natural field conditions. It is found that electrical resistivity bears positive correlation with cohesion and an inverse correlation with angle of internal friction and CBR. Due to fragmentation of soil samples on compressive loading as the percentage of sand increase, UCS and ER are less correlated for the soil samples studied.
- The results of this study reveal that by properly handling the uncertainties and ubiquitous resistivity measurement errors, Electrical Resistivity tomography can be applied as a pre investigation method on sites, prior to direct testing methods like SPT to reduce labour, cost and time involved. Although the field ER values depend on a number of factors at site, generally there exists a good correlation between SPT and ER. In that direct and inverse relations are investigated. However, a few inconsistent relations also exists between SPT and ER. Water content, soil type, stiffness of the soil layers, develop a direct relation between SPT and ER. However, compaction/bulk density, soil layers submerged under the water table, salt concentration ensue inverse relation between ER and SPT. Gravelly soils and hard porous laterites gave higher SPT and higher ER values. Fine grained soils, even at large depths, gave lower SPT and lower ER values. Dry soil, at locations where water table was very low showed higher resistivity values.
- Comparisons done on laboratory and field electrical resistivity data showed fairly good correlations. The difference in resistivity could be due to the inability to produce the

exact field conditions in the laboratory. It is also noted that the lab resistivity is generally higher than the field resistivity and generally correlate quite well with surface measurements.

- By the time an unconfined compressive strength test can be performed to check the quality of the soil-cement/lime, the material will be hardened in the field and if it does not meet strength, performance criteria, the material will have to be removed, collapsed and remixed with additional cement/lime which is a very time and cost consuming task. At this phase, electrical measurements of soil-cement/lime material saves a great deal of expense and time by predicting the strength properties without hardening of the material. Quantitative relations developed for predicting 7 day strength of soil-cement/lime mix, using resistivity of the soil-cement/lime samples at freshly prepared state, after 1 hour curing help to decide whether the soil-cement/lime mix meets the desired strength and performance criteria. This offers the option of the soil-cement/lime mix to be upgraded (possibly with additional cement or lime) in its fresh state itself, if it does not fulfil the performance criteria, rather than wasting the material after hardening.
- It is seen that the liquid limit, plasticity index, specific gravity, plastic limit, shrinkage limit and pH decreases with increase in the amount of phosphoric acid added to the soil. The decrease in plasticity index with the increase in the percentage of acid content indicates the growth of particle size from clay size to silt size. The soil changes from highly plastic (natural sample) to medium plastic and becomes poorly graded. This happens because of the stacking of unit layers of smectite mineral by its reaction with phosphoric acid.
- Shrinkage limit need not be always less than plastic limit. For acid content of 10 N shrinkage limit even exceeds plastic limit, i.e. plastic limit exists at partially saturated condition. Water content v/s resistivity curves can be used to predict the shrinkage limit values of soil. This assessment holds true for both contaminated as well as bentonite mixed shedi soil samples.
- Individual mineral constituents of the soil were identified using X-Ray diffraction technique. SEM images clearly shows that by the addition of phosphoric acid to the soil, individual soil particles get stacked together and voids get bigger.

- Bentonite clays are active in nature (activity > 1.25) because of the presence of montmorillonite mineral. Whereas shedi soil is inactive (activity < 0.75) due to the presence of kaolinite mineral. Active clays show higher conductivity. Hence presence of bentonite imparts conductivity to soil blends. SEM images of bentonite mixed shedi soil show the flaky nature of montmorillonite as well as the sheet like structure of kaolinite.
- The electrical resistivity of the soil sample is sensitive to the moulding water content and degree of saturation initially and becomes stable once the soil is fully saturated. In this study, it is observed and verified that, the point where a well compacted soil is “just saturated” is clearly captured by the resistivity-water content profile, which is a good estimate of the “shrinkage limit” of the soil. This assessment is proven valid with phosphoric acid contaminated shedi soils and bentonite blended shedi soils. This method can be suggested as a good alternative for conventional shrinkage limit determination (using shrunken dry soil pats and mercury), especially for highly expansive soils for which the exact volume determination of the dried pat is very difficult. Hence, resistivity measurements prove to be a quick method for assessing the shrinkage limit of soils. The variation of electrical resistivity with other index properties are also studied for the bentonite blended and acid contaminated shedi soils.

## **8.2 Limitations**

The role of geophysical testing in geotechnical studies is sometimes looked at as a more probable rather than certain approach when it comes to making a precise subsurface soil profile. However, it can be possible to employ the modern 2D and 3D electrical resistivity soil profiling techniques combined with a few boreholes data to make a true and correct subsurface profile, which can be used confidently by geotechnical engineers. The correlations of physical properties on electrical resistivity in the study are obtained by single factor analysis method, but its effects are actually working in a combined pattern. Caution should be exercised in the presence of metal pipes, cables, fences and electrical grounds, which can distort the resistivity measured and complicate the interpretation.

### **8.3 Scope for Future Work**

- The correlations are site-specific and require a detailed study to establish its validity and restrictions. More field tests have to be conducted in various flat and sloping geological environments for getting more summed up conclusions.
- It is necessary to develop correlations between ER and Geotechnical parameters of soils with high salt content such as marine clay, soils contaminated with alkali, ammonia, Urea, Sodium Carbonate etc. which alter the basic geotechnical characteristics of the soil.
- It is necessary to conduct a detailed study on the relation between pore tortuosity and electrical resistivity, so that electrical measurements could provide a methodology for quantifying the pore tortuosity in soil.

## REFERENCES

Adebisi, N. O., Ariyo, S. O. and Sotikare, P. B. (2016). "Electrical resistivity and geotechnical assessment of subgrade soils in southwestern part of Nigeria." *Journal of African Earth Sciences*, 119 (2016), 256-263.

Abidin, M. H. B. Z., Saad, R. B., Ahmad, F. B., Wijeyesekera, D. C. and Baharuddin, M. F. B. T. (2012). "Integral Analysis of Geoelectrical (Resistivity) and Geotechnical (SPT) Data in Slope Stability Assessment." *Academic J. of Science*, ISSN: 2165-6282, 1(2), 305–316.

Abidin, M. H. B. Z, Wijeyesekera, D. C, Saad, R. B. and Ahmad, F. B. (2013). "The Influence of Soil Moisture Content and Grain Size Characteristics on its Field Electrical Resistivity." *Electronic Journal of Geotechnical Engineering*. 18, 699-705.

Abidin, M. H. B. Z., Saad, R. B., Ahmad, F. B., Wijeyesekera, D. C. and Baharuddin, M. F. B. T. (2014). "Correlation Analysis between Field Electrical Resistivity Value (Erv) and Basic Geotechnical Properties (Bgp)." *Soil Mechanics and Foundation Engineering*, Russian Original, 51(3), 118-125.

Abu-Hassanein, Z. S., Craig H. B., and Lisa R. B. (1996). "Electrical resistivity of compacted clays." *J. of geotechnical engineering*, ASCE, 122, 397-406.

Abu-Hassanein, Z. S., Zeyad, S., Blotz, L. R., Craig, H. B., and Xiadong, W. (1995). "Determining bentonite content in soil – bentonite mixtures using electrical conductivity." *Geotechnical testing J*, GTJODJ, ASCE, 19, 51-57.

Adli, Z. H., Musa, M. H. and Arifin, M. N. K. (2010). "Electrical Resistivity of Subsurface: Field and Laboratory Assessment." *Int. J. of Environmental, Earth Science and Engineering*, World Academy of Science, Engineering and Technology, 4(9), 1-4.



Ahmed, A. M. and Sulaiman, W. N. (2001). "Evaluation of Groundwater and Soil Pollution in a Landfill Area Using Electrical Resistivity Imaging Survey." *Environmental Management*, 28(5), 655–663.

Akinlabi, I. A. and Adeyemi, G. O. (2014). "Determination of Empirical Relations between Geoelectrical Data and Geotechnical Parameters in Foundation Studies for a proposed Earth Dam." *The Pacific J. of Science and Technology*, 15(2), 278-287.

Aleva, G. J. J., and Creutzberg, D. (1994). "Laterites: concepts, geology, morphology, and chemistry." (Wageningen, The Netherlands: International Soil Reference and Information Center).

Anderson, N., Cardimona, S. and Newton, T. (2003). "Application of Innovative Non-Destructive Methods to Geotechnical and Environmental Investigation". *Report by Missouri Department of Transportation Project Operations Division*.

Archie, G. E. (1942). "The Electrical Resistivity Log as an Aid in Determining Some Reservoir Characteristics." *Transactions of the AIME, American Institute of Mining, Metallurgical, and Petroleum Engineers*, 146(01), 54-62.

Arora, T. and Ahmed, S. (2010). "Electrical structure of an unsaturated zone related to hard rock aquifer". *Current Science*, 99(2), 216-220.

Arrubarrena-Moreno, M. and Arango-Galván, C. (2013). "Use of electrical resistivity tomography in the study of soil pollution caused by hydrocarbons: Case study in Puebla (México)." *Boletín de la Sociedad Geológica Mexicana*, 65(2), 410-426.

Arulanandan, K. (1991). "Dielectric method for prediction of porosity of saturated soil." *J. of Geotechnical Engineering*. ASCE, 117(2), 319-330.

Assa'ad, A. (1998). "Differential Upheaval of Phosphoric Acid Storage Tanks in Aqaba, Jordan," *ASCE, J. of Performance of Constructed Facilities*, 112, 71-76.

Asif, A. R., Ali, S. S., Noreen, N., Ahmed, W., Khan, S., Khan, M. Y. and Waseem, M. (2016). "Correlation of electrical resistivity of soil with geotechnical engineering parameters at Wattar area district Nowshera, Khyber Pakhtunkhwa, Pakistan." *J. of Himalayan Earth Sciences*. 49(1), 124-130.

Bai, W., Kong, L. and Guo, A. (2013). "Effect of Physical Properties on Electrical Conductivity of Compacted Lateritic Soil." *J. of Rock Mechanics and Geotech. Engg.* Elsevier, 5(2013), 406-411.

Ballukraya, P. N. (1996). "Differentiating conductive and resistive inhomogenities: A new approach in groundwater exploration." *Current Science*, 71(11), 926-930.

Bell F. G. (1996). "Lime stabilisation of clay minerals and soils", *Engineering Geology*, 42, 223-237.

Bery, A. A. (2016). "Slope Monitoring Study using Soil Mechanics Properties and 4-D Electrical Resistivity Tomography Methods." *Soil Mechanics and Foundation Engineering*, 53(1), 24-29.

Bery, A. A. and Saad, R. (2012). "Tropical Clayey Sand Soil's Behaviour Analysis and Its Empirical Correlations via Geophysics Electrical Resistivity Method and Engineering Soil Characterizations." *International J. of Geosciences*, 3, 111-116.

Bhangale, L. A. and Bhosale, S. S. (2010). "Stabilized Soil Evaluation Using Laboratory Electrical Resistivity Cell." *Indian Geotechnical Conference, Geotrendz*, December 16-18, IGS Mumbai Chapter & IIT Bombay, 333-336.

Bhatt, S. and Jain, P. K. (2014). "Correlation between electrical resistivity and water content of sand –a statistical approach." *American Int. J. of Research in Science, Technology, Engineering & Mathematics*, 6(2), 115-121.

Bhat, A. M., Rao, H. B. and Singh, D. N. (2007). "A Generalized Relationship for Estimating Dielectric Constant of Soils." *Journal of ASTM International*, 4(7), 1-17.

Bhoi, A. K. (2012). "An Assessment of Electrical Resistivity Soundings Data by Different Interpretation Techniques." *International J. of Biological, Ecological and Environmental Sciences (IJBEES)*, 1(3), 108-112.

Bhowmick, A. N. and Baweja, B. K. (1977). "On the use of surface electrical resistivity survey for groundwater investigation in Panipat-Sonepat area, Haryana." *Geophysical case histories of India*, 1. 187-199.

Bose, R. N. and Ramakrishna, T. S. (1977). "Electrical Resistivity for Groundwater in the Deccan Trap country of Sangli District, Maharashtra." *J. of hydrology*, 38. 209-221.

Bryson, L. S. (2005). "Evaluation of Geotechnical Parameters using Electrical Resistivity Measurements." *GSP 133, Earthquake Engineering and Soil Dynamics*, ASCE, 1-12.

BS: 1377--Part 2, 1990, British Standard Methods of Test for Soil for Engineering Purposes. Part 2: "Classification Tests: Cone penetration test".

Cabalar, A. F. (2007). "A New Approach for the Electrical Resistance of compacted Soils." *EJGE*, Available at <http://www.ejge.com/2007/Ppr0790/Abs0790.htm>.

Cardimona, S. (2002). "Electrical Resistivity Techniques for Subsurface Investigation." *Proceedings of The 2nd Annual Conference on the Application of Geophysical and NDT Methodologies to Transportation Facilities and Infrastructure*. [www.dot.ca.gov/hq/esc/.../061cardimona\\_resistivity\\_overview.pdf](http://www.dot.ca.gov/hq/esc/.../061cardimona_resistivity_overview.pdf)

Castelblanco, M. J. A., Pereira, J. M., Delage, P. and Cui, Y. J. (2012). "The influence of changes in water content on the electrical resistivity of a natural unsaturated loess." *ASTM Geotechnical Testing Journal*, 35 (1), 11-17.

Chen, L., Yan-Jun, D., Liu, M. and Jin, F. (2011). "Evaluation of Cement Hydration Properties of Cement-Stabilized Lead-Contaminated Soils using

Electrical Resistivity Measurement.” *J. of Hazardous, Toxic, and Radioactive waste*. ASCE.

Chung, D. D. L. and Jingyao, C. (2004). “Microstructural effect of the shrinkage of cement-based materials during hydration, as indicated by electrical resistivity measurement.” *J. Cement and Concrete Research*, Elsevier, 34(10), 1893-1897.

Clement, R. and Moreau, S. (2016). “How should an electrical resistivity tomography laboratory test cell be designed? Numerical investigation of error on electrical resistivity measurement.” *J. of Applied Geophysics*. Elsevier. 127, 45–55.

Cosentini, R. M., Vecchia, G. D., Foti, S., and Musso, G. (2012). “Estimation of the hydraulic parameters of unsaturated samples by electrical resistivity tomography.” *Geotechnique*, 62(7), July 2012, 583-594.

Cosenza, P., Marmet, E., Rejiba, F., Cui, Y. J., Tabbagh, A. and Charlery, Y. (2006). “Correlations between geotechnical and electrical data: A case study at Garchy in France.” *J. of Applied Geophysics*, Science Direct, 60, 165–178.

Dong, B., Zhang, J., Wang, Y., Fang, G., Liu, Y. and Xing, F. (2016). “Evolutionary trace for early hydration of cement paste using electrical resistivity method.” *Construction and Building Materials*, Elsevier, 119, 16-20.

Dafalla, M. A. and Fouzan, A. Al Fouzan. (2012). “Influence of Physical Parameters and Soil Chemical Composition on Electrical Resistivity: A Guide for Geotechnical Soil Profiles.” *International J. of electrochemical science*, 7 (2012), 3191- 3204.

Drnevich, V. P., Carlos, E. Z., Jung, S. and Clarke, J. P. (2008). “Electrical conductivity of soils and soil properties.” *Geocongress 2008*, ASCE, 316-323.

Elarabi, H. and Ali Jabir, M. (2013). "Experimental evaluation of soil resistivity in lateritic soil of western sudan." *Ozean J. of Applied Sciences* 6(1), 11-20.

Eltarabily, M. G. A., Negm, A. M., Valeriano, O. C. S., and Gafar, K. E. (2015). "Effects of di-ammonium phosphate on hydraulic, compaction and shear strength characteristic of sand and clay soils." *Arab J Geosci.* 8, 10419–10432.

Eve, A. S. and Keys, D. A. (1954), *Applied Geophysics*, Cambridge at the university press. 142.

Fallah-Safari, M., Hafizi, M. K. And Ghalandarzadeh, A. (2013), "The relationship between clay geotechnical data and clay electrical resistivity" *Bollettino di Geofisica Teorica ed Applicata*, 54(1), 23-38.

Fallah-Safari, M., Mohammad, K. H., and Abbas, G. (2010), "Correlation between electrical resistivity data and Geotechnical data on a clay soil" *Proceedings of the 19th International Geophysical Congress and Exhibition of Turkey – November 2010*.

Fukue, M., Minato T., Horibe, H. and Taya, N. (1999). "The micro-structures of clay given by resistivity measurements." *Engineering Geology*, Elsevier Science 54, 43–53.

Gagliano, M. (2010). "Assessment of Electrical Resistivity Method to Map Groundwater Seepage Zones in Heterogeneous Sediments at Mirror Lake, NH. *M. Sc. Thesis, Temple University Graduate Board*.

Gardi, S. Q. S. (2014). "2D Electrical Resistivity Tomography Survey for Shallow Environmental Study at Wastewater Valley of Southwestern Erbil City, Iraqi Kurdistan Region." *Research J. of Environmental and Earth Sciences*, 6(5), 266-277.

Gautam, P. K. and Sastry, R. G. (2013). “Geotechnical site characterization through geoelectrics.” *Proceedings of 10th Biennial International Conference & Exposition*, 1-5.

Gayathri, G. (2006) “Studies on Factors Affecting Shrinkage Limit of Soils.” *M Tech Dissertation*, National Institute of Technology Karnataka, Surathkal.

George, V., Ramakrishna, H., Vardhana, M. V., Santosh, G. and Gotamey, D. (2012). “A Accelerated Consolidation of Coir Reinforced Lateritic Lithomarge Soil Blends with Vertical Sand Drains for Pavement Foundations.” *EJGE*, 17, 2115-2132.

Giao, P. H., Chung, S. G., Kim, D.Y. and Tanaka, H. (2003). “Electric imaging and laboratory resistivity testing for geotechnical investigation of Pusan clay deposits.” *J. of Applied Geophysics*, Science Direct, Elsevier, 52, 157– 175.

Gidigasu, M. D. (1976). “Laterite soil engineering: pedogenesis and engineering principles.” (Amsterdam ; New York: Elsevier Scientific Pub. Co).

Gingine, V., Dias, A. S. and Cardoso, R. (2016). “Compaction Control of Clayey Soils using Electrical Resistivity Charts.” *Advances in Transportation Geotechnics 3*. The 3<sup>rd</sup> International Conference on Transportation Geotechnics, 143, 803-810, Elsevier.

Gunn, D. A, Reeves, H., Chambers, J. E., Pearson, S. G., Haslam, E., Raines, M. R., Tragheim, D. G., Lovell, J. M., Tilden, S. R., Ghataora, G., Burrow, M., Weston, P., Thomas. A. and Nelder, L. M. (2007). “Assessment of Embankment Condition using Combined Geophysical and Geotechnical Surveys. <https://www.bgs.ac.uk/downloads/start.cfm?id=1866>

Gunn, D. A., Chambers, J. E., Uhlemann, S., Wilkinson, P. B., Meldrum, P. I., Dijkstra, T. A., Haslam, E., Kirkham, M., Wragg, J., Holyoake, S., Hughes, P. N., Hen-Jones, R. and Glendinning, S. (2015). “Moisture monitoring in clay

embankments using electrical resistivity tomography.” *Construction and Building Materials*, Elsevier, Science Direct, Constr Build Mater, 92, 82-94.

Hassan, A. and Toll, D. G. (2013). “Electrical Resistivity Tomography for Characterizing Cracking of Soils.” *Geo-Congress*, ASCE, 818-827.

Hamzah, U. Ismail, M. A. and Samsudin, A. R. (2008). “Geophysical techniques in the study of hydrocarbon-contaminated soil.” *Bulletin of the Geological Society of Malaysia*, 54, 133-138.

Hausmann, M. R. (1990). “Engineering principles of ground modification.” McGraw-Hill, New York.

Hen-Jones, R. M., Hughes, P. N., Stirling, R. A., Glendinning, S., Chambers, J. E., Gunn, D. A. and Cui, Y. J. (2017). “Seasonal effects on geophysical–geotechnical relationships and their implications for electrical resistivity tomography monitoring of slopes.” *Acta Geotechnica*, Springer Publications, 2017, 1-15.

Herman, R. (2001). “An introduction to electrical resistivity in geophysics.” *American Association of Physics Teachers*. 69(9), 943-952.

Huntley, D. (1986). “Relations between permeability and electrical resistivity in granular aquifers.” *Groundwater*, 24(4), 466-474.

Holtz, D. R., Kovacs, W. D. and Sheahan, T. C. (2015). “An Introduction to Geotechnical Engineering.” Pearson India Education Services Pvt. Ltd., 863.

Hong-jing, J., Shun-qun, L. and Lin, L. (2014). “The relationship between the electrical resistivity and saturation of unsaturated soil.” *EJGE*, 19, 3739-3746.

IS:2720 (Part 2)-1973 Methods of Test for Soils Part 2, “Determination of Water Content.” (second revision). Bureau of Indian Standards, New Delhi.

IS: 2720 (Part 7) - 1980, Methods of test for soils: Part 7, “Determination of water content- dry density relation using light compaction.” (second revision). Bureau of Indian Standards, New Delhi.

IS: 2720 (Part 8) – 1983. Methods of test for soils: Part 8, “Determination of water content-dry density relation using heavy compaction.” Bureau of Indian Standards, New Delhi.

IS: 2720 (Part 3/ Section I) - 1980, Method of test for soils: Part 3, “Determination of specific gravity.” (first revision). Bureau of Indian Standards, New Delhi.

IS: 2720(Part 4) - 1985, Methods of test for soils, Part 4: “Grain size analysis.” Bureau of Indian Standards, New Delhi.

IS 2720 (Part 5)-1985: Methods of test for soils: “Determination of liquid and plastic limit.” Bureau of Indian Standards, New Delhi.

IS 2720 (Part 6)-1972: Methods of test for soils: “Determination of shrinkage factors.” Bureau of Indian Standards, New Delhi.

IS 2720 (Part 17)-1986: Methods of test for soils, Part 17: “Laboratory determination of permeability.” Bureau of Indian Standards, New Delhi.

IS: 2720 (Part 10) - 1991, Methods of test for soils: Part 10, “Determination of unconfined compressive strength.” (second revision).

IS 2720 (Part 11) – 1993, Methods of test for soils: Part 11, “Determination of the shear strength parameters of a specimen tested in unconsolidated undrained triaxial compression without the measurement of pore water pressure.” Bureau of Indian Standards, New Delhi.

IS: 4332 (Part 3)-1967. Methods of test for stabilized soils: Part 3, “Test for Determination of Moisture Content- Dry density relation for Stabilized Soil Mixtures.” Bureau of Indian Standards, New Delhi.



IS: 2720 (Part 26)-1987. Method of test for soils: Part 26: "Determination of pH value." Bureau of Indian Standards, New Delhi.

Islam, T., Chik, Z., Mustafa, M. M. and Sanusi, H. (2012). "Estimation of Soil Electrical Properties in a Multilayer Earth Model with Boundary Element Formulation." *Mathematical Problems in Engineering*, Hindawi Publishing Corporation, Article ID 472457, 1-13.

Jee, W. W. and Sang-Gui, H. (2007). "Feasible Boulder treatment methods for soft ground shielded TBM." *Underground Space- the 4<sup>th</sup> Dimension of Metropolises-Bartal, Hrdina, Romancov & Ziamalv(eds) (c) Taylormand Francis Group, London*. Google Books, 217-222.

Jia, Y., Liu, X., Zheng, J., Shan, H. and Honglei. (2013). "Field and laboratory resistivity monitoring of sediment consolidation in China's Yellow River estuary." *Engineering Geology*, Science Direct, 164, 77–85.

Jun-hua, W., Jun-ping, Y. and Charles, W. W. N. (2012). "Theoretical and experimental study of initial cracking mechanism of an expansive soil due to moisture-change." *J. of Central South University*, Springer, 19(5), 1437-1446.

Kabir, S. A. S. M., Hossain, D. and Abdullah, R. (2011). "2-D Electrical Imaging In Some Geotechnical Investigation of Madhupur Clays, Bangladesh." *J. Geological Society of India*, 77, 73-81.

Kahraman, S. and Yeken, T. (2010). "Electrical resistivity measurement to predict uniaxial compressive and tensile strength of igneous rocks." *Bull. Mater. Sci., Indian Academy of Sciences*, 33(6), 731–735.

Kalinski, R. and Kelly, W. (1994). "Electrical-Resistivity Measurements for Evaluating Compacted-Soil Liners." *J. Geotech. Engrg., ASCE*, 120(2), 451–457.

Kelly, W. E. (1978). "Goelectric Sounding for estimating aquifer Hydraulic Conductivity." *Groundwater*, 15(6), 420-425.

Kelly, W. E. (1985). "Electrical resistivity for estimating Groundwater recharge." *J. Irrig. Drain Eng.* 111, 177-180.

Khalil, M. A., Fernando A., and Santos, M. (2009). "Influence of Degree of Saturation in the Electrical Resistivity–Hydraulic Conductivity Relationship." *Surveys in Geophysics*, Springer, November 2009, 30(6), 601-615.

Kibria, G. (2011). "Determination of Geotechnical Properties of Clayey Soil from Resistivity Imaging (RI)." *M. S. Thesis, The University of Texas at Arlington.*

Kibria, G. and Hossain, M. S. (2012). "Investigation of Geotechnical Parameters Affecting Electrical Resistivity of Compacted Clays." *J. of geotechnical and geo environmental engineering*, ASCE, 138, 1520-1529.

Kim, J. H., Hyung-Koo, Y. and Jong-Sub, L. (2011). "Void Ratio Estimation of Soft Soils Using Electrical Resistivity Cone Probe." *J. of geotechnical and geo environmental engineering*, ASCE, 137, 86-93.

Kishore, N. K. and Bhagat, M. (2006). "Study of soil resistivity variation with salinity." *Proceedings of First International Conference on Industrial and Information Systems, ICIIS 2006, 8 - 11 August 2006, Sri Lanka.* 1-5.

Kosinski, W. K. and Kelly, W. E. (1981). "Geoelectric soundings for predicting aquifer properties." *GroundWater* 19, 163-171.

Loke M. H. (2004). "Tutorial: 2D and 3D Electrical Imaging Surveys." [https://pangea.stanford.edu/research/groups/sfmf/docs/DCResistivity\\_Notes.pdf](https://pangea.stanford.edu/research/groups/sfmf/docs/DCResistivity_Notes.pdf)

Li, Z., Xiao, L., and Wei, X. (2007). "Determination of Concrete Setting Time using Electrical Resistivity Measurement." *J. Mater. Civ. Eng.*, 19(5), 423–427.

Liao, Y. and Wei, X. (2014). "Relationship between Chemical Shrinkage and Electrical Resistivity for Cement Pastes at Early Age." *J. Mater. Civ. Eng.*, 26(2), 384–387.

Liu, S. Y., Du, Y. J., Han, L. H. and Gu, M. F. (2008). "Experimental study on the electrical resistivity of soil–cement admixtures." *Environmental Geology*, Springer, 54, 1227-1233.

Mahmoud, M. A. A. N. (2013). "Reliability of using standard penetration test (SPT) in predicting properties of silty clay with sand soil." *Int. J. of Civil and Structural Engineering* 3(3), 545-556.

Meshram, S. A., Khadse, S P. and Meshram, D. C. (2013). "Interpretation and Optimization of Resistivity Studies Data for the Shallow Subsurface Geology along The Cauvery –Vaigai Link Canal Project- (A Case Study)." *International Refereed J. of Engineering and Science (IRJES)*, 2(1), 25-29.

Michael. M. (2012). "Relationship between electrical resistivity and basic geotechnical parameters for marine clays." *Canadian Geotechnical, J.* 49(10), 1158-1168.

Michot, D., Hallaire, V., Besnard, S., Chirie, G., Besnard, Y. and Dutin, G. (2010). "Characterization of soil structure and water infiltration spatial variability using electrical resistivity tomography at decimetre scale. A study of two contrasted soil tillage modalities." *Proceedings of 19th World Congress of Soil Science, Soil Solutions for a Changing World.* 18- 20.

Mitchell, J. and Soga, K. (2005). "Fundamentals of soil behaviour." John Wiley and Sons, Inc., Hoboken, NJ.

Montafia, A. (2013). "Influence of Physical Properties of Marine Clays on Electric Resistivity and Basic Geotechnical Parameters." *Geotechnics and Geohazards*, 1-150.

Mostafa, M. S., Afify, N., Gaber, A. and Abozid, E. F. (2003). "Electrical Resistivity of Some Basalt and Granite Samples from Egypt." *Egypt. J. Sol.*, 26(1), 25-32.

Nayak, S. and Sarvade, P. G. (2012). “Effect of Cement and Quarry Dust on Shear Strength and Hydraulic Characteristics of Lithomargic Clay.” *Geotech Geol Eng*, Springer, 30, 419–430.

Nolan, B. T., Campell, D. L. and Senterfit, R. M. (1998). “Depth of the base of the Jackson Aquifer, based on geophysical exploration, southern Jackson Hole, Wyoming, USA.” *Hydrogeology journal*. Springer, 6, 374-382.

Nitterberg, F. (1982). “Geotechnical Properties and Behaviour of Calcretes in South and Southwest Africa. Geotechnical Properties, Behaviour, and Performance of Calcareous Soils.” ASTM STP 777. *American Society for Testing and Materials*, 296-309.

Ogungbe, A. S., Olowofela, J. A., Da-Silva, O. J., Alabi, A. A. and Onori, E. O. (2012). “The influence of changes in water content on the electrical resistivity of a natural unsaturated loess.” *ASTM Geotechnical Testing Journal*, 35 (1), 11-17.

Oh, S. and Sun, C. G. (2008). “Combined analysis of electrical resistivity and geotechnical SPT blow counts for the safety assessment of fill dam.” *Environmental Geology*, Springer, 54, 31-42.

Osman, S. B. S., Jusoh, H and Abdul, H. (2016). “Behavior of Electrical Resistivity in Sandy Clay Loam Soil with Respect to its Strength Parameters.” *ARPN Journal of Engineering and Applied Sciences*. 11(8), 5433-5438.

Osman, S. B. S. and Siddiqui, F. I. (2014). “Possible Assessment on Sustainability of Slopes by using Electrical Resistivity: Comparison of Field and Laboratory Results.” *Energy, Environment, Biology and Biomedicine*, 60-73.

Owusu-Nimo, F. (2011). “Investigating linkages between the engineering and petrophysical properties of unconsolidated geomaterials and their geoelectrical parameters.” *Ph.D thesis*, Department of Civil and Environmental Engineering, Duke University.

Ozcep, F., Yildirim, E., Tezel, O., Asci, M. and Karabulut, S. (2010). "Correlation between electrical resistivity and soil-water content based artificial intelligent techniques." *International J. of Physical Sciences*. 5 (1), 047-056, January, 2010. *Soil and Tillage Research*, Science Direct, 83(2), 173–193

Parikh, H. N., Ayachit, V. V. and Chakravarthy, N. C. V. N. (1990). "Goelectrical resistivity surveys for groundwater prospecting in granitic area of Idar and Godhra blocks of Gujarat state: An analytical study." *Journ. Assoc. Expl. Geophys*, 11(1), 33-44.

Patangay, N. S., Sirsailanath, A. and Bhimasankaram, V. L. S. (1977). "Prediction of Groundwater yield of wells in granites by means of resistivity sounding method." *Geophysical case histories of India*, 1, 161-168.

Piegari, E. and Di Maio, R., (2012). "A study of stability analysis of pyroclastic covers based on electrical resistivity measurements." *J. Geophys. Eng.* 9, 191-200.

Piegari, E. and Di Maio, R. (2013). "Estimating soil suction from electrical resistivity." *Nat. Hazards Earth Syst. Sci.*, 13, 2369–2379.

Piegari, E. and Di Maio, R. (2014). "Simulations of landslide hazard scenarios by a geophysical safety factor." *Nat Hazards*, Springer, 73:63–76.

Pozdnyakova, L. (1999). "Electrical properties of soils." *Ph.D thesis*, Department of Renewable Resources, University of Wyoming, Laramie, WY.

Putiska, R., Nikolaj, M. and Dostal, I. and Kusnirak, D. (2012). "Determination of cavities using electrical resistivity tomography." *Contributions to Geophysics and Geodesy*. 42(2), 201–211.

Qazi, W. H., Osman, S. B. A. B. S and Memon, M. B. (2016). "Prediction of Soil Engineering Properties using Electrical Resistivity Values at Controlled

Moisture Content-A Conceptual Paper.” *ARPJ Journal of Engineering and Applied Sciences*. 11(6), 3684-3589.

Ramaiah, J. B., Kate, J. M. and Shanker, H. (2010). “Interpretation and Assessment of Electrical Resistivity Soundings Data.” *Proceedings of Indian Geotechnical Conference – 2010, GEOTrendz*, 41-44.

Ramakrishnegowda, C. (2005). “Impact of Contaminants on Geotechnical Behaviour of Soil.” Ph.D thesis, NITK Surathkal, India.

Rao, B. V. (2002). “Goelectrical gata based statistical modelling for yield of bore wells in a typical Khondalitic terrain.” *Journal of Applied Hydrology*. 15(2,3), 1-8.

Rao, K. V. R., Mathur, S. P. and Bhimasankaram, V. L. S., 1977. Location of Groundwater inflow horizons in granites by resistivitymetry logging. *Geophysical case histories of India*, 1, 201-209.

Razali, M. N. F. B and Osman, S. B. A. S. (2011). “Non-Quantitative Correlation of Soil Resistivity with Some Soil Parameters.” *Proceedings of National Postgraduate Conference (NPC), 19-20 Sept.* Published in IEEE Explore, Electronic ISBN: 978-1-4577-1884-7.

Robertson, E. I., and Macdonald, W. J. P. (1962). “Electrical resisivity and ground temperature at Scott Base, Antarctica.” *New Zealand Journal of Geology and Geophysics*. Taylor & Francis, 5(5), 797-809.

Rogers, J. D. (2006). “Subsurface Exploration Using the Standard Penetration Test and the Cone Penetrometer Test.” *Environmental & Engineering Geoscience*, 12(2), 161–179.

Sabet, M. A. (1975). “Vertical Electrical Resistivity Soundings to Locate Ground Water Resources: A Feasibility Study.” *A publication of Virginia Water*

*Resources Research Center Virginia Polytechnic Institute and State University Blacksburg, Bulletin 73.*

Samouelian, A., Isabelle, C., Guy, R., Alain, T., and Ary, B. (2003). "Electrical Resistivity Imaging for Detecting Soil Cracking at the Centimetric Scale." *Soil science society of America J.* 675. 1319–1326.

Samouelian, A., Cousin, I., Tabbagh, A., Bruand, A., Richard, G. (2005). "Electrical Resistivity Survey in Soil Science: A Review." *Soil and Tillage Research*, 83 (2), 173-193.

Sarma, V. V. J. (1977). "A case history of the application of the geoelectrical surveys in delineation of hydrogeological sections of Khondalitic zones of Eastern Ghats." *Geophysical case histories of India*, 1. 211-218.

Seladji, S., Cosenzaa, P., Tabbagh, A., Ranger, J. and Richard, J. (2010). "The effect of compaction on soil electrical resistivity: A laboratory investigation." *European J. of Soil Science*, 61(6) 1043–1055.

Sentenac, P. and Zielinski, M. (2009). "Clay fine fissuring monitoring using miniature geoelectrical resistivity arrays." *Environmental Earth Science*, Springer, 59, 205–214.

Seo, S. Y., Hong, S. S., and Lee, J. S. (2013). "Electrical Resistivity of Soils due to Cyclic Freezing and Thawing." *ISCORD 2013: Planning for Sustainable Cold Regions*. ASCE, 149-154.

Seokhoon, Oh. Chang-Guk, S. (2008). "Combined analysis of electrical resistivity and geotechnical, SPT blow counts for the safety assessment of fill dam." *Environmental Geology*. Springer, 54, 31–42.

Sharma, K. K. and Jayashree, S. (1998). "Identification of zones of corrosive groundwater using resistivity method." *Journ. of Geophysics*, 19(4), 225-229.

Shivashankar, R. Nayak, S. Srinath, K., Bhat, Arun Kumar K. and Rao, Shubhananda (2016), "Properties and Behaviour of laterites and lithomargic clays of coastal Karnataka" Proceedings of International conference on Soil and Environment (ICSE) at IISc Bangalore, July 22-23, 2016, paper No. 83, Session 2, 1-8.

Shivashankar, R., Ravi Shankar, A. U. and Jayamohan, J. (2015), "Some Studies on Engineering Properties, Problems, Stabilization and Ground Improvement of Lithomargic Clays", Paper No.3095, Geotechnical Engg. Journal of SEAGS and AGSSEA, 46(4), December 2015, ISSN 0046-5828, pp.68-80, Special issue on problematic soils including contaminated soils.

Siddiqui, F. I., Baharom, S., and Osman, A. B. S. (2012). "Electrical Resistivity based Non-Destructive Testing Method for Determination of Soil's Strength Properties." *Advanced Materials Research*, 488-489, 1553-1557.

Singh, Y. (2013). "Electrical Resistivity Measurements: A Review." *International Journal of Modern Physics: Conference Series*, 22, 745–756.

Sirhan, A. and Hamidi, M. N. (2013). "Detection of soil and groundwater domestic pollution by the electrical resistivity method in the West Bank, Palestine." *Near Surface Geophysics*, 11(4), 371 – 380.

Sivapullaiah, P. V., Guru Prasad, B. and Allam, M. M. (2009). "Effect of Sulfuric Acid on Swelling Behavior of an Expansive Soil." *Soil and Sediment Contamination: An Int. J.* Taylor and Francis, 18:121–135.

Sivapullaiah, P. V. (2015). "Surprising soil behaviour: is it really!!!" *Indian Geotechnical Journal*, 45(1), 1–24.



Smith, R. C. and Sjogren, D. B. (2006). "An evaluation of electrical resistivity imaging (ERI) in Quaternary sediments, southern Alberta, Canada." *Geosphere*, The Geological Society of America, 2, 287-298.

Spragg, R., Villani, C., Snyder, K., Bentz, D., Bullard, J. W. and Weiss, J. (2013). "Electrical Resistivity Measurements in Cementitious Systems: Observations of Factors that Influence the Measurements." *Annual Compendium of Papers of the 92nd Annual Meeting of the Transportation Research Board*, January 2013. Washington, D.C.

Sreedeeep, S. and Singh, D. N. (2005). "Estimating Unsaturated Hydraulic Conductivity of Fine-Grained Soils using Electrical Resistivity Measurements." *J. of Applied Geophysics*, Science Direct, 59, 126– 139.

Sreedeeep, S., Reshma, A. C. and Singh, D. N. (2004). "Measuring Soil Electrical Resistivity Using a Resistivity Box and a Resistivity Probe." *Geotechnical Testing Journal*, 27(4), 411-415.

Sridharan, A., Nagaraj, T. S., and Sivapullaiah, P. V. (1981). "Heaving of soil due to acid contamination." *Proc. X International Conference Soil Mechanics and Foundation Engineering, Stockholm, Balkema*, 2, 383-386.

Sridharan, A. and Prakash, K. (1998). "Mechanism Controlling the Shrinkage Limit of Soils." *Geotechnical Testing J. GTJODJ*, 21, 3, 240-250.

Srinivasan, K., Poongothai, S. and Chidambaram, S. (2013). "Identification of Groundwater Potential Zone by using GIS and Electrical Resistivity Techniques in and around the Wellington Reservoir, Cuddalore District, Tamilnadu, India, *European Scientific Journal*, 9(17), 312-331.

Sudha, K., Israil, M., Mittal, S. and Rai, J. (2009). "Soil characterization using electrical resistivity tomography and geotechnical investigations." *J. of Applied Geophysics*, Science Direct. 67, 74–79.

Syed, B. A. and Siddiqui, F. I. (2012). "Use of Vertical Electrical Sounding (VES) method as an Alternative to Standard Penetration Test (SPT)." *Proceedings of the Twenty-second (2012) International Offshore and Polar Engineering Conference*, 871-875.

Toll, D. G., Hassan, A. A., King, J. M., Asquith, J. D. (2013). "New Devices for Water Content Measurement." *Proceedings of the 18th International Conference on Soil Mechanics and Geotechnical Engineering, Paris, 2013*. 1199-1202.

Tong, L., Liu, L., Cai, G. and Du, G. (2013). "Assessing coefficient of the earth pressure at rest from shear wave velocity and electrical resistivity measurements." *Engg. Geology*. Elsevier, Science Direct, 163, 122-131.

Verma, K., Rao, M. K. and Rao, C. V. (1980). "Resistivity investigations for Groundwater in metamorphic areas near Dhanbad, India." *Groundwater* 18(1), 44-55.

Vita, D. P., Agrello, D. and Ambrosino, F. (2006). "Landslide susceptibility assessment in ash-fall pyroclastic deposits surrounding Mount Somma-Vesuvius: Application of geophysical surveys for soil thickness mapping." *J. of Applied Geophysics*. 59, 126– 139.

Voronin, A. D. (1986). "The Bases of Soil Physics." Mosk. Gos. Univ., Moscow.

Wang, Z., Zeng, Q., Wang, L., Yao, Y. and Li, K. (2014). "Electrical resistivity of cement pastes undergoing cyclic freeze-thaw action." *Journal of Materials in Civil Engineering*, ASCE, 1-33.

Wei, X. and Li, Z. (2006). "Early Hydration Process of Portland Cement Paste by Electrical Measurement." *J. Mater. Civ. Eng.*, ASCE, 18(1), 99–105.

Wei, X., Xiao, L. and Li, Z. (2012). "Prediction of standard compressive strength of cement by the electrical resistivity measurement," *Construction and Building Materials*, 31, 341–346.

Wei, X., Tian, K. and Xiao, L. (2010). "Prediction of compressive strength of Portland cement paste based on electrical resistivity measurement." *Advances in Cement Research*, 2010, 22(3), 165–170.

Yamasaki, M. T., Peixoto, A. S. P. and Lodi, P. C. (2013). "Evaluation of Electrical Resistivity in a Tropical Sandy Soil Compacted." *EJGE*, 19/C, 629-644.

Zha, F., Liu, S., and Du, Y. (2006). "Evaluation of Swell-Shrinkage Properties of Compacted Expansive Soils Using Electrical Resistivity Method." *Advances in Unsaturated Soil, Seepage, and Environmental Geotechnics*, ASCE, 143-151.

Zha, F., Liu, S., Du, Y. (2007). "Evaluation of change in structure of expansive soils upon swelling using Electrical Resistivity Measurements." *Advances in Measurement and Modeling of Soil Behavior*, ASCE, 1-10.

Zhang, D., Chen, L. and Liu, S. (2012). "Key parameters controlling electrical resistivity and strength of cement treated soils." *J. of Central South University*, Springer, 19, 2991-2998.

## LIST OF PUBLICATIONS

### Journals

Nimi Ann Vincent, R. Shivashankar, K. N. Lokesh, V.L. Gayathri, (2015). “Investigating Linkages between Electrical Resistivity and Physical Characteristics of Unsaturated Soils”. *Journal of Civil Engineering and Environmental Technology*. 2(13) 46-50.

Nimi Ann Vincent, R. Shivashankar, and K. N. Lokesh: “Laboratory and Field Electrical Resistivity Studies on Laterites and Lateritic Soils” *Electronic Journal of Geotechnical Engineering (EJGE)*, 2017 (22.07) [Accepted May 03, 2017], pp 2637- 2664. Worldwide web of geotechnical engineers, ISSN 1089-3032. Available at [ejge.com](http://www.ejge.com).  
<http://www.ejge.com/2017/JourTOC22.07.htm>,

Nimi Ann Vincent, R. Shivashankar, K. N. Lokesh, Jinu Mary Jacob, (2017) “Laboratory Electrical Resistivity Studies on Cement Stabilized Soil”. *International Scholarly Research Notices*. Vol. 2017, Article ID 8970153, 15 pages. doi:10.1155/2017/8970153, Hindawi publications.

R. Shivashankar, Nimi Ann Vincent, Divya Nath and K. N. Lokesh (2018), “Soil Resistivity Studies related to Corrosive Nature of Soil for Buried Pipes”, Paper ID 10, International Symposium on Lowland Technology (ISLT2018), September 26-28, 2018, at Hanoi Vietnam; Organized by International Association of Lowland Technology (IALT), Institute of Lowland and Marine Research (ILMR) Japan and Thuy Loi University, Hanoi, Vietnam (to be published in a special issue of Lowland Technology International Journal, scopus indexed).

### National and International Conferences

Nimi Ann Vincent, K. N. Lokesh, R. Shivashankar, “Electrical Resistivity measurements- a versatile testing technique in Civil Engineering.” Proceedings of the first annual conference on innovations and developments in civil engineering, ACIDIC-2014, NITK, Surathkal, India. 19-20, May 2014, vol 1. 339-346.

Nimi Ann Vincent, R. Shivashankar, K. N. Lokesh, V.L. Gayathri, “Investigating Linkages between Electrical Resistivity and Physical Characteristics of Unsaturated

Soils”. Proceedings of the eighth International conference on Recent Advances in “Civil Engineering, Architecture and Environmental Engineering for Sustainable Development”. 11-12 July 2015, JNU, New Delhi.

Nimi Ann Vincent, R. Shivashankar and K. N. Lokesh (2017), "Some studies on laboratory and field electrical resistivities of soils", Indian Geotechnical Conference 2017 GeoNEst, 14-16 December 2017, IIT Guwahati, India (Th01\_037).

Divya Nath, Nimi Ann Vincent, R. Shivashankar and K. N. Lokesh (2017), “Electrical resistivity studies on lateritic soils”, Indian Geotechnical Conference 2017 GeoNEst, 14-16 December 2017, IIT Guwahati, India (Th01\_211).

R. Shivashankar, Nimi Ann Vincent and K. N. Lokesh (2018) "Geotechnical and Electrical Properties of Laterites and Lateritic Soils", 4<sup>th</sup> GeoShanghai International Conference, May 27-30 2018. Submission ID:B0289, Main Organizer Tongji University, Shanghai, PR China.

## CURRICULUM VITAE

**NIMI ANN VINCENT**

Pathrapankal,  
Ponkunnam,  
Kottayam-686506  
Kerala.

**Email:nimiannvincent@gmail.com**

**Mobile: +91-8547864346**

---

### Education:

Qualification	Institution	University/Board
Ph.D. (Geotechnical Engineering)	National Institute of Technology, Karnataka, Surathkal, Mangalore	NITK, Surathkal
M Tech (Geotechnical Engineering)	National Institute of Technology, Karnataka, Surathkal, Mangalore	NITK, Surathkal
B.Tech(Civil Engineering)	College of Engineering Trivandrum	Kerala University
Twelth	Arya Central School, Trivandrum	Central Board of Secondary Education
Tenth	Nirmala Bhavan English Higher Secondary, School	Kerala Secondary Education Examination Board

**Work Experience:** Working as Assistant Professor in Amal Jyothi College of Engineering, Kottayam, Kerala, from July 2012 to present.

## APPENDIX

**Apparent Resistivity data obtained by conducting VES at 14 selected locations in NITK Campus**

AB /2	MN/ 2	NITK1	NITK2	NITK3	NITK4	NITK5	NITK6	NITK7	NITK8	NITK9	NITK10	NITK11	NITK12	NITK13	NITK14
		$\rho_a(\text{ohm-m})$	$\rho_a(\text{ohm-m})$	$\rho_a(\text{ohm-m})$	$\rho_a(\text{ohm-m})$	$\rho_a(\text{ohm-m})$	$\rho_a(\text{ohm-m})$	$\rho_a(\text{ohm-m})$	$\rho_a(\text{ohm-m})$	$\rho_a(\text{ohm-m})$	$\rho_a(\text{ohm-m})$	$\rho_a(\text{ohm-m})$	$\rho_a(\text{ohm-m})$	$\rho_a(\text{ohm-m})$	$\rho_a(\text{ohm-m})$
0.5	0.25	4255.93	338.42	1011.01	195.60	1004.17	321.12	319.18	956.38	2151.01	734.26	1846.16	3327.05	883.65	436.15
1	0.25	3096.65	589.04	1395.33	209.28	1960.48	263.23	325.75	1377.29	2581.49	1005.16	2607.43	2762.03	975.53	620.86
1	0.5	3200.17	804.19	1554.38	199.99	2003.80	331.06	350.41	1602.37	386.54	1122.42	2801.12	3180.15	1100.59	1200.37
1.5	0.5	1972.52	739.04	1071.42	233.37	1616.91	238.42	324.95	1535.62	2158.93	1155.30	2685.22	2120.03	907.12	974.69
2	0.5	1685.96	797.51	753.36	277.41	1345.59	240.68	242.70	1484.31	1871.54	1081.47	2655.51	1988.88	862.46	1266.26
2.5	0.5	1506.43	768.11	632.01	317.07	1211.59	250.89	217.84	1352.43	1527.24	1045.38	2693.50	1731.17	847.68	1558.02
2.5	1	1607.20	727.69	788.02	320.48	1293.28	236.22	250.87	1332.48	1582.98	935.06	2411.40	1673.33	976.40	1443.39
3	1	1455.62	712.00	672.35	366.15	1260.90	229.47	217.66	1310.55	1298.68	881.68	2424.27	1572.95	960.68	1742.01
3.5	1	1293.89	642.98	557.39	403.91	1195.99	236.49	211.64	1176.87	1166.97	851.76	2414.99	1572.45	915.30	1995.10
4	1	1233.81	551.76	502.77	438.95	933.70	217.59	216.74	1095.37	1036.10	840.60	2275.95	1415.37	875.74	2189.67
4.5	1	1221.71	522.15	488.20	480.48	799.84	210.68	220.01	1035.83	915.26	814.50	2090.25	1173.99	844.12	2385.08
5	1	1179.71	501.34	471.46	520.05	694.48	225.56	221.58	972.59	570.69	780.30	1957.75	1162.59	799.99	2448.36
5	2	1002.86	545.97	610.74	470.53	954.46	234.93	241.40	1000.77	580.71	755.86	1881.42	1157.92	971.56	2329.71
6	2	1136.33	481.60	581.60	506.04	901.48	215.88	236.87	812.56	643.82	722.55	1773.57	980.65	861.28	2101.13
7	2	1076.34	427.72	455.77	550.23	932.83	188.87	252.19	836.37	598.35	709.56	1590.15	792.17	746.76	1952.35
8	2	1032.31	358.60	317.95	557.19	884.61	159.85	261.34	718.97	577.68	640.91	1405.51	688.16	719.23	1782.69
9	2	979.19	320.63	118.43	567.85	655.74	135.13	253.68	623.03	524.73	570.72	1232.38	688.04	586.74	1555.50
10	2	874.36	269.07	104.96	603.61	624.45	122.64	263.02	542.90	445.22	504.42	1056.88	644.65	495.44	1382.29

10	4	1020.25	308.11	256.89	579.53	663.18	140.53	223.39	616.59	446.85	552.00	1105.55	647.69	803.86	1470.33
12	4	801.13	188.56	221.21	562.03	472.32	115.53	221.13	436.55	379.30	494.15	850.20	585.87	497.80	1168.13
14	4	641.71	115.76	139.34	525.00	363.30	102.84	201.22	306.89	362.10	417.38	674.09	548.70	343.14	936.95
16	4	511.12	80.18	130.35	510.19	338.28	97.47	135.60	215.07	345.04	347.18	518.77	495.19	270.42	724.99
18	4	420.50	81.74	120.60	477.19	317.40	87.00	158.20	170.49	331.12	297.44	410.30	411.22	213.84	534.75
20	4	370.71	93.44	488.50	422.35	297.31	82.79	135.56	140.15	321.28	243.80	329.87	359.96	142.60	419.00
20	8	363.64	91.00	90.30	459.29		68.85			327.61	271.16				578.49
25	8	345.62	98.67		358.40		62.07			299.25	174.43				228.07
30	8	253.71									129.67				